

**BIOCHEMICAL CHARACTERIZATION OF THE BVDV RNA-DEPENDENT  
RNA POLYMERASE DURING INITIATION AND ELONGATION OF RNA  
SYNTHESIS**

by

**Claudia M. D'Abramo**

Experimental Medicine  
McGill University, Montreal  
August 2006

A thesis submitted to McGill University in partial fulfillment of the requirements of the  
degree of Doctor of Philosophy

© **Claudia M. D'Abramo, 2006**



Library and  
Archives Canada

Bibliothèque et  
Archives Canada

Published Heritage  
Branch

Direction du  
Patrimoine de l'édition

395 Wellington Street  
Ottawa ON K1A 0N4  
Canada

395, rue Wellington  
Ottawa ON K1A 0N4  
Canada

*Your file    Votre référence*

*ISBN: 978-0-494-32346-5*

*Our file    Notre référence*

*ISBN: 978-0-494-32346-5*

#### NOTICE:

The author has granted a non-exclusive license allowing Library and Archives Canada to reproduce, publish, archive, preserve, conserve, communicate to the public by telecommunication or on the Internet, loan, distribute and sell theses worldwide, for commercial or non-commercial purposes, in microform, paper, electronic and/or any other formats.

The author retains copyright ownership and moral rights in this thesis. Neither the thesis nor substantial extracts from it may be printed or otherwise reproduced without the author's permission.

#### AVIS:

L'auteur a accordé une licence non exclusive permettant à la Bibliothèque et Archives Canada de reproduire, publier, archiver, sauvegarder, conserver, transmettre au public par télécommunication ou par l'Internet, prêter, distribuer et vendre des thèses partout dans le monde, à des fins commerciales ou autres, sur support microforme, papier, électronique et/ou autres formats.

L'auteur conserve la propriété du droit d'auteur et des droits moraux qui protègent cette thèse. Ni la thèse ni des extraits substantiels de celle-ci ne doivent être imprimés ou autrement reproduits sans son autorisation.

---

In compliance with the Canadian Privacy Act some supporting forms may have been removed from this thesis.

Conformément à la loi canadienne sur la protection de la vie privée, quelques formulaires secondaires ont été enlevés de cette thèse.

While these forms may be included in the document page count, their removal does not represent any loss of content from the thesis.

Bien que ces formulaires aient inclus dans la pagination, il n'y aura aucun contenu manquant.

  
**Canada**

## ABSTRACT

The RNA-dependent RNA polymerase (RdRp) of viruses belonging to the *Flaviviridae* family, including the hepatitis C virus (HCV) and bovine viral diarrhea virus (BVDV) is critical for viral replication. The major goal of this PhD study was to biochemically characterize the role of the polymerase during initiation and elongation of RNA synthesis, utilizing the BVDV RdRp as a model system. We showed that the BVDV polymerase efficiently incorporates chain-terminating nucleoside analogues, which ultimately arrest RNA synthesis. The incorporated chain-terminators, however, can be removed from the primer terminus in the presence of pyrophosphate (PPi). These results suggest that the phosphorolytic excision of incorporated chain-terminators is a possible mechanism that can diminish the efficiency of this class of compounds against viral RdRps. The chain-terminators then served as valuable tools in subsequent experiments to analyze the functional role(s) of the RdRp-associated GTP-specific binding site (G-site) and the consequences of GTP binding during the initiation of RNA synthesis. The results provide biochemical evidence for the existence of a G-site in the BVDV enzyme, and suggest that GTP binding controls template positioning during *de novo* initiation. Finally, through the development of a novel ribonuclease-based footprinting assay, it was determined that catalytically active complexes contact the newly synthesized RNA during elongation of RNA synthesis with approximately 6-7 base pairs. The polymerase moves along the template according to the position where RNA synthesis is arrested. Taken together, this study provides novel insight into mechanisms involved during initiation and elongation of RNA replication of viruses belonging to the *Flaviviridae* family. The ability of RdRps to excise incorporated chain-

terminators points to possible shortcomings of nucleoside analogue inhibitors that are under development as antiviral agents for the treatment of infection with HCV.



## RÉSUMÉ

L'ARN polymérase ARN-dépendant (ApAd) d'origine virale joue un rôle clé dans la réplication des virus appartenant à la famille des *Flaviviridae*, dont font partie le virus de l'hépatite C (VHC) et le virus de la diarrhée bovine virale (VDBV). L'objectif principal de cette étude de doctorat était de caractériser biochimiquement le rôle de cette polymérase durant l'initiation et l'élongation du processus de synthèse de l'ARN en utilisant l'ApAd du VDBV comme modèle. Nous avons démontré que la polymérase de VDBV incorpore efficacement les analogues de nucléosides capable de terminer la chaîne d'ARN, ce qui entraîne l'arrêt de la synthèse d'ARN. Cependant, ces nucléosides terminaux peuvent être enlevés du bout de l'amorce en présence de pyrophosphate (PPi). Ces résultats suggèrent que l'excision phosphorolytique des nucléosides terminaux peut contribuer à la réduction de l'efficacité de cette classe de produits ciblant les ApAd viraux. Par la suite, ces nucléosides terminaux ont servi d'outils importants pour exécuter d'autres expériences, soit analyser le rôle du site spécifique de liaison de GTP (site-G) et observer l'effet de la présence de GTP durant l'initiation de la synthèse d'ARN. Les résultats fournissent une preuve biochimique de la présence du site-G dans l'enzyme de VDBV et suggèrent que la liaison du GTP contrôle l'emplacement de la matrice d'ADN durant l'initiation *de novo*. En dernier lieu, avec le développement d'un test d'empreinte à base d'ARNase-H, nous avons déterminé que les complexes d'enzymes catalytiquement actives entrent en contact avec approximativement 6-7 paires de bases de l'ARN nouvellement synthétisé pendant l'élongation de la synthèse. La polymérase se déplace le long de la matrice selon la position où la synthèse d'ARN se termine. En conclusion, ces études aident à comprendre les mécanismes impliqués durant l'initiation et l'élongation

de la réplication d'ARN des virus appartenant à la famille des *Flaviviridae*. La capacité des ApAds d'exciser les nucléosides terminaux incorporés souligne l'insuffisance des analogues de nucleosides terminaux présentement en développement comme agents antiviraux pour le traitement de l'hépatite C.

## PREFACE

This thesis was written in accordance with McGill University guidelines (available at <http://www.mcgill.ca/gps/programs/thesis/guidelines/preparation>). The format of the thesis conforms to the “Manuscript-based thesis” option and consists of:

- 1) Abstract in English and French
- 2) Acknowledgements
- 3) Rationale and Objectives
- 4) Literature Review
- 5) Experimental Research
- 6) Conclusion
- 7) References

Original publications presented in chapter 2 to 4 are either published or will soon be submitted for publication:

**Chapter 2:** C.M. D’Abramo, L. Cellai and M. Götte. Excision of Incorporated Nucleotide Analogue Chain-terminators can diminish their Inhibitory Effects on Viral RNA-dependent RNA polymerases. *J Mol Biol*, 2004, 337(1):1-14.

**Chapter 3:** C.M. D’Abramo, J. Deval, C.E. Cameron, L. Cellai and M. Götte. Control of Template Positioning during *De Novo* initiation of RNA Synthesis by the BVDV NS5B Polymerase. *J Biol Chem*, 2006, 281(34): 24991-24998.

**Chapter 4:** C.M. D'Abramo, L. Cellai and M. Götter. Comparative Footprints of the Bovine Viral Diarrhea Virus RNA-dependent RNA polymerase complexes during Elongation. Manuscript in preparation for *Virology*.

#### Contribution of Authors:

All data presented in chapters 2-4 are from experiments performed by myself under the direct supervision of Dr. Matthias Götter. Luciano Cellai chemically synthesized all RNA and chimeric RNA-DNA templates utilized. In chapter 3, Dr. Jerome Deval prepared Figure 6, while Dr. Craig E. Cameron critiqued the manuscript and offered suggestions for revision.

#### This thesis contains 4 chapters:

Chapter 1 includes a comprehensive literature review relevant to the work presented in this thesis. Chapters 2 to 4 include original publications that are either published or will soon be submitted for publication. A final general discussion is presented in Chapter 5. Chapters 2, 3, and 4 contain their own reference sections, which are found at the end of each corresponding section. The references for chapters 1 and 5 are compiled at the end of the thesis.

## **ACKNOWLEDGEMENTS**

This thesis is the result of many years of hard work through which I have been associated and supported by many people. Firstly, I would like to express my sincerest gratitude to my supervisor, Dr. Matthias Götte, whose help, critical judgment, encouragement and guidance, both throughout my project and during the preparation of this thesis, have contributed to the mainstream of my research. I learned a great deal through his knowledge and ascertained the basis and fundamentals of scientific research.

I also wish to thank my fellow colleagues who have familiarized me with numerous techniques, and assisted me with their helpful comments and suggestions during the whole tenure of my research project. They have always offered a motivating, enthusiastic, and stimulating working environment, and I truly enjoyed my interactions with them.

My family deserves my heartfelt acknowledgement for continuously supporting me throughout all my studies. I am deeply indebted to my parents, Mary and Tony D'Abramo, who have taught me the value of hard work through their own example. I firmly believe they are responsible for instilling in me the desire to always pursue the frontiers of knowledge and education. Through their moral framework and work ethics, which they provided me while growing up, I have been able to accomplish the goals I set out for myself. A special thanks to my brother, Joseph for enduring my complaints, yet believing in me and my work.

The encouragement provided by my friends has also been a constant form of motivation. Thank you all for listening and for lending me your shoulders to lean on during the rough times.

Finally, my deepest and loving thanks go to my best friend and husband, Krikor Bijian. He has been my tower of strength and sustenance throughout this entire process. I thank him for helping me realize that I can be successful in all aspects of life. His endless encouragement, love, understanding, and most of all patience, were indispensable in ensuring my success in completing this work. Thank you for believing in me and for supporting me through a long journey that is finally coming to an end!

This research has been supported and funded by various organizations including the Canadian Institutes of Health Research (CIHR) and Fonds de recherche en santé du Québec (FRSQ).

## **TABLE OF CONTENTS**

<b>ABSTRACT</b>	ii
<b>RÉSUMÉ</b>	iv
<b>PREFACE</b>	vi
<b>ACKNOWLEDGEMENTS</b>	viii
<b>TABLE OF CONTENTS</b>	x
<b>LIST OF FIGURES AND TABLES</b>	xv
<b>LIST OF ABBREVIATIONS</b>	xvii
 <b>CHAPTER 1 – GENERAL INTRODUCTION</b>	 1
1.1 Discovery and Epidemiology of HCV	2
1.2 Molecular Biology of HCV	4
1.2.1 The Viral Genome and Polyprotein Processing	4
1.3 The Viral Proteins	7
1.3.1 Core Protein	7
1.3.2 E1 and E2 Envelope Glycoproteins	8
1.3.3 P7	9
1.3.4 NS2	10
1.3.5 NS3	11
1.3.6 NS4A/NS4B	13
1.3.7 NS5A	14
1.3.8 NS5B	15
1.4 The Viral Life Cycle	15

1.4.1	Attachment and Entry into Host Cells	17
1.4.2	Translation and Polyprotein Processing	18
1.4.3	RNA Replication Process	19
1.4.4	Virion Assembly and Release	23
1.5	HCV Model Systems	23
1.5.1	Primary Cell Cultures and Cell Lines	24
1.5.2	The Replicon System	25
1.5.3	The JFH-1 System	27
1.5.4	BVDV	28
1.6	The Viral RNA-dependent RNA polymerase	32
1.6.1	Biochemical Characteristics of Recombinant NS5B	32
1.6.2	Structural Features of RdRps	35
1.6.3	<i>De Novo</i> Initiation Mechanism by RdRps	41
1.7	Nucleoside Analogue Inhibitors of HCV polymerase	45
1.7.1	Non-Nucleoside Analogue Inhibitors	51
1.8	Thesis Objectives	56
<b>2.</b>	<b>CHAPTER 2 – EXCISION OF INCORPORATED NUCLEOTIDE ANALOGUE CHAIN-TERMINATORS DIMINISH THEIR INHIBITORY EFFECTS ON VIRAL RNA-DEPENDENT RNA POLYMERASES</b>	<b>58</b>
	Preface to Chapter 2	59
	Abstract	60
	Introduction	62



Materials and Methods	65
Chemicals and nucleic acids	65
Expression and purification of BVDV NS5B protein	66
RNA synthesis and chain-termination assay	66
Pyrophosphorolysis and rescue of chain-terminated RNA synthesis	67
Results	68
Inhibition of RNA synthesis in the presence of 3'-dNTPs	68
Phosphorolytic excision of incorporated chain-terminators	70
Requirements for divalent metal ions	72
Formation of a dead end complex	74
Discussion	75
Figures	80
References	98
 <b>3. CHAPTER 3 - CONTROL OF TEMPLATE POSITIONING DURING <i>DE NOVO</i> INITIATION OF RNA SYNTHESIS BY THE BVDV NS5B POLYMERASE</b>	 102
Preface to Chapter 3	103
Abstract	104
Introduction	105
Materials and Methods	107
Enzymes and nucleic acids	107
Primer extension assay	108
De novo initiation assay	109



Discussion	151
Figures	155
References	164
<b>5. CHAPTER 5 – GENERAL DISCUSSION</b>	<b>167</b>
5.1 Initiation vs. Elongation	168
5.2 Future Therapeutic Implications	176
5.3 Final Conclusion	179
<b>CONTRIBUTION TO ORIGINAL KNOWLEDGE</b>	<b>180</b>
<b>REFERENCES</b>	<b>183</b>

## LIST OF FIGURES

### Chapter 1:

Figure 1: Genome Organization and Polyprotein Processing of HCV RNA	5
Figure 2: HCV Life Cycle	16
Figure 3: Initiation of the RNA Replication Process	22
Figure 4: Comparison of the HCV genome and subgenomic replicon system	26
Figure 5: Comparison of the structural organization of the HCV and BVDV genome	30
Figure 6: Comparison of RdRp crystal structures	36
Figure 7: Chemical structures of selected inhibitors of HCV NS5B polymerase	46
Figure 8: Crystal structure of HCV RdRp detailing the location of binding pockets for three classes of NNIs	52

### Chapter 2:

Figure 1: Chemical structures of nucleoside analogue inhibitors of RdRps	81
Figure 2: Inhibition of RNA synthesis in the presence of 3'dNTPs	82
Figure 3: PPi-dependent rescue of chain-terminated RNA synthesis	84
Figure 4: Rescue of RNA synthesis in the presence of trap	89
Figure 5: Requirements for divalent metal ions	91
Figure 6: Formation of a dead end complex (DEC)	93

Figure 7: Models of complexes involved in nucleotide-binding, chain termination, phosphorolytic excision, and DEC formation	96
---	----

### Chapter 3:

Figure 1: Schematic model of G-site dependent <i>de novo</i> initiation of RNA synthesis by the BVDV RdRp	121
Figure 2: Heterogeneous priming of the GG dinucleotide primer during primer-dependent initiation of RNA synthesis	123
Figure 3: Effect of incoming nucleotide on template positioning	125
Figure 4: Difference in template positioning during <i>de novo</i> and dinucleotide-primed initiation	127
Figure 5: Effect of G-site specific mutation during <i>de novo</i> and dinucleotide-primed initiation of RNA synthesis	129
Figure 6: Difference in template positioning between BVDV and HCV polymerases	131
Figure 7: Model of GTP-facilitated <i>de novo</i> initiation of RNA synthesis by the BVDV polymerase	133

### Chapter 4:

Figure 1: Use of RNA-DNA chimeric templates as substrates for BVDV RdRp	155
Figure 2: Footprints of arrested polymerization complexes generate a protection of 11 to 12 nucleotides	157
Figure 3: Translocation of arrested enzyme complexes	160
Figure 4: Schematic model of the interaction between BVDV RdRp and its nucleic acid substrate during elongation	162

## LIST OF ABBREVIATIONS

3'-dNTPs	3'-deoxyribonucleoside triphosphates
3D <sup>pol</sup>	poliovirus polymerase
3TC	lamivudine
Å	angstroms
ApoA1	apolipoprotein A1
ARFP	alternative reading frame protein
Arg (R)	arginine
ASGPr	asialoglycoprotein receptor
ATP	adenosine triphosphate
BVDV	bovine viral diarrhea virus
C (Cys)	cysteine
C, E1, E2, p7	structural proteins
cAMP	cyclic adenosine monophosphate
cDNA	complementary DNA
CP	cytopathic
CRE	cis-acting RNA element
CSFV	classical swine fever virus
D (Asp)	aspartic acid
DNA	deoxyribonucleic acid
dNTPs	deoxynucleoside triphosphate
E0 (E <sup>ms</sup> )	BVDV envelope glycoprotein with RNase activity
E. coli	Escherichia coli
EDTA	ethylene-diamine-tetra-acetic-acid
eIF	eukaryotic translation initiation factor
EMCV	encephalomyocarditis virus
ER	endoplasmic reticulum
FdC	2'-deoxy-2'- $\alpha$ -fluorocytidine
G (Gly)	glycine
G418	neomycin sulfate (geneticin)

GBV-B	GB virus type B
GFP	green fluorescent protein
Grb2	growth factor receptor-binding protein 2
G-site	GTP-specific binding site
GST	glutathione S-transferase
GTP	guanosine triphosphate
GTPase	hydrolyses GTP
H (His)	histidine
HAV	hepatitis A virus
HBV	hepatitis B virus
HCV	hepatitis C virus
HCC	hepatocellular carcinoma
HCMV	human cytomegalovirus
HIV-1	human immunodeficiency virus type-1
hnRNP C	heterogeneous nuclear ribonucleoprotein C
hnRNP K	heterogeneous nuclear ribonucleoprotein K
HSV	herpes simplex virus
HVR	hypervariable region
IFN	interferon
IMPDH	inosine monophosphate dehydrogenase
IRES	internal ribosomal entry site
ISDR	interferon sensitivity determining region
JEV	Japanese encephalitis virus
JFH-1	HCV genotype 2a replicon
K (Lys)	lysine
kb	kilobase
kDa	kiloDalton
L (Leu)	leucine
LDL	low-density lipoprotein
LT-BR	lymphotoxin B receptor
M (Met)	methionine

MAPK	mitogen-activated protein kinase
MEK1	mitogen-activated protein kinase kinase 1
Met (M)	methionine
Mg <sup>2+</sup>	magnesium ion
MKK6	mitogen-activated protein kinase kinase kinase 6
Mn <sup>2+</sup>	manganese ion
mRNA	messenger RNA
N site	nucleotide binding site
NaCl	sodium chloride
NANB	non-A, non-B hepatitis
NBM	nucleotide binding motif
NCP	noncytopathic
<i>neo</i>	neomycin phosphotransferase
NHC	b-D-N4-hydroxycytidine
NNIs	non-nucleoside inhibitors
N <sup>pro</sup>	pestivirus autoprotease
NS2, NS3, NS4, NS5	non-structural proteins
NTP	nucleoside triphosphate
NTPase	nucleoside triphosphatase
NTPi	initiating nucleotide
NTPi+1	first NTP substrate
ORF	open reading frame
P (Pro)	proline
P site	priming site
PCBP2	poly (rC)-binding protein 2
PEG	polyethylene glycol
PePHD	PKR/eIF2 $\alpha$ phosphorylation homology domain
PTB	polypyrimidine-tract-binding protein
PKR	double-stranded RNA-dependent protein kinase
PPi	pyrophosphate
PRK2	protein-kinase C-related kinase 2



R (Arg)	arginine
RdRp	RNA-dependent RNA polymerase
RNA	ribonucleic acid
RNase	ribonuclease
RT	reverse transcriptase
RT-PCR	reverse transcription polymerase chain-reaction
S (Ser)	serine
SDS	sodium dodecyl sulfate
SL	stem-loop
SNARE	soluble NSF (N-ethylmaleimide sensitive factor) attachment
SR-BI	scavenger receptor class B type 1
SV40	simian virus 40
T (Thr)	threonine
TMD	transmembrane domain
TNFxxR1	tumor necrosis factor receptor 1
TNTase	terminal transferase
Tris-HCl	tris-hydrochloric acid buffer
UTR	untranslated region
Y (Tyr)	tyrosine
Zn <sup>2+</sup>	zinc ion

## **CHAPTER 1**

### **GENERAL INTRODUCTION**

## **1. GENERAL INTRODUCTION**

Human liver disease caused by the hepatitis C virus (HCV) has become a serious public health issue worldwide. First recognized as post-transfusion “non-A, non-B hepatitis”, the elucidation of the HCV viral sequence in 1989 by Choo *et al.*<sup>1</sup> has led to the extensive and rapid growth in both basic and clinical HCV research. To date, a large number of scientific articles on HCV have been published, addressing several topics such as viral genetic analysis, functional analysis of viral proteins, virus-host interactions, adaptive immune responses, and the mechanisms of drug action and viral persistence. The following chapter provides a brief summary of the discovery and epidemiology of HCV, as well as the current status of the molecular biology of HCV, the viral life cycle, and HCV model systems. This is followed by a comprehensive review of the literature focused on the viral RNA-dependent RNA polymerase (RdRp) that forms the basis for the hypotheses of this thesis.

### **1.1 Discovery and Epidemiology of HCV**

For many years, it was believed that both hepatitis A (HAV) and hepatitis B virus (HBV) were the major causative agents responsible for infectious hepatitis. However, even after the development of preventative and diagnostic methods, it became increasingly clear that the majority of cases of post-transfusion hepatitis that continued to occur was not caused by either HAV or HBV infections, and was therefore termed “non-A, non-B” (NANB) hepatitis. In 1989, after a large number of trials were conducted,

Choo *et al.*<sup>1</sup> succeeded in isolating and cloning part of the HCV genome sequence by immunoscreening a cDNA library derived from the plasma of a chimpanzee chronically infected with the serum from a patient with NANB hepatitis. Antibody detection systems for the diagnosis of HCV were developed by Kuo *et al.*<sup>2</sup> that same year and eventually led to the development of assays with improved sensitivity and specificity. This, in turn, allowed for wide-scale screening of blood and blood products, and ultimately resulted in the prevention of new infections. Today, antibody detection systems, along with DNA amplification methods such as reverse transcription polymerase chain-reaction (RT-PCR), are used as diagnostic tests for HCV infection and help define the prevalence, incidence, and transmission of HCV. It is currently estimated that HCV infection afflicts over 200 million people worldwide<sup>3</sup>, with nearly 35 000 new cases and 10 000-12 000 deaths occurring annually in the United States alone. The rates of HCV infection show significant geographic variations resulting in disease prevalence ranging from 1%-2% in North America, 2% in Japan, 3%-6% in Pakistan and up to 22% in Egypt<sup>4</sup>. Genotype distribution also varies considerably. On the basis of differences in the genomic sequence, HCV can be divided into six distinct genotypes and more than fifty subtypes, with genotype 1a and 1b prevailing in the United States, genotype 3 most common in India, and genotype 4 predominant in Africa and in the Middle East<sup>5</sup>.

The first effective therapy against HCV infection, namely interferon (IFN)-based therapy, was identified before the discovery of the virus itself and was used to treat NANB hepatitis in 1986. Today, combination regimens of polyethylene glycol (PEG)-modified interferon and ribavirin have become the predominant antiviral therapy for

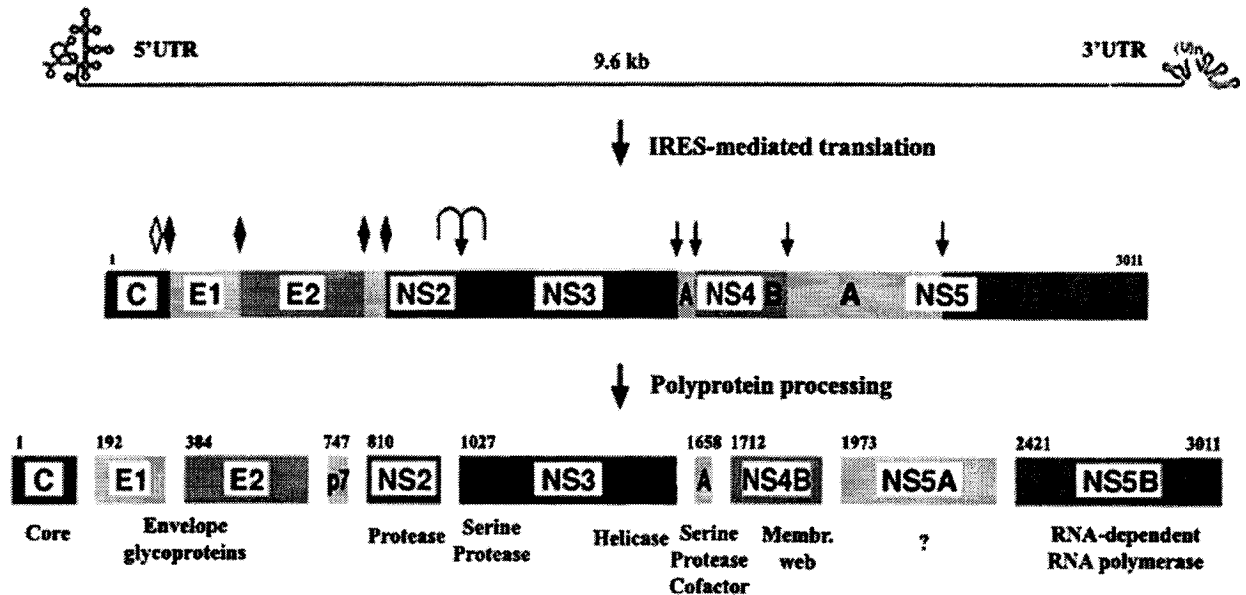
HCV<sup>6; 7</sup>. Trials have shown that this current standard treatment induces a sustained virological response in about 40%-80% of patients with chronic HCV, depending on the HCV genotype<sup>8; 9; 10</sup>. Despite these significant advances, the number of HCV infected patients is expected to rise within the next 10-20 years, making it HCV is one of the greatest public health threats faced in this century. Chronic HCV infection has also been implicated in the rising incidence of hepatocellular carcinoma (HCC) and is the leading cause of liver transplantation in the United States<sup>4</sup>. Consequently, there is an urgent need for the development of newer and more effective therapy in combating the progression of the disease. Progress toward developing a vaccine or new therapeutic strategies however, depends on the continued research on the mechanisms of protective immunity, the molecular biology of the virus, and the complete elucidation of the HCV life cycle.

## **1.2 Molecular Biology of HCV**

### **1.2.1 The Viral Genome and Polyprotein Processing**

The elucidation of the HCV genome structure led to its classification as a distinct member within the family *Flaviviridae*<sup>11</sup>, a family of positive-strand RNA viruses that consist of the flaviviruses, which include Japanese encephalitis virus (JEV), dengue virus and West Nile, the animal pathogenic pestiviruses such as the classical swine fever virus (CSFV) and bovine viral diarrhea virus (BVDV), and the recently cloned GB-viruses. These viruses all have diverse biological properties but appear to be similar in terms of virion morphology, genome organization, and RNA replication.

**Figure 1: Genome Organization and Polyprotein Processing of HCV RNA**



*Schematically depicted at the top is the HCV positive-strand viral genome containing a 9.6-kb open reading frame (ORF) that is flanked on either ends by 5' and 3'UTRs. Internal ribosomal entry site (IRES)-mediated translation yields a polyprotein of approximately 3000 amino acids long, depending on the HCV genotype, which is processed into mature structural (C-p7) and non-structural (NS2-NS5B) proteins. Solid diamonds indicate ER signal peptidase cleavage sites, the cyclic arrow represents the autocatalytic cleavage of the NS2-NS3 junction, and the solid arrows denote the NS3/NS4 proteinase complex cleavage sites. Amino acid positions are shown above each protein. (Adapted from Moradpour et al.<sup>12</sup>).*

The genomic organization and proteolytic processing of the HCV polyprotein are illustrated schematically in Fig. 1. HCV contains a positive-sense, single-stranded RNA genome of approximately 9.6 kb in length<sup>13</sup>. The genome contains a single open reading frame (ORF) encoding a polyprotein that varies in length from 3010-3030 amino acids according to isolate and genotype, and is flanked by 5' and 3' untranslated regions (UTR)<sup>14</sup> (Fig. 1, top). Both 5' and 3'UTR contain a number of highly conserved *cis*-acting RNA elements (CREs) essential for polyprotein translation and genome replication. These structures include the 5'-proximal stem-loop structure and internal ribosome entry site (IRES) within 5'UTR that mediates cap-independent translation initiation of the HCV polyprotein, and a highly conserved 98 nucleotide long RNA element designated as the X-tail at the 3'UTR, important for the initiation of minus-strand synthesis during HCV RNA replication. The viral proteins are translated as a single polyprotein precursor that undergoes extensive post-translational processing by both host and viral enzymes into structural (C, E1, E2, p7) and non-structural (NS2, NS3, NS4A, NS4B, NS5A, NS5B) proteins (Fig. 1, bottom). For most of the HCV proteins, distinct functions have been described. The structural proteins appear to be involved in viral assembly and in the export and infection of new cells, while the non-structural proteins play various important roles in viral genome replication and encode for proteases (NS2, NS3), a helicase (NS3) and an RNA-dependent RNA polymerase (NS5B). Recently, another protein of unknown function, designated the F-protein or ARFP (for alternative-reading-frame-protein) has been identified and is synthesized by means of ribosomal frameshifting in the sequence encoding the N-terminal region of the

polyprotein within the core gene<sup>15; 16</sup>. Whether this protein is expressed in patients during HCV infection remains to be determined.

### **1.3 The Viral Proteins**

#### **1.3.1 Core Protein**

The first structural protein encoded by the HCV ORF is a 22 kDa highly basic, RNA binding core (C) protein, considered to be involved in the formation of the viral nucleocapsid. The HCV core can undergo post-translational processing by cleavage in its hydrophobic C-terminal end to give rise to two additional core products, 19 and 16 kDa in length<sup>17</sup>; however, it is unknown at this time which precise length of the core is required for viral encapsidation. In addition to its role in nucleocapsid formation, the C-protein has been reported to interact with a variety of cellular proteins including the heterogeneous nuclear ribonucleoprotein K (hnRNP K), the lymphotoxin B receptor (LTBR), the tumor necrosis factor receptor 1 (TNF-R1), DEAD box protein (DDX3, DBX, CAP-Rf) (Reviewed in McLauchlan<sup>18</sup>), as well as modulate cellular gene transcription<sup>19</sup> and participate in signal transduction pathways<sup>20</sup>. Its roles in other biological functions such as apoptotic cell death<sup>21; 22</sup> and immune modulation<sup>23; 24; 25; 26</sup> have also been studied extensively, although the conflicting data have led to distinct conclusions. Clearly, the array of effects mediated by the viral core protein suggests its significant role in HCV pathogenesis.



### 1.3.2 E1 and E2 Envelope Glycoproteins

The viral envelope is produced from two envelope glycoproteins E1 and E2, essential for host-cell entry through their role in receptor binding and inducing fusion with the host cellular membrane<sup>27</sup>. Both E1 and E2 are type-1 transmembrane glycoproteins containing a large N-terminal ectodomain and a short C-terminal hydrophobic transmembrane domain (TMD) region, which contributes to important protein functions such as membrane anchoring<sup>28</sup>, ER retention<sup>29; 30; 31; 32</sup> and E1-E2 heterodimer formation<sup>33; 34</sup>. Extensive characterization of the E1-E2 heterodimer complexes, stabilized by noncovalent interactions<sup>35</sup> and/or disulfide-linked aggregates<sup>27</sup>, have suggested that the noncovalent oligomeric complexes are the prebudding form of the virus<sup>36</sup>.

E1 and E2 have also been extensively studied in terms of antigenic variation. Within the N-terminal sequence of the E2 envelope glycoprotein are two extreme hypervariable regions (HVR), HVR-1 and HVR-2. These regions are caused by random mutations and by selection of mutants capable of escaping from the immune pressures of protective B-cell or T-cell responses. HVR-1 appears to be one of the main targets of anti-HCV neutralizing responses. Support for this concept is based on the finding that HCV-negative chimpanzees are protected from HCV infection when inoculated with hyperimmune rabbit serum raised against a synthetic peptide representing the HVR-1<sup>37</sup>. The implication of these findings suggests that mutations in HVR-1 may render the host immune response ineffective, as seen in patients with chronic HCV infection. Antibodies

raised against HVR-1 were also found to prevent viral entry into cells<sup>38</sup>. In fact, a number of cell surface molecules have been found to interact with the envelope protein, implicating E2 as a critical protein involved in targeting the virus to the host cell<sup>39; 40; 41; 42; 43; 44; 45</sup>.

Aside from its role in immune evasion and viral entry, E2 protein has been associated with resistance to interferon- $\alpha$ -based therapy by inhibiting the IFN- $\alpha$  inducible double-stranded RNA-dependent protein kinase (PKR) *in vitro*<sup>46</sup>. Within the C-terminal end of E2 lies a 12 amino acid sequence termed PKR/eIF2 $\alpha$  phosphorylation homology domain (PePHD), which is analogous to the phosphorylation site of PKR and the eukaryotic translation initiation factor (eIF)2 $\alpha$ . Interaction of PePHD with PKR abolishes its kinase activity, and ultimately blocks its inhibitory effect on protein synthesis<sup>46</sup>.

### 1.3.3 P7

Until recently, very little information was known about the structural protein p7. It appears that p7 is a small, membrane-spanning protein of approximately 63 amino acids in length and consists of two TMDs connected by a cytoplasmic loop<sup>47</sup>. P7 is often incompletely cleaved from E2, resulting in a mixture of E2-p7 proteins whose specific function, if any, remains unknown. Although not required for RNA replication *in vitro*<sup>48</sup>, studies have demonstrated that p7 is critical for infectivity of HCV *in vivo*<sup>49</sup>. This is further supported by functional data obtained from the p7 of the related pestivirus, BVDV, which indicate that p7 is necessary for the generation of infectious virions in cell

culture<sup>50</sup>. Based on its structural and membrane-permeability properties, the p7 protein is suggested to be an ion channel<sup>51; 52; 53</sup> and belongs the viroporin family. In fact, Griffin *et al.*<sup>51</sup> reported that recombinant HCV p7 proteins form hexamers and possess ion channel activity that could ultimately be blocked by amantadine, a known ion channel inhibitor. While detailed function of the p7 protein in the viral life cycle remains to be determined, its role in viral particle release and maturation is becoming increasingly apparent. In the future, the p7 protein may prove to be an attractive target for antiviral drug development.

#### 1.3.4 NS2

The biological function of the NS2 protein is still unclear. It appears that the C-terminal end of NS2, along with the N-terminal end of NS3, encodes for a  $Zn^{2+}$ -dependent metalloprotease<sup>54</sup> that is required for the proteolytic cleavage at the NS2-NS3 junction. It has been demonstrated that NS2 is not essential for HCV replication *in vitro*<sup>55</sup>, however, cleavage at the NS2-NS3 junction by this protease is a pivotal step in HCV replication *in vivo*, such that it is required to release the NS3 serine protease for downstream polyprotein processing in the nonstructural region. In BVDV, the absence of cleavage at this site is found in viruses that are non-cytopathic<sup>56</sup>. NS2 has also been shown to interact with NS3, although the precise role and functional significance of these NS2/NS3 interactions remain unknown. Clearly, this interaction represents an attractive antiviral target.

### 1.3.5 NS3

#### i) NS3-4A Serine Protease

The NS3 protein of the HCV genome is a multifunctional protein that encodes for protease activity, located in the N-terminal one-third end of the protein, and for RNA helicase/nucleoside triphosphatase (NTPase) activity, found in the C-terminal two-thirds portion of the protein. The NS3 protease is necessary for cleavage of the downstream protein junctions (NS4A/4B, NS4B/NS5A, NS5A/NS5B) into functional, individual viral proteins that can assemble into replication complexes, and has therefore been the focus of extensive studies. Several studies have confirmed that the NS3 protease contains the catalytic triad formed by the amino acid residues, His-1083, Asp-1107 and Ser-1165, characteristic of serine proteases<sup>57; 58; 59</sup>. The crystal structure of the protease domain alone<sup>60; 61</sup>, in complex with its NS4A cofactor<sup>62; 63; 64</sup>, and more recently, in complex with specific inhibitors<sup>65; 66; 67</sup>, have been solved by several groups. Based on the success of inhibitors targeting the protease enzyme of other viruses such as the human immunodeficiency virus type-1 (HIV-1), the NS3 serine protease emerged as a major target for the design of specific inhibitors. Initial efforts at designing specific inhibitors were challenging because of its unusually shallow substrate-binding site. The finding that NS3 protease is inhibited by N-terminal hexapeptide cleavage products<sup>68; 69</sup>, however, led to the discovery of several effective peptide inhibitors *in vitro*, including the molecules BILN 2061<sup>70</sup> and VX-950<sup>71</sup>.

## ii) NS3 Helicase

The NTPase/helicase activity associated with NS3 resides in the C-terminal 500 amino acid residues of the protein. Based on both structural and biochemical analysis, the HCV DExH/D-box helicase is a three-domain protein whose putative biological role is to assist in viral replication by unwinding double-stranded replication intermediates, displacing proteins from the RNA genome, and/or removing regions of RNA secondary structures (Reviewed in Kwong *et al.*<sup>72</sup>). In fact, Lam *et al.*<sup>73</sup> have recently provided conclusive evidence that shows the absolute requirement for RNA unwinding by the NS3 helicase during viral replication in cells. Domains 1 and 2 of the NS3 helicase share several conserved motifs characteristic of superfamily 2 helicases, while Domain 3 is a novel domain that does not contain motifs conserved with other helicases<sup>74</sup>. To initiate unwinding, the NS3 helicase requires a single-stranded region with a 3'-end overhang strand, and is able to separate DNA/DNA, RNA/RNA and RNA/DNA duplexes. The associated NTPase activity is believed to fuel the energy needed for unwinding through NTP hydrolysis, or more specifically, ATP hydrolysis (Reviewed in Borowski *et al.*<sup>75</sup>). Although both the protease and helicase activities of NS3 can be expressed independently, very little evidence suggests that they are separated during the viral life cycle. Aside from its role in viral replication, NS3 also has been found to interact with several cellular proteins including TBK1<sup>76</sup>, protein kinase A and C, p53, and histones H2B and H4. The biological relevance of these interactions remains to be determined (Reviewed in Tellinghuisen *et al.*<sup>77</sup>).

### 1.3.6 NS4A/NS4B

The NS4A protein acts as an essential cofactor for the NS3 serine protease. With its central domain directly implicated in interacting with NS3, NS4A markedly increases the conformational stability of the protease by orientating its catalytic residues in an optimal orientation, as well as contributes to the formation of the protease substrate binding site<sup>62; 78</sup>. NS4A also recruits the NS3 protease to the ER membrane and has been found to interact with both NS4B and NS5A<sup>79</sup>. It is hypothesized that these interactions are necessary for the formation of a viral replication complex.

Little is known about the function of the NS4B product other than it appears to induce a specific membrane alteration of the ER, referred to as an ER-derived membranous web that is suggested to serve as a platform for the formation of the HCV replication complex<sup>80</sup>. Direct evidence that this membranous web is the site of RNA replication and represents the replication complex was obtained by Egger *et al.*<sup>80</sup> who observed similar intracellular membrane alterations containing all the NS proteins, as well as the genomic HCV RNA, in replicon harboring cells. Further demonstration that NS4B interacts with NS5B and with NS5A strongly suggests that it is a component of the replication complex<sup>81</sup>. NS4B has also been found to contain a nucleotide binding motif (NBM) mediating GTPase activity that may be required for its membrane-altering ability<sup>82</sup>.

### 1.3.7 NS5A

The NS5A region codes for a phosphoprotein that exists as two phosphorylated forms, a basally phosphorylated form of 56 kDa and a hyperphosphorylated form of 58 kDa. Hyperphosphorylation of NS5A is dependent on the presence of other non-structural proteins, particularly NS4A<sup>83</sup>. To date, several kinases capable of phosphorylating NS5A have been identified and include AKT, MEK1, MKK6, cAMP-dependent protein kinase A- $\alpha$  and casein kinase II<sup>84</sup>. It has recently been proposed that the phosphorylation state of NS5A has a regulatory function in HCV RNA replication<sup>85; 86</sup>. In addition, NS5A is believed to be an essential component of the multi-protein replication complex and was shown to interact independently with all the non-structural proteins, including NS5B<sup>81; 87</sup>.

A definitive role of NS5A in HCV replication, however, is currently unknown. NS5A has been implicated in modulating the response to IFN- $\alpha$ . Studies first performed in Japan<sup>88</sup> described a correlation between mutations within a discrete region of NS5A, termed the interferon sensitivity determining region (ISDR), and increased sensitivity to IFN- $\alpha$  therapy. The plausible mechanism behind which NS5A mediates IFN- $\alpha$  resistance could be explained by its ability to disrupt the dimerization of PKR and thus interfere with PKR function, although these findings are deemed controversial. NS5A has also been shown to bind to a range of cellular signaling molecules including the growth factor receptor-binding protein 2 (Grb2), the SNARE-like protein hVAP-33, the apolipoprotein A1 (ApoA1), p53, and amphiphysin II, to name a few (Reviewed in Macdonald and Harris<sup>84</sup>). Through these interactions, NS5A can modulate all three MAPK signaling pathways, with varying cellular effects, as well as mediate both extrinsic and intrinsic

stimulated apoptosis (Reviewed in Macdonald and Harris<sup>84</sup>). Additionally, studies with subgenomic HCV replicons have shown that cell culture-adaptive mutations cluster mainly in the central portion of the NS5A protein<sup>89</sup>, indicating that NS5A is involved in viral replication, either directly or indirectly, through interactions with host regulatory factors. The physiological significance of many of these protein interactions remains to be determined and will, in turn, facilitate a better understanding of the critical role of NS5A in HCV replication.

### **1.3.8 NS5B**

Based on the primary amino acid sequence of the NS5B region, particularly its highly conserved Gly-Asp-Asp (GDD) amino acid motif, NS5B was predicted to act as an RNA-dependent RNA polymerase (RdRp). This prediction has subsequently been confirmed and the polymerase has been studied extensively both biochemically and structurally. Given its key role in viral replication, the polymerase is considered to be one of the most attractive targets for drug discovery efforts. The role of the polymerase in replication will be discussed in subsequent sections of the chapter.

## **1.4 The Viral Life Cycle**

Systems that support HCV replication *in vitro*<sup>90; 91; 92</sup> are only emerging now, 17 years after the discovery of the virus. Species-restriction of the hepatitis C virus, which has limited infection models to the chimpanzee<sup>93</sup> or immunodeficient mice carrying



engrafted human livers<sup>94</sup>, along with the inherent difficulties in culturing the virus, have made unraveling the details of HCV replication quite challenging. Since a great deal of information is known about other members of the *Flaviviridae* family, the use of different models systems have significantly contributed to a developing model of the steps involved in the HCV life cycle, as summarized in Fig. 2 below. It is only now with the development of the infectious JFH-1 cell-culture system that detailed analysis and confirmation of most of what is known about the viral life cycle can be made.

**Figure 2: HCV Life Cycle**

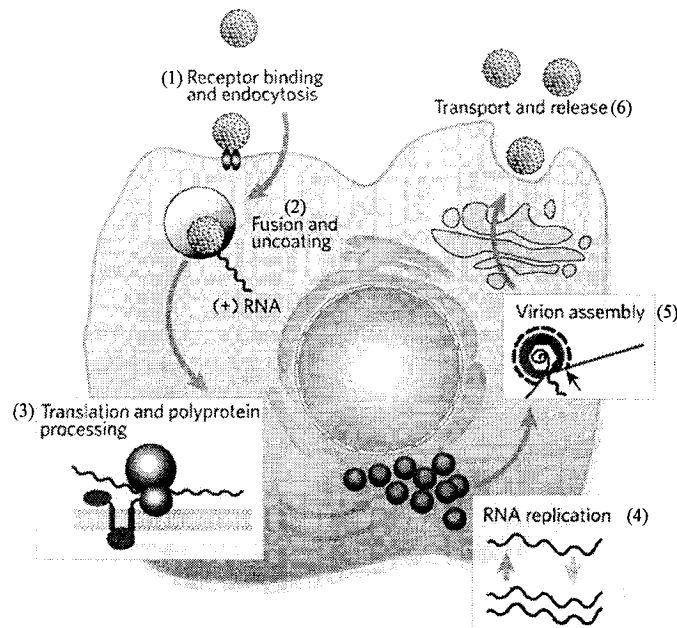


*Illustration of a hypothetical model of the HCV life cycle. Viral particles enter the cell, possibly through interaction with CD81 receptor and/or additional co-receptors (step 1). Upon viral entry and uncoating, the viral genome is released into the cytoplasm of the cell (step 2), where it carries out three main functions: as a messenger RNA (mRNA) for IRES-mediated translation of the viral polyprotein (step 3), as a template for viral*

*replication (step 4), and as a genome to be packaged within newly forming virions (step 5). Note that RNA replication occurs at the ER-membrane in a specific membranous web, where the viral proteins and/or additional host cell factors, form a replication complex. Newly assembled viral particles exit the cell via the Golgi (step 6). (Adapted from Lindenbach et al. <sup>95</sup>)*

#### **1.4.1 Attachment and Entry into Host Cells**

Infection begins with the attachment of a protein present at the surface of the virion to the surface of the host cell, a process that may require more than one type of receptor and/or co-receptor. Like most viruses, HCV takes advantage of many cellular proteins for viral entry into its host cell. The first such cellular factor to be identified, based on binding studies with the E2 envelope glycoprotein, is the human tetraspanin CD81<sup>39</sup>. CD81 is expressed on the surface of many different cell types and is involved in membrane-fusion processes, suggesting a role for CD81 in the fusion phase of viral entry. Although the involvement of CD81 in HCV viral entry has been confirmed by several groups<sup>39; 96; 97; 98; 99</sup>, the fact that ectopic expression of this molecule in non-hepatic cell lines does not lead to viral entry suggests that the virus requires additional molecules to gain entry into the cell. Among them is a second E2-binding protein, the human scavenger receptor class B type I (SR-BI)<sup>40; 96</sup>. SR-BI is predominantly high in hepatocytes and supports the hypothesis that HCV is a hepatotropic virus. Like CD81, additional studies are needed to determine the exact role of SR-BI in HCV entry and at what entry stage it is required. Several other candidate receptors for HCV have been

proposed including the mannose binding lectins DC-SIGN and L-SIGN, low-density lipoprotein (LDL) receptor, the asialoglycoprotein receptor (ASGPr) and glycosaminoglycans (Reviewed in Cocquerel *et al.*<sup>100</sup>).

#### **1.4.2 Translation and Polyprotein Processing**

Upon viral entry and uncoating, the viral RNA genome is released from the nucleocapsid into the cytoplasm of the host cell where it will carry out three main functions: as an mRNA for translation of the viral polyprotein, as a template for viral replication, and as a genome to be packaged within newly forming virions. Translation of the HCV genome is mediated by a high-ordered structure of about 340 nucleotides long located within the 5'UTR, termed the internal ribosome entry site (IRES). Three of the four highly structured domains (II, III, and IV) within the 5'UTR, together with the first 24 to 40 nucleotides of the core-encoding region constitute the IRES region. The HCV IRES binds directly to the host cell small ribosomal subunit (40S) in the absence of pre-initiation factors, and induces a conformational change that positions the AUG initiation codon in close proximity to or at the P-site of the ribosome<sup>101; 102</sup>. This complex, in turn, binds to the eIF 3 and to the ternary complex of Met-tRNA-eIF2-GTP, which eventually enables the formation of the translationally active ribosomal complex. This HCV IRES-mediated mechanism of translation is shared by other related viruses such as the GBV-B virus and the pestiviruses, BVDV and CSFV<sup>103; 104; 105</sup>. However, it is fundamentally different from initiation on encephalomyocarditis virus (EMCV), poliovirus and/or cellular mRNAs IRES elements, which appear to require the presence of additional eIFs

(Reviewed in Hellen and Sarnow<sup>106</sup>). Translation of the HCV genome results in the production of a single, long polyprotein precursor that is proteolytically cleaved by host and virally-encoded proteases to yield the individual structural and non-structural proteins.

A number of cellular factors have been shown to interact with the HCV IRES. These include the polypyrimidine-tract-binding protein (PTB), the human La antigen, the poly (rC)-binding protein 2 (PCBP2), the heterogeneous nuclear ribonucleoprotein L and ribosomal protein factors S9. Although unclear, it is hypothesized that these proteins function by increasing the efficiency of translation by stabilizing secondary and tertiary IRES structures (Reviewed in Dasgupta *et al.*<sup>107</sup>). The HCV IRES is highly conserved compared to the rest of the genome and utilizes a mechanism for translation initiation that is distinct from most eukaryotic pathways thereby strengthening its validity as a potential target for drug development. In fact, RNA-based drugs such as ribozymes and antisense oligonucleotides targeting the HCV IRES are currently underway and show promising results in reducing HCV RNA translation and replication in cell culture<sup>107; 108</sup>. Although these approaches have shown limited efficacy *in vivo*, they do confirm the proof-of-concept that blockage of IRES-mediated translation can be important for the future development of antiviral therapy.

#### **1.4.3 RNA Replication Process**

The signals that induce a switch from translation to RNA replication are currently unknown, although it has been speculated that the binding of certain cellular factors (i.e.,

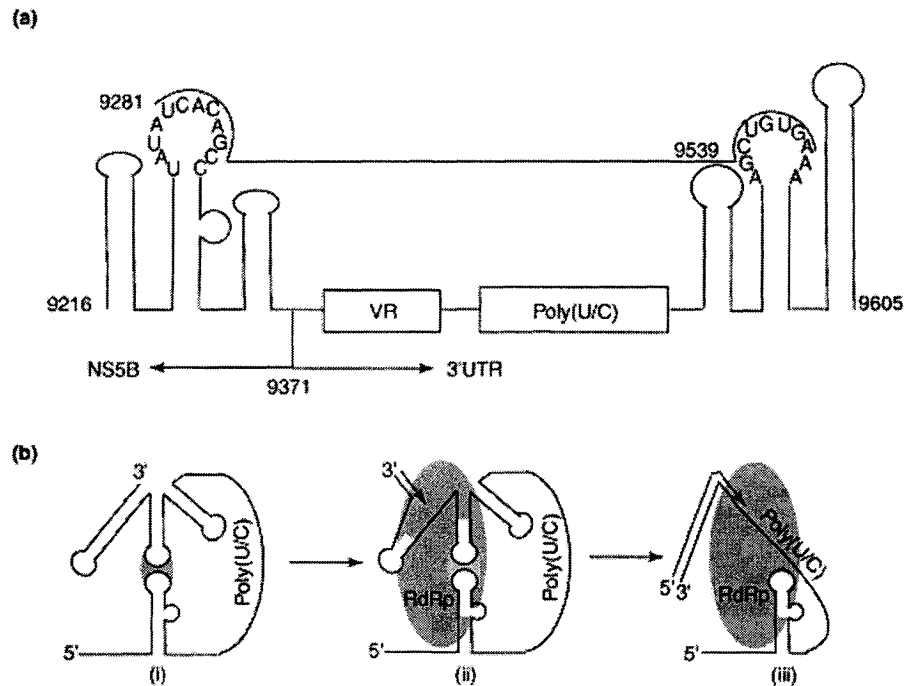
PTB) to both 5' and 3'UTRs may be important in modulating translation versus replication. The site of the replication process, as identified in replicon-containing Huh-7 cells, occurs at the ER-membrane in a specific membranous web. Here the viral proteins, along with the replicating RNA and host cell factors, form a membrane-associated replication complex that is analogous to other positive-strand RNA viruses<sup>109</sup>. The NS5B polymerase, which plays a key role in the replication process, then synthesizes a complementary minus-strand copy of the genome, which in turn, is used for the synthesis of additional genome-length RNAs. Genetic studies have revealed the requirement for CREs within the 3'UTR during RNA replication<sup>110</sup>. The 3'UTR of the HCV genome is composed of three main regions: a highly variable region, a polypyrimidine poly (U/UC) tract of variable length, and a highly conserved 98-nucleotide long region, designated as the X-tail. Three stem-loop (SL) structures have been identified in the X-tail region, designated SL1, SL2 and SL3 and are important for replication.

In addition to the 3'UTR, the core and NS5B encoding regions are also predicted to contain functional RNA elements. Through the use of computer-based secondary structure prediction programs and enzymatic and chemical probing, six SL structures were identified within the NS5B coding region by several groups<sup>111; 112; 113; 114</sup>; 5BSL1 (codons 111-128), 5BSL2 (codons 333-342) and the 5BSL3 cruciform (codons 539-591), which is folded into 4 RNA structures (i.e., 5BSL3.1, 5BSL3.2, 5BSL3.3 and 5BSL3.4). Subsequent mutational studies using the subgenomic replicon system revealed that 5BSL3.2 is indispensable for HCV replication<sup>114</sup>. Upon further analysis, Friebe and co-workers<sup>115</sup> demonstrated that the loop region of 5BSL3.2 can form important kissing-loop

interactions with the loop region of SL2 in the 3'UTR, and that this interaction involves a highly conserved sequence motif (CACAGC) within the upper loop of 5BSL3.2. These findings have resulted in the development of a model for the initiation of minus-strand RNA synthesis, which is summarized in Fig3. This model predicts that, through Watson-Crick base pairing between the loop region of 5BSL3.2 and that of SL2 in the 3'UTR, the 3' end of the genome folds into a closed loop formation which ultimately facilitates binding of the NS5B polymerase to the 3' end of the genome to initiate minus-strand synthesis<sup>110</sup>. Although not essential for replication *in vitro*, it cannot be excluded that the other predicted SL structures within the NS5B region may function in different stages of the HCV life cycle, like in RNA packaging and virion assembly.

It has been suggested that the formation of the kissing-loop interaction may require the presence of additional host cell factors. A series of cellular proteins have already been reported to bind to the 3'UTR<sup>116; 117; 118; 119; 120</sup>. In a recent study, Harris *et al*<sup>121</sup> identified more than 70 proteins and confirmed earlier findings that showed an association between the PTB protein<sup>116; 117</sup>, the La antigen<sup>119</sup>, the heterogeneous nuclear ribonucleoprotein C (hnRNP C)<sup>118</sup>, the HuR protein<sup>120</sup> and the 3' end of the HCV genome. Although the roles of these proteins in HCV replication have yet to be analyzed, possible mechanisms involve viral RNA stabilization, splicing, and regulation of host gene expression.

**Figure 3: Initiation of the RNA Replication Process**



(A) Schematic representation of the various stem-loop (SL) structures located at the 3'-end of the HCV RNA are important for virus replication. The SL-structures located in the coding region of NS5B (5BSL3.1, 3.2, 3.3) are separated from those present in the 3'UTR (SL I, II, III) by the variable region (VR) and the poly (U/C) tract. (B) Model for the initiation of minus-strand RNA synthesis. According to this model, the loop region of SL3.2 in NS5B forms important kissing-loop interactions with the loop region of SL2 in the 3'UTR (step i). This interaction allows the 3'end of the genome to fold into a closed loop formation, which facilitates binding of the NS5B polymerase to the 3' end of the genome to initiate minus-strand synthesis (steps ii and iii). Nucleotides and numbering correspond to the HCV1bCon1 (AJ238799) sequence. (Adapted from Seeger<sup>110</sup>).

#### 1.4.4. Virion Assembly and Release

Despite the significant advances made in elucidating the earlier steps of the HCV life cycle, the assembly of the viral genome, as well as the release of newly synthesized viral particles, is still poorly understood. The establishment of efficient systems that permit propagation of the virus in cells will aid in the establishment of these goals.

### 1.5 HCV Model Systems

For many years, progress in the HCV field has been hampered by the lack of a small animal model and/or a reliable cell culture system that can efficiently support viral replication. Since the discovery of the virus, a number of articles supporting cell lines as appropriate *in vitro* model systems for HCV have been published, but none with great acceptance as a robust model system for HCV replication. The discovery of the subgenomic replicon system in 1999 by Lohmann and coworkers<sup>48</sup> represented a milestone in HCV research. With it came the establishment of the infectious JFH-1 cell-culture system, which allows for the study of the complete viral life cycle *in vitro*. The following is a brief description of the different HCV model systems that led up to the development of the JFH-1 system.



### 1.5.1 Primary Cell Cultures and Cell Lines

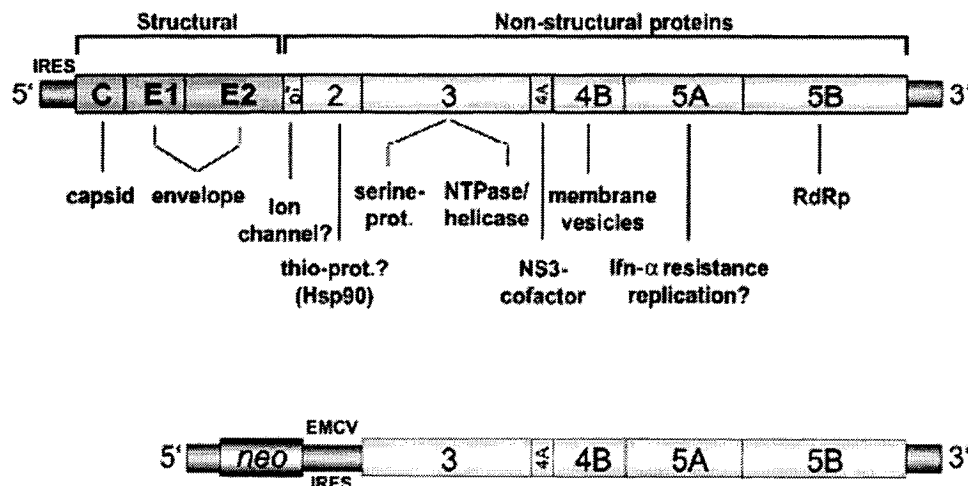
Initial attempts in establishing efficient systems to propagate HCV *in vitro* included the infection or transfection of cultured cells. Seeing how the chimpanzee is the only animal that can reliably be infected with HCV, several groups used primary chimpanzee hepatocytes or primary human hepatocytes that were either infected *ex vivo* or isolated from chronically infected patients to propagate HCV in cell culture. Despite evidence for short-term viral replication, these systems were clearly limited by the availability of cells, poor reproducibility, and low levels of viral titre (Reviewed in Bartenschlager and Lohmann<sup>122</sup>). These limitations, combined with the difficulty in maintaining human hepatocytes in a differentiated form within a culture system, led researchers to seek support for HCV replication in immortalized human hepatocyte-based cell lines. Some of the most detailed studies have been conducted with PH5CH cells, a cell line derived from normal human hepatocytes immortalized by transfection with simian virus 40 (SV40) large T antigen. In these studies, evidence for HCV replication was based on the prolonged detection of positive-strand HCV RNA for more than 100 days of culture, and on the strong selection of distinct variants, as determined by analysis of the HCV sequence in the E2 protein<sup>123; 124</sup>. However, the recurrent findings of limited HCV replication, along with the inconsistency and irreproducibility of results, limited the use of these cells as an accepted model for HCV replication. The majority of other cell lines studied for infection by HCV included human B or T cell lines, in particular Daudi cells, MOLT-4, MT-2 and HPB-Ma (Reviewed in Bartenschlager and Lohmann<sup>122</sup>).

### 1.5.2. The Replicon System

Improvements in the development of a cell-based system for HCV production were largely based on the transfection of *in vitro* transcribed HCV RNA into the human hepatoma cell line Huh-7. The transfection of cultured cells with cloned viral DNA or with *in vitro* transcripts offers several advantages; it avoids the potential block of infection at the level of viral entry, and the inoculum (i.e., *in vitro* transcribed RNA genome) is usually well-defined, available in large quantities, and can be manipulated for genetic analysis of viral functions. A major breakthrough came in 1999, with the establishment of the HCV subgenomic replicon system by Lohmann and coworkers<sup>48</sup>. The prototype replicon was derived from the consensus genotype 1b clone termed Con1, isolated from the liver tissue of a chronically infected patient. As depicted in Figure 4, the replicon RNA was modified such that the structural region of HCV, from the core to p7 or to NS2, was replaced by a gene encoding for the selectable marker neomycin phosphotransferase (*neo*). The resulting replicon was bicistronic such that expression of the *neo* gene was directed by the HCV IRES, while expression of the HCV nonstructural proteins (NS3-NS5B) was directed by the EMCV IRES, located downstream of the *neo* gene. Initial transfection of replicons into Huh-7 cells led to the selection of a low number of colonies resistant to neomycin sulfate (G418), containing self-replicating HCV RNA. Upon further analysis, it was determined that certain single amino acid substitutions, referred to as cell-culture adaptive mutations, increased the efficiency of replication by more than 10<sup>5</sup>-fold<sup>125; 126; 127</sup>. These conserved mutations were found in every non-structural protein, although most appeared to cluster in the central region of

NS5A<sup>128</sup>. The exact function of these mutations is currently unknown, although it has been suggested that they may directly or indirectly affect interactions with host cell factors. Interestingly, Bukh *et al.*<sup>129</sup> found that the replication efficiency of replicons with adaptive mutations are highly attenuated in chimpanzees, leading to the conclusion that although cell culture adaptive mutations are required for viral replication *in vitro*, they are lethal for virus production. It is unclear how these mutations preclude infectious particle production.

**Figure 4: Comparison of the HCV genome and subgenomic replicon system**



*Schematic representation of the HCV genome organization (top) and the structure of the HCV subgenomic replicon (bottom). The original replicon RNA was modified such that the structural region of HCV, from the core to p7 or to NS2, was replaced by the neo gene encoding for neomycin phosphotransferase. The expression of the HCV nonstructural proteins (NS3-NS5B) is directed by the EMCV IRES, located downstream of the neo gene, while the expression of the neo gene is directed by the HCV IRES located in the 5'UTR. (Adapted from Bartenschlager *et al.*<sup>130</sup>).*

Since its discovery, the replicon system has been improved substantially giving rise to the development of a large number of replicons including replicons derived from genotypes 1a<sup>131; 132</sup> and 2a<sup>133</sup>, full-length replicons<sup>134</sup>, systems expressing easily quantifiable marker enzymes (i.e., firefly luciferase)<sup>126</sup>, as well as systems that can track functional replication complexes in living cells through the insertion of green fluorescent protein (GFP) in NS5A<sup>135</sup>. Amplification of HCV RNA has also been expanded to other host cells including HeLa epithelial cells and mouse hepatoma cells<sup>136</sup>.

### 1.5.3. The JFH-1 System

Despite these significant improvements, the replicon system still does not permit analysis of the complete viral life cycle. Substantial progress has been made, however, with the development of the infectious JFH-1 cell culture system by Wakita *et al.*<sup>91</sup>. The JFH-1 system is derived from a genotype 2a replicon, isolated from the serum of a Japanese patient with fulminant hepatitis C<sup>133</sup>. Transfection of *in vitro* transcribed full-length JFH-1 RNA sequences in Huh 7 cells was shown to result in the secretion of viral particles that could be passed in cell culture, and that were infectious in both chimpanzee and mouse animal models, thereby confirming the authenticity of HCV grown in cell culture<sup>91; 92; 137</sup>. Improved colony formation and high efficiency RNA replication of the JFH-1 replicon has been demonstrated not only in Huh 7 cells, but also in other liver-derived cell lines such as HepG2 and IMY-N9<sup>138</sup>, as well as non-hepatic cell lines such as HeLa and HEK293<sup>139</sup>. Interestingly, replicons derived from JFH-1 cDNA cells do not require adaptive mutations for efficient replication *in vitro*<sup>91</sup>.

The development of a robust cell culture system for HCV infection is definitely a major breakthrough in HCV research. The JFH-1 system has already been proven invaluable by enabling researchers to study the different aspects of the virus life cycle including viral entry, cytoplasmic release, the assembly of viral particles, and host-virus interactions. Additionally, the JFH-1 system facilitates the comparison between replicons of distinct genotypes<sup>140</sup>. It has been suggested that patients infected with HCV of different genotypes have different clinical profiles and responses to antiviral treatment. Genotypes 2 and 3 are susceptible to IFN- $\alpha$ , while genotype 1 has a lower response rate to interferon-based therapies<sup>141</sup>. Comparisons between replicons of distinct genotypes can help determine the mechanisms of viral persistence. In the future, the establishment of such a novel cell culture system will not only contribute to the current understanding of the basic HCV biology, but will also reveal new aspects of HCV replication, facilitate the development of specific antiviral compounds that inhibit unexplored targets, and contribute to the development of an effective HCV vaccine.

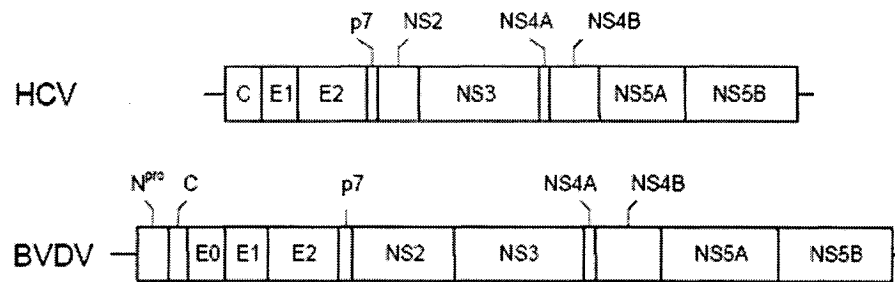
#### **1.5.4. BVDV**

As mentioned above, recent advances now permit the study of the complete life cycle of HCV in cell culture<sup>90; 91; 92</sup>. Nonetheless, surrogate viruses such as BVDV are still often applied as valuable model systems for HCV replication, and to study the activity of inhibitors for use against HCV<sup>142; 143</sup>. Even with the development of robust HCV cell culture systems, insights into the mechanism of inhibition of anti-BVDV compounds provide important information for the development of novel HCV inhibitors

and for the study of the mechanisms of drug action and drug resistance (Reviewed in Buckwold *et al.*<sup>144</sup>).

The pestivirus BVDV, a major pathogen of cattle, belongs to the *Flaviviridae* family of positive-strand RNA viruses and is closely related to HCV<sup>145</sup>. Due to the action of the virus in cell culture, BVDV is divided into cytopathic (cp) and noncytopathic (ncp) strains<sup>56</sup>. The viral genome is approximately 12.5 kb in size and varies in length between cp and ncp isolates, due to the insertion of cellular sequences, large in-frame deletions, or gene rearrangements. These genomic rearrangements result in the processing of the NS2/3 polypeptide into individual, mature NS2 and NS3 proteins, correlating with cytopathogenicity in BVDV-infected cells. In cells infected with ncp BVDV, cleavage at the NS2/3 site does not occur and the NS2-3 gene is expressed as a read-through product<sup>56; 146</sup>. Like HCV, the BVDV genome consists of a large ORF with UTRs at both the 5' and 3' ends, and codes for functionally equivalent gene products, as depicted in Figure 5. IRES-mediated translation of the BVDV genome yields a single polypeptide represented by NH<sub>2</sub>-N<sup>pro</sup>-C-E0-E1-E2-P7-NS2-NS3-NS4A-NS4B-NS5A-NS5B-COOH. This polypeptide is subsequently cleaved to give rise to four structural (C, E0, E1, and E2) and six nonstructural (NS2-NS5B) proteins. The N-terminus of the pestivirus polypeptide consists of two additional proteins, N<sup>pro</sup> and E0, which are not found in HCV. N<sup>pro</sup> is an autoprotease that functions to release the core protein by autoproteolysis, while E0 or E<sup>ns</sup> is an additional envelope glycoprotein with ribonuclease (RNase) activity (Reviewed in Lindenbach and Rice<sup>145</sup>).

**Figure 5: Comparison of the structural organization of the HCV and BVDV genome**



*Schematic representation of the HCV (top) and BVDV (bottom) genome organization. Both genomes encode for a single polyprotein that is processed into structural (C-p7) and non-structural (NS2-NS5B) proteins by means of viral and host proteases. The N-terminus of the pestivirus polyprotein consists of two additional proteins, N<sup>pro</sup> and E0, which are not found in the HCV polyprotein. N<sup>pro</sup> functions as an autoprotease, while E0 (also known as E<sup>ns</sup>) is an envelope glycoprotein with associated RNase activity. (Adapted from Buckwold et al.<sup>144</sup>).*

In addition to the fact that HCV and BVDV share similarities in terms of their genomic organization and mode of polyprotein translation and processing, the viruses also share conserved motifs within the 5'UTR, NS3, and NS5 regions, all of which are considered to be major targets for HCV antiviral drug development. These similarities, along with the fact that BVDV has a well-established cell culture system with common strains readily available from the American Type Culture Collection (ATCC), makes BVDV an important and widely utilized surrogate virus to study HCV replication and identify specific inhibitors. Several studies have demonstrated how specific NS5B

inhibitors have already been discovered using BVDV<sup>142; 147; 148; 149</sup>. For instance, Baginski *et al.*<sup>142</sup> identified the compound VP32947 as an effective inhibitor of BVDV replication in cell culture. *In vitro* selection of drug resistance conferring mutations located in the NS5B coding region provides strong evidence to show that this compound antagonizes the function of the polymerase. Similarly, by screening a nucleoside library with the BVDV cell culture system, Stuyver *et al.*<sup>147</sup> identified the base-modified ribonucleoside analogue, b-D-N4-hydroxycytidine (NHC) as an inhibitor of both BVDV and HCV RNA production. Although the exact mechanism of inhibition remains elusive, the authors hypothesize that NHC acts as a weak alternative substrate for the viral polymerase. The cyclic urea derivative compound-1453 was also identified and characterized as a specific inhibitor of BVDV replication<sup>148</sup>. Viruses resistant to this compound contain a specific mutation mapped to the NS5B polymerase. Compound-1453 also directly inhibited BVDV RNA polymerase activity in a membrane-based assay, suggesting that it specifically targets the NS5B replicase and affects the activity of the polymerase complex<sup>148</sup>. Recently, a highly selective inhibitor of pestivirus replication, BPIP, was reported<sup>149</sup>. Identification of a drug resistance conferring mutation in the viral RdRp strongly suggests that this compound interferes with viral polymerase activity. Structural analogues of this molecule were also found to exhibit anti-HCV activity, thereby implicating how distinct changes to a class of inhibitors of pestivirus replication may result in molecules with anti-HCV activity. The agreement between the activities of other inhibitors of the HCV and BVDV polymerases, however, is still unknown and remains an important area for future studies, especially since the NS5B protein is an important target for the development of novel antiviral inhibitors against HCV. The remainder of the



chapter will focus on the role of the HCV polymerase in replication, highlight some of its interesting features both structurally and biochemically, as well as compare it to other well-characterized RdRps, in particular to the BVDV RdRp.

## **1.6 The Viral RNA-dependent RNA polymerase**

### **1.6.1 Biochemical Characteristics of Recombinant NS5B**

Initial studies aimed at characterizing the NS5B protein of the HCV genome involved the expression of active recombinant protein from bacterial or insect cells. Progress in this area, however, appeared to be quite challenging. The first active recombinant NS5B protein was reported only 7 years after the identification of the HCV genome. In their study, Behrens and coworkers<sup>150</sup> expressed an untagged, full-length NS5B protein of HCV genotype 1b using a baculovirus expression system. The extraction and purification of this untagged NS5B, however, required the use of high concentrations of salts, glycerol, and non-ionic detergent. The expression of histidine-tagged NS5B in insect cells followed shortly thereafter<sup>151</sup>, along with the generation of active NS5B protein in bacterial cells, expressed as either GST fusion, affinity-tagged at the N- or C-terminus, full-length or C-terminal truncated forms of the protein<sup>151; 152; 153; 154; 155; 156; 157</sup>. Many of these modifications resulted in soluble and easily purified protein. Some of the difficulties in expressing, purifying, and studying recombinant NS5B can be attributed to the insoluble and inactive nature of the full-length protein. NS5B contains a hydrophobic C-terminal transmembrane domain of 21 amino acids and belongs to a class

of membrane proteins termed tail-anchored proteins<sup>158; 159; 160</sup>. Through the use of several different experimental approaches, it has been demonstrated that this C-terminal domain crosses the ER membrane phospholipid bilayer as a transmembrane segment. Expression of the truncated NS5B protein in mammalian cells revealed that the C-terminal truncation altered the localization pattern of the protein<sup>153</sup>. Although essential for anchorage to the perinuclear membrane and for HCV replication in cells<sup>160; 161</sup>, deletion of this C-terminal hydrophobic domain increases the solubility of the NS5B recombinant protein without compromising RdRp activity *in vitro*<sup>153; 154</sup>. In fact, enzymatic activities of various full-length and truncated forms of NS5B have been demonstrated using both homopolymeric and heteropolymeric RNA templates<sup>150; 151; 153; 154; 162</sup>. This reported lack of specificity for HCV genomic sequences *in vitro* suggests that additional viral proteins and/or host cellular factors are required to mediate specific interactions between the polymerase and the viral RNA genome *in vivo*. These interactions may also be essential in maintaining optimal polymerase activity. For instance, experiments conducted by Carroll *et al.*<sup>163</sup> demonstrated that only a small fraction of purified NS5B recombinant protein was active and capable of processive synthesis, especially when compared to the catalytic efficiency observed for the poliovirus polymerase (3D<sup>pol</sup>) and HIV-1 RT. Interaction of NS5B with other non-structural proteins, in particular, NS3, NS4A and NS5A have been described and proven to modulate RdRp activity in various ways<sup>87; 164</sup>. Shiota *et al.*<sup>87</sup> reported a dose-dependent inhibitory effect of NS5A on RdRp activity, due to the direct interaction between NS5A and NS5B through two binding regions of NS5A. Mutational analysis further demonstrated that these two regions in NS5A are indispensable for HCV replication in the HCV replicon system, suggesting a modulating role of NS5A for RdRp

activity in HCV replication<sup>165</sup>. In another report, interaction of NS5B with NS3 and NS4B has been described to have both positive and negative modulatory influences on RdRp activity, respectively<sup>166</sup>. In addition to its interactions with other non-structural proteins, NS5B has been shown to interact with itself to form functional oligomers. Oligomerization of NS5B has been detected both *in vitro* and in mammalian cells<sup>167; 168</sup>. Using various biochemical methods including chemical cross-linking, gel filtration and yeast two-hybrid system, Wang *et al.*<sup>167</sup> demonstrated the ability of NS5B protein to form an oligomeric complex, and identified several potential amino acid motifs condensed at two interfaces of the polymerase that are critical for oligomerization. Subsequent mutational analyses by Qin *et al.*<sup>168</sup> identified two amino acid residues, Glu18 and His502, which are important for NS5B protein-protein interactions and for RdRp catalytic activity. Based on these results, the authors hypothesized that the low catalytic efficiency of the polymerase observed *in vitro* can be explained by interactions between inactive NS5B proteins and active enzyme forms. Finally, several groups have reported specific interactions between NS5B and a number of host cellular proteins including a SNARE-like protein (hVAP-33)<sup>169</sup>, cyclophilin B<sup>170</sup>, eIF4AII<sup>171</sup>, protein-kinase C-related kinase 2 (PRK2)<sup>172</sup>, p68<sup>173</sup> and nucleolin<sup>174; 175</sup>. All of these interactions were shown to modulate RdRp activity which may, in turn, affect HCV replication. An important interaction is that mediated between NS5B and PRK2, the cellular kinase responsible for phosphorylation of NS5B. Although NS5B phosphorylation was shown to have a positive effect on HCV replication in replicon-containing cells<sup>172</sup>, the mechanisms by which phosphorylated NS5B regulates HCV replication are still largely unknown. Subsequent experiments are required to determine the specific phosphorylation site(s) on NS5B, and

to establish the possible mechanisms by which phosphorylation modulates RdRp activity. It is possible that the specific interactions mentioned earlier with viral and/or cellular proteins, and the oligomerization of NS5B may be influenced by NS5B phosphorylation or by a phosphorylation-induced conformational change in the enzyme.

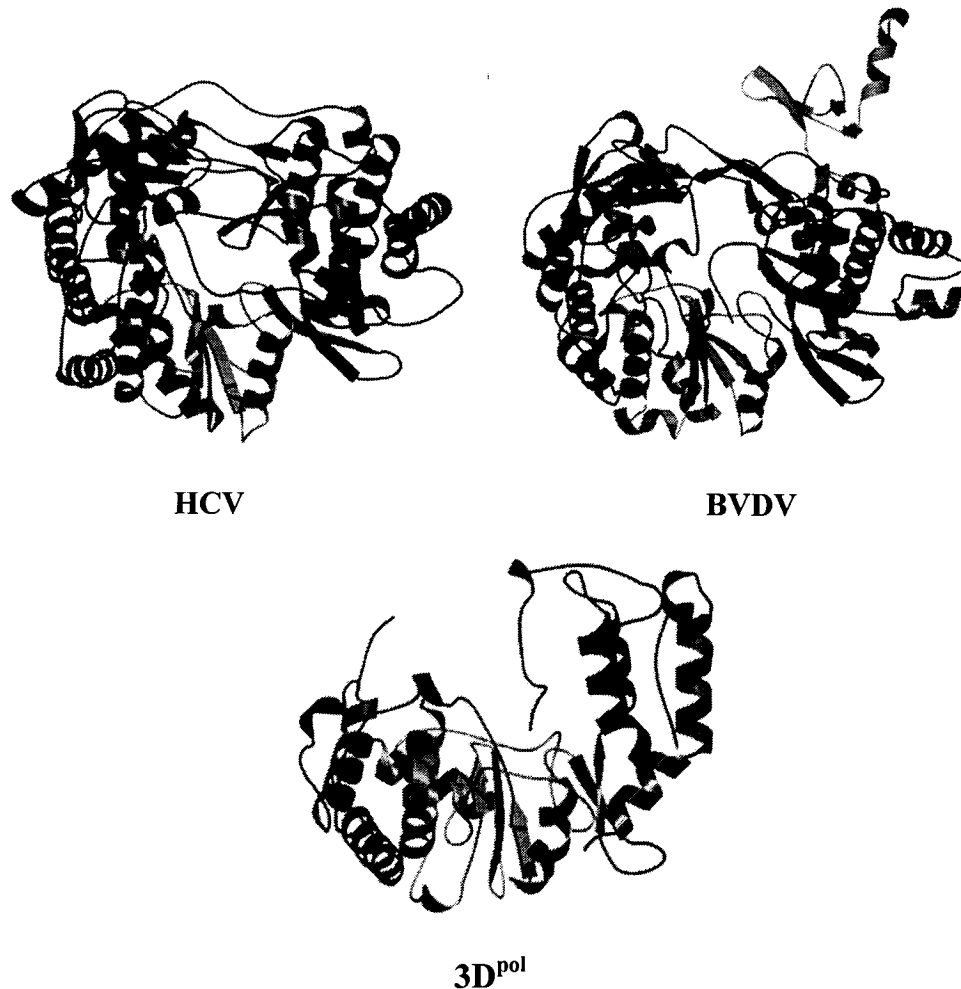
In addition to RdRp activity, NS5B has been reported to possess terminal transferase activity (TNTase), the ability to catalyze the addition of nontemplated nucleotides to the 3'-end of RNA<sup>150, 176</sup>. This activity was originally believed to result from cellular enzyme contaminants present in purified NS5B enzyme preparations<sup>151,156; 177</sup>. However, subsequent experiments later provided evidence to show that TNTase activity is indeed an inherent property of not only HCV RdRp, but also of BVDV polymerase<sup>176</sup>. Whether this property is essential for replication *in vivo* remains to be established. It has been suggested that TNTase is utilized by RNA viruses as a mechanism to maintain the integrity of the ends of their viral genomes, which contain the sequences required for initiation of RNA synthesis. In agreement with this is the observation that HCV polymerase-dependent TNTase activity was able to restore the ability to initiate RNA synthesis on an initiation-defective RNA template<sup>176</sup>.

### **1.6.2 Structural Features of RdRps**

As noted above, the availability of soluble forms of the HCV NS5B protein permitted detailed biochemical characterization of the HCV polymerase. Despite this, a number of unanswered questions still remained; questions about the processes of

initiation and elongation, and about unique structural features of the HCV polymerase that can be targeted for drug development. Insights to these questions were made possible by detailed structural analyses of the HCV polymerase.

**Figure 6: Comparison of RdRp crystal structures**



*Structures of HCV, BVDV and poliovirus RdRps resemble a right hand with fingers (blue), palm (green), and thumb (red) domains. The N-terminal region of the BVDV RdRp structure is colored yellow. Note that the fingers domain of the poliovirus polymerase is mostly disordered. (Adapted from Choi et al.<sup>178</sup>).*

The three-dimensional crystal structure of the HCV polymerase of genotype 1b, with or without an incoming nucleotide, has been reported by several groups<sup>179; 180; 181; 182; 183</sup> and has led to the understanding of the overall structure of the enzyme and the architecture of its active site. In all reported structures and as displayed in Figure 6 above, the HCV NS5B contains the classic palm, fingers and thumb structural domains, characteristic of all known RNA and DNA polymerases. Unlike the open structures of most DNA polymerases, such as the Klenow fragment from *Escherichia coli* (*E.coli*) and HIV-1 RT<sup>184</sup>, extensive interactions between the fingers and the thumb domains allows the HCV polymerase to form a fully encircled active site to which the RNA template and NTP substrates access through two positively charged tunnels<sup>180</sup>. This closed catalytic pocket is not unique to HCV, and has also been identified as an unique feature of BVDV<sup>185</sup> and bacteriophage phi6<sup>186</sup> polymerases.

In HCV NS5B, this closed conformational state is attributed to the  $\Lambda$ 1-loop that extends from the fingers to the thumb domain and suggests the possibility of a concerted movement between the two domains during enzyme translocation<sup>187</sup>. In their study, Labonte *et al.*<sup>187</sup> showed by analytical ultracentrifugation experiments that substitution of the amino acid residue Leu30 by serine or arginine impairs the ability of the thumb domain to remain in a closed conformation, due to a local perturbation in the  $\Lambda$ 1-loop. This, in turn, resulted in a non-functional protein and gave rise to the idea that the HCV RdRp can adopt both “open” and “closed” conformational states. Further structural evidence for the existence of two conformations of NS5B came from the elucidation of the crystal structure of HCV RdRp from genotype 2a<sup>188</sup>. Structures of two crystal forms

of the enzyme were described; a “closed” conformation that is believed to be the active form of the enzyme, and an “open” conformation that is inactive. More importantly, the authors revealed that the conformation of an NS5B-inhibitor-bound structure resembled that of the “open” (inactive) form of the polymerase. In this inactive form, movement of the  $\Lambda$ 1-loop from the thumb domain, due to inhibitor binding, reduced fingers-thumb interactions, and thus caused the enzyme to adopt an “open” form. Overall, these studies provide evidence that the  $\Lambda$ 1-loop is indeed responsible for determining the active state of HCV polymerase.

As in other known polymerases, the catalytic core of HCV NS5B is located within the palm domain and is conserved in virtually all polymerases. The palm domain contains 5 of the 8 conserved sequence motifs; motifs A, B, C and D are found in all classes of polymerases, while motif E is unique to RTs and RdRps. These motifs are both catalytic and structural, and contain highly conserved residues that carry out specific functions such as metal ion coordination and sugar selection (Reviewed in O'Reilly and Kao<sup>189</sup>). Of importance is the highly conserved GDD sequence located in motif C that is absolutely required for catalytic RdRp activity. Interestingly, motif D contains a lysine at position 345. This amino acid residue is found in all RTs and nearly all classes of polymerases, except for HCV NS5B, where it is replaced by an arginine. Mutational analysis revealed that substitution of this arginine to a lysine in HCV NS5B created an enzyme that exhibited a 52% increase in RdRp activity compared to wild-type enzyme *in vitro*<sup>151</sup>. The basis for this stimulation is currently unknown, although the presence of an arginine residue which reduces RdRp activity may help explain the low levels of HCV replication

observed in infected cells. Finally, the palm domain contains two conserved aspartic acid residues (Asp220 and Asp318) that chelate two divalent metal ions and are essential for polymerization. The metal ions are positioned such that they are involved in the precise alignment of the primer and incoming nucleotide, thereby supporting the two-metal ion mechanism of catalysis<sup>190</sup>.

The thumb domain, consisting of the C-terminal region, is the most diverse feature among the polymerase structures. In HCV, the thumb domain contains a novel structural feature referred to as the  $\beta$ -hairpin<sup>179; 180; 181</sup>. It is composed of 12 amino acid residues and protrudes toward the active site of the polymerase, imposing steric hindrance that restricts binding to double-stranded RNA structures. This unique feature is suggested to be involved in ensuring terminal initiation of RNA synthesis by correctly positioning the 3'-end of the template at the active site. Supporting this hypothesis are experiments showing that shortening of the  $\beta$ -hairpin by 8 amino acids did not disrupt RdRp activity *in vitro*, but did allow for increased internal initiation from pre-annealed duplex RNA<sup>191</sup>. Interestingly, truncations of the  $\beta$ -hairpin were shown to completely abolish viral replication in replicon-containing cells, demonstrating its essential role in viral replication *in vivo*<sup>192</sup>. On the basis of these findings, it was also concluded that a positional shift of the  $\beta$ -hairpin is necessary to accommodate the elongation of the nascent double-stranded RNA product. Despite this shift, the  $\beta$ -hairpin is believed to maintain contact with the template substrate and act as a “flap” that positions the substrate in the correct orientation during elongation. A structural element known as the  $\beta$ -thumb region has also been identified in the thumb domain of BVDV, and is proposed



to play a similar role as the  $\beta$ -hairpin in HCV NS5B in allowing only single-stranded RNA to access the active site<sup>185</sup>. In contrast, poliovirus 3D<sup>pol</sup>, which initiates RNA synthesis through priming with the viral Vg protein, lacks an analogous loop and contains a wider template channel that can accommodate binding to a template/primer complex during initiation<sup>191; 193</sup>. Along with the  $\beta$ -hairpin, a regulatory motif in the C-terminal tail of RdRp, just upstream of the membrane anchor domain, is buried within the putative RNA binding region and may also function in regulating initiation<sup>194</sup>.

Another notable feature of the HCV RdRp is the recently identified low affinity GTP-binding site located 30Å away from the active site of the polymerase, at the interface between the fingers and thumb domain<sup>182</sup>. The functional role of this GTP-binding pocket is currently unknown, although it is speculated that binding of GTP to this site serves as a conformational switch between the initiation and elongation of RNA synthesis<sup>182</sup>. Further mutational analysis of the amino acid residues defining this GTP-binding pocket revealed that the mutants catalyzed RNA synthesis as efficiently as wild-type enzyme *in vitro*, but either impaired or completely abolished HCV RNA replication in the cell-based replicon system<sup>178</sup>. Based on these results, the authors suggested that the binding of GTP to this site may modulate the structure of the polymerase to allow for efficient interactions with viral and/or cellular proteins involved in the formation of the replication complex. Unfortunately, no conformational change was observed in the crystal structure of HCV NS5B bound to GTP, suggesting that the presence of RNA may be required for this change to occur. Crystallographic data has also pointed to the existence of a GTP-specific binding site (G-site) in BVDV NS5B, located ~ 4 to 6Å

upstream of the active site of the polymerase<sup>185</sup>. Based on structural comparisons between the BVDV RdRp-GTP complex, and related polymerases with an RNA template, it has been suggested that the 3'-hydroxyl group of the bound GTP helps position the initiating nucleotide in a favorable orientation that facilitates its attack on the first nucleotide substrate<sup>185</sup>. Notably, the requirements for high concentrations of GTP in both HCV and BVDV enzymes, as well as GTP binding to the GTP-specific binding site appear to mediate important yet different functions during viral replication. The exact nature of these functions is an area that remains to be largely explored.

### **1.6.3 *De Novo* Initiation Mechanism by RdRps**

Initiation is one of the most critical and complex steps in the replication of viral genomes, especially since the precise terminal sequences have to be strictly maintained. Many viruses have evolved mechanisms such as primer-dependent and *de novo* synthesis through which precise terminal initiation is ensured. Primer-dependent initiation of RNA synthesis is used *in vivo* by many polymerases including the poliovirus 3D<sup>pol</sup>, where the viral VPg protein covalently linked to the terminal end of the genome, acts as a primer to which the polymerase adds nucleotides in a template complementary manner<sup>193</sup>. Polymerases of RNA viruses such as bacteriophage phi6<sup>186</sup>, HCV<sup>177; 195; 196; 197; 198; 199</sup>, and BVDV<sup>200; 201</sup>, however, have been reported to initiate RNA synthesis *in vitro* by both primer-dependent and primer-independent (*de novo*) mechanisms. *De novo* initiation of RNA synthesis by the HCV polymerase has been detected when utilizing either RNAs derived from the HCV 3'UTR<sup>196; 199</sup>, full-length HCV RNA genome<sup>177</sup>, and nonviral or

homopolymeric RNAs<sup>195; 197</sup> as templates. According to the *de novo* initiation model of RNA synthesis, complementary RNA is initiated at the 3'-end of the genome where the initiating nucleotide (NTPi), rather than a protein or oligonucleotide primer, provides the 3'-hydroxyl group for nucleotidyl transfer to a second NTP.

The initial focus of many studies was to identify essential features in the RNA template and/or the NS5B polymerase required for initiating RNA synthesis *de novo*. It has been determined that RdRps have a specificity for cytidylate as the preferred template initiation nucleotide, although the preferred position in the template can significantly differ among viruses<sup>195; 202</sup>. HCV RdRp directs synthesis strictly from the 3'-terminal cytidylate, while BVDV RdRp can use either the 3'-terminal or penultimate cytidylate<sup>196</sup>. Subsequent research further confirmed the specificity for initiation pyrimidines by HCV NS5B<sup>195; 197; 198; 199</sup>. Notably, the 3' end of both positive and negative strands of the HCV RNA genome starts with a pyrimidine followed by two purine bases. Such arrangements may be required to ensure that initiation occurs directly from the 3'-end of the genome<sup>203</sup>. Changes to nucleotides adjacent to the initiation cytidylate (i.e., at positions +2 and +3) were also shown effect *de novo* initiation. For instance, RNAs that contained deoxynucleotides at these positions were ineffective templates for RNA synthesis<sup>202</sup>. Like other polymerases, both HCV and BVDV RdRps require higher concentrations of the initiation nucleotide, with a preference for GTP as NTPi<sup>201; 202; 204; 205</sup>. In an attempt to further characterize the requirements for NTPi, Ranjith-Kumar *et al.*<sup>205</sup> examined whether several GTP analogs could substitute for NTPi during initiation *in vitro*. In contrast to BVDV and GBV RdRps, HCV RdRp was the most capable of accepting a range of GTP

analogues, and it was determined that the triphosphate portion of GTP was not essential for initiation of HCV RNA synthesis *de novo*. For instance, the lack of one or two phosphates in NTPi significantly increased HCV RNA synthesis, while the use of guanosine was able to initiate synthesis at approximately 80% compared to GTP. It was also shown that HCV RdRp can use short oligonucleotides as substitutes for NTPi<sup>206</sup>. These short oligonucleotides may be produced by the polymerase during abortive initiation. On the basis of these findings, it was concluded that the NTPi requirements for HCV RdRp seem to be less strict than those for BVDV RdRp, which was able to efficiently utilize only GTP for *de novo* synthesis<sup>205</sup>. The authors attributed this difference to the fact that cytidylate is the 3'-terminal nucleotide for both positive and negative strands of the BVDV RNA genome while for HCV, uridylate and cytidylate are present at the 3' termini of positive and negative strands respectively. The same group later went on to show that the presence of divalent metal ions, either  $Mn^{2+}$  or  $Mg^{2+}$ , can also affect the specificity of the initiation reaction. Although both metal ions were found to support *de novo* synthesis, the presence of  $Mn^{2+}$  significantly increased the amount of *de novo* initiated products by HCV and BVDV RdRps<sup>207</sup>. Overall, these findings highlight the fact that specific requirements for *de novo* initiation differ between viral RdRps.

Finally, several groups have reported the initiation of RNA synthesis *in vitro* by HCV NS5B through a copy-back mechanism<sup>150; 151</sup>. In the copy-back mechanism, templates adopt a hairpin conformation due to the presence of short complementary sequences at the 3'-end of the template which allows it to hybridize internally. The 3'-

end hydroxyl group of the template is then used as a primer for polymerization, leading to the synthesis of a double-stranded molecule in which the template and newly synthesized RNA product remain covalently linked. Copy-back elongation, however, is considered to be unique to *in vitro* experimental conditions. It is unlikely that this mechanism is used *in vivo* since it would lead to loss of terminal sequences, as well as require additional enzymatic functions to cleave the link between the template and newly synthesized RNA strand. Rather, based on the structure of RdRps, and on functional analyses of RNA synthesis of RdRps *in vitro*, it is generally accepted that *de novo* synthesis is the more biologically relevant mechanism of initiation for HCV replication. Several studies support this *de novo* initiation hypothesis. For one, *de novo* initiation has been reported to be the mechanism utilized for the replication of many plus-stranded RNA viruses, including the related bacteriophage phi6<sup>208</sup>. The presence of the  $\beta$ -hairpin near the catalytic pocket of HCV NS5B, which functions to correctly position the 3'-end of the template, provides part of the structural basis for *de novo* initiation<sup>180; 191</sup>. Additionally, the crystal structure of NS5B in complex with nucleotides reported the presence of three distinct nucleotide binding sites in the catalytic site of the HCV polymerase, whose geometry is remarkably similar to that observed in the *de novo* initiation complex of the phi6 polymerase, thereby yielding a credible model for *de novo* initiation of RNA synthesis<sup>182; 186</sup>. Despite this ample evidence supporting *de novo* synthesis, it is currently unknown at this time which mechanism is utilized by the virus to initiate replication in infected cells. Of importance is the demonstration that that poliovirus 3D<sup>pol</sup>, which is known to initiate *in vivo* with a primer, has also been shown capable of *de novo* initiation *in vitro* under special reaction conditions<sup>209; 210</sup>. This observation indicates that the

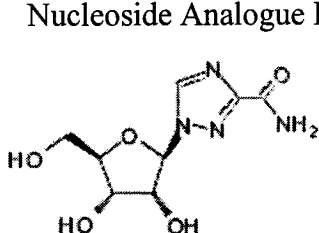
detection of *de novo* initiation *in vitro* does not establish it as a biologically relevant mechanism in infected cells. Clearly, additional experiments are required in determining the mechanism(s) and specificity of HCV RNA replication *in vivo*, which in turn, will aid in the identification of compounds that specifically target the replication process.

### **1.7 Nucleoside Analogue Inhibitors of HCV polymerase**

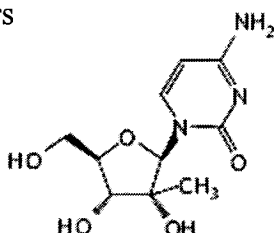
Prominent success in the use of polymerase inhibitors for the treatment of other viral infections (i.e., HIV-1, HBV and herpes viruses) has prompted extensive research efforts for the development of inhibitors targeting the enzymes responsible for HCV replication. Given that polymerase inhibitors are the largest class of approved antiviral drugs, the HCV NS5B polymerase is regarded as one of the most promising targets for the development of anti-HCV compounds. In recent years, researchers have witnessed rapid advances in the identification of potent inhibitors targeting NS5B polymerase activity. Currently, compounds belonging to three classes of HCV NS5B inhibitors, namely nucleoside analogue inhibitors, non-nucleoside inhibitors (NNIs), and pyrophosphate (PPi)-analogues, are either under preclinical evaluation or have advanced to clinical trials (Reviewed in De Francesco and Migliaccio<sup>108</sup>). The chemical structures of selected NS5B polymerase inhibitors are depicted in Figure 6.

**Figure 7: Chemical structures of selected inhibitors of HCV NS5B polymerase**

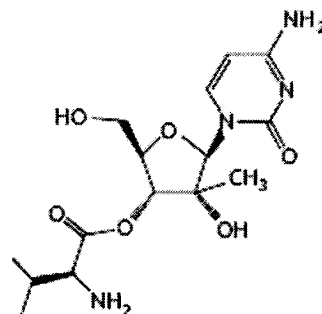
**Nucleoside Analogue Inhibitors**



**Ribavirin**

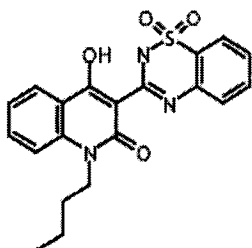


**2'-C-methyl-cytidine**

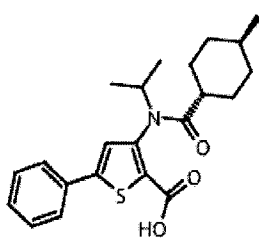


**NM283**

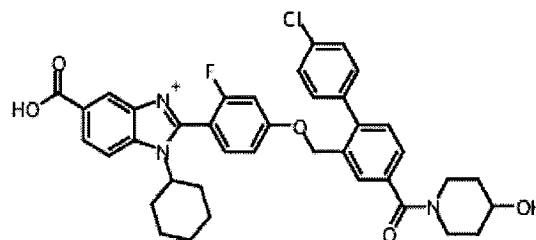
**Non-nucleoside Inhibitors (NNIs)**



**Thiadiazine derivative**



**Thiophene derivative**



**Benzimidazole derivative**

*Examples of nucleosides analogue inhibitors: ribavirin, 2'-C-methylcytidine and its oral prodrug, NM283, as well as representative examples of different classes of NNIs: benzimidazoles, benzothiadiazines, and thiopenes. (Adapted from Neyts<sup>211</sup>).*

Nucleoside analogue inhibitors are an important class of compounds that can target viral polymerases and are already used in the clinic to treat infection with HIV-1, HBV, herpes simplex virus (HSV), and the human cytomegalovirus (HCMV). These compounds are all simple pyrimidine or purine nucleosides with modifications made mainly to the ribose portion. The majority of antiviral nucleoside analogues is administered as prodrugs and must be intracellularly phosphorylated by the sequential action of viral and/or cellular kinases to their corresponding 5'-triphosphate derivatives. Once converted to their active form, these compounds function as alternative substrates by competing with cellular NTP pools for incorporation by the viral polymerase into the nascent RNA product. Many of these inhibitors can induce premature termination of RNA synthesis after incorporation, and thus act as chain-terminators due to the lack of a 3'-hydroxyl group that is essential to attack the  $\alpha$ -phosphate of the incoming NTP.

In the last few years, a number of novel nucleoside analogues with the potential to inhibit the activity of HCV RdRp have been described. For instance, the base-modified ribonucleoside analogue, b-D-N4-hydroxycytidine (NHC) has been found to inhibit production of both HCV and BVDV RNA by acting as a weak alternative substrate for the viral polymerase<sup>147</sup>. HCV NS5B has also been reported to be a mediator of the antiviral activity of ribavirin, a guanosine analogue that is used in current drug regimens to treat HCV infections. Unlike the nucleoside analogues directed against HIV-1 RT which lack the 3'-hydroxyl group, ribavirin contains a normal ribose moiety and does not appear to cause chain termination. Rather, this analogue has been shown to increase error frequency for both poliovirus genomic RNA and hepatitis C replicon synthesis<sup>212; 213; 214</sup>.



Magg *et al.*<sup>215</sup> demonstrated that the triphosphate form of ribavirin is accepted by the RNA polymerase of HCV and poliovirus. Although the efficiency of incorporation was decreased by a factor in the  $10^4$  to  $10^5$  range compared to the natural purine nucleotides, the enzymes incorporated the analogue opposite both cytosine and uracil, leading to transition mutations (A-to-G, G-to-A). Ribavirin is therefore considered to be a powerful mutagen and is thought to exert its antiviral activity through the accumulation of replicative errors, which in turn, results in lethal mutagenesis of the viral genome and diminished viral replication fitness. These findings are further supported by data showing that a ribavirin resistance-conferring mutation in poliovirus 3D<sup>pol</sup> increased fidelity<sup>216</sup>. The ability of the monophosphorylated form of ribavirin to inhibit inosine monophosphate dehydrogenase (IMPDH) and cause moderate depletions of cellular GTP pools has been postulated to accentuate this mutagenic effect by decreasing the concentration of the natural nucleotide within the cell, and thus increasing the frequency of ribavirin triphosphate incorporation. There is also a possibility that ribavirin or ribavirin analogues may compete for binding into the GTP binding pocket of HCV RdRp and inhibit the stimulating effects normally induced by the binding of GTP to this site. Another interesting analogue shown to be a potent inhibitor of HCV NS5B is 2'-deoxy-2'- $\alpha$ -fluorocytidine triphosphate (FdC). Experiments have demonstrated, however, that FdC induces cytostasis in HCV replicon-containing cells, due to the inhibition of one or more cellular targets<sup>217</sup>. The fact that FdC and other 2'-fluoronucleosides have limited selectivity, acting as substrates and chain-terminating inhibitors for several human polymerases, makes them unlikely candidates for the treatment of HCV infection<sup>217</sup>. Canonical 3'-deoxyribonucleoside triphosphates (3'-dNTP), which lack the 3'-hydroxyl

group, were also found to function as highly effective chain-terminators for HCV NS5B-mediated RNA synthesis *in vitro*; however, cell culture testing revealed a much weaker cellular activity of the corresponding nucleosides for inhibition of HCV genome replication<sup>218</sup>. More interestingly are studies on several compounds carrying a 2'-methyl moiety that were found to strongly inhibit HCV RdRp activity *in vitro* and in cell culture<sup>219; 220; 221</sup>. These compounds, referred to as non-obligate chain-terminators, diminish the binding and/or incorporation of the next nucleotide and cause chain-termination once incorporated, despite the presence of the 3'-hydroxyl group. It appears that the addition of a methyl group at the 2' position of the sugar moiety is sufficient to cause chain-termination. As well, the presence of the 3'-hydroxyl group is important for substrate recognition by cellular kinases for phosphorylation to their active triphosphate forms<sup>218; 222</sup>. One member of this group of compounds, the prodrug of 2'-C-methylcytidine (i.e., NM283), is currently in Phase 2 clinical trials. This compound, initially identified as an inhibitor of BVDV, exhibits potent inhibition against various genotype RdRps, and thus has the potential to be active against many clinically relevant viral variants<sup>220; 223</sup>. Despite these promising results, *in vitro* resistance selection experiments using the HCV replicon system have demonstrated that a number of 2'-C-methyl analogues, including 2'-C-methylcytidine, are readily susceptible to the development of drug resistance<sup>220; 223</sup>. A single point mutation (S282T) within the active site of NS5B is sufficient to confer resistance by increasing the ability of the polymerase to discriminate between the inhibitor and its natural NTP counterpart. The exact effect of replacing serine 282 with threonine on the NS5B structure is currently unknown, although replicons harboring this mutation have decreased replication fitness<sup>223</sup>. The

possibility that additional resistance mechanisms diminish the inhibitory effects of this class of compounds *in vivo* warrants further investigation. Recent studies have identified a novel group of 4'-substituted nucleoside analogues as yet another promising class of inhibitors for HCV replication<sup>224</sup>. More specifically, the compound 4'-azidocytidine was found to inhibit HCV replication in replicon-containing cells with a similar potency comparable to that of 2'-C-methylcytidine. The analogue has been shown to function as a competitive inhibitor of RNA synthesis by preventing further elongation once incorporated into nascent RNA by the HCV polymerase. Given its promising preclinical profile, 4'-azidocytidine will soon enter clinical evaluation<sup>224</sup>.

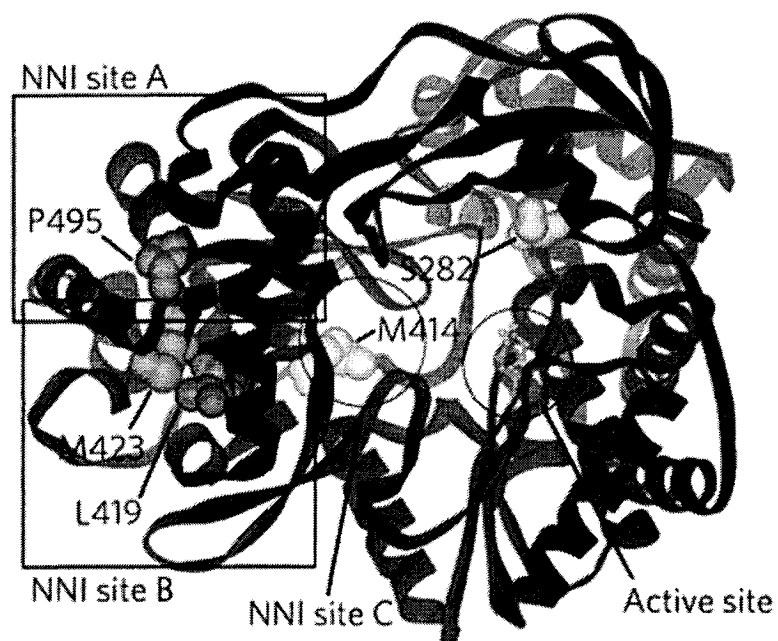
Tremendous progress has been made toward the discovery of effective HCV antiviral compounds. Despite this, new therapy options for the treatment of HCV infection are still urgently required. Currently, ribavirin in combination with IFN- $\alpha$  is the only nucleoside analogue used for the treatment of HCV infection. However, the weak antiviral effects observed *in vitro* and in clinical studies suggest that improved HCV-targeted drugs with higher selectivity and inhibitory potency are required. As seen above, the development of novel nucleoside analogues holds great promise for drug discoverers. The first group of anti-HCV nucleoside analogues yielded promising results in early clinical trials. The success of these inhibitors will greatly be influenced by their ability to be selective against numerous HCV viral variants and to prevent the emergence of escape mutants. Future therapeutic regimens for HCV infection may almost certainly involve combinations of several drugs such as nucleoside or non-nucleoside analogue inhibitors,

as well as drugs that target different viral proteins to control infection and prevent the emergence of drug-resistant viruses.

### **1.7.1 Non-Nucleoside Inhibitors of HCV Polymerase**

Over the years, a number of structurally diverse non-nucleoside inhibitors (NNIs) of the HCV polymerase have been independently identified by several laboratories<sup>225; 226; 227; 228; 229; 230; 231; 232; 233; 234</sup>. Among the compounds documented, representative molecules from each of the three different classes of NNIs, based on benzimidazoles, thiophenes or benzothiadiazines derivatives, are either in preclinical development, or under investigation in early clinical trials (Reviewed in De Francesco and Migliaccio<sup>108</sup>). These inhibitors bind directly to the viral polymerase and block RNA synthesis through an allosteric mode of inhibition. Based on the location of resistance conferring mutations and on the determination of the crystal structure of NS5B in complex with the analogues, it has been determined that these inhibitors bind to three distinct, non-overlapping binding sites on the surface of the NS5B protein<sup>226; 235; 236; 237; 238</sup>, as depicted in Figure 7.

**Figure 8: Crystal structure of the HCV RdRp detailing the location of binding pockets for the three classes of NNIs**



*The thumb, palm, and fingers domain of the HCV NS5B polymerase are colored in blue, green, and red respectively, while the two catalytic aspartic acids located in the active site are colored in yellow. Based on resistance data, the location of the binding site for the inhibitors of the benzimidazole (NNI site A), thiophene (NNI site B), and thiadiazine (NNI site C) class of NNIs are indicated. The amino acid residues responsible for resistance to benzimidazole (P495), thiophene (L419 or M423), or thiadiazine (M414) are also shown. (Adapted from De Francesco and Migliaccio<sup>108</sup>).*

The benzimidazole class of NS5B inhibitors bind to a site that encompasses the interface between the thumb domain and the  $\Lambda$ 1-loop of the fingertip domain<sup>239</sup>. At least three different types of NNIs based on thiophene, phenylalanine, and dihydropyranone derivatives bind to a common site on an elongated hydrophobic cleft in the thumb domain, near the C-terminus of the polymerase. Replicons resistant to these compounds contain mutations at amino acid residues Met423 and Leu419 at the base of the thumb, which is close to, yet distinct from the site occupied by benzimidazole-based inhibitors<sup>226; 238</sup>. Finally, inhibitors of the benzothiadiazine series bind to site which is located in the inner surface of the thumb domain, close to the active site of the enzyme<sup>237</sup>. Despite binding to different sites on the polymerase, biochemical and structural studies have suggested that these allosteric inhibitors function via a common mechanism by impeding with the conformational transition needed for the formation of a productive RNA-enzyme elongation complex<sup>236; 240</sup>. This inhibition occurs non-competitively with RNA template or NTPs. Once this conformational transition occurs, the polymerase is no longer sensitive to inhibition. This observation is supported by studies which have shown that the addition of compounds to pre-formed polymerase-RNA complexes results in residual enzyme activity, even at saturating inhibitor concentrations<sup>237; 241</sup>. It is conceivable that the binding site is no longer accessible due to changes in the conformational behavior of the polymerase during polymerization. As such, the potency of NNIs may critically depend on both the binding site accessibility and the conformation of the polymerase.

The first NNIs of the HCV polymerase to enter clinical trials (i.e., JTK-109 and JTK-003) are part of a series of compounds based on a benzimidazole or indole core<sup>108</sup>.

In general, compounds of the benzimidazole series have been shown to have specific antiviral activity against the HCV polymerase and can effectively inhibit the replication of subgenomic replicons with no apparent cytotoxicity<sup>235</sup>. Detailed interactions between the polymerase and an analogue belonging to this class of inhibitors, as revealed by crystallographic studies, have shown that these compounds bind to a site within the thumb domain in a cavity that is normally occupied by the fingers domain<sup>239</sup>. Inhibitor binding to this location appears to cause a perturbation of the interaction between the fingertip  $\Lambda$ 1-loop and the thumb domain, forcing the enzyme to adopt an “open”, inactive conformation<sup>239</sup>. The binding of thiophene inhibitors also induces a conformational change of the enzyme toward an “open” form, suggesting a common mechanism of inhibition<sup>188</sup>. It has also been suggested that both these classes of inhibitors may exert a second mode of inhibition by affecting the integrity of the allosteric GTP-binding site. In agreement with this hypothesis is the identification that resistance to benzimidazole inhibitors arises through a mutation of the amino acid residue Pro495 with either alanine or leucine<sup>236</sup>. Notably, GTP binding to the GTP-binding pocket also involves interaction with Pro495<sup>182</sup>. Recently, a detailed comparison of the crystal structures of unbound NS5B with that of the NS5B protein in complex with thiophene-based inhibitors has shown that inhibitor binding induces large conformational changes in the binding site residues Pro495 to Arg505, some of which are also involved in GTP recognition<sup>242</sup>. Additionally, Tomei *et al.*<sup>236</sup> have demonstrated the antagonistic effects that high concentrations of GTP have on the inhibition potency by this class of compounds. There is also evidence to suggest that these classes of NNIs may have an effect on the oligomerization process of the HCV polymerase by perturbing the position of His502,

one of the amino acid residues involved in NS5B protein-protein interactions<sup>242</sup>. Recently, Powers *et al.*<sup>243</sup> have reported a new series of NNIs for HCV NS5B that utilize yet another distinct mechanism of inhibition. These compounds bind to the amino acid residue Cys366 located in the hydrophobic pocket around the  $\beta$ -hairpin, approximately 8 Å away from the GDD motif of the active site. Based on the X-ray structure information obtained, compound binding at this position is unlikely to interfere with the active site, or compete with nucleotide binding. Rather, inhibition likely occurs through stabilization of the  $\beta$ -hairpin. By interacting with the compound, the  $\beta$ -hairpin is positioned in such a way that may inhibit the conformational change in the thumb domain required for template binding, or for the formation of the initiation platform. Inhibitor binding also blocks the template channel and thus interferes with the advancement of the RNA template strand<sup>243</sup>. Pfefferkorn *et al.*<sup>244; 245</sup> has reported a series of NNIs which also bind in the hydrophobic pocket around the  $\beta$ -hairpin where C366 is located, although interactions with the  $\beta$ -hairpin were not observed with this specific class of inhibitors.

Over the years, it has become increasingly evident that multiple regions of the NS5B thumb domain are potential antiviral targets for allosteric inhibition. This is in contrast to HIV-1 RT for which all known NNIs have been shown to bind to the same site of the enzyme. This is of particular relevance considering the possible requirement for combination therapy based on the use of multiple NNIs as the future therapeutic regimen for HCV infection.



## 1.8 Thesis Objectives

As shown above, a vast number of structural and biochemical studies have been carried out on the HCV polymerase. Despite this, many important questions on the topic of initiation and elongation remain. For instance, the exact initiation mechanism utilized by HCV RdRp is still unclear. Moreover, the functions of many of the structural features involved in initiation, as well as the signals that regulate the switch from initiation to elongation remain to be elucidated. The answers to these questions will be crucial with regards to the development of specific antiviral agents directed against the viral polymerase, as well as will facilitate the understanding of the underlying mechanism(s) associated with drug resistance.

When I began my PhD project, I was interested in studying the fundamental aspects of the mechanisms of initiation and elongation of viral RdRps. Preliminary data have suggested that related viruses such as BVDV can be utilized as surrogate model systems for the analysis of HCV replication and the evaluation of antiviral inhibitors, especially since its polymerase behaves favorably with regards to its expression and purification, as compared to the HCV RdRp<sup>142; 143; 144; 246</sup>. The first objective of the thesis was therefore to develop a tool to arrest the BVDV polymerase complex at different template positions with the use of chain-terminators, in an attempt to study the structural and functional nature of these complexes during initiation and elongation. The second major objective was to assess the potential of these inhibitors as antiviral agents to treat infection with HCV. As such, Chapter 2 describes the biochemical mechanisms

associated with the inhibition of BVDV RNA synthesis by 3'dNTPs. Previous studies with HIV-1 RT have shown that the incorporation of a chain-terminator is not always an irreversible process. Rather, the incorporated chain-terminator can be removed from the primer terminus through phosphorolytic cleavage in the presence of pyrophosphate (PPi)<sup>247</sup> or a PPi donor<sup>248</sup>. We therefore questioned whether phosphorolytic excision is a possible mechanism that can diminish the efficiency of nucleotide analogues directed against viral RdRps. These chain-terminators then served as valuable tools in subsequent experiments to obtain information about specific initiation events that occur during BVDV RNA synthesis, as well as to analyze the functional role(s) of the G-site and the consequences of GTP binding during initiation (Chapter 3). Finally, Chapter 4 describes the development of a ribonuclease-based footprinting assay used to obtain structural information about catalytically active complexes that exist during the elongation of BVDV RNA synthesis.

## **CHAPTER 2**

### **EXCISION OF INCORPORATED NUCLEOTIDE ANALOGUE CHAIN- TERMINATORS CAN DIMINISH THEIR INHIBITORY EFFECTS ON VIRAL RNA-DEPENDENT RNA POLYMERASES**

This chapter was adapted from an article that appeared in *Journal of Molecular Biology*, 2004, 337(1):1-14.

## **Preface to Chapter 2:**

Although the HCV polymerase was shown to efficiently incorporate 2'-hydroxyl, 3'-deoxynucleoside triphosphates (3'-dNTPs) and cause effective chain termination in cell-free assays, further analyses showed that the corresponding nucleosides functioned as poor inhibitors in replicon-harboring cells. Several parameters including metabolic activation, as well as the efficiency and accuracy of nucleotide incorporation can greatly influence susceptibility to this specific class of compounds. Phosphorolytic excision of incorporated chain-terminators is another mechanism that can also severely compromise the potency of both classical and non-obligate chain-terminators. Previous biochemical studies with HIV-1 RT have shown that chain-termination is not always irreversible, and that the removal of the nucleotide analogue through phosphorolytic cleavage in the presence of either PPi or a PPi donor may eventually rescue RNA synthesis. On the basis of these reports, we questioned whether PPi-mediated excision is likely to be an important factor that can influence the potency of chain-terminating nucleotides against viral RdRps.

## Abstract

Bovine viral diarrhea virus (BVDV) is amongst the best-characterized members of the *Flaviviridae* that includes the hepatitis C virus (HCV). The virally encoded RNA-dependent RNA polymerase (RdRp) plays a crucial role during replication and therefore represents an important target for the development of antiviral drugs. Here we studied biochemical mechanisms associated with the inhibition of BVDV RNA synthesis by 2'-hydroxyl, 3'-deoxynucleoside triphosphates (3'-dNTPs). All four nucleotide analogues are effectively incorporated and act as chain-terminators. However, relatively low, physiologically relevant concentrations of pyrophosphate (PPi) are sufficient to drive the reaction backwards, which results in primer unblocking and rescue of RNA synthesis. Metal ion requirements for nucleotide incorporation and pyrophosphorolysis are similar; the efficiency of both reactions is higher with  $Mn^{2+}$  as compared to  $Mg^{2+}$ . Complexes containing chain-terminated primer strands are stable in the presence of heparin, which increases the probability that pyrophosphorolysis occurs before the enzyme can dissociate from its nucleic acid substrate. In contrast to the reverse transcriptase of the human immunodeficiency virus type-1 (HIV-1 RT), the BVDV RdRp may not recruit NTP pools as PPi-donors. Conversely, we found that the efficiency of primer unblocking is severely compromised in the presence of increasing concentrations of the NTP that is complementary to the next template position. These data suggest that the incoming NTP can access its designated binding site, which, in turn, prevents the catalytically competent complexation of PPi. The results of this study provide novel insights into mechanisms involved in pyrophosphorolysis associated with viral RdRps, and suggest that the

excision reaction is likely to be an important parameter that can affect susceptibility to nucleotide analogue inhibitors directed against viral RdRps.

## Introduction

Bovine viral diarrhea virus (BVDV) is a member of the Pestivirus genus in the *Flaviviridae* family, which includes important human pathogens like the hepatitis C virus (HCV). Both BVDV and HCV contain a plus-stranded RNA genome, which encodes a single polyprotein that is processed into individual structural and non-structural proteins. The virally encoded RNA-dependent RNA polymerase (RdRp), termed NS5B (nonstructural protein 5B), is essential for the production of minus-strand intermediates and the plus-stranded RNA genome. The development of replicon systems has greatly advanced our understanding of the molecular biology of the HCV virus<sup>1; 2; 3</sup>; however, cell culture systems that facilitate continuous viral replication remain to be established. The study of related pestiviruses such as BVDV became an important approach to gain information not only in regard to the molecular biology of positive-strand RNA viruses, but also in regard to the discovery and development of novel antiviral drugs that inhibit replication of members of the *Flaviviridae* family.

Non-nucleosidic small molecule compounds that effectively inhibit replication of BVDV in cell culture have recently been described<sup>4,5</sup>. Although the exact mechanism involved in inhibition of viral replication remains to be elucidated, the *in vitro* selection of drug resistance conferring mutations located in the NS5B coding region provide strong evidence to show that these compounds antagonize the function of the BVDV enzyme. Nucleoside analogue inhibitors represent another important class of compounds that can target viral RdRps. 2'-deoxynucleoside analogue inhibitors are used in the clinic to treat

infection with the human immunodeficiency virus type 1 (HIV-1), herpes simplex virus (HSV), hepatitis B virus (HBV) and the human cytomegalovirus (HCMV). These compounds are intracellularly phosphorylated, and compete with cellular dNTP pools for incorporation by viral DNA polymerases. Many of these inhibitors act as chain-terminators due to the lack of a 3' hydroxyl group that is essential to attack the  $\alpha$ -phosphate of the incoming deoxynucleoside triphosphate (dNTP). Novel nucleoside analogues with the potential to inhibit the activity of RNA polymerases of viruses belonging to the *Flaviviridae* family are currently under investigation.

Stuyver et al. (2003)<sup>6</sup> showed that the base-modified ribonucleoside analogue,  $\beta$ -D-N<sup>4</sup>-hydroxycytidine (NHC, Fig. 1A) inhibits production of HCV and BVDV RNA. However, the mechanism of action remains elusive, since this compound does not appear to inhibit the polymerization process and attempts to select for resistant strains have been unsuccessful. Various mechanisms have been associated with the antiviral effects of the guanosine analogue ribavirin<sup>7</sup> (Fig. 1B). The monophosphorylated form of ribavirin causes moderate depletions of cellular GTP pools through inhibition of inosine monophosphate dehydrogenase, which may help to explain its broad spectrum of antiviral activities. More recently, it has been demonstrated that the triphosphate form of ribavirin is accepted by the RNA polymerase of HCV and poliovirus suggesting a direct effect on viral replication<sup>8,9</sup>. However, ribavirin does not appear to cause chain-termination. The drug contains a 3' hydroxyl group, which allows continuation of RNA synthesis, albeit with diminished rates<sup>9</sup>. Ribavirin is incorporated opposite cytidine and also opposite uridine, which has been shown to be associated with an increased mutation rate and



diminished viral replication fitness<sup>8; 10</sup>. These findings and conclusions are strongly supported by recent data showing that a ribavirin resistance-conferring mutation in the RdRp of poliovirus increased fidelity<sup>11</sup>.

Chain-termination has been demonstrated with 2'-methylated nucleoside analogues that are effectively incorporated by the HCV NS5B enzyme<sup>12</sup> (Fig. 1C). Although these compounds contain the 3' hydroxyl group, they block the continuation of RNA synthesis once incorporated into the growing strand. Increased intracellular concentrations of their triphosphate forms correlated well with increased drug susceptibility in replicon systems. Thus, metabolic activation as well as the efficiency and accuracy of nucleotide incorporation are important factors that can influence susceptibility to nucleoside analogue inhibitors. However, these parameters may not suffice to assess the efficiency of members of this family of compounds. 2'-hydroxyl, 3'-deoxynucleoside triphosphates (3'-dNTPs) have been shown to act as highly efficient chain-terminators of HCV RNA synthesis in cell-free assays, while the corresponding nucleosides are poor inhibitors in cell-based replicon systems<sup>13; 14</sup> (Fig. 1D). The reason for this disparity is unknown.

Insufficient phosphorylation of the nucleoside diphosphate metabolite is a possible factor, considering that the 3'-hydroxyl group appears to play an important role in substrate recognition by homologues of the human nucleoside diphosphate kinase<sup>15</sup>; however, it is also conceivable that high rates of nucleotide incorporation may not necessarily translate into efficient chain-termination. Previous biochemical studies with

the reverse transcriptase (RT) of the human immunodeficiency virus type-1 (HIV-1) have shown that the incorporation of a chain-terminator is not always irreversible. The incorporated chain-terminator can be removed from the primer terminus through phosphorolytic cleavage in the presence of either pyrophosphate (PPi)<sup>16</sup>, or in the presence of NTPs<sup>17</sup>, that were shown to act as PPi donors. Such unblocking of the primer may severely compromise the potency of nucleoside analogue inhibitors. Notably, mutations that confer resistance to these drugs can sometimes dramatically increase the rates of excision of chain-terminating nucleotides<sup>18; 19</sup>. Here we studied the effects of both incorporation and excision of 2'-hydroxyl, 3' deoxynucleoside monophosphates (3'-dNMPs) on RNA synthesis by the RdRp of BVDV. Our data suggest that the PPi-mediated excision is likely to be an important factor that can influence the potency of chain-terminating nucleotides against viral RdRps.

## **Materials and Methods**

**Chemicals and nucleic acids** - The RNA template substrate used in this study was derived from the 3'end of the minus-strand BVDV genome<sup>20</sup>. Sequences of the nucleic acid substrate utilized are as follows:

5'-CCUUUUCUAAUUCUCGUAUAC (T-21 template), 5'-GG (primer).

All RNA oligonucleotides were chemically synthesized. The RNA template was further purified on 12% polyacrylamide-7M urea gels containing 50 mM Tris-borate (pH 8.0) and 1 mM EDTA, followed by elution from gel slices in a buffer containing 500 mM

NH<sub>4</sub>Ac and 0.1% SDS. 5' end-labelling of the RNA primer was performed with [ $\gamma$ -<sup>32</sup>P]ATP and T4 polynucleotide kinase according to the manufacturer's recommendation (Invitrogen). Ribonucleoside triphosphates were purchased from Roche and 3'-dNTPs were purchased from TriLink BioTechnologies.

**Expression and purification of BVDV NS5B protein** - We generated a truncated version of the BVDV NS5B enzyme to facilitate its purification. This protein, termed NS5B $\Delta$ 18, lacks the 18 C-terminal residues. The coding sequence was amplified from an infectious cDNA clone (pACNR/BVDV NADL-XbaI)<sup>48</sup>. *EcoRI* and *XhoI* sites were engineered into the PCR primers to facilitate cloning into the expression vector pET-21b (Novagen). The truncated protein was expressed in *E.coli* strain BL21 (DE3) (Novagen). Purification was conducted using a combination of metal ion affinity and ion exchange chromatography as previously described<sup>49</sup>. The eluted protein was dialyzed against a buffer containing 10 mM Tris-HCl pH 7.5, 10 % glycerol, 5 mM DTT, 600 mM NaCl. The protein was stored at -80°C in 50% glycerol.

**RNA synthesis and chain-termination assay** - Standard reaction mixtures consisted of 0.75  $\mu$ M of RNA template (T-21), 0.75  $\mu$ M BVDV NS5B and 0.25  $\mu$ M 5'-end labelled primer in a buffer containing 20 mM Tris-HCl pH 7.5, 50 mM NaCl, 1 mM DTT, 0.15 mM MnCl<sub>2</sub> and 100  $\mu$ M NTPs. Reactions were initiated by the addition of enzyme at room temperature. The efficiency of chain-termination was monitored in reaction mixtures as described above except that each of the four NTPs was added at a constant concentration of 10  $\mu$ M in the presence of increasing concentrations of 3'-dNTPs

as specified in the figure legends. Samples were precipitated with ethanol, heat-denatured for 5 min at 95°C, and resolved on 12 % polyacrylamide–7M urea gels. IC<sub>50</sub> values were obtained by quantifying the relative amount of full-length versus chain-terminated products. Determinations of K<sub>m</sub> and k<sub>cat</sub> values were performed using gel-based assays essentially as previously described<sup>50</sup>. Kinetic parameters were determined in ‘running start’ experiments, in which the correct NTP or the chain-terminator, respectively, was added at different concentrations to the reaction mixture.

**Pyrophosphorolysis and rescue of chain-terminated RNA synthesis** - Rescue of RNA synthesis was studied at a single template position using a similar assay as recently described for HIV-1 RT<sup>24</sup>. Reaction mixtures consisted of 0.75 μM template, 0.75 μM BVDV NS5B enzyme and 0.25 μM 5'-end labelled primer in a 20 μl volume containing 20 mM Tris-HCl pH 7.5, 50 mM NaCl, 1 mM DTT, 0.15 mM MnCl<sub>2</sub>, 100 μM ATP/UTP and 100 μM 3'-dCTP. Reactions were allowed to proceed for 30 min to ensure efficient extension of the primer and incorporation of the 3'-dCTP. The excision of the 3'-dCTP was initiated by the addition of different concentrations of either PPi or ATP and other NTPs that potentially act as PPi donors. A mixture of 200 μM CTP and 100 μM 3'-dGTP was simultaneously added in the reaction mixture to enable rescue of RNA synthesis. Pyrophosphorolysis was assayed by the addition of various concentrations of PPi, in the absence of other NTPs. The effect of the next NTP on PPi-dependent rescue was monitored as described above except that the excision of 3'-dCTP was initiated by adding 100 μM PPi, 200 μM CTP and different concentrations of correctly templated (GTP) or incorrect (ATP or UTP) NTPs.

## Results

**Inhibition of RNA synthesis in the presence of 3'-dNTPs** - Throughout this study, we utilized a short synthetic RNA template (T-21) and a C-terminal truncated version of the BVDV NS5B enzyme as a model system to scrutinize the effects of chain-terminators on RNA synthesis by RdRps. We initially established cell-free assays in order to analyze the incorporation of chain-terminating nucleotides into the growing RNA chain (Fig. 2). Previous studies have demonstrated that viral RdRps, including BVDV NS5B, are capable of initiating RNA synthesis either *de novo*, i.e. in the absence of a primer, or in the presence of short dinucleotide primers<sup>20; 21; 22; 23</sup>. The latter conditions facilitate the analysis of efficiency of RNA synthesis, since the formation of reaction products can be monitored by extension of the 5'-end-labelled primer. Throughout this study we used an end-labelled GG-dinucleotide primer, which, we found, is more efficiently used compared to a GU-primer that is complementary to the two 3' terminal residues of the template (data not shown). The incorporation of chain-terminators was analyzed in the presence of increasing concentrations of 3'-dNTPs. Each of the four NTPs was used at a constant concentration of 10  $\mu$ M. The results show that formation of the full-length product was compromised concomitantly with an increase in concentrations of the different 3'-dNTPs (Fig. 2). Concentrations required to inhibit the formation of the full-length product by 50% ( $IC_{50}$ ) were in a range between 2 to 10  $\mu$ M (Table 1), which suggests that the modified nucleotides are efficiently incorporated. Steady-state kinetic parameters were determined for the incorporation of 3'-dGTP and GTP at a later stage after the initiation of RNA synthesis, i.e. at position +7. The catalytic

efficiency was similar for 3'-dGTP ( $k_{cat}/K_m = 2.45 \mu\text{M}^{-1}\text{min}^{-1}$ ,  $K_m = 0.2 \mu\text{M}$ ), and GTP ( $k_{cat}/K_m = 2.3 \mu\text{M}^{-1}\text{min}^{-1}$ ,  $K_m = 0.2 \mu\text{M}$ ). These data show that relatively low  $K_m$  values can facilitate the incorporation of the chain-terminator and its natural counterpart at this advanced stage of the reaction; however, we note that  $K_m$  values for nucleotide incorporation can be considerably higher at early stages after immediately following initiation of the reaction (see below).

Differences in  $\text{IC}_{50}$  values between the four different analogues correlated well with differences in the number of possible incorporation sites (Table 1). Lower  $\text{IC}_{50}$  values correlated with an increasing number of template positions that provided complementarity to the nucleotide analogue. All four chain-terminators are preferentially incorporated opposite the expected, complementary template sites (compare Fig. 2A-D). The absence of doublets (double bands) shows that the initiation of RNA synthesis occurs precisely from a single position. The patterns of chain-termination suggest that initiation takes place from the penultimate template position (+2), as indicated in the sequence alignments shown in Fig. 2. This interpretation is consistent with a previous study, in which differences in the length of final reaction products have been indicative for different sites of initiation with GG- and GU-dinucleotide primers<sup>22</sup>.

We also noted the appearance of additional bands that did not correspond to correct incorporation events (asterisks, Fig. 2B and 2C). These bands point to incorporation events opposite template uridines, early after initiation at positions +3 and +5. GTP and/or 3'-dGTP are possible candidates in this regard, considering that G:U

mispairs are the easiest to form. Consistent with this proposal is the observation that increased concentrations of 3'-dGTP correlated with increased chain-termination opposite uridine at position +5 (Fig. 2C). Moreover, nucleotide mixtures with higher concentrations of NTPs, including higher concentrations of ATP, i.e. the correct nucleotide for positions +3 and +5, completely prevented the appearance of these bands (see below, Fig. 3B/C). In fact, the  $K_m$  value for incorporation of ATP ( $K_{m, ATP} = 14.8 \mu\text{M}$ ) was relatively high at these early stages after initiation. Thus, to overcome the possible formation of G:U mispairs, we increased the concentration of ATP and UTP from 10  $\mu\text{M}$  to 100  $\mu\text{M}$  in the following experiments.

**Phosphorolytic excision of incorporated chain-terminators** - We next studied the effects of exogenously added PPi on the efficiency of chain-termination. As previously described in the context of HIV-1 RT<sup>24</sup>, we utilized an assay that allowed us to monitor the excision of the chain-terminator and the subsequent rescue of RNA synthesis at a single template position (Fig. 3A). RNA synthesis was initiated in the presence of a nucleotide mixture that permitted RNA extension up to template position +6, at which point the incorporation of 3'-dCTP blocked further RNA synthesis (Fig. 3B, lane C1). The reaction was almost completed after 30 min, since the subsequent addition of the natural nucleotide CTP and 3'-dGTP, which is complementary to the next template position, did not yield significant amounts of the longer product (Fig. 3B, lane 1). However, the simultaneous addition of increasing concentrations of PPi caused an accumulation of the longer product. The band at position +6 disappeared concomitantly with increased chain-termination at position +7 (Fig. 3B, lanes 2-14; left panel). These

data demonstrate that the incorporation of the chain-terminator is not irreversible. The nucleotide analogue is susceptible to phosphorolytic excision, which is a prerequisite for the ensuing rescue of RNA synthesis. To drive the reaction forward we used significantly higher concentrations of 3'-dGTP (100  $\mu$ M) than the  $K_m$  value ( $K_{m,3'-dGTP} = 0.2 \mu$ M). The addition of PPi alone allowed us to directly monitor pyrophosphorolysis. The 3'-dCTP chain-terminator was efficiently removed at position +6, concomitant with an increase of a product at position +5 (Fig. 3C; left panel).

These findings are reminiscent of properties described for HIV-1 RT<sup>16</sup>. Both HIV-1 RT and BVDV NS5B can recruit PPi to catalyze the excision of incorporated chain-terminators; however, in contrast to the retroviral DNA polymerase<sup>17</sup>, the BVDV RdRp might be unable to use its natural NTPs substrates as PPi donors. Increasing concentrations of ATP, and the simultaneous presence of CTP and 3'-dGTP, did not significantly promote the rescue of chain-terminated RNA synthesis (Fig. 3B, right panel). The increase in the amount of product at position +7 is almost negligible as compared to the control reaction in the absence of higher concentrations of ATP (Fig. 3B, compare lane C2 with lanes 1 to 14; right panel). These data are in good agreement with the low levels of ATP-dependent phosphorolytic cleavage shown in Fig. 3C.

The PPi-mediated rescue of RNA synthesis occurred most effectively in a window of concentrations between 80 and 300  $\mu$ M (Fig. 3E). Higher concentrations of PPi inhibited the reaction, which is attributable to a blockage of RNA synthesis (Fig. 3D). However, we also noted that the addition of PPi prior to the start of the reaction inhibited



RNA synthesis at significantly lower concentrations as observed in the context of the combined excision and rescue reaction (compare Figs. 3 B with D, and E with G). 50% inhibition of RNA synthesis was seen at a concentration of approximately 100  $\mu$ M PPi. In contrast, the rescue of RNA synthesis was highly efficient under these conditions, suggesting that the initiation is more sensitive to PPi-mediated inhibition as compared to later stages of the reaction. It is conceivable that the negatively charged PPi interferes with nucleotide and/or the dinucleotide binding, which appears to be less relevant at later stages of the reaction when the interaction with the template provides an additional anchor for the growing primer strand. The exogenous addition of ATP shows similar effects, although less pronounced.

Notably, the sequence of excision and rescue of RNA synthesis is highly processive. The addition of a trap, i.e. heparin, from the start of the reaction, at concentrations as low as 0.5  $\mu$ g/ $\mu$ l, ultimately inhibited the initiation of RNA synthesis (Fig. 4B, left panel). In contrast, the addition of heparin after initiation and chain-termination took place, simultaneously with the addition of PPi and nucleotides, had little effect on the rescue of RNA synthesis (Fig. 4B; right panel). These data suggest that the complex containing the chain-terminated primer is considerably stable, and dissociation between enzyme and nucleic acid substrate at this advanced stage of RNA synthesis may only occur infrequently.

**Requirements for divalent metal ions** - Like all other polymerases, BVDV NS5B and HCV NS5B require divalent metal ions to catalyze the incorporation of

nucleotides. Previous biochemical data have shown that RdRps are capable of recruiting both  $\text{Mn}^{2+}$  and  $\text{Mg}^{2+}$ , albeit at different optimal concentrations<sup>25; 26; 27</sup>. In good agreement with these studies, we found that  $\text{Mn}^{2+}$  supports RNA synthesis in a range between 0.15 and 1.25 mM, while  $\text{Mg}^{2+}$  is most efficiently used in a range between 2.0 and 8.0 mM (Fig. 5A; left and right panels). Effects of the nature and concentration of the divalent metal ion on the excision and rescue of RNA synthesis are unknown. Considering that the excision of an incorporated nucleoside monophosphate is the reverse reaction of its incorporation, one would predict very similar, if not identical requirements for the metal cofactor.

To test this hypothesis we analyzed the effects of increasing concentrations of  $\text{Mn}^{2+}$  and  $\text{Mg}^{2+}$  on the efficiency of rescue of RNA synthesis. The efficiency of the rescue reaction peaked at concentrations of 0.3 mM  $\text{Mn}^{2+}$ . Concentrations higher than 0.60 mM specifically blocked the rescue reaction (product formation at position +7), while RNA synthesis (product formation at position +6) is still effective at 1.25 mM  $\text{Mn}^{2+}$  (Fig. 5B, left panel). Thus, it appears that relatively high concentrations of  $\text{Mn}^{2+}$  diminish the rescue reaction due to a diminution in pyrophosphorolysis. To test this directly, we looked at PPi-mediated excision in the absence of ensuing rescue events (Fig. 5C, left panel). The data obtained support the aforesaid, and show that higher concentrations of  $\text{Mn}^{2+}$  exert differential effects on nucleotide incorporation and pyrophosphorolysis. The excision (product formation at position +5) is efficient below concentrations of 0.3 mM  $\text{Mn}^{2+}$ , while higher concentrations are inhibitory. In contrast, RNA synthesis is still detectable at concentrations as high as 2.5 mM. These differences

are not evident with  $Mg^{2+}$ . The efficiency of RNA synthesis peaks in the same range of  $Mg^{2+}$  concentrations, as seen with the rescue of RNA synthesis (Fig. 5B; right panel). Pyrophosphorolysis is generally weak in the presence of  $Mg^{2+}$  (Fig. 5C; right panel). The chain-terminator, which is still present in the reaction mixture, is likely to be reincorporated after its excision.

**Formation of a dead end complex** - The concentration of NTPs is another important factor that may influence the efficiency of pyrophosphorolysis. Previous biochemical studies with DNA polymerases have shown that the presence of the nucleoside triphosphate that is complementary to the next template position following the incorporated chain-terminator can diminish the efficiency of excision<sup>18; 28</sup>. Blockage of the reaction has been linked to the formation of a stable ternary complex composed of enzyme, nucleic acid substrate and the bound nucleotide<sup>29</sup>. Such constellation, referred to as dead-end complex (DEC), may prevent the competent binding of PPi.

Here we studied the influence of increasing concentrations of NTPs on the phosphorolytic excision of incorporated chain-terminators and the ensuing rescue of RNA synthesis. In contrast to the previous experiments, we monitored the reaction by looking at the ratio of the blocked primer at position +6 and the full-length product. Thus, the addition of 3'-dGTP, that was previously used to monitor rescue events, was replaced with the addition of increasing concentrations of either the next correct complementary NTP (GTP) or incorrect NTPs (ATP and UTP) (Fig. 6A). The results show that the presence of GTP significantly decreased the efficiency of PPi-dependent rescue of RNA

synthesis (Fig. 6B, left). The concentration required to inhibit the reaction by 50% was determined to be approximately 250  $\mu$ M for GTP (Fig. 6C). These data suggest that the correct nucleotide facilitates the formation of a stable DEC. Inhibition of rescue of RNA synthesis was less pronounced in the presence of nucleotides that mismatched with the next template position, i.e. ATP (Fig. 6B, middle) and UTP (Fig. 6B, right), respectively. The concentration required to inhibit the reaction by 50% was approximately an order of magnitude higher as determined for GTP (Fig. 6C). Together, these results provide strong evidence to show that both pyrophosphorolysis and its NTP-dependent inhibition are important parameters that can influence the efficiency of nucleoside analogue inhibitors directed against viral RdRps.

## Discussion

In this study, we analyzed the phosphorolytic excision of chain-terminating nucleotides in the context of viral RdRps using the BVDV NS5B enzyme as an example. The major results obtained are discussed with the help of simplified models to illustrate possible scenarios that involve binding of PPi and NTPs, nucleotide incorporation, and the requirements for its excision. Our data are in some cases reminiscent of properties described for HIV-1 RT. As recently suggested for the retroviral DNA polymerase<sup>30</sup>, we distinguish between the nucleotide binding site (N-site) and the primer binding site (P-site) that constitute the active center<sup>30; 31; 32; 33</sup>. In this model, productive RNA synthesis requires that the incoming nucleotide, which can be a chain-terminator, binds to the N-site, while the 3' end of the primer occupies the P-site (Fig. 7A). Crystal structure models

of different polymerases<sup>34; 35</sup>, including structures of truncated forms of the HCV NS5B enzyme<sup>36; 37; 38; 39</sup>, suggest that two divalent metal ions, referred to as metal ions A and B, are involved in the precise alignment of primer and incoming nucleotide. The relative positions of the two metal ions suggest that metal ion A facilitates the attack of the 3'OH group of the primer terminus to the  $\alpha$ -phosphorous of the incoming NTP, while metal ion B stabilizes the leaving group, i.e. PPi<sup>34; 35</sup>.

Immediately after bond-formation, the newly generated PPi occupies the binding sites for the  $\beta$ - and  $\gamma$ -phosphates of the formerly bound nucleotide triphosphate. The same configuration also permits the nucleophilic attack of PPi on the terminal phosphodiester bond (Fig. 7B). However, studies with DNA polymerases have shown that weak binding of PPi, associated with its rapid release from the active site prevent the excision of incorporated nucleotides during active DNA synthesis<sup>40,41</sup>. In contrast, the polymerase of the duck hepatitis B virus shows high-affinity binding to PPi, which appears to be an exception in this regard<sup>42</sup>. Pyrophosphorolysis gains importance when the polymerization process is blocked by chain-terminators, provided that PPi is present at sufficiently high concentrations. Here we show that the BVDV NS5B enzyme promotes the excision of incorporated 3'-dNTPs in the presence of exogenously added PPi. Pyrophosphorolysis, and the ensuing rescue of RNA synthesis, is highly effective within a range of physiologically relevant concentrations of PPi of approximately 100  $\mu$ M<sup>43</sup>. However, the local intracellular PPi concentrations close to the membrane associated replicase complex of flaviviruses<sup>14</sup> have yet not been determined, and it remains to be seen whether high levels of PPi can be maintained in this environment. The metal ion requirements for

nucleotide incorporation and pyrophosphorolysis are similar but not identical. The efficiency of both reactions is higher with  $Mn^{2+}$  as compared to  $Mg^{2+}$ . At the same time we note that pyrophosphorolysis is sensitive to inhibition with increased concentrations of  $Mn^{2+}$ . This may reflect differential metal ion affinities with respect to the two different metal binding sites A and B, as recently proposed for the RT enzyme of yeast Ty1<sup>44</sup>. It is conceivable that  $Mn^{2+}$  binds to the B site with relatively high affinity, which may stabilize the complex with PPi. At this point, we also consider the possible existence of additional, low affinity metal binding site(s) that may affect the specific binding of PPi (Fig. 7B). These questions are important and warrant further detailed investigation, which is beyond the scope of this study.

Unlike HIV-1 RT, viral RdRps may not be able to recruit ATP or other NTPs as a PPi donor to catalyze the excision of incorporated chain-terminators (Fig. 7C). Previous biochemical data with the retroviral enzyme provided evidence for the existence of an ATP binding pocket that is located in close proximity to the active site of the enzyme<sup>18</sup>. Resistance conferring mutations appear to modulate this binding site, which helps to explain why the relevant mutant enzymes increase rates of ATP-dependent primer unblocking<sup>30; 45</sup>. ATP must bind in the reverse orientation to allow the  $\beta$ -, and  $\gamma$ -phosphates to act as a PPi-donor (Fig. 7C). Unlike HIV-1 RT, which shows low affinity to NTPs<sup>46</sup>, RdRps recruit NTPs as their natural substrates for incorporation. Thus, it is unlikely that such reverse binding plays an important role in this context. In fact, our data provide strong evidence to show that the incoming nucleotide binds to complexes with a chain-terminated primer predominantly in the correct orientation. First, NTP-dependent

primer unblocking is difficult to detect, even at millimolar concentrations of ATP or other NTPs. Second, we have shown that high concentrations of NTPs inhibit the PPi-mediated removal of the chain-terminator in dose-dependent fashion. These data suggest that the presence of nucleotide triphosphates promote the formation of a ternary dead-end complex (DEC).

Using site-specific footprinting techniques, we have recently demonstrated that the presence of the next nucleotide forces HIV-1 RT to translocate a single position further downstream<sup>33</sup>. Such a scenario is illustrated in Fig. 7D. The primer terminus occludes the N-site immediately after the incorporation of the last nucleotide (Fig. 7B). The 3'end of the primer must then translocate into the P-site to allow binding of the next nucleotide (Fig. 7D). The P-site occupation brings the active center in a position that facilitates nucleotide incorporation, but disfavors nucleotide removal (compare Figs. 7B and D). Excision can only occur when the incorporated chain-terminator occupies the N-site<sup>31; 33</sup>. For HIV-1 RT, access to N- and P-sites are controlled by a translocational equilibrium that depends on multiple parameters including the concentration of the next nucleotide<sup>33</sup>. The data in this study suggest the existence of similar control mechanisms for BVDV NS5B. First, the 3'end of the primer does not appear to move ultimately into the P-site, as shown by the fact that pyrophosphorolysis occurs efficiently in the absence of NTPs. Second, the NTP concentration required to block pyrophosphorolysis is significantly lower with the correctly templated nucleotide, as compared to nucleotides that form mispairs with the template.

Taken together, our data show that viral RdRps can excise incorporated chain-terminators in PPi-dependent reactions. Primer unblocking reactions may be relevant *in vivo* as proposed for HIV. The efficiency of rescue of RNA synthesis will critically depend on the available local concentrations of PPi and NTPs. High NTP concentrations promote the formation of a DEC that diminishes excision, and high concentrations of PPi promote excision. We also found that chain-terminated complexes are heparin-stable, which increases the probability that pyrophosphorolysis eventually occurs before the enzyme can dissociate from its nucleic acid substrate. These questions merit further investigation in the HCV system. Although both HCV and BVDV NS5B enzymes behave similarly in various biochemical assays<sup>22; 23; 25; 47</sup>, it remains to be seen whether the RdRp of HCV also promotes the excision of incorporated nucleotides to better understand the diminished potency of 3'-deoxyribonucleosides in cell-culture-based replicon systems<sup>13</sup>. Both a possible poor metabolic activation, as well as the PPi-mediated excision of incorporated nucleotide analogue should be considered in this regard. The latter reaction may also be considered in the context of nucleoside analogues that contain the 3'-hydroxyl group, e.g. ribavirin or the 2'-modified nucleosides. These inhibitors, once incorporated opposite correct or incorrect template positions, diminish the efficiency of incorporation of the following nucleotide<sup>9; 12</sup>, which likely diminishes the overall production of viral RNA. This effect might be neutralized, at least in part, if the incorporated nucleoside monophosphate is effectively removed from the primer terminus. Thus, the excision of nucleotide analogue inhibitors adds to the repertoire of reactions that may be of importance regarding the assessment of drug susceptibilities in the context of both wild type and resistant mutant viruses.



**Table 1**

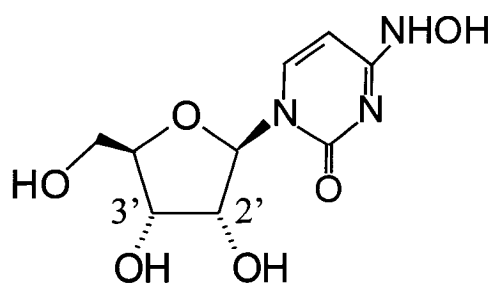
<b>Chain-terminator</b>	<b>IC<sub>50</sub> (μM) <sup>a</sup></b>	<b>Number of Possible Incorporation Sites</b>
3'-dATP	1	10
3'-dCTP	12	1
3'-dGTP	2	4 (6) <sup>b</sup>
3'-dUTP	4	3

<sup>a</sup> Values are averages of at least three independent measurements

<sup>b</sup> The number in parenthesis indicate 'correct' and the two 'incorrect' incorporation sites at positions +3 and +5

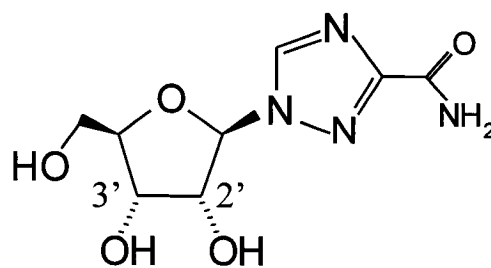
**Figure 1**

**A**



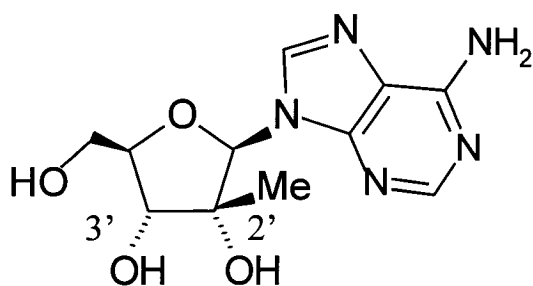
$\beta$ -D-N<sup>4</sup>-hydroxycytidine (NHC)

**B**



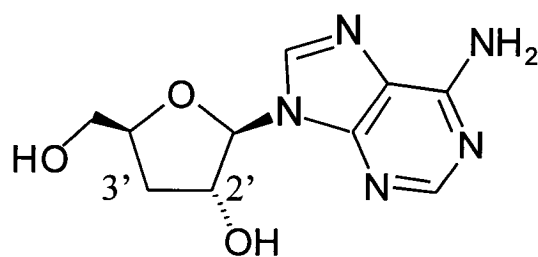
ribavirin

**C**



2'-C-methyladenosine

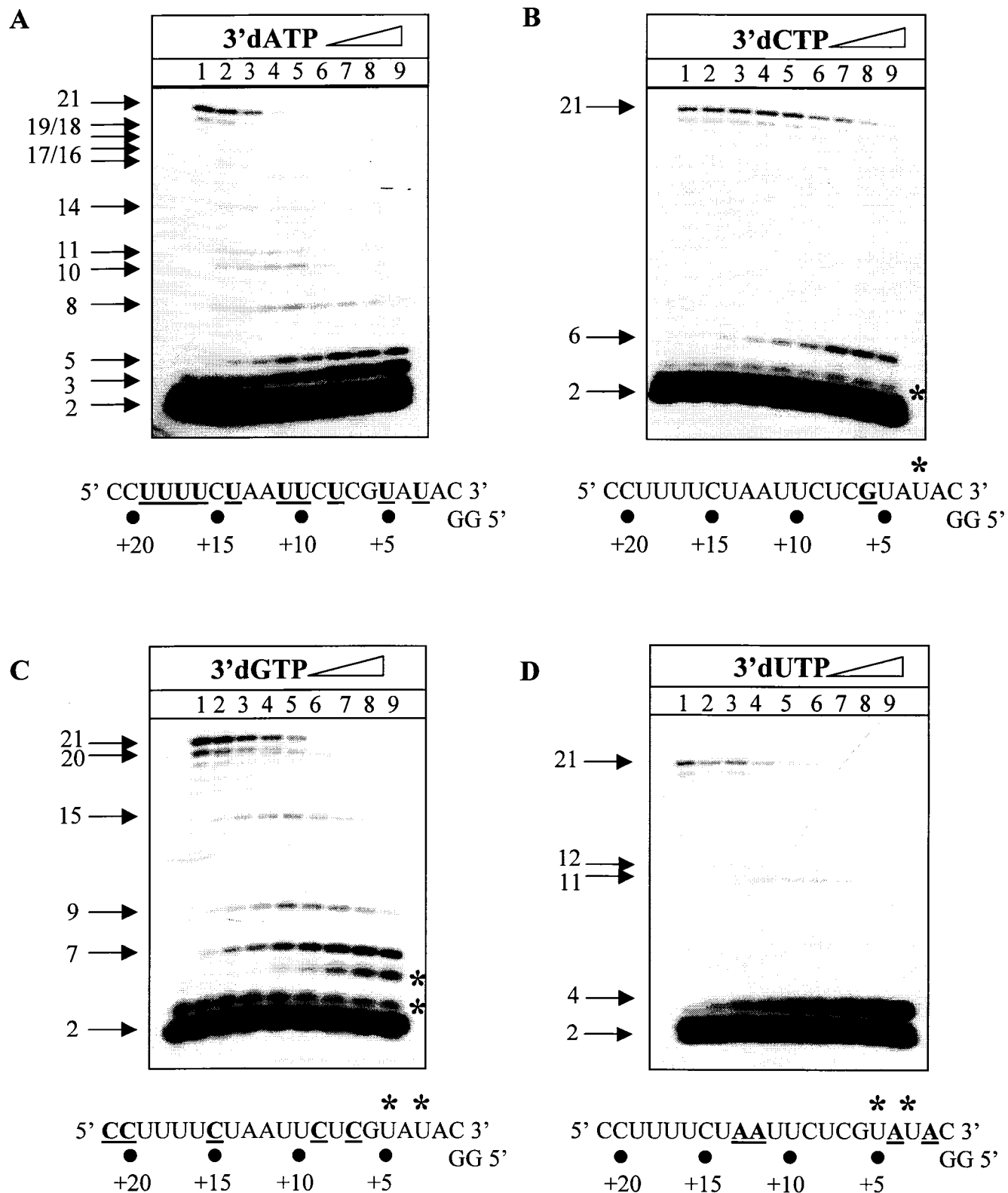
**D**



3'-deoxyadenosine

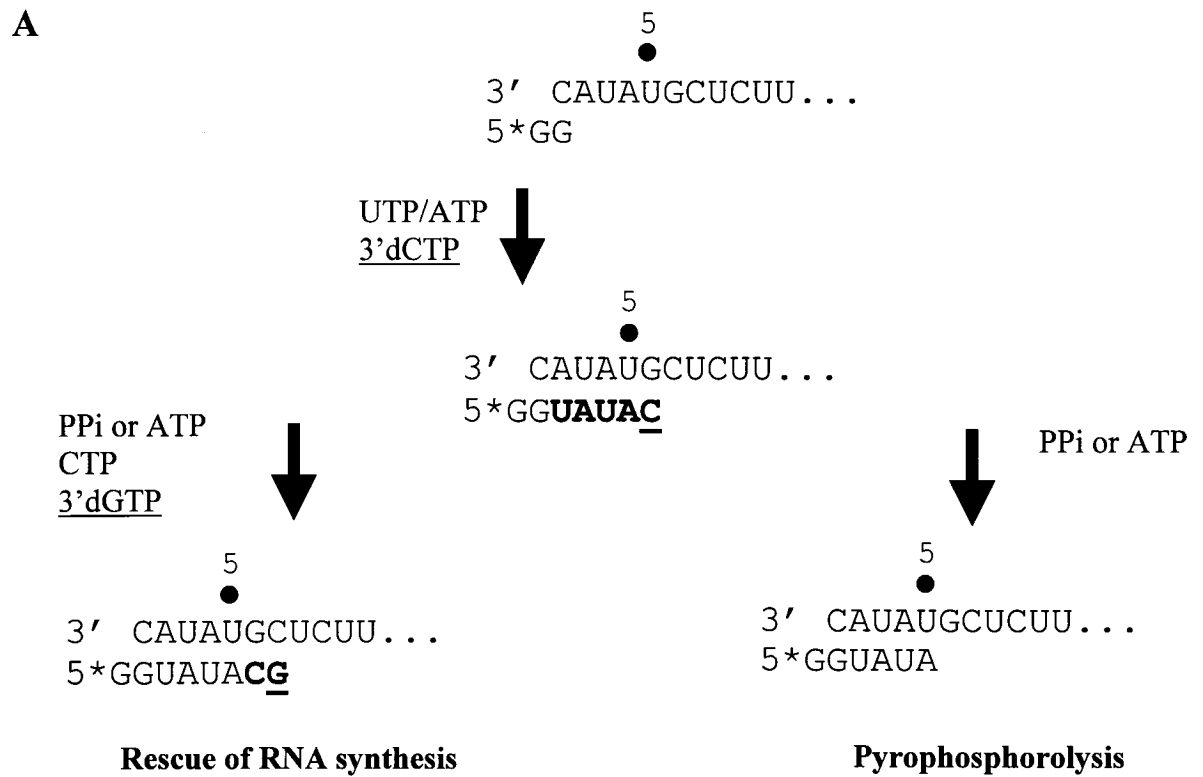
**Figure 1: Chemical structures of nucleoside analogue inhibitors of RdRps.**

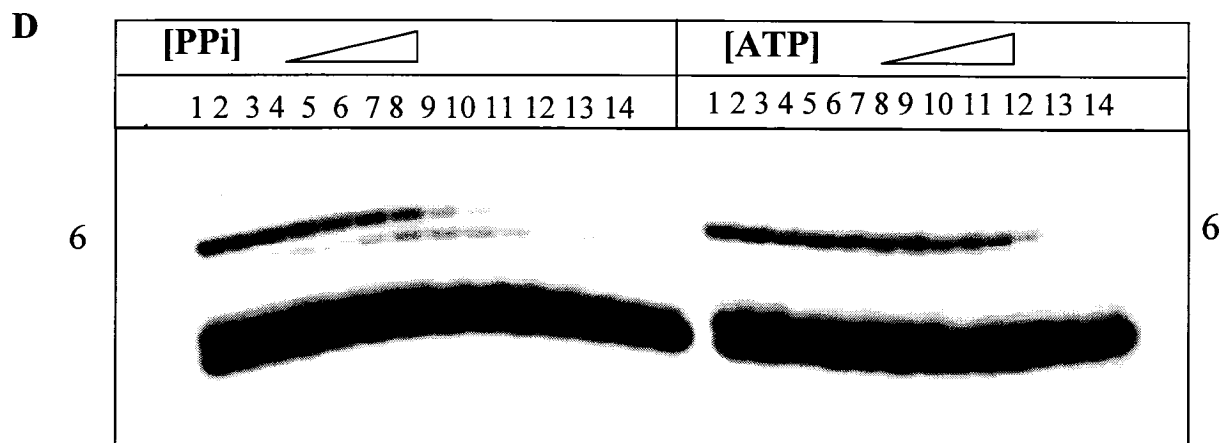
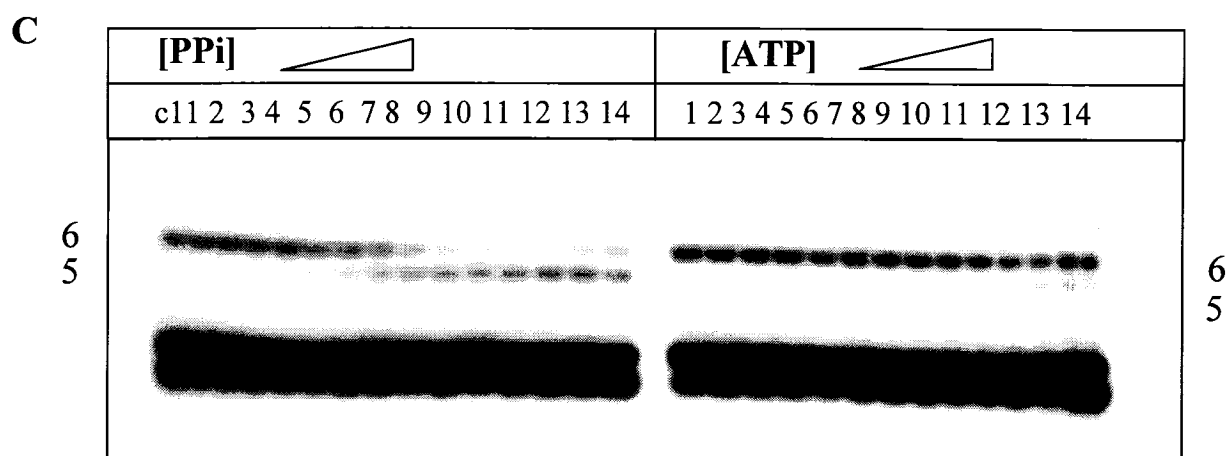
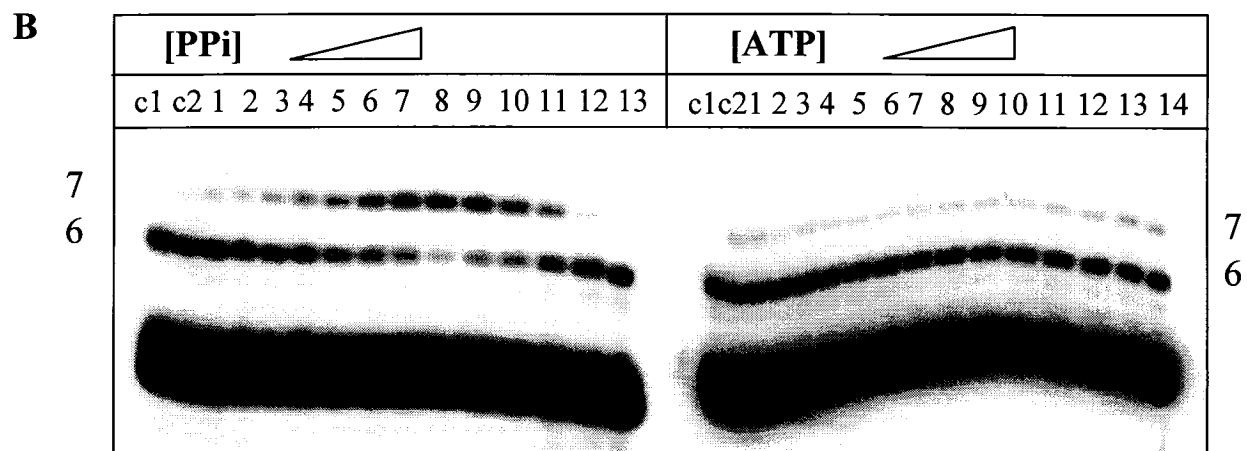
# Figure 2

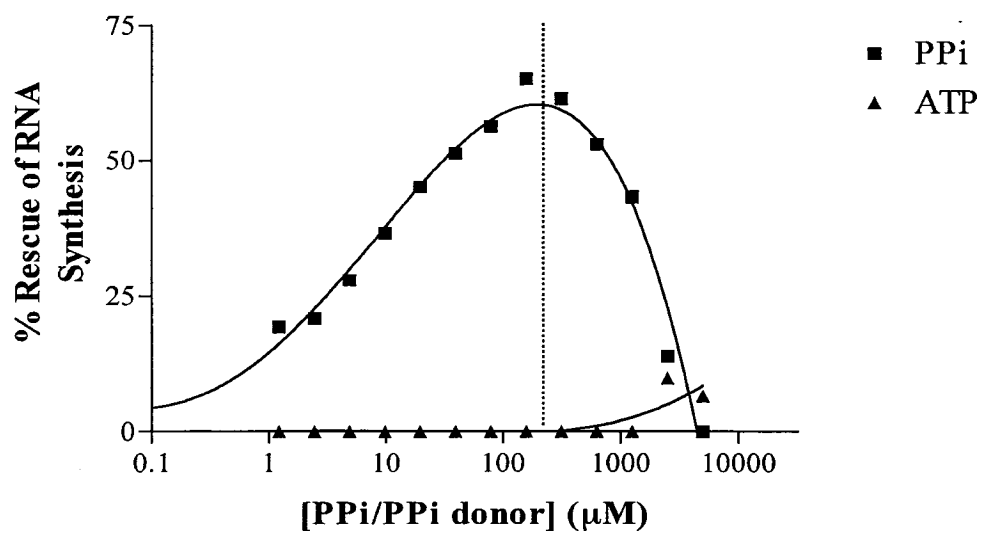
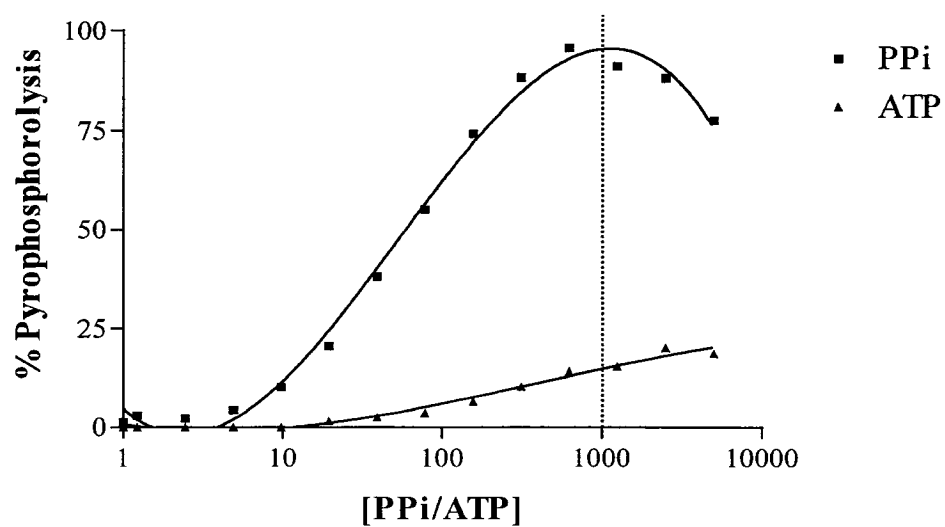
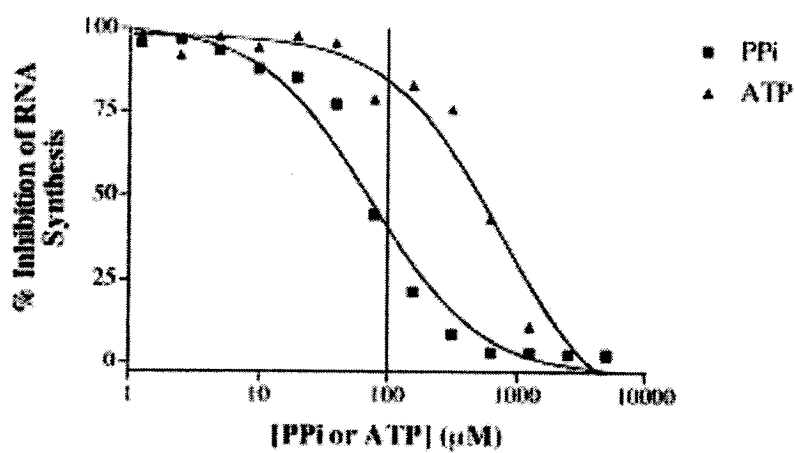


**Figure 2: Inhibition of RNA synthesis in the presence of 3'dNTPs.** Effects of increasing concentrations of each of the four 3'-dNTPs on the formation of full-length product: (A) 3'-dATP, (B) 3'-dCTP, (C) 3'-dGTP, (D) and 3'-dUTP. The nucleoside analogue was added to reaction mixtures containing the RNA template, the 5'-end-labelled dinucleotide primer (GG), and constant concentrations of 10  $\mu$ M of each of the four natural NTPs. Lane 1 is a control in the absence of nucleoside analogue triphosphates. Lanes 2-9 show reactions in the presence of the following concentrations of 3'-dNTPs: (0.78 $\mu$ M, 1.56 $\mu$ M, 3.125 $\mu$ M, 6.25 $\mu$ M, 12.5 $\mu$ M, 25 $\mu$ M, 50 $\mu$ M and 100 $\mu$ M). Reactions were allowed to proceed for 60 min. Correct sites of incorporation of the chain-terminator are indicated by arrows. Asterisks denote possible mismatch formation. Note that the numbering refers to the underlined template positions, and not to the length of the primer, since initiation takes place from the correct C:G base pair at template position +1 (see text).

# Figure 3





**E****F****G**

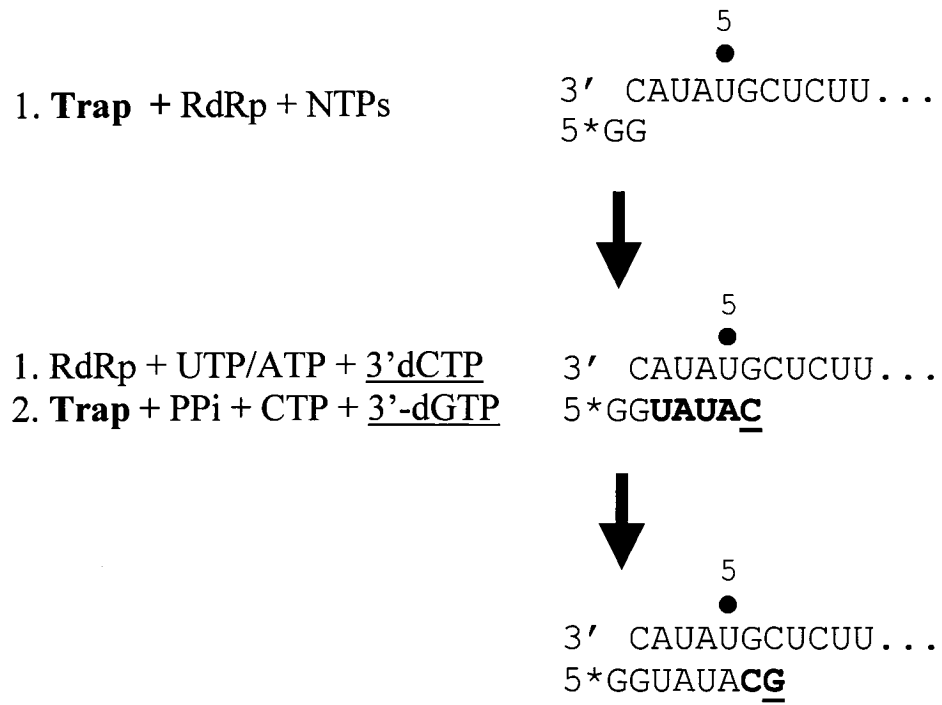
**Figure 3: PPi-dependent rescue of chain-terminated RNA synthesis.** (A) Schematic description of the assay utilized to monitor excision of the chain-terminator and the ensuing rescue of RNA synthesis at a single template position. The template and the 5'-end labelled dinucleotide primer were incubated with BVDV NS5B and a nucleotide cocktail that included 100  $\mu$ M of UTP, ATP, and 3'-dCTP. Reactions were allowed to proceed for 30 min. Newly incorporated nucleotides are shown in bold. The incorporation of the chain-terminator opposite template position +6 is underlined. Rescue of RNA synthesis was initiated by the addition of a mixture containing PPi or ATP, 200  $\mu$ M of CTP and 100  $\mu$ M of 3'-dGTP. The efficiency with which 3'-dGMP is incorporated serves as a direct measure for the efficiency of rescue of RNA synthesis. The addition of PPi or ATP alone allows direct monitoring of pyrophosphorolysis. (B) Effects of different concentrations of PPi (left panel) and ATP (right panel) on the combined excision and rescue of RNA synthesis. Lane C1 is a control that shows chain-termination at position +6 after a 30 min reaction. Lanes 1-14 show the rescue of chain-terminated RNA synthesis in the presence of different concentrations of PPi or ATP: 0 $\mu$ M, 1.22 $\mu$ M, 2.4 $\mu$ M, 4.9 $\mu$ M, 9.8 $\mu$ M, 19.5 $\mu$ M, 39 $\mu$ M, 78 $\mu$ M, 156 $\mu$ M, 312.5 $\mu$ M, 625 $\mu$ M, 1.25mM, 2.5mM and 5mM. PPi, or ATP, was added together with 200  $\mu$ M of CTP and 100  $\mu$ M of 3'-dGTP. Lane C2 is a control reaction that contained CTP and 3'-dGTP in the absence



of ATP. (C) Effects of different concentrations of PPi (left panel) and ATP (right panel) on nucleotide excision. Lane C1 is a control that shows chain-termination of the template at position +6 after 30 min, as described in A. Varying concentrations of PPi or ATP were added in lanes 1-14 to monitor the phosphorolytic excision of the nucleoside analog. (D) Effects of different concentrations of PPi and ATP on the initiation of RNA synthesis. Reactions were initiated in the presence of 100  $\mu$ M of UTP, ATP, 3'-dCTP and different concentrations of PPi (left panel) or ATP (right panel), as described above. (E), (F), (G) Graphic representation of data shown under B, C, and D, respectively.

# Figure 4

A



B

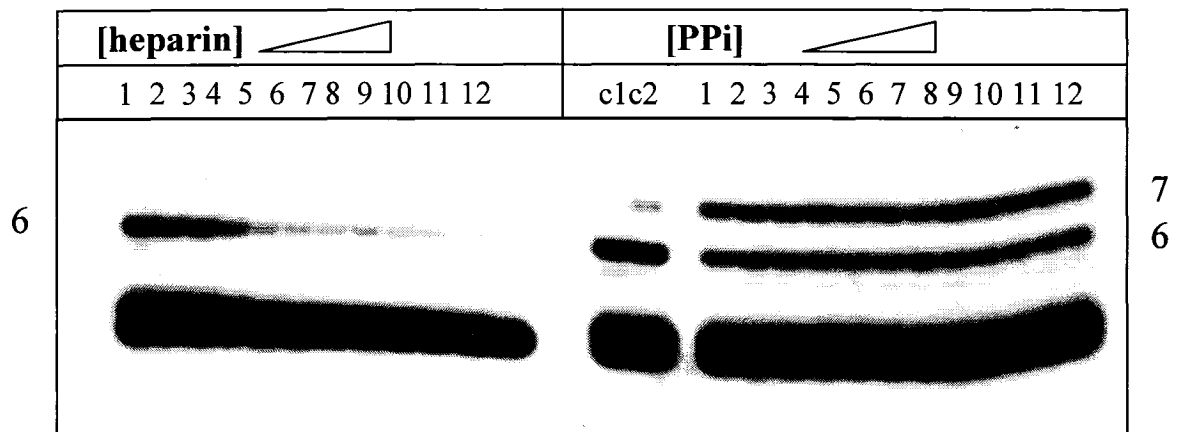


**Figure 4: Rescue of RNA synthesis in the presence of trap:** (A) Schematic representation of the experimental procedure. Reactions were conducted according to the conditions specified in Fig. 3. The addition of heparin together with the addition of PPi, allows the study of the rescue of RNA synthesis under processive reaction conditions. (B) Effect of heparin on the initiation of RNA synthesis (left panel) and combined excision/rescue reactions (right panel). Increasing concentrations of heparin were added to reactions containing 100 $\mu$ M UTP/ATP and 3'-dCTP: 0ng/ $\mu$ l, 0.5ng/ $\mu$ l, 1.0ng/ $\mu$ l, 2.0ng/ $\mu$ l, 4.0ng/ $\mu$ l, 8.0ng/ $\mu$ l, 15.0ng/ $\mu$ l, 0.03 $\mu$ g/ $\mu$ l, 0.06 $\mu$ g/ $\mu$ l, 0.125 $\mu$ g/ $\mu$ l, 0.25 $\mu$ g/ $\mu$ l and 0.5 $\mu$ g/ $\mu$ l (lanes 1-12). Excision reactions were monitored in the presence of increasing concentrations of 100  $\mu$ M PPi. Heparin was added together with PPi, CTP, and 3'-dGTP. The 3'-dCTP terminated primer prior to the initiation of PPi is shown in lane C1. Lane C2 shows a control reaction that contained CTP and 3'-dGTP in the absence of PPi.

# Figure 5

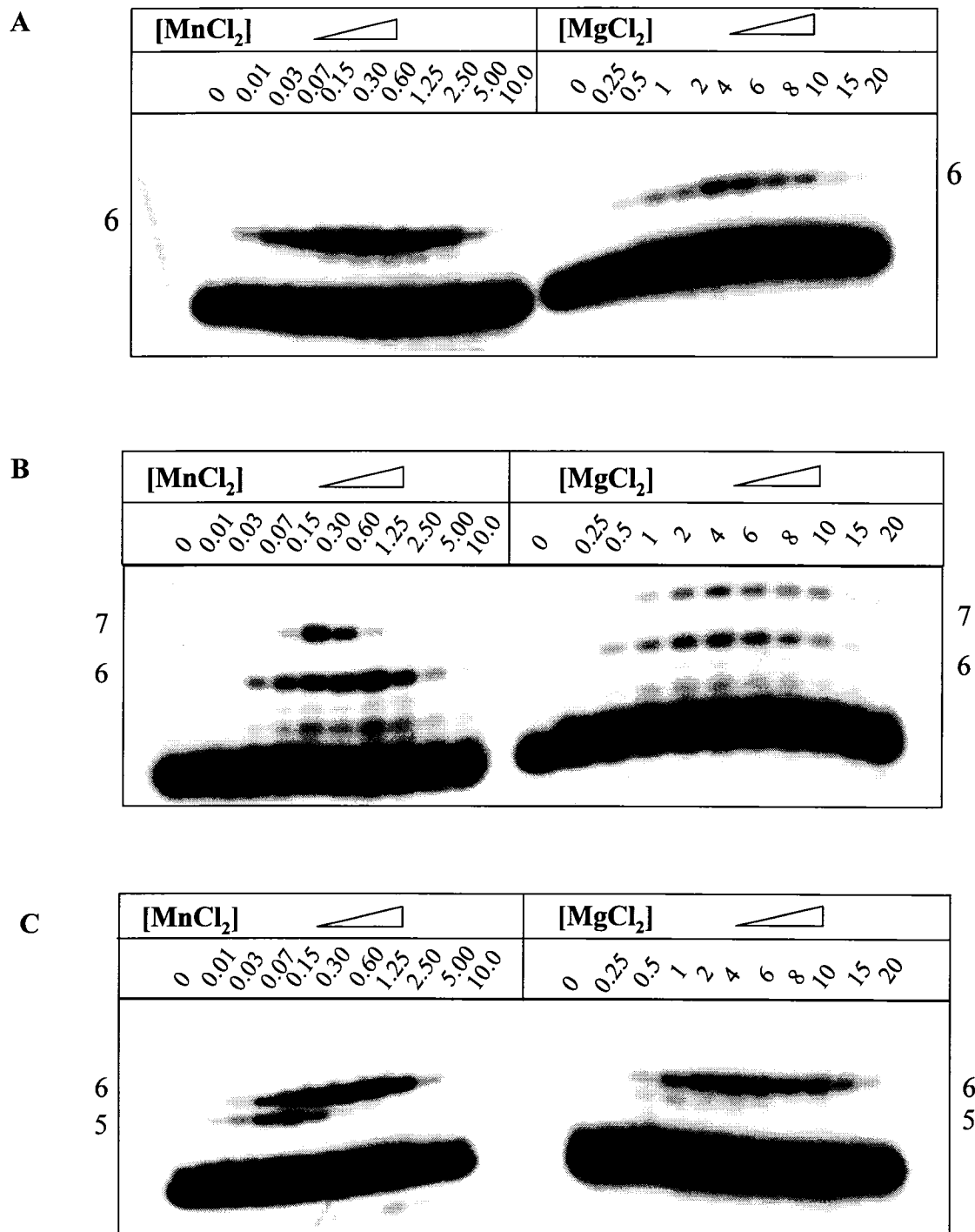
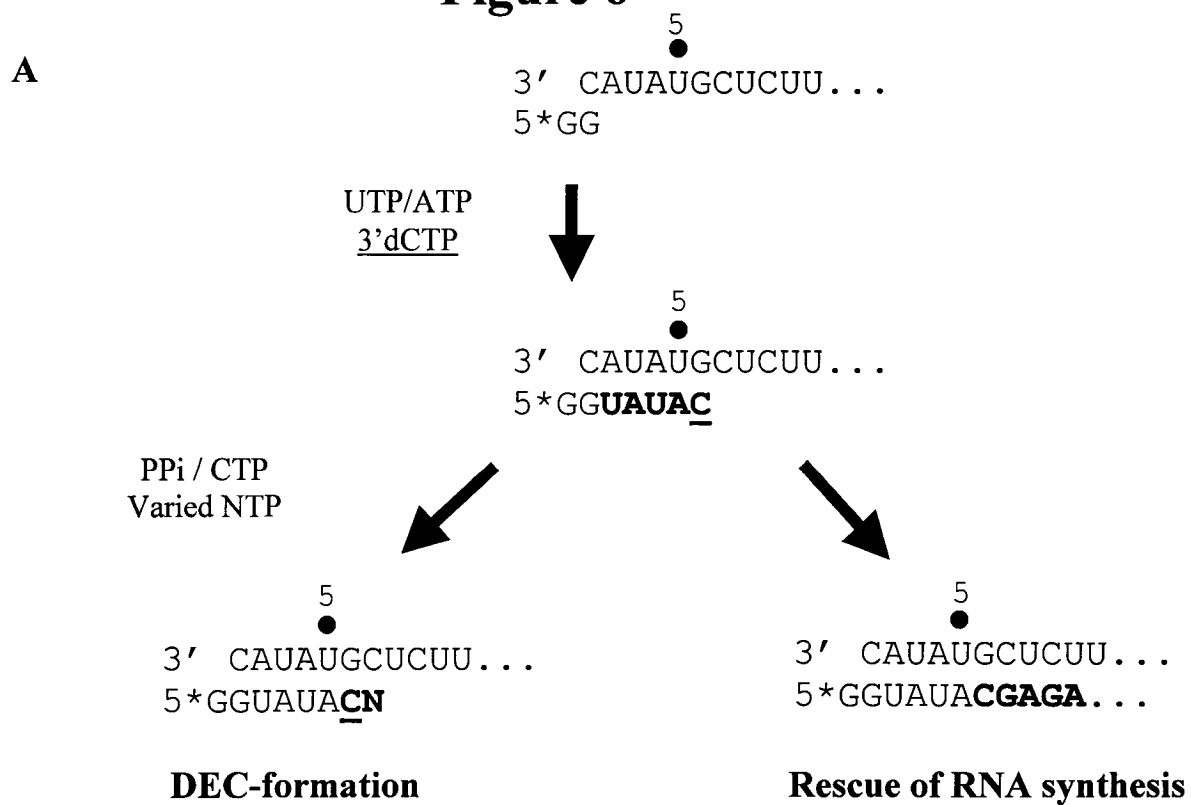
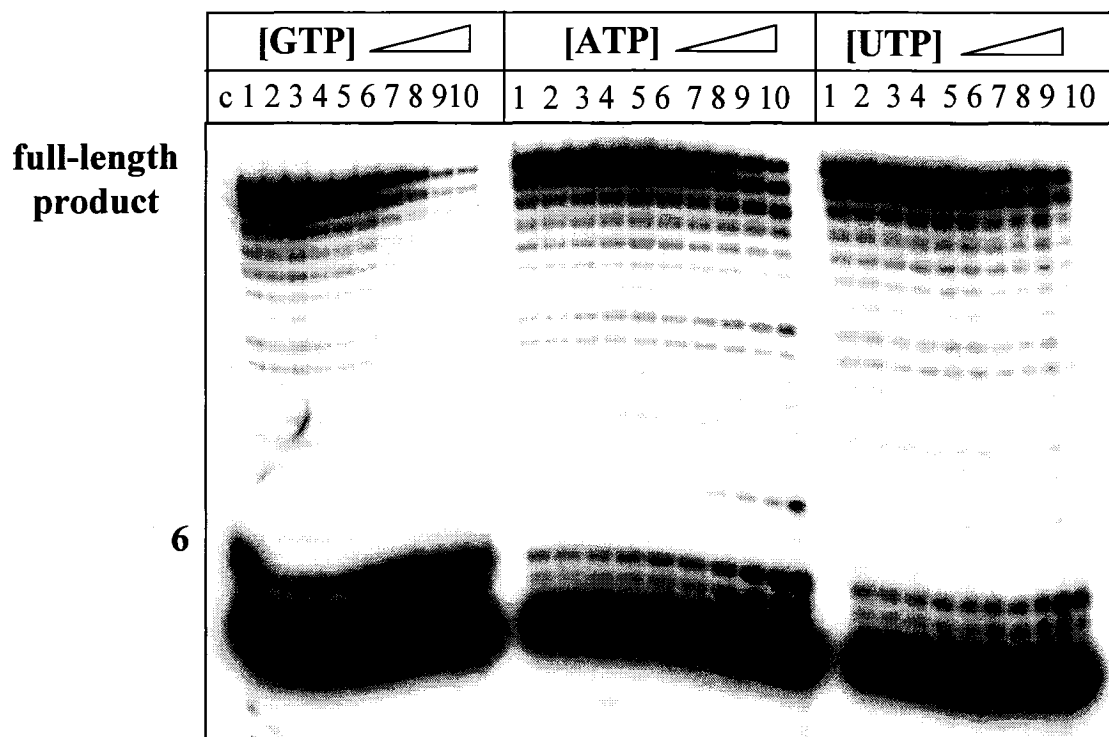


**Figure 5: Requirements for divalent metal ions.** Effects of increasing concentrations of  $\text{MnCl}_2$  (left panel) and  $\text{MgCl}_2$  (right panel) on RNA synthesis (A), rescue of RNA synthesis (B) and phosphorolytic cleavage of 3'-dCTP chain-terminator (C). Reactions were conducted according to the conditions specified in Fig. 3 using a constant concentration of 100  $\mu\text{M}$  PPI. The initiation of RNA synthesis, the excision of the chain-terminator, and the ensuing rescue reaction were all performed at different concentrations of the metal cofactor, as indicated.

# Figure 6



**B**



C

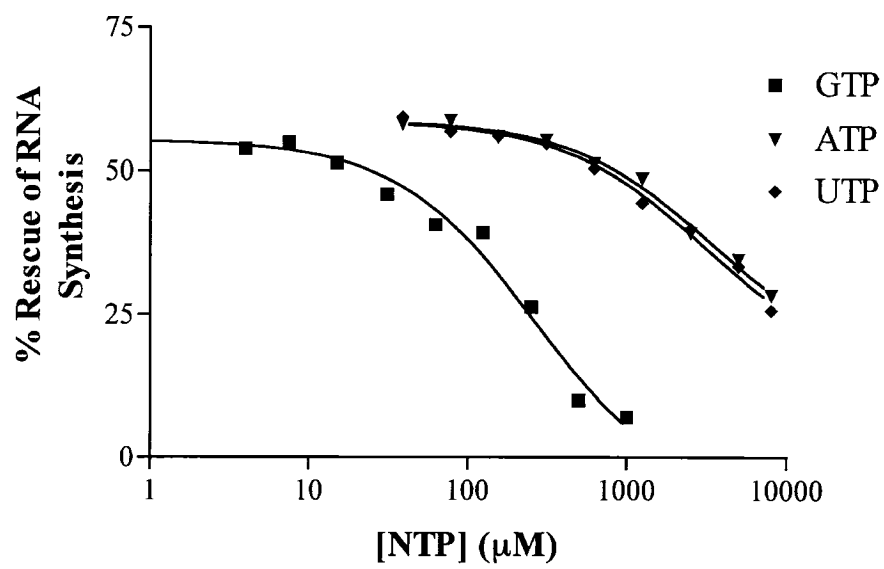
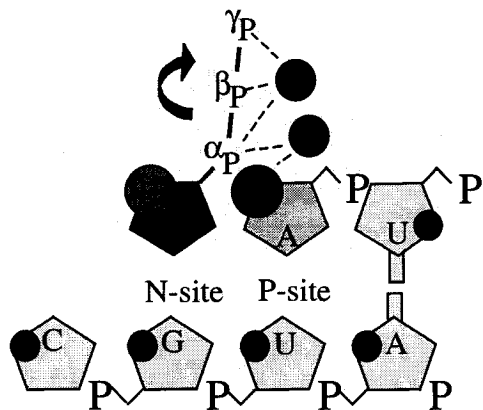


**Figure 6: Formation of a dead-end-complex (DEC).** (A) Schematic representation of the strategy used to determine the effects of the templated NTP on efficiency of rescue of RNA synthesis. The basic set-up is identical to the approach described in Fig. 3A., except that the addition of the 3'-dGTP was replaced with the addition of either GTP (next correct complementary nucleotide) or ATP or UTP (incorrect nucleotides). (B) Lane C shows a 30 min reaction to produce the 3'-dCTP-terminated primer. Lanes 1-10 show the rescue of RNA synthesis, monitored through the formation of the full-length product in the presence of increasing concentrations of GTP (left), ATP (middle), or UTP (right). Concentrations of GTP: 0 $\mu$ M (lane 1), 3.9 $\mu$ M (lane 2), 7.8 $\mu$ M (lane 3), 15.6 $\mu$ M (lane 4), 31.25 $\mu$ M (lane 5), 62.5 $\mu$ M (lane 6), 125 $\mu$ M (lane 7), 250 $\mu$ M (lane 8), 500 $\mu$ M (lane 9) and 1mM (lane 10). Concentrations of the next ATP or UTP in lanes 1-10 are 19.5 $\mu$ M, 39 $\mu$ M, 78 $\mu$ M, 156 $\mu$ M, 312.5 $\mu$ M, 625 $\mu$ M, 1.25mM, 2.5mM, 5.0mM, and 8.0mM, respectively. (C) Graphic representation of data shown in (B). The concentrations of GTP, ATP and UTP required to inhibit the rescue of RNA synthesis by 50% are indicated below.

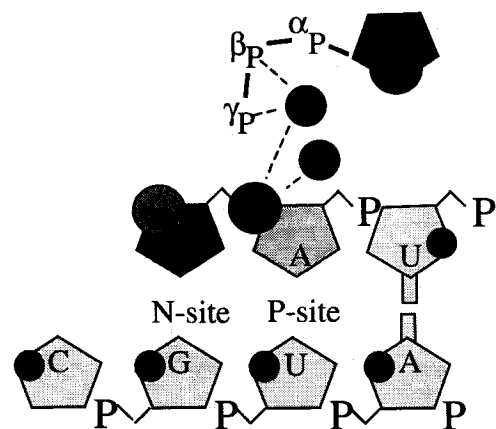
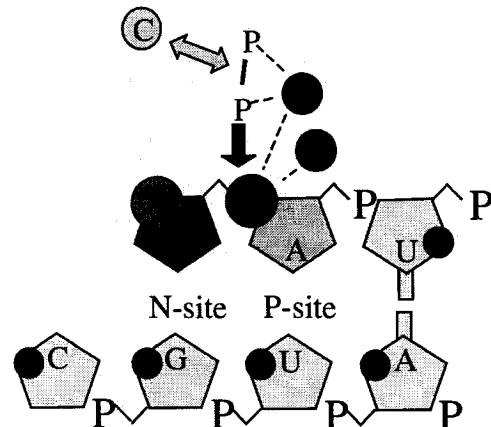


**Figure 7**

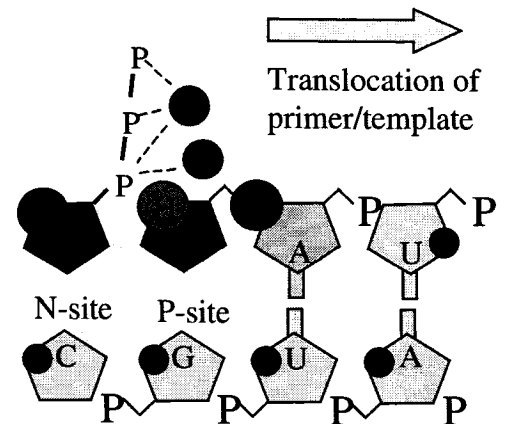
**A. Nucleotide Incorporation**



**B. Pyrophosphorolysis**



**C. NTP-dependent Excision**



**D. DEC-Formation**

**Figure 7: Models of complexes involved in nucleotide binding, chain-termination, phosphorolytic excision, and DEC-formation.** The proposed models describe events that take place directly at the active site, and do not rely on specific assumptions with respect to nucleic acid binding characteristics<sup>30; 31; 32; 33</sup>. Primer/template sequences are identical with sequences used throughout this study. (A) Nucleotide incorporation. The incoming nucleotide (middle blue), which is the chain-terminating 3'-dCTP, in this case, binds to the nucleotide binding site termed the N-site. The primer terminus (light blue) occupies the priming site or P-site. Specific binding sites for divalent metal ions (pink circles) are shown in close proximity to the  $\alpha$ -,  $\beta$ -, and  $\gamma$  phosphates of the incoming nucleotides, according to the two-metal ion mechanism proposed by Steitz (1999)<sup>35</sup>. The attack of the 3'-OH-group (red) of the 3'-end of the primer, and the ensuing release of PPi is indicated by the red arrow. (B) Pyrophosphorolysis. PPi occupies the binding sites that are occupied by the  $\beta$ -, and  $\gamma$  phosphates of the incoming nucleotides in A. Putative additional  $Mn^{2+}$  site(s) (C, yellow) might alter the specific binding mode at relatively high concentration of the metal ion (see text). (C) NTP-dependent primer unblocking. NTPs can only act as PPi-donors if the  $\alpha$ - and  $\beta$ -phosphates are in a position to attack the incorporated chain-terminator. This requires reverse binding of the NTP substrate, which is unlikely in the context of RdRps. (D) DEC-formation. Following the incorporation of the chain-terminator, the 3'-end of the primer must leave the N-site to allow binding of the next nucleotide. The translocation of the nucleic acid substrate (grey arrow) brings the chain-terminator to the P-site. Primer unblocking through phosphorolytic excision cannot occur in this configuration.

## References

1. Blight, K. J., Kolykhalov, A. A. & Rice, C. M. (2000). Efficient initiation of HCV RNA replication in cell culture. *Science* 290, 1972-4.
2. Lohmann, V., Korner, F., Koch, J., Herian, U., Theilmann, L. & Bartenschlager, R. (1999). Replication of subgenomic hepatitis C virus RNAs in a hepatoma cell line. *Science* 285, 110-3.
3. Bartenschlager, R. (2002). Hepatitis C virus replicons: potential role for drug development. *Nat Rev Drug Discov* 1, 911-6.
4. Baginski, S. G., Pevear, D. C., Seipel, M., Sun, S. C., Benetatos, C. A., Chunduru, S. K., Rice, C. M. & Collett, M. S. (2000). Mechanism of action of a pestivirus antiviral compound. *Proc Natl Acad Sci U S A* 97, 7981-6.
5. Sun, J. H., Lemm, J. A., O'Boyle, D. R., 2nd, Racela, J., Colonno, R. & Gao, M. (2003). Specific inhibition of bovine viral diarrhea virus replicase. *J Virol* 77, 6753-60.
6. Stuyver, L. J., Whitaker, T., McBrayer, T. R., Hernandez-Santiago, B. I., Lostia, S., Tharnish, P. M., Ramesh, M., Chu, C. K., Jordan, R., Shi, J., Rachakonda, S., Watanabe, K. A., Otto, M. J. & Schinazi, R. F. (2003). Ribonucleoside analogue that blocks replication of bovine viral diarrhea and hepatitis C viruses in culture. *Antimicrob Agents Chemother* 47, 244-54.
7. Graci, J. D. & Cameron, C. E. (2002). Quasispecies, error catastrophe, and the antiviral activity of ribavirin. *Virology* 298, 175-80.
8. Crotty, S., Maag, D., Arnold, J. J., Zhong, W., Lau, J. Y., Hong, Z., Andino, R. & Cameron, C. E. (2000). The broad-spectrum antiviral ribonucleoside ribavirin is an RNA virus mutagen. *Nat Med* 6, 1375-9.
9. Maag, D., Castro, C., Hong, Z. & Cameron, C. E. (2001). Hepatitis C virus RNA-dependent RNA polymerase (NS5B) as a mediator of the antiviral activity of ribavirin. *J Biol Chem* 276, 46094-8.
10. Crotty, S., Cameron, C. E. & Andino, R. (2001). RNA virus error catastrophe: direct molecular test by using ribavirin. *Proc Natl Acad Sci U S A* 98, 6895-900.
11. Pfeiffer, J. K. & Kirkegaard, K. (2003). A single mutation in poliovirus RNA-dependent RNA polymerase confers resistance to mutagenic nucleotide analogs via increased fidelity. *Proc Natl Acad Sci U S A* 100, 7289-94.
12. Carroll, S. S., Tomassini, J. E., Bosserman, M., Getty, K., Stahlhut, M. W., Eldrup, A. B., Bhat, B., Hall, D., Simcoe, A. L., LaFemina, R., Rutkowski, C. A., Wolanski, B., Yang, Z., Migliaccio, G., De Francesco, R., Kuo, L. C., MacCoss, M. & Olsen, D. B. (2003). Inhibition of hepatitis C virus RNA replication by 2'-modified nucleoside analogs. *J Biol Chem* 278, 11979-84.
13. Shim, J., Larson, G., Lai, V., Naim, S. & Wu, J. Z. (2003). Canonical 3'-deoxyribonucleotides as a chain terminator for HCV NS5B RNA-dependent RNA polymerase. *Antiviral Res* 58, 243-51.
14. Lai, V. C., Dempsey, S., Lau, J. Y., Hong, Z. & Zhong, W. (2003). In vitro RNA replication directed by replicase complexes isolated from the subgenomic replicon cells of hepatitis C virus. *J Virol* 77, 2295-300.
15. Gallois-Montbrun, S., Chen, Y., Dutartre, H., Sophys, M., Morera, S., Guerreiro, C., Schneider, B., Mulard, L., Janin, J., Veron, M., Deville-Bonne, D. & Canard, J. (2003). Inhibition of hepatitis C virus RNA replication by 2'-modified nucleoside analogs. *J Biol Chem* 278, 11979-84.

- B. (2003). Structural analysis of the activation of ribavirin analogs by NDP kinase: comparison with other ribavirin targets. *Mol Pharmacol* 63, 538-46.
16. Arion, D., Kaushik, N., McCormick, S., Borkow, G. & Parniak, M. A. (1998). Phenotypic mechanism of HIV-1 resistance to 3'-azido-3'-deoxythymidine (AZT): increased polymerization processivity and enhanced sensitivity to pyrophosphate of the mutant viral reverse transcriptase. *Biochemistry* 37, 15908-17.
  17. Meyer, P. R., Matsuura, S. E., So, A. G. & Scott, W. A. (1998). Unblocking of chain-terminated primer by HIV-1 reverse transcriptase through a nucleotide-dependent mechanism. *Proc Natl Acad Sci U S A* 95, 13471-6.
  18. Meyer, P. R., Matsuura, S. E., Mian, A. M., So, A. G. & Scott, W. A. (1999). A mechanism of AZT resistance: an increase in nucleotide-dependent primer unblocking by mutant HIV-1 reverse transcriptase. *Mol Cell* 4, 35-43.
  19. Mas, A., Parera, M., Briones, C., Soriano, V., Martinez, M. A., Domingo, E. & Menendez-Arias, L. (2000). Role of a dipeptide insertion between codons 69 and 70 of HIV-1 reverse transcriptase in the mechanism of AZT resistance. *Embo J* 19, 5752-61.
  20. Kao, C. C., Del Vecchio, A. M. & Zhong, W. (1999). De novo initiation of RNA synthesis by a recombinant flaviviridae RNA-dependent RNA polymerase. *Virology* 253, 1-7.
  21. Kao, C. C., Singh, P. & Ecker, D. J. (2001). De novo initiation of viral RNA-dependent RNA synthesis. *Virology* 287, 251-60.
  22. Ranjith-Kumar, C. T., Gutshall, L., Kim, M. J., Sarisky, R. T. & Kao, C. C. (2002). Requirements for de novo initiation of RNA synthesis by recombinant flaviviral RNA-dependent RNA polymerases. *J Virol* 76, 12526-36.
  23. Zhong, W., Ferrari, E., Lesburg, C. A., Maag, D., Ghosh, S. K., Cameron, C. E., Lau, J. Y. & Hong, Z. (2000). Template/primer requirements and single nucleotide incorporation by hepatitis C virus nonstructural protein 5B polymerase. *J Virol* 74, 9134-43.
  24. Gotte, M., Arion, D., Parniak, M. A. & Wainberg, M. A. (2000). The M184V mutation in the reverse transcriptase of human immunodeficiency virus type 1 impairs rescue of chain-terminated DNA synthesis. *J Virol* 74, 3579-85.
  25. Ranjith-Kumar, C. T., Kim, Y. C., Gutshall, L., Silverman, C., Khandekar, S., Sarisky, R. T. & Kao, C. C. (2002). Mechanism of de novo initiation by the hepatitis C virus RNA-dependent RNA polymerase: role of divalent metals. *J Virol* 76, 12513-25.
  26. Zhong, W., Uss, A. S., Ferrari, E., Lau, J. Y. & Hong, Z. (2000). De novo initiation of RNA synthesis by hepatitis C virus nonstructural protein 5B polymerase. *J Virol* 74, 2017-22.
  27. Hardy, R. W., Marcotrigiano, J., Blight, K. J., Majors, J. E. & Rice, C. M. (2003). Hepatitis C virus RNA synthesis in a cell-free system isolated from replicon-containing hepatoma cells. *J Virol* 77, 2029-37.
  28. Tabor, S. & Richardson, C. C. (1990). DNA sequence analysis with a modified bacteriophage T7 DNA polymerase. Effect of pyrophosphorolysis and metal ions. *J Biol Chem* 265, 8322-8.

29. Tong, W., Lu, C. D., Sharma, S. K., Matsuura, S., So, A. G. & Scott, W. A. (1997). Nucleotide-induced stable complex formation by HIV-1 reverse transcriptase. *Biochemistry* 36, 5749-57.
30. Boyer, P. L., Sarafianos, S. G., Arnold, E. & Hughes, S. H. (2001). Selective excision of AZTMP by drug-resistant human immunodeficiency virus reverse transcriptase. *J Virol* 75, 4832-42.
31. Sarafianos, S. G., Clark, A. D., Jr., Das, K., Tuske, S., Birktoft, J. J., Ilankumaran, P., Ramesha, A. R., Sayer, J. M., Jerina, D. M., Boyer, P. L., Hughes, S. H. & Arnold, E. (2002). Structures of HIV-1 reverse transcriptase with pre- and post-translocation AZTMP-terminated DNA. *Embo J* 21, 6614-24.
32. Sarafianos, S. G., Clark, A. D., Jr., Tuske, S., Squire, C. J., Das, K., Sheng, D., Ilankumaran, P., Ramesha, A. R., Kroth, H., Sayer, J. M., Jerina, D. M., Boyer, P. L., Hughes, S. H. & Arnold, E. (2003). Trapping HIV-1 reverse transcriptase before and after translocation on DNA. *J Biol Chem* 278, 16280-8.
33. Marchand, B. & Gotte, M. (2003). Site-specific footprinting reveals differences in the translocation status of HIV-1 reverse transcriptase: Implications for polymerase translocation and drug resistance. *J Biol Chem*.
34. Doublie, S., Sawaya, M. R. & Ellenberger, T. (1999). An open and closed case for all polymerases. *Structure Fold Des* 7, R31-5.
35. Steitz, T. A. (1999). DNA polymerases: structural diversity and common mechanisms. *J Biol Chem* 274, 17395-8.
36. O'Farrell, D., Trowbridge, R., Rowlands, D. & Jager, J. (2003). Substrate complexes of hepatitis C virus RNA polymerase (HC-J4): structural evidence for nucleotide import and de-novo initiation. *J Mol Biol* 326, 1025-35.
37. Lesburg, C. A., Cable, M. B., Ferrari, E., Hong, Z., Mannarino, A. F. & Weber, P. C. (1999). Crystal structure of the RNA-dependent RNA polymerase from hepatitis C virus reveals a fully encircled active site. *Nat Struct Biol* 6, 937-43.
38. Bressanelli, S., Tomei, L., Rey, F. A. & De Francesco, R. (2002). Structural analysis of the hepatitis C virus RNA polymerase in complex with ribonucleotides. *J Virol* 76, 3482-92.
39. Bressanelli, S., Tomei, L., Roussel, A., Incitti, I., Vitale, R. L., Mathieu, M., De Francesco, R. & Rey, F. A. (1999). Crystal structure of the RNA-dependent RNA polymerase of hepatitis C virus. *Proc Natl Acad Sci U S A* 96, 13034-9.
40. Hsieh, J. C., Zinnen, S. & Modrich, P. (1993). Kinetic mechanism of the DNA-dependent DNA polymerase activity of human immunodeficiency virus reverse transcriptase. *J Biol Chem* 268, 24607-13.
41. Dahlberg, M. E. & Benkovic, S. J. (1991). Kinetic mechanism of DNA polymerase I (Klenow fragment): identification of a second conformational change and evaluation of the internal equilibrium constant. *Biochemistry* 30, 4835-43.
42. Urban, S., Fischer, K. P. & Tyrrell, D. L. (2001). Efficient pyrophosphorolysis by a hepatitis B virus polymerase may be a primer-unblocking mechanism. *Proc Natl Acad Sci U S A* 98, 4984-9.
43. Barshop, B. A., Adamson, D. T., Vellom, D. C., Rosen, F., Epstein, B. L. & Seegmiller, J. E. (1991). Luminescent immobilized enzyme test systems for inorganic pyrophosphate: assays using firefly luciferase and nicotinamide-

- mononucleotide adenylyl transferase or adenosine-5'-triphosphate sulfurylase. *Anal Biochem* 197, 266-72.
44. Bolton, E. C., Mildvan, A. S. & Boeke, J. D. (2002). Inhibition of reverse transcription in vivo by elevated manganese ion concentration. *Mol Cell* 9, 879-89.
  45. Chamberlain, P. P., Ren, J., Nichols, C. E., Douglas, L., Lennerstrand, J., Larder, B. A., Stuart, D. I. & Stammers, D. K. (2002). Crystal structures of Zidovudine- or Lamivudine-resistant human immunodeficiency virus type 1 reverse transcriptases containing mutations at codons 41, 184, and 215. *J Virol* 76, 10015-9.
  46. Cases-Gonzalez, C. E., Gutierrez-Rivas, M. & Menendez-Arias, L. (2000). Coupling ribose selection to fidelity of DNA synthesis. The role of Tyr-115 of human immunodeficiency virus type 1 reverse transcriptase. *J Biol Chem* 275, 19759-67.
  47. Zhong, W., Gutshall, L. L. & Del Vecchio, A. M. (1998). Identification and characterization of an RNA-dependent RNA polymerase activity within the nonstructural protein 5B region of bovine viral diarrhea virus. *J Virol* 72, 9365-9.
  48. Mendez, E., Ruggli, N., Collett, M. S. & Rice, C. M. (1998). Infectious bovine viral diarrhea virus (strain NADL) RNA from stable cDNA clones: a cellular insert determines NS3 production and viral cytopathogenicity. *J Virol* 72, 4737-45.
  49. Lai, V. C., Kao, C. C., Ferrari, E., Park, J., Uss, A. S., Wright-Minogue, J., Hong, Z. & Lau, J. Y. (1999). Mutational analysis of bovine viral diarrhea virus RNA-dependent RNA polymerase. *J Virol* 73, 10129-36.
  50. Boosalis, M. S., Petruska, J. & Goodman, M. F. (1987). DNA polymerase insertion fidelity. Gel assay for site-specific kinetics. *J Biol Chem* 262, 14689-96.

## **CHAPTER 3**

### **CONTROL OF TEMPLATE POSITIONING DURING *DE NOVO* INITIATION OF RNA SYNTHESIS BY THE BVDV NS5B POLYMERASE**

This chapter was adapted from an article that appeared in *Journal of Biological Chemistry* (*in press*, 2006).

### **Preface to Chapter 3:**

Based on the data presented in Chapter 2, which showed that the BVDV polymerase was able to efficiently incorporate chain-terminating nucleotides to arrest RNA synthesis, we utilized these nucleotide analogues as tools in subsequent experiments to study the specific events that take place during initiation of RNA synthesis. Currently, the understanding of the mechanisms involved during *de novo* initiation of RNA synthesis by RdRps remains incomplete. Recent crystallographic data have shown that the BVDV polymerase binds an additional GTP to a guanosine-specific binding site (G-site), just upstream of the active center. In contrast, a so-called “allosteric” GTP-specific binding pocket is located at a position further away from the active site of the HCV polymerase. For both enzymes, the underlying function of this G-site, as well as the consequences of GTP binding during initiation is unknown. We thus explored the functional role(s) of this G-site during *de novo* initiation of RNA synthesis and analyzed whether *de novo* initiation by RdRps is based on a common mechanism.



## Abstract

The RNA-dependent RNA polymerase (RdRp) of the hepatitis C virus (HCV) and the bovine viral diarrhea virus (BVDV) are able to initiate RNA synthesis *de novo* in the absence of a primer. Previous crystallographic data have pointed to the existence of a GTP-specific binding site (G-site) that is located in the vicinity of the active site of the BVDV enzyme. Here we have studied the functional role of the G-site, and present evidence to show that specific GTP binding affects the positioning of the template during *de novo* initiation. Following the formation of the first phosphodiester bond, the polymerase translocates relative to the newly synthesized dinucleotide, which brings the 5' end of the primer into the G-site, releasing the previously bound GTP. At this stage, the 3' end of the template can remain opposite to the 5' end of the primer, or be repositioned to its original location before RNA synthesis proceeds. We show that the template can freely move between the two locations, and both complexes can isomerize to equilibrium. These data suggest that the bound GTP can stabilize the interaction between the 3' end of the template and the priming nucleotide, preventing the template to overshoot and extend beyond the active site during *de novo* initiation. The HCV enzyme utilizes a dinucleotide primer exclusively from the blunt end; the existence of a functionally equivalent G-site is therefore uncertain. For the BVDV polymerase we show that *de novo* initiation is severely compromised by the T320A mutant that likely affects hydrogen bonding between the G-site and the guanine base. Dinucleotide primed reactions are not influenced by this mutation, which supports the notion that the G-site is located in close proximity but not at the active site of the enzyme.

## Introduction

Despite structural and functional differences among various viral polymerases, previous biochemical and crystallographic data suggested that several distinct steps define a minimum, general mechanism of DNA or RNA synthesis<sup>1; 2; 3; 4</sup>. These steps involve binding of the nucleoside triphosphate, a conformational change that traps the nucleotide substrate, formation of the first phosphodiester bond, and the release of pyrophosphate (PPi). The addition of the next nucleotide requires that the polymerase translocates a single position further downstream relative to the primer/template. This movement clears the nucleotide binding site in a processive mode of polymerization before the enzyme dissociates from its nucleic acid substrate. Such a mechanism is likely to be relevant during elongation of a growing DNA or RNA chain; however, the initiation of the reaction is often more complex. Initiation in the absence of a primer, referred to as *de novo* initiation, is of particular interest in this regard.

Viral RNA-dependent RNA polymerases (RdRps) that belong to members of the *Flaviviridae* family, which includes the hepatitis C virus (HCV) and the related bovine viral diarrhea virus (BVDV), were shown to initiate RNA synthesis *de novo*<sup>5; 6; 7; 8; 9; 10; 11; 12</sup>. Both HCV and BVDV contain a plus-stranded RNA genome, which encodes a single polyprotein that is processed into several structural and non-structural proteins<sup>13</sup>. The non-structural protein 5B (NS5B) shows RdRp-activity that is required for viral replication<sup>14; 15; 16; 17; 18</sup>. A minimum mechanism of *de novo* initiation likely involves binding of the initiating nucleotide (NTPi) at a specific site of the enzyme referred to as

the priming or initiation site (P-site)<sup>19</sup>. For polymerases that recruit a primer, the P-site is occupied by the 3'-terminal nucleotide of the primer. The first NTP substrate (NTP<sub>i</sub>+1) that is later attached to the primer terminus (primed RNA synthesis) or to the initiating nucleotide (*de novo* initiation, Fig. 1) binds to the nucleotide binding site (N-site, also referred to as catalytic site or substrate site). Both nucleotides NTP<sub>i</sub> and NTP<sub>i</sub>+1 need to be aligned such that the 3'OH group of the initiating nucleotide in the P-site can attack the  $\alpha$ -phosphate of the nucleotide substrate in the N-site. Following catalysis, the release of PP<sub>i</sub>, and translocation, the 3' end of the newly formed dinucleotide (NTP<sub>i</sub>+1) occupies the P-site and the next incoming nucleotide (NTP<sub>i</sub>+2) gains access to the N-site, which permits another cycle of RNA synthesis<sup>20</sup>.

Nucleotide binding to both P- and N-sites is likely to be necessary, but not sufficient to efficiently initiate RNA synthesis in the absence of a primer. Crystallographic data suggested that both BVDV NS5B and the HCV enzyme form specific GTP binding sites, albeit at different locations<sup>21; 22</sup>. In the HCV enzyme, a low-affinity G-specific binding site is seen 30Å away from the polymerase active site<sup>21</sup>. Possible effects on RNA synthesis, if any, would be mediated indirectly if one considers the long distance. In contrast, the structure of the BVDV polymerase bound to a GTP substrate revealed the existence of a GTP-specific binding site, herein referred to as G-site, that is located  $\approx 4$  to 6Å upstream of the P-site<sup>22</sup>. This is supported by superimposing the BVDV structural data onto the solved crystal structure of the related phi6 ( $\phi$ 6) bacteriophage polymerase with bound template and an initiating GTP<sub>i</sub><sup>20</sup>. The 3'-OH group of the bound GTP is seen in the vicinity of the  $\alpha$ - and  $\beta$ - phosphates of the modeled

nucleotide that occupies the P-site. This location suggests a possible role in the process of *de novo* initiation. Based on this model, it has been proposed that the bound GTP helps to position the initiating NTP<sub>i</sub> in an orientation that facilitates the attack on the first nucleotide substrate NTP<sub>i+1</sub> (Fig. 1).

*De novo* initiation requires that the 3' end of the template interacts specifically with the initiating nucleotide NTP<sub>i</sub><sup>23; 24</sup>. Here we show that the GTP-specific binding site of BVDV NS5B can control the precise positioning of the template strand. A dinucleotide primer with a guanosine monophosphate (GMP) at its 5' end binds preferentially to a 3'-recessed template. Specific binding of the 5' terminal guanosine to the G-site, and, by extension, specific binding of GTP during *de novo* initiation, appears to prevent overshooting of the template. Based on comparative analyses of *de novo*- and dinucleotide-primed reactions, we propose a model for early steps of G-site dependent RNA synthesis by BVDV NS5B.

## Material and Methods

**Enzymes and nucleic acids** – Truncated versions of the BVDV (BVDVΔ18) and HCV (HCVΔ21) NS5B, which lack the 18 or 21 C-terminal residues respectively, were generated to facilitate their expression and purification<sup>26; 38; 39</sup>. The coding sequence of the BVDV enzyme was amplified from an infectious cDNA clone (pACNR/BVDV NADL-XbaI)<sup>40</sup>. *EcoRI* and *XhoI* sites were engineered into the PCR primers to facilitate cloning into the expression vector pET-21b (Novagen). The BVDVΔ18 protein was

expressed in *Escherichia coli* and purified as described previously<sup>26</sup>. The plasmid encoding the BVDV $\Delta$ 18 was then utilized as the parental clone for the construction of the GTP-binding site mutants. Mutant enzymes T320A and Y581F were generated through site-directed mutagenesis using the Stratagene Quick-change kit according to the manufacturer's protocol. The HCV $\Delta$ 21 NS5B sequence inserted into the expression vector pET-22 (Novagen) was also expressed in *Escherichia coli* and purified utilizing a combination of metal ion affinity and ion exchange chromatography<sup>25</sup>. The sequences of all clones were confirmed by sequencing at the McGill University and Genome Quebec Innovation Centre.

The RNA template substrates utilized in this study were:

5'-AACCGUAUCCAAAACAGUCC-3' (T-20 template, HCV),

5'-CCUUUUCUAAUUCUCGUAUAC-3' (T-21 template, BVDV) and

5'-CCUUUUCUAAUUCUCGUAUACC-3' (T-22 template, BVDV) while 5'-GG-3', and 5'-GGG-3' served as RNA primers. All RNA oligonucleotides were chemically synthesized. The RNA templates were further purified on 12% polyacrylamide-7M urea gels containing 50 mM Tris-borate pH 8.0 and 1 mM EDTA, followed by elution from gel slices in a buffer containing 500 mM NH<sub>4</sub>Ac and 0.1% SDS. 5'-end-labelling of the RNA primers was conducted with [ $\gamma$ -<sup>32</sup>P]ATP and T4 polynucleotide kinase according to the manufacturer's recommendation (Invitrogen).

**Primer extension assay** – Primer extension assay was performed as described previously<sup>27</sup>. Briefly, standard reaction mixtures consisted of 0.75  $\mu$ M of RNA template

(T-21 or T-22), 0.75  $\mu$ M BVDV NS5B and 0.25  $\mu$ M 5'-end labelled primer in a buffer containing 20 mM Tris-HCl pH 7.5, 50 mM NaCl, 1 mM DTT, and 100  $\mu$ M NTPs. Reactions were initiated by the addition of 0.15 mM  $\text{MnCl}_2$  and incubated at room temperature for 30 minutes, unless otherwise stated. The effect of primer binding on chain-termination was monitored in reaction mixtures as described above except that each of the four NTPs was added at a constant concentration of 10  $\mu$ M in the presence of increasing concentrations of 3'-dNTPs (TriLink Biotechnologies). All subsequent chain-termination reactions consisted of 100  $\mu$ M ATP, 100  $\mu$ M GTP, 100  $\mu$ M UTP and 100  $\mu$ M 3'-dCTP. The HCV $\Delta$ 21 primer extension assay was conducted with the following modifications: 1  $\mu$ M T-20 template, 1  $\mu$ M HCV enzyme and 200 nM 5'-end labeled primer were added to a buffer containing 20 mM Tris-HCl pH 8.0, 10 mM NaCl, 1 mM DTT, 0.2 mM  $\text{MnCl}_2$  and 10  $\mu$ M NTPs and incubated at room temperature for 60 minutes.

**De novo initiation assay** – Reaction mixtures for the *de novo* initiation assay are similar to those described for the primer extension assay except that the concentration of NTPs was modified to include 100  $\mu$ M 3'-dCTP, 100  $\mu$ M GTP, 100  $\mu$ M UTP, 10  $\mu$ M ATP and 1  $\mu$ Ci [ $\alpha$ - $^{32}$ P] ATP (Amersham). Reactions were initiated by the addition of 0.15 mM  $\text{MnCl}_2$  and incubated at room temperature for 30 minutes, unless otherwise stated. To monitor whether the products obtained during primer-dependent and *de novo* initiation reactions are identical, GMP (Sigma) was added to *de novo* reactions at varied concentrations. For both assays, reaction mixtures were stopped with 100  $\mu$ l of a solution containing 0.3 M  $\text{NH}_4\text{Ac}$ , 1  $\mu$ g bulk tRNA and 90 % isopropanol. Samples were

precipitated with ethanol, heat-denatured for 5 minutes at 95°C, and resolved on 12 % polyacrylamide–7M urea gels. Quantification of product bands was performed using a phosphor-imager (Bio-Rad Molecular Imager FX).

## Results

**Experimental Design** - Both the BVDV and HCV NS5B are capable of utilizing dinucleotide primers to initiate RNA synthesis<sup>25; 26</sup>. Such reactions could mimic early stages of RNA synthesis immediately following the formation of the first phosphodiester bond. Moreover, a complex with a dinucleotide primer has also been compared with an initiation complex that contains GTP and the initiating NTPi in the G-site and P-site, respectively<sup>22; 25</sup>. For the BVDV enzyme, the 5'-terminal guanosine of a 5'-GG-3' or 5'-GN-3'-type primer may thus occupy the G-site. Our recent biochemical studies provided support for this notion<sup>27</sup>. We have utilized a 5'-end labelled GG-dinucleotide primer and a short 21-mer RNA template (T-21) as a model system to study the incorporation of chain-terminating 3'-deoxynucleotide triphosphates (3'-dNTPs). The 3'-terminal CA-sequence of the T-21 template provides only partial complementarity with the GG primer; however, the efficiency of RNA synthesis was significantly higher as compared to reactions with the matching GU primer. With the GG primer, we found that chain-terminated elongation products were always a single nucleotide longer than one would expect from the length of the template. These findings show that the 5'-terminal guanosine of the primer can indeed extend beyond the 3'-end of the template to interact with the G-site, while the 3'-terminal guanosine occupies the P-site<sup>27</sup>. At the same time,

these data raise the question as to whether G-site binding, and, in turn, “overhang priming” may also occur when the dinucleotide GG primer is perfectly complementary to the 3’end of the template. To address this issue, we devised a 22-mer as model RNA template (T-22) that contains an additional cytidine at its 3’-terminus and is otherwise identical to T-21 (Fig. 2A). This template is designed to allow both “overhang priming”, which is indicative of specific interactions between G-site and the 5’terminal guanosine of the dinucleotide primer, and “blunt-end priming”, which is indicative of perfect Watson and Crick base-pairing between the two guanosine residues of the primer and the two 3’terminal cytidines of the template (Fig. 2A).

With the T-21 template, the BVDV NS5B enzyme extends the GG primer to generate a major full-length product of 22 nucleotides in length (Fig. 2B; left panel). In contrast, we observed a mixture of products containing 22 and 23 nucleotides in length when T-22 was utilized as a template (Fig. 2B; right panel). The mixture of products points to differences in priming locations; however, it cannot be excluded that template independent nucleotide additions may have confounded the results<sup>28</sup>. Moreover, there are also shorter products that point to truncations at the 5’end of the RNA template. To control for these problems, we included chain-terminating 3’-dNTPs in the reaction mixture and looked for the appearance of duplex bands that would unambiguously show heterogeneous priming. Increasing concentrations of 3’-dCTP were added to reactions containing either T-21 (Fig. 2C; left panel) or T-22 (Fig. 2C; right panel). The use of T-21 shows a single band at position +7, while reactions with the T-22 template show two



distinct bands at positions +7 and +8, which is indicative of blunt-end and overhang priming, respectively.

#### **Parameters affecting the ratio between overhang and blunt-end priming -**

The incorporation of the first nucleotide requires that the NTP substrate binds to the N-site. At the same time, the dinucleotide GG primer occupies the G- and P-site. Both the dinucleotide primer and the nucleotide substrate must bind in this configuration to allow the chemical step. However, the appearance of two distinct reaction products suggests that the template strand is not located at a fixed position. The precise positioning of the template may crucially depend on base complementarity with the incoming nucleotide. To test this hypothesis, we varied systematically the concentration of the incoming nucleotide opposite template positions  $n$ ,  $n+1$ ,  $n+2$ , and  $n+3$  (Fig. 3A). The results show that increasing concentrations of GTP (opposite template position  $n$  and  $n+1$ ) provide conditions that favor overhang priming (8-mer product) (Fig. 3B, lanes 5-8; right panel). Low concentrations of GTP yield the shorter 7-mer product, which is gradually replaced by the 8-mer product as the concentration of GTP increases (Fig. 3B, lanes 1-5; right panel). Longer products are not seen, which indicates that priming cannot take place from template position  $n$ . Two connected template nucleotides are perhaps required to stabilize a fragile alignment between the two reacting residues that are located in the P- and N-sites, respectively.

The effect of the incoming nucleotide on the positioning of the template becomes evident with increasing concentrations of UTP, which is complementary to template

position  $n+2$  (Fig. 3A). Increasing concentrations of this substrate facilitates RNA synthesis through blunt-end priming (7-mer product) (Fig. 3B, lanes 5-10; middle panel). Varying concentrations of ATP, that binds opposite template position  $n+3$ , has no effect on the mode of priming (Fig. 3B; left panel). The ratio between overhang and blunt-end priming remains unchanged when increasing the concentration of ATP. This result was expected, since priming from position  $n+3$  would involve a mismatch at the P-site (Fig. 3A). Together the data show that the template can freely move between two positions, which allow both overhang priming and blunt-end priming. A third reaction product, that migrates a little faster, is probably the result of an unspecific priming event that could involve G: U misincorporation in the beginning of the reaction (asterisks, Fig. 3B). This product is not seen in the absence of GTP, while it becomes dominant when increasing the concentrations of GTP (Fig. 3B, lanes 5-10; right panel). Alternatively, it is also possible that increasing concentrations of GTP may promote internal binding of the GG dinucleotide.

***De novo* initiation versus dinucleotide-primed reactions** - A dinucleotide is the first reaction product during *de novo* initiation. After formation of the first phosphodiester bond, the newly synthesized dinucleotide must translocate to clear the N-site for the next incoming nucleotide. The dinucleotide would then occupy the G- and P-site, which raises the question whether *de novo* initiation and dinucleotide-primed RNA synthesis give rise to the same distribution of reaction products. To study which of the two priming modes may adequately mimic events that take place during *de novo* initiation, we looked at product formation in the presence of [ $\alpha$ - $^{32}$ P] ATP (Fig. 4). Time

course experiments show a single dominant product, and a faint band that migrates a little higher (Fig. 4; middle panel). The spacing between both bands is reminiscent of the spacing seen between the two products generated with the dinucleotide primer (Fig. 4; left panel). However, the corresponding fragments do not co-migrate because the initiating GTP utilized during *de novo* initiation remains attached to the product in its triphosphate form, while the GG-primer contains a (radiolabelled) guanosine monophosphate at its 5' terminus. To confirm whether these products are identical to those obtained during primer-dependent synthesis, we tested the effects of increasing concentrations of GMP during the *de novo* reaction (Fig. 4, lanes 9-16). We found that increasing concentrations of GMP yielded reaction products that co-migrated with the two products generated with the dinucleotide primer; however, the ratio of the two reaction products differs significantly. Dinucleotide-primed synthesis favors the 8-mer product, while *de novo* initiation provides conditions that favor the 7-mer product.

**Mutational analysis of the G-site** - The crystal structure of the BVDV NS5B complex with GTP points to several residues that lie in close proximity to the guanine base<sup>22</sup>. These include H499, R517, K525, and R529 that are found in close proximity to the phosphate groups, and residues T320, P321, L322, Y581, and L677 that are found in close proximity to the base moiety. T320 and Y581 appear to interact through hydrogen bonds with positions N1, N2, and O6 of guanine. We generated mutant enzymes to study the effects of structural changes at crucial positions on both *de novo* initiation and dinucleotide primed reactions. The efficiency of RNA synthesis was monitored in the presence of increasing concentrations of GTP (Fig. 5). We found that *de novo* initiation

with a T320A change is severely compromised (Fig. 5; right panel). In contrast, the efficiency of dinucleotide primed RNA synthesis remains largely unaffected, which shows that the active site of the enzyme is intact. Thus, this mutation affects selectively the formation of the first phosphodiester bond during *de novo* initiation. We have also tested the Y581F mutant that potentially disrupts hydrogen bonding between guanine O6 and the hydroxyl group of the side chain. However, this mutant behaves essentially like the wild type enzyme (data not shown). It appears that the Y581F change alone may not be sufficient to influence GTP binding.

**Template positioning during initiation of RNA synthesis by HCV NS5B** – We next compared early events of RNA synthesis by BVDV and HCV NS5B. We devised another model template, since T-21 and T-22 were poorly accepted by the HCV enzyme. As for BVDV, we utilized a short synthetic RNA template (T-20) which contains two cytidines at its 3'-end (Fig. 6). We observed the presence of single bands during incorporation of the 3'-dGTP chain-terminator, which indicates that the HCV polymerase, unlike the BVDV enzyme, preferentially positions the GG primer to bind complementary to the 3'-end of the template (Fig. 6, lanes 3 and 5; left panel). Overhang priming takes place only when the binding of at least two nucleotides is pre-established, as in the presence of a GGG primer (Fig. 6, lane 3; right panel). Thus, a functionally equivalent G-site, as described for the BVDV enzyme, is not evident in HCV NS5B.

## Discussion

A minimum requirement for *de novo* initiation of RNA synthesis by BVDV and HCV RdRps involves binding of the initiating nucleotide (NTP<sub>i</sub>) to the P-site and binding of the first NTP substrate (NTP<sub>i</sub>+1) to the N-site. Crystallographic data have shown that the BVDV polymerase binds an additional GTP to a guanosine-specific binding site, herein referred to as G-site, just upstream of the active center<sup>22</sup>. However, the functional role of this GTP-binding pocket remains elusive. Based on structural comparisons between the BVDV RdRp-GTP complex, and related polymerases with an RNA template, with and without an incoming nucleotide, it has been suggested that the 3'-OH of the bound GTP may help orient the 3'OH group of NTP<sub>i</sub> to attack the first nucleotide substrate<sup>21; 29; 30; 31; 32</sup>. The biochemical data shown in this study corroborates the existence of a GTP binding site at this position; however, we invoke an alternative functional role for the bound GTP. We provide strong evidence to show that binding of GTP to the G-site can affect the precise positioning of the template, which leads us to suggest that the bound GTP may facilitate the alignment between the 3'terminus of the template and the priming nucleotide. Both suggestions are not mutually exclusive, and the bound GTP could play a dual role in promoting *de novo* initiation by orienting the priming nucleotide, and by controlling the positioning of the template. We developed a model that helps to reconcile the biochemical and crystallographic data. This model covers early stages during *de novo* initiation by BVDV NS5B, including the formation of the first phosphodiester bond, polymerase translocation and incorporation of the second nucleotide substrate (Fig. 7).

A possible configuration with the bound nucleotides involved in the initiation reaction is schematically shown in Fig. 7A. The G-site, P-site, and N-site accommodate the three nucleotides involved: GTP, NTPi, and NTPi+1, respectively (step 1). The 3' end of the template is located in close proximity to the priming position opposite to the initiating NTPi. This model is supported by biochemical data showing that *de novo* RNA synthesis yields products that match the length of the template (blunt-end priming); however, the structural determinants that control the positioning of the template remain to be defined. The study and comparison of dinucleotide primed reactions and *de novo* initiation of RNA synthesis shed light on this problem.

Following catalysis, the enzyme must translocate relative to the newly synthesized dinucleotide in order to clear the N-site for the next nucleotide substrate (Fig. 7A, steps 2 and 3). For polymerizing enzymes in the elongation stage, it is assumed that the primer/template substrate forms a stable duplex that moves as a whole relative to the enzyme. During *de novo* initiated reactions, such movement brings the 3'-end of the newly synthesized dinucleotide to the P-site and its 5'-end to the G-site, while the formerly bound GTP is released (Fig. 7A, step 3). The N-site is now accessible for the next nucleotide, and its incorporation yields products that match the size of the template (blunt-end priming). Our data show that blunt-end priming dominates during *de novo* initiation. In contrast, dinucleotide-primed reactions give rise to longer products that originate from overhang priming. To explain these data, we suggest that the template can be repositioned to its initial location following translocation, and both complexes may isomerize to equilibrium (Fig. 7A, step 4). We propose that the existence and occupancy

of the G-site promotes template repositioning, which is illustrated in Fig. 7B. Following enzyme translocation, the 5'-terminal G of the newly synthesized dinucleotide is either in contact with the 3'-terminal base of the template (complex 1), or with the G-specific binding site (complex 2). It is unlikely that the 5'-terminal G can interact simultaneously with the G-site and the complementary 3'-end of the template strand, given that both contacts engage positions O6, N1, and N2 of the guanine base<sup>22</sup>. Thus, the repositioning of the template appears to be facilitated by the loss of interactions with the 5'-terminal guanosine of the primer strand (Fig. 7B, complex 2 and 3). The movement of the template relative to the dinucleotide involves breakage of only a single base pair under these conditions, which is probably compensated by the newly formed interaction between the primer and the G-site. The intermediate complex, shown in Fig. 7B (complex 2), may not exist as illustrated. It is conceivable that the conformational change at the 5'-terminal guanosine of the primer might be accompanied by, or even triggers template repositioning. Regardless of the precise mechanism, the data suggest that the 3'-terminal cytosine of the template is unlikely to be found in the vicinity of the G-site if this pocket is occupied with the 5'-terminal guanosine of the primer. Thus, both the specifically bound GTP during *de novo* initiation, and the 5'-terminal GMP in the context of dinucleotide-primed reaction, could restrict the free movement of the template and lock its 3'-end in close proximity to the P-site.

Our data further support the notion that both complexes can isomerize to reach an equilibrium. We found that the ratio of blunt-end priming and overhang priming depends critically on the concentration of NTPs opposite template positions  $n+1$  and  $n+2$ , which

provides strong evidence to show that the template can indeed freely move between these locations. The existence of an isomerization equilibrium can also explain why the *de novo* reaction is preferentially blunt-end primed, while dinucleotides are preferentially overhang primed. We suggest that the incubation of enzyme, dinucleotide primer, and template pre-establishes the equilibrium, and the most stable configuration will predominate. This appears to be the complex with the 5'-end of the primer interacting with the G-site and the 3'-end of the template base-pairing with the 3'-end of the primer (Fig. 7B, complex 3). As a result, overhang priming is favored. A dinucleotide product is also generated during *de novo* initiation; however, in this case, blunt-end priming is favored. Thus, binding and incorporation of the next nucleotide is probably faster than the isomerization step and the ensuing repositioning of the template.

Taken together, the results of this study show that the GTP-binding site of the BVDV RdRp can affect the positioning of the template strand, which, in turn, affects the mode of priming. Such effects are not seen with the HCV enzyme (Fig. 6). In this case, dinucleotide-primed reactions give rise to identical products that have been originated from blunt-end priming. Overhang priming is only seen when initiating the reaction with a trinucleotide GGG primer that extends beyond the 3'-terminus of the template. It is therefore unlikely that the HCV enzyme contains a functionally equivalent G-specific binding site adjacent to the active site. Here the requirement for high concentrations of GTP may have different reasons, which remains to be addressed<sup>33; 34; 35; 36; 37</sup>. For the BVDV enzyme, high concentrations of GTP, and, ultimately its binding to the G-site could help orient the priming nucleotide, and binding of GTP may also help position the



3'-end of the template to facilitate the formation of the first phosphodiester bond. However, the comparison of reactions carried out by BVDV NS5B and the HCV enzyme shows that *de novo* initiation by RNA polymerases is not necessarily based on a common, unifying mechanism.

# Figure 1

G-site dependent *De Novo* Initiation

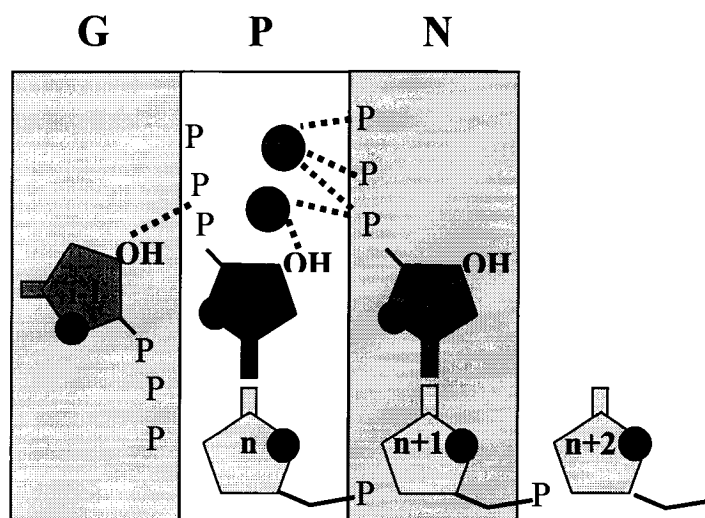


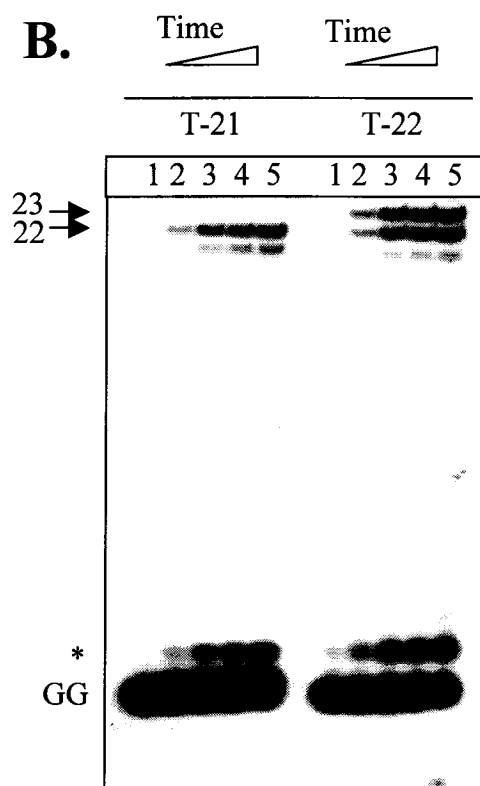
**Fig. 1. Schematic model of G-site dependent *de novo* initiation of RNA synthesis by the BVDV RdRp.** *De novo* initiation of RNA synthesis involves binding of the initiating nucleotide (GTP<sub>i</sub>; red) at the priming or initiation site (P-site; white box) and binding of the first NTP substrate (GTP<sub>i+1</sub>; blue) to the nucleotide binding site (N-site; purple box). GTP (i-1; green) bound to the GTP-specific binding site (G-site; green box) is positioned in such a way that its 3'-hydroxyl group is located in the vicinity of the  $\alpha$ - and  $\beta$ -phosphates of the initiating nucleotide. Specific binding sites for divalent metal ions (pink circles A and B) are shown in close proximity to the  $\alpha$ -,  $\beta$ -, and  $\gamma$ - phosphates of the first nucleotide substrate.

# Figure 2

**A.**

Template	Mode of Primer Binding	Product Size (nt)
T-21	3' CAUAUGCUCUUAUCUUUCC 5*GGUAUAC...	22
Overhang priming		
Blunt-end priming	3' CCAUAUGCUCUUAUCUUUCC 5*GGUAUAC...	22
T-22	or	
Overhang priming	3' CCAUAUGCUCUUAUCUUUCC 5*GGUAUAC...	23

**B.**



**C.**

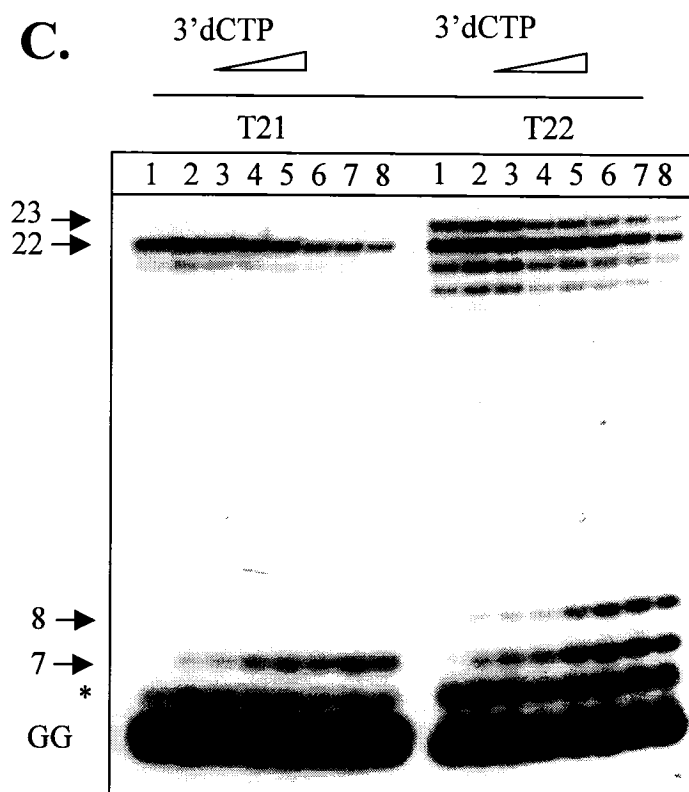


**Fig. 2. Heterogeneous priming of the GG dinucleotide primer during primer-dependent initiation of RNA synthesis.** (A) Schematic representation of the template/primer systems used in this study as well as possible binding positions of the 5'-end-labelled dinucleotide primer (\*GG, bolded) and expected full-length product sizes. (B) Time course reactions comparing the extension of the 5'-end labelled GG dinucleotide primer utilizing T-21 (left panel) and T-22 (right panel) as templates. Lanes 1-5 show reactions after 0, 5, 15, 30, and 60 min. (C) Incorporation of 3'-dCTP at increasing concentrations during heterogeneous priming after a 30 min reaction. Lanes 1-8 show reactions in the presence of 0, 1.5, 3.125, 6.25, 12.5, 25, 50, and 100  $\mu$ M 3'-dCTP, while maintaining each of the four natural NTPs at 10  $\mu$ M. Arrows denote chain-termination incorporation sites while the asterisk denotes possible unspecific priming events. Note that the numbering refers to the length of the primer.

# Figure 3

**A.**

			Priming position	Product Length (nt)
	GP <u>N</u>			
5*GG	<u>G</u>		n	9
	CCAUAUG <u>C</u> U...			
5*GG	<u>G</u>	Overhang priming	n+1	8
	CCAUAUG <u>C</u> U...			
5*GG	<u>U</u>	Blunt-end priming	n+2	7
	CCAUAUG <u>C</u> U...			
5*GG	<u>A</u>		n+3	6
	CCAUAUG <u>C</u> U...			

**B.**

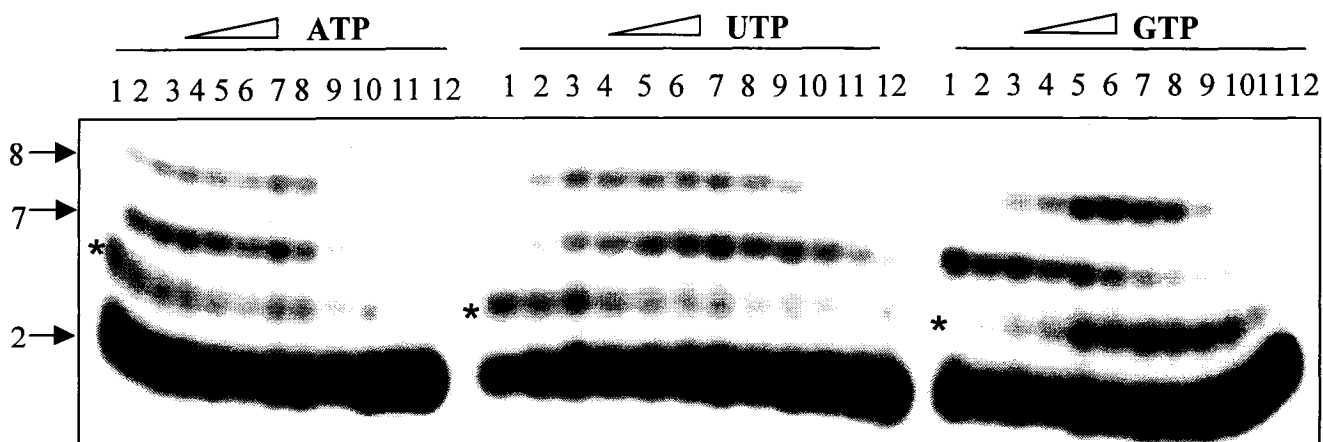


**Fig. 3. Effect of incoming nucleotide on template positioning.** (A) Schematic description depicting the priming position of the incoming nucleotides tested (bolded), as well as the expected chain-terminated product lengths. Note that blunt-end priming results in the formation of a 7-mer product while overhang priming forms an 8-mer product. Site of 3'-dCTP incorporation is underlined. (B) Effect of increasing concentrations of ATP (left panel), UTP (middle panel), and GTP (right panel) on template positioning (lanes 1-12: 0, 2.5, 5, 10, 19.5, 40, 80, 156, 312.5, and 625  $\mu$ M, and 1.25 and 2.5 mM). Reactions were conducted with the T-22 template and incubated for 30 min. Asterisks denote possible unspecific priming events such as G:U misincorporation or internal binding of the GG primer.

# Figure 4

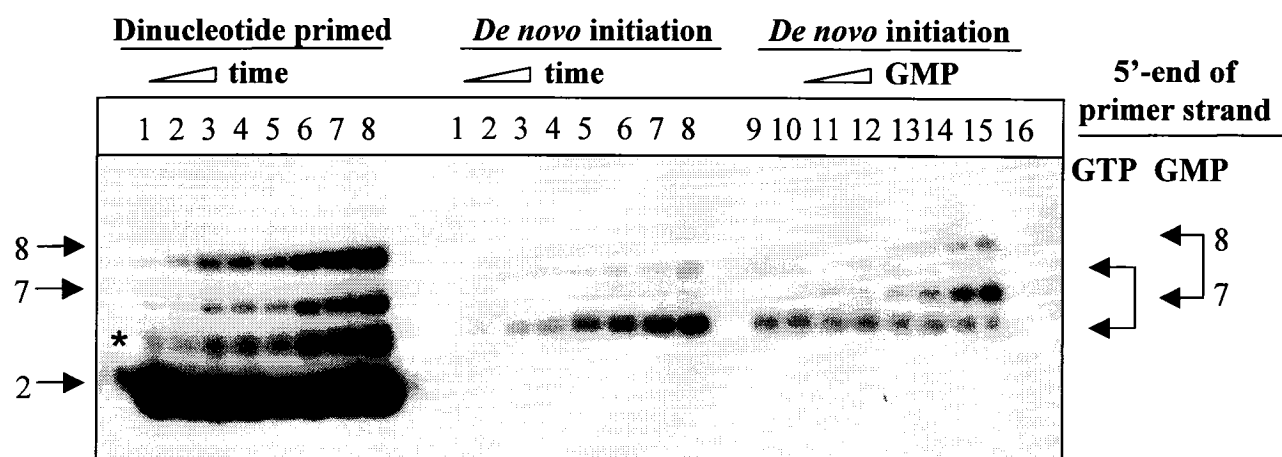




**Fig. 4. Difference in template positioning during *de novo* and dinucleotide-primed initiation.** Time course experiments comparing the incorporation of 3'-dCTP during dinucleotide-primed (left panel) and *de novo* (middle panel) initiation of RNA synthesis. Reactions were conducted with the T-22 template and were incubated for 0, 5, 10, 15, 30, 45, 60, and 120 min (lanes 1-8). For *de novo* reactions, a mixture of GTP and UTP was used at 100  $\mu$ M and ATP at 1  $\mu$ M to allow for the incorporation of [ $\alpha$ - $^{32}$ P] ATP, which is used as a tracer. To confirm whether the products generated between the two priming modes were identical, GMP was added at increasing concentrations during *de novo* initiation for 30 min (right panel). Lanes 9-16 show reactions in the presence of 0, 19.5, 40, 80, 156, 312.5, and 625  $\mu$ M, and 1.25 mM GMP. The 5'-end of the primer strand for the dinucleotide-primed (GMP) and *de novo* (GTP) reactions, as well as positions of products formed (double-arrows) are indicated. Asterisks denote possible unspecific priming events such as G:U misincorporation or internal binding of the GG primer.

# Figure 5

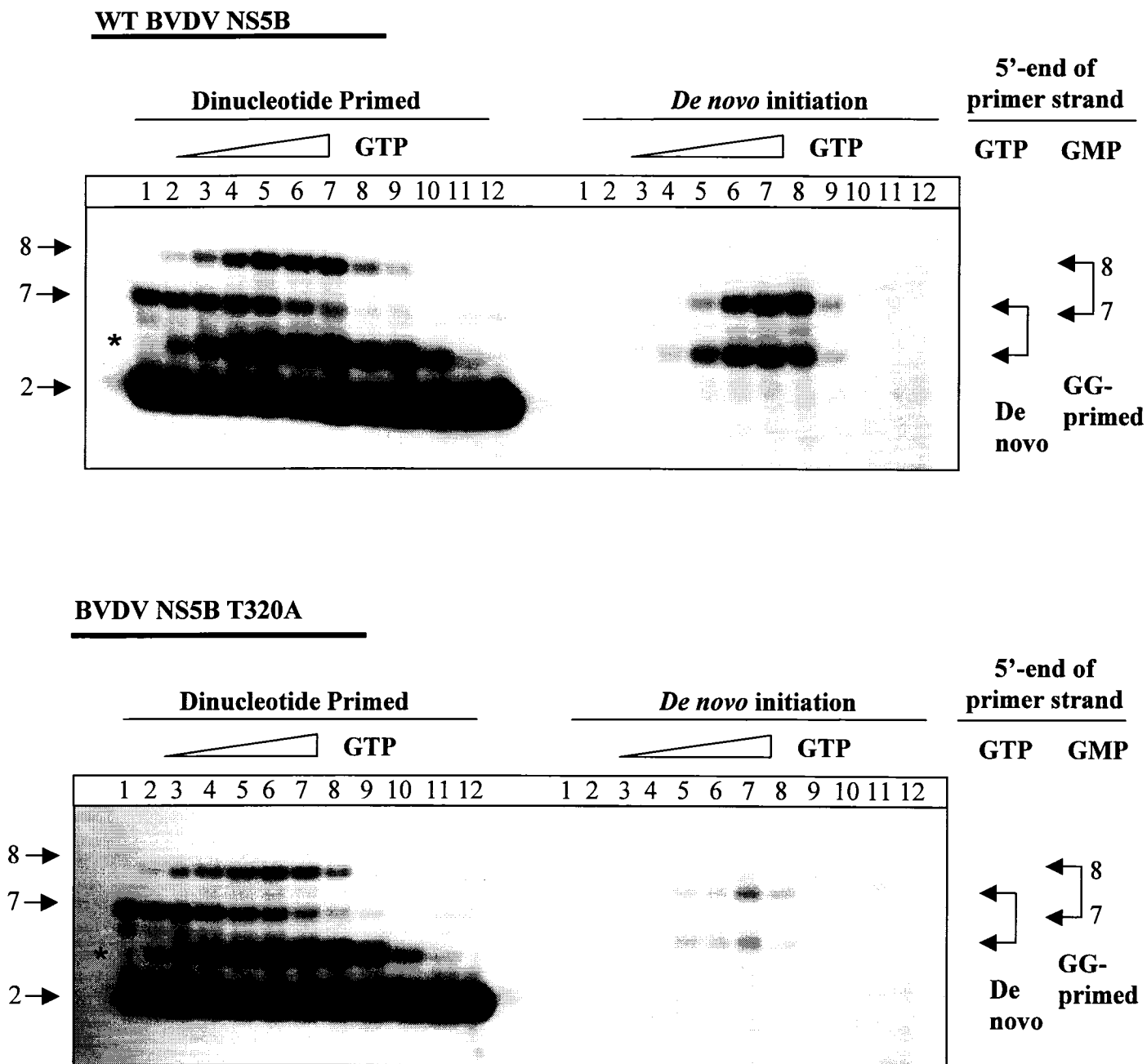


**Fig. 5. Effect of G-site specific mutation during *de novo* and dinucleotide-primed initiation of RNA synthesis.** Comparison of the effect of G-site specific mutation at position T320A (A) with wild-type enzyme (B) on the incorporation of 3'-dCTP during dinucleotide-primed (left panel) and *de novo* (right panel) initiation of RNA synthesis. Lanes 1-12 show reactions that were allowed to proceed for 30 min in the presence of 0, 2.5, 5, 10, 19.5, 40, 80, 156, 312.5, and 625  $\mu$ M, and 1.25 and 2.5 mM GTP. Asterisks denote possible unspecific priming events such as G:U misincorporation or internal binding of the GG primer. The 5'-end of the primer strand for the dinucleotide-primed (GMP) and *de novo* (GTP) reactions, as well as the positions of products formed (double-arrows) are indicated.

Figure 6

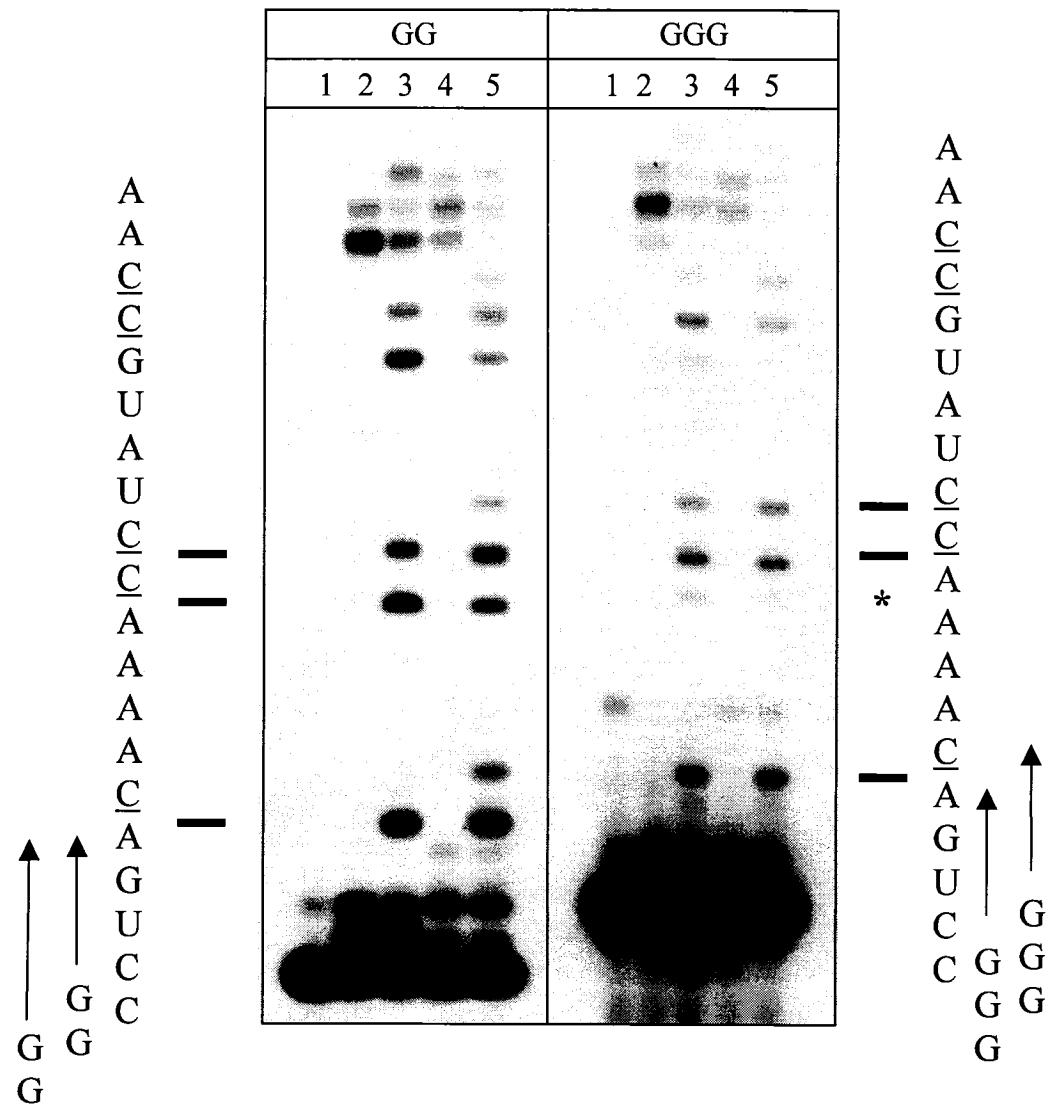


**Fig. 6. Difference in template positioning between BVDV and HCV polymerases.**

Each panel shows reactions conducted with the T-20 template and 5'-end labelled dinucleotide (GG, left panel) or trinucleotide (GGG, right panel) primer during full-length extension (lanes 2 and 4) or the incorporation of 3'-dGTP (lanes 3 and 5) by the HCV (lanes 2 and 3) or BVDV (lanes 4 and 5) RdRp. Lane 1 is a control which shows unextended primer. Reactions were incubated for 60 or 120 min, depending on whether GG or GGG was used respectively. Template positions for the incorporation of 3'-dGTP are underlined. Possible binding positions of GG and GGG primers are also shown. A minor product, represented by an asterisk, is generated through blunt-end priming of the GGG primer to the 3'-end of the template.

# Figure 7

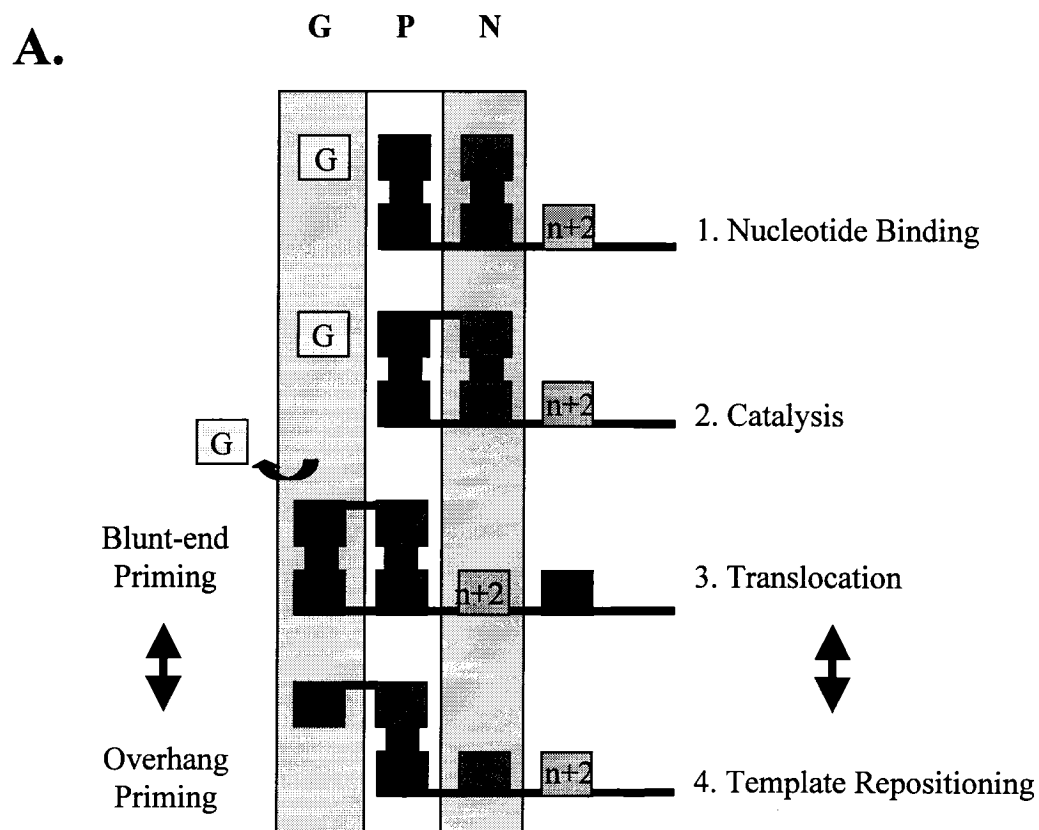


**Figure 7**

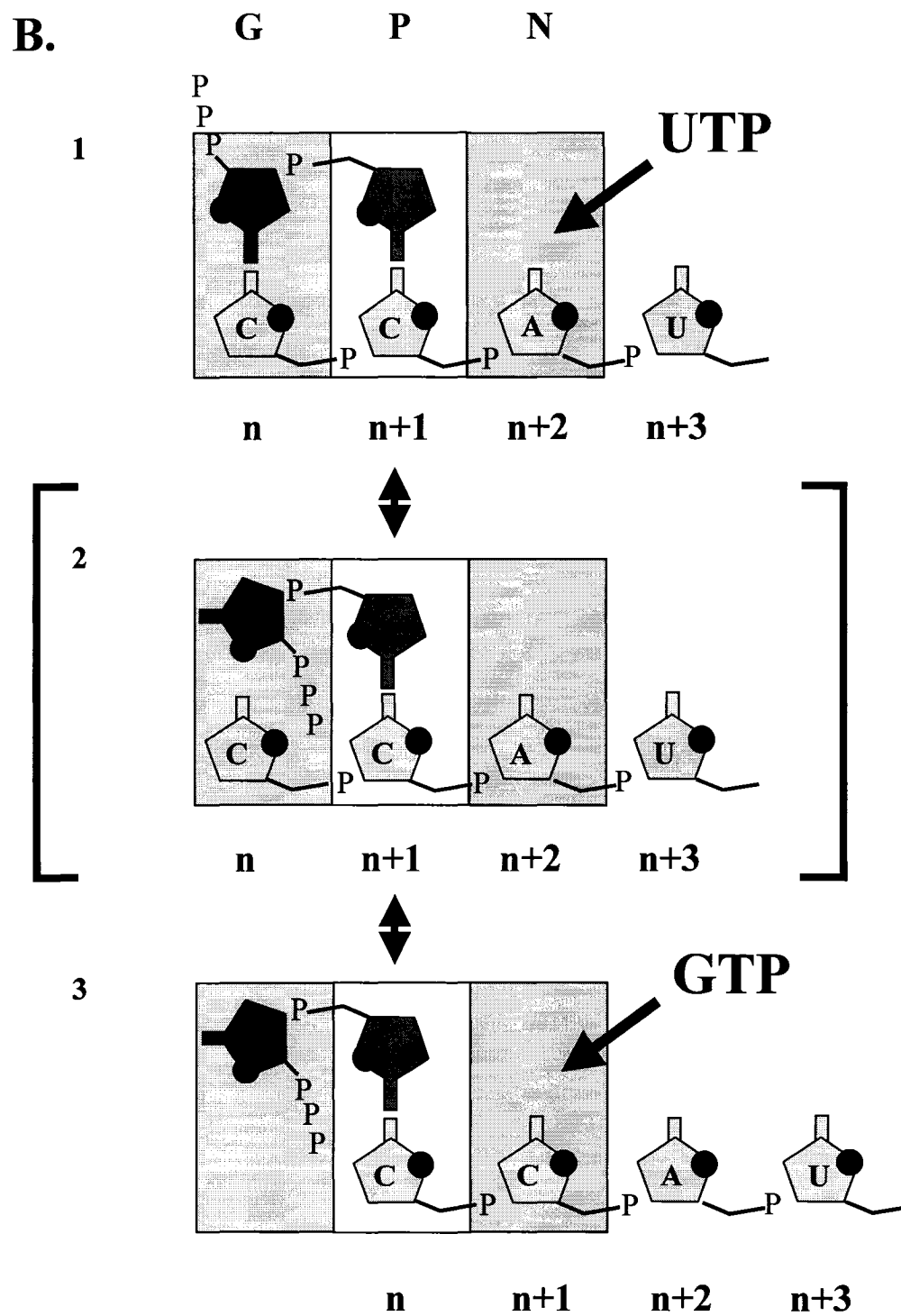


**Fig. 7. Model of GTP-facilitated *de novo* initiation of RNA synthesis by the BVDV polymerase.** (A) The initial stages of RNA synthesis by BVDV RdRp can be divided into four steps: nucleotide binding (step 1), catalysis (step 2), translocation (step 3), and template repositioning (step 4). In this model, repositioning of the template is triggered by the bound GTP. (B) Following enzyme translocation, the 3'-end of the newly synthesized dinucleotide occupies the P-site (white box) and the 5'-end interacts with the complementary 3'-end of the template strand (complex 1). A conformational change at the 5'-terminal guanosine of the primer strand initiates its loss of contact with the templated base and facilitates specific interaction with the G-site (complex 2). The loss of terminal base-pairing may trigger repositioning of the template to its original location. RNA synthesis resumes with a 3'-recessed template (complex 3). The isomerization equilibrium is controlled by the concentration of NTPs at template positions  $n+1$  (GTP) and  $n+2$  (UTP).



## References

1. Jager, J. & Pata, J. D. (1999). Getting a grip: polymerases and their substrate complexes. *Curr Opin Struct Biol* **9**, 21-8.
2. Steitz, T. A. (1997). DNA and RNA polymerases: structural diversity and common mechanisms. *Harvey Lect* **93**, 75-93.
3. deHaseth, P. L., Zupancic, M. L. & Record, M. T., Jr. (1998). RNA polymerase-promoter interactions: the comings and goings of RNA polymerase. *J Bacteriol* **180**, 3019-25.
4. Patel, P. H., Jacobo-Molina, A., Ding, J., Tantillo, C., Clark, A. D., Jr., Raag, R., Nanni, R. G., Hughes, S. H. & Arnold, E. (1995). Insights into DNA polymerization mechanisms from structure and function analysis of HIV-1 reverse transcriptase. *Biochemistry* **34**, 5351-63.
5. Kao, C. C., Del Vecchio, A. M. & Zhong, W. (1999). De novo initiation of RNA synthesis by a recombinant flaviviridae RNA-dependent RNA polymerase. *Virology* **253**, 1-7.
6. Luo, G., Hamatake, R. K., Mathis, D. M., Racela, J., Rigat, K. L., Lemm, J. & Colonno, R. J. (2000). De novo initiation of RNA synthesis by the RNA-dependent RNA polymerase (NS5B) of hepatitis C virus. *J Virol* **74**, 851-63.
7. Ranjith-Kumar, C. T., Gutshall, L., Kim, M. J., Sarisky, R. T. & Kao, C. C. (2002). Requirements for de novo initiation of RNA synthesis by recombinant flaviviral RNA-dependent RNA polymerases. *J Virol* **76**, 12526-36.
8. Kao, C. C., Singh, P. & Ecker, D. J. (2001). De novo initiation of viral RNA-dependent RNA synthesis. *Virology* **287**, 251-60.
9. Zhong, W., Uss, A. S., Ferrari, E., Lau, J. Y. & Hong, Z. (2000). De novo initiation of RNA synthesis by hepatitis C virus nonstructural protein 5B polymerase. *J Virol* **74**, 2017-22.
10. Kim, M. J., Zhong, W., Hong, Z. & Kao, C. C. (2000). Template nucleotide moieties required for de novo initiation of RNA synthesis by a recombinant viral RNA-dependent RNA polymerase. *J Virol* **74**, 10312-22.
11. Sun, X. L., Johnson, R. B., Hockman, M. A. & Wang, Q. M. (2000). De novo RNA synthesis catalyzed by HCV RNA-dependent RNA polymerase. *Biochem Biophys Res Commun* **268**, 798-803.
12. Ranjith-Kumar, C. T., Kim, Y. C., Gutshall, L., Silverman, C., Khandekar, S., Sarisky, R. T. & Kao, C. C. (2002). Mechanism of de novo initiation by the hepatitis C virus RNA-dependent RNA polymerase: role of divalent metals. *J Virol* **76**, 12513-25.
13. Reed, K. E. & Rice, C. M. (2000). Overview of hepatitis C virus genome structure, polyprotein processing, and protein properties. *Curr Top Microbiol Immunol* **242**, 55-84.
14. Lohmann, V., Korner, F., Herian, U. & Bartenschlager, R. (1997). Biochemical properties of hepatitis C virus NS5B RNA-dependent RNA polymerase and identification of amino acid sequence motifs essential for enzymatic activity. *J Virol* **71**, 8416-28.

15. Ferrari, E., Wright-Minogue, J., Fang, J. W., Baroudy, B. M., Lau, J. Y. & Hong, Z. (1999). Characterization of soluble hepatitis C virus RNA-dependent RNA polymerase expressed in *Escherichia coli*. *J Virol* **73**, 1649-54.
16. Behrens, S. E., Tomei, L. & De Francesco, R. (1996). Identification and properties of the RNA-dependent RNA polymerase of hepatitis C virus. *Embo J* **15**, 12-22.
17. Yamashita, T., Kaneko, S., Shiota, Y., Qin, W., Nomura, T., Kobayashi, K. & Murakami, S. (1998). RNA-dependent RNA polymerase activity of the soluble recombinant hepatitis C virus NS5B protein truncated at the C-terminal region. *J Biol Chem* **273**, 15479-86.
18. Zhong, W., Gutshall, L. L. & Del Vecchio, A. M. (1998). Identification and characterization of an RNA-dependent RNA polymerase activity within the nonstructural protein 5B region of bovine viral diarrhea virus. *J Virol* **72**, 9365-9.
19. van Dijk, A. A., Makeyev, E. V. & Bamford, D. H. (2004). Initiation of viral RNA-dependent RNA polymerization. *J Gen Virol* **85**, 1077-93.
20. Butcher, S. J., Grimes, J. M., Makeyev, E. V., Bamford, D. H. & Stuart, D. I. (2001). A mechanism for initiating RNA-dependent RNA polymerization. *Nature* **410**, 235-40.
21. Bressanelli, S., Tomei, L., Rey, F. A. & De Francesco, R. (2002). Structural analysis of the hepatitis C virus RNA polymerase in complex with ribonucleotides. *J Virol* **76**, 3482-92.
22. Choi, K. H., Groarke, J. M., Young, D. C., Kuhn, R. J., Smith, J. L., Pevear, D. C. & Rossmann, M. G. (2004). The structure of the RNA-dependent RNA polymerase from bovine viral diarrhea virus establishes the role of GTP in de novo initiation. *Proc Natl Acad Sci U S A* **101**, 4425-30.
23. Shim, J. H., Larson, G., Wu, J. Z. & Hong, Z. (2002). Selection of 3'-template bases and initiating nucleotides by hepatitis C virus NS5B RNA-dependent RNA polymerase. *J Virol* **76**, 7030-9.
24. Kao, C. C., Yang, X., Kline, A., Wang, Q. M., Barket, D. & Heinz, B. A. (2000). Template requirements for RNA synthesis by a recombinant hepatitis C virus RNA-dependent RNA polymerase. *J Virol* **74**, 11121-8.
25. Zhong, W., Ferrari, E., Lesburg, C. A., Maag, D., Ghosh, S. K., Cameron, C. E., Lau, J. Y. & Hong, Z. (2000). Template/primer requirements and single nucleotide incorporation by hepatitis C virus nonstructural protein 5B polymerase. *J Virol* **74**, 9134-43.
26. Lai, V. C., Kao, C. C., Ferrari, E., Park, J., Uss, A. S., Wright-Minogue, J., Hong, Z. & Lau, J. Y. (1999). Mutational analysis of bovine viral diarrhea virus RNA-dependent RNA polymerase. *J Virol* **73**, 10129-36.
27. D'Abramo, C. M., Cellai, L. & Gotte, M. (2004). Excision of incorporated nucleotide analogue chain-terminators can diminish their inhibitory effects on viral RNA-dependent RNA polymerases. *J Mol Biol* **337**, 1-14.
28. Ranjith-Kumar, C. T., Gajewski, J., Gutshall, L., Maley, D., Sarisky, R. T. & Kao, C. C. (2001). Terminal nucleotidyl transferase activity of recombinant Flaviviridae RNA-dependent RNA polymerases: implication for viral RNA synthesis. *J Virol* **75**, 8615-23.

29. Ago, H., Adachi, T., Yoshida, A., Yamamoto, M., Habuka, N., Yatsunami, K. & Miyano, M. (1999). Crystal structure of the RNA-dependent RNA polymerase of hepatitis C virus. *Structure Fold Des* **7**, 1417-26.
30. Lesburg, C. A., Cable, M. B., Ferrari, E., Hong, Z., Mannarino, A. F. & Weber, P. C. (1999). Crystal structure of the RNA-dependent RNA polymerase from hepatitis C virus reveals a fully encircled active site. *Nat Struct Biol* **6**, 937-43.
31. O'Farrell, D., Trowbridge, R., Rowlands, D. & Jager, J. (2003). Substrate complexes of hepatitis C virus RNA polymerase (HC-J4): structural evidence for nucleotide import and de-novo initiation. *J Mol Biol* **326**, 1025-35.
32. Leveque, V. J., Johnson, R. B., Parsons, S., Ren, J., Xie, C., Zhang, F. & Wang, Q. M. (2003). Identification of a C-terminal regulatory motif in hepatitis C virus RNA-dependent RNA polymerase: structural and biochemical analysis. *J Virol* **77**, 9020-8.
33. Qin, W., Luo, H., Nomura, T., Hayashi, N., Yamashita, T. & Murakami, S. (2002). Oligomeric interaction of hepatitis C virus NS5B is critical for catalytic activity of RNA-dependent RNA polymerase. *J Biol Chem* **277**, 2132-7.
34. Wang, Q. M., Hockman, M. A., Staschke, K., Johnson, R. B., Case, K. A., Lu, J., Parsons, S., Zhang, F., Rathnachalam, R., Kirkegaard, K. & Colacino, J. M. (2002). Oligomerization and cooperative RNA synthesis activity of hepatitis C virus RNA-dependent RNA polymerase. *J Virol* **76**, 3865-72.
35. Ferron, F., Bussetta, C., Dutartre, H. & Canard, B. (2005). The modeled structure of the RNA dependent RNA polymerase of GBV-C Virus suggests a role for motif E in Flaviviridae RNA polymerases. *BMC Bioinformatics* **6**, 255.
36. Lohmann, V., Overton, H. & Bartenschlager, R. (1999). Selective stimulation of hepatitis C virus and pestivirus NS5B RNA polymerase activity by GTP. *J Biol Chem* **274**, 10807-15.
37. Cai, Z., Liang, T. J. & Luo, G. (2004). Effects of mutations of the initiation nucleotides on hepatitis C virus RNA replication in the cell. *J Virol* **78**, 3633-43.
38. Yuan, Z. H., Kumar, U., Thomas, H. C., Wen, Y. M. & Monjardino, J. (1997). Expression, purification, and partial characterization of HCV RNA polymerase. *Biochem Biophys Res Commun* **232**, 231-5.
39. Ishii, K., Tanaka, Y., Yap, C. C., Aizaki, H., Matsuura, Y. & Miyamura, T. (1999). Expression of hepatitis C virus NS5B protein: characterization of its RNA polymerase activity and RNA binding. *Hepatology* **29**, 1227-35.
40. Mendez, E., Ruggli, N., Collett, M. S. & Rice, C. M. (1998). Infectious bovine viral diarrhea virus (strain NADL) RNA from stable cDNA clones: a cellular insert determines NS3 production and viral cytopathogenicity. *J Virol* **72**, 4737-45.

## **CHAPTER 4**

### **CONSECUTIVE FOOTPRINTS OF THE BOVINE VIRAL DIARRHEA RNA-DEPENDENT RNA POLYMERASE COMPLEXES DURING ELONGATION**

This chapter was adapted from a manuscript that is in preparation for submission for *Virology*.

## **Preface to Chapter 4:**

Another area requiring additional characterization includes specific interactions between the polymerase and its nucleic acid substrate after the initiation of RNA synthesis. Our biochemical studies in Chapter 2 have shown that the BVDV RdRp enzyme complex can be arrested at different positions along the template strand during elongation. These arrested complexes are insensitive to the addition of heparin, indicating that they are quite stable during elongation and thereby facilitate a footprinting approach. As such, we developed a ribonuclease-based footprinting assay to obtain information about catalytically active complexes that exist during the elongation of BVDV RNA synthesis.

## Abstract

Little is known about the interaction between the bovine viral diarrhea virus (BVDV) RNA-dependent RNA polymerase (RdRp) and its nucleic acid substrate. We developed a ribonuclease (RNase) H-based footprinting assay to obtain information with respect to the enzyme-nucleic acid interface during elongation of RNA synthesis. Chimeric RNA-DNA templates were utilized as substrates for BVDV RdRp to generate RNA/DNA hybrids that are recognized by *E. coli* RNase H. The BVDV polymerase was able to extend the chimeric templates and *E. coli* RNase H mediated cleavage of the RNA product strand. Footprints of arrested polymerization complexes suggest that the enzyme complex sits on the template with a protection of 11 to 12 nucleotides in length. Considering that the RNase H active center contacts the substrate by at least 5 base pairs, we suggest that RdRp contacts the newly synthesized RNA with approximately 6 to 7 base pairs. This protection moves along the template according to the position where RNA synthesis is arrested. This novel enzymatic footprinting technique facilitates the study of mechanisms involved in polymerase elongation and translocation.

## Introduction

The pestivirus bovine viral diarrhea virus (BVDV) is one of the best characterized members of the *Flaviviridae* family, which also includes the hepatitis C virus (HCV). Both viruses contain a positive-strand RNA genome that encodes for a single polypeptide that is processed by host and virally encoded proteases to generate mature structural and nonstructural proteins required for viral assembly and viral genome replication<sup>1</sup>. The NS5B protein (non-structural protein 5B) functions both as a catalytic RNA-dependent RNA polymerase (RdRp) and as a cooperative RNA-binding protein that is required for viral RNA synthesis, and therefore represents an important target for drug development<sup>2; 3; 4; 5; 6</sup>.

Crystal structures of RdRps from various RNA viruses including HCV, poliovirus, bacteriophage phi6, and BVDV have greatly expanded the knowledge of the structure and functions of this class of enzymes<sup>7; 8; 9; 10; 11; 12</sup>. Similar to other polymerases, the general shape of RdRps resembles a right hand with fingers, palm, and thumb domains. Unlike the open structures of most DNA polymerases, such as the Klenow fragment from *Escherichia coli* (*E.coli*) and the human immunodeficiency virus type-1 reverse transcriptase (HIV-1 RT), RdRps contain an encircled active site through which the RNA template and NTP substrates must gain access<sup>9; 13</sup>. RdRps have also been postulated to adopt an open conformational state, although this “open” form of the enzyme is considered inactive<sup>14</sup>.

Despite the elucidation of several structures of RdRps, with or without an incoming nucleotide, little is known with regards to the specific interactions between the polymerase and its nucleic acid substrate. This is in part due to the fact that most of the crystallographic data available do not include structures of the enzyme associated with an RNA template. As such, several models of the ternary complex and of RNA template binding have been proposed on the basis of structural comparisons among the available RdRp structures, in particular to that of the related bacteriophage phi6 polymerase<sup>8; 11; 15</sup>. In fact, the phi6 structural data has provided the framework for biochemical studies on the initiation mechanism of RNA synthesis by RdRps<sup>11</sup>. According to this model, the template strand enters a highly charged template channel leading to the active site of the enzyme. Initially, the template overshoots the active site and binds to a specificity pocket within the C-terminal domain. In the presence of incoming nucleotides, however, the template ratchets back to the active site to form the initiation complex. One intriguing feature of the phi6 initiation complex is the presence of a C-terminal platform loop that protrudes into the active site and forms stacking interactions with the incoming nucleotides. A similar structural element known as the  $\beta$ -hairpin has also been identified in the thumb domain of both HCV and BVDV RdRp, and has been suggested to stabilize the initiation complex<sup>7; 8; 9; 12; 16</sup>.

Although several biochemical studies have analyzed how the RNA template can interact with the NS5B polymerase to form a stable initiation complex, little information is known about specific interactions between the enzyme and its nucleic acid substrate during elongation. Our previous biochemical studies on BVDV RdRp have shown that the enzyme complex can be arrested at different positions along the template strand



during elongation through the incorporation of chain-terminating nucleotides. These complexes are heparin stable which facilitates a footprinting approach<sup>17</sup>. Here we developed a ribonuclease (RNase) H-based footprinting assay to obtain structural information on catalytically active complexes that exist during the elongation of BVDV RNA synthesis. RNase H enzymes are a class of RNA-binding proteins that specifically cleave the RNA moiety of RNA-DNA hybrids<sup>18</sup>. As such, chimeric RNA-DNA templates were utilized as substrates for BVDV RdRp to generate RNA/DNA hybrid products that are recognized by *E. coli* RNase H. Footprints of arrested polymerization complexes suggest that the BVDV RdRp contacts the newly synthesized RNA with approximately 6 to 7 base pairs. The priming strand beyond 6 to 7 base pairs is cleaved by *E. coli* RNase H. These findings suggest that the primer and template maintain their duplex form and share the same exit.

## **Materials and Methods:**

**Enzymes and nucleic acids** – Construction of the plasmid used for the expression and purification of BVDV NS5B containing a deletion of 24 C-terminal residues (BVDV $\Delta$ 24) was performed as described previously<sup>17</sup>. Briefly, the DNA sequence encoding BVDV NS5B (pACNR/BVDV NADL-XbaI) was cloned into the bacterial expression vector pET21b (Novagen), which contains a polyhistidine tag at the C-terminal end to allow for affinity purification<sup>19</sup>. The sequence of the NS5B protein was confirmed by sequencing at the McGill University and Genome Quebec Innovation Centre. The final BVDV enzyme preparation was dialyzed against a buffer containing

10mM Tris-HCl (pH 7.5), 10% (v/v) glycerol, 5mM DTT, 600mM NaCl and stored at -80°C in 50% glycerol.

The chimeric RNA/DNA template substrates utilized in this study include:

R/D1: 5'-CCT CTA TAC AGC TTC ATA CTT TCT AAu ucu cua uac-3';

R/D2: 5'-CCT CTA TGC ACC TTC ATA CTT TCT AAu ucu cua uac-3';

R/D/R5: 5'-cgu cua aac ugc cac a ACC CAC ACA CAC aca cac aac-3';

R/D/R6: 5'-cgu cua aac ugc cac ac ACC CAC ACA CAC aca cac aac-3';

R/D/R7: 5'-cgu cua aac ugc cac aac ACC CAC ACA CAC aca cac aac-3';

with the RNA portion of the templates represented by lower-case letters and the DNA portion by upper-case letters. All chimeric oligonucleotides were chemically synthesized and purified by UV shadowing at 254nm on 8% denaturing polyacrylamide gels. Purified templates were eluted from excised gel slices in a buffer containing 500mM NH<sub>4</sub>Ac and 0.1% SDS. After ethanol precipitation, the concentration of nucleic acids was determined spectrophotometrically. 5' end-labelling of the dinucleotide RNA primer, 5'-GG-3', was performed using T4 polynucleotide kinase and [ $\gamma$ -<sup>32</sup>P]ATP according to the manufacturer's recommendation (Invitrogen).

**Nucleotide Incorporation Assay** – Standard nucleotide incorporation assays were conducted in a primer-dependent manner. In a reaction volume of 20 $\mu$ l, 0.75  $\mu$ M chimeric template, 0.75  $\mu$ M BVDV NS5B and 0.25  $\mu$ M 5'-end labelled GG primer were added to a buffer containing 20 mM Tris-HCl pH 7.5, 50 mM NaCl, 1 mM DTT and 100

μM NTPs. Reactions were initiated by the addition of 0.15 mM MnCl<sub>2</sub> and incubated for 30 minutes at room temperature.

***E.coli* RNase H Protection Assay** – *E.coli* RNase H protection assay was monitored in reactions similar to those described above except that 100 μM of the nucleoside analogue, 3'-dCTP or 3'-dATP (TriLink Biotechnologies), replaced the natural NTP in the reaction to arrest the BVDV enzyme complex at specific positions along the template strand. Reaction mixtures were initiated by the addition of 0.15 mM MnCl<sub>2</sub> and incubated at room temperature for 30 minutes. The resulting RNA-DNA hybrid product was then subjected to cleavage by the addition of a combined mixture of increasing concentrations of *E. coli* RNase H (MBI Fermentas) and 8 mM MgCl<sub>2</sub>. RNase H preparations were diluted from stock solutions directly before use. Reactions were incubated at 37°C for 10 minutes. For control purposes, the enzyme complex was heat inactivated at 95°C for 5 minutes followed by the re-annealing of the RNA-DNA hybrid product at 72°C for 15 min and slow cooling to room temperature, prior to the addition of 1.25U of *E. coli* RNase H. All reaction mixtures were stopped with 100 μl of a solution containing 0.3M NH<sub>4</sub>Ac, 1μg bulk tRNA and 90% isopropanol. Samples were precipitated with ethanol, heat-denatured for 5 min at 95°C, and finally resolved on 12 % polyacrylamide–7M urea gels.

## Results:

**Experimental Rationale** – A number of reagents, either enzymatic or chemical that promote specific cleavages in RNA or DNA are available and can be utilized in footprinting assays<sup>20</sup>. For our purposes, the use of enzymes were chosen over a number of possible chemical cleavage agents because the extent of digestion with an enzyme is easily controlled and the end-chemistry at the site of cleavage is homogeneous (i.e., one cleavage product produced by cutting corresponds to one nucleotide position on the template). Our previous biochemical studies on BVDV RdRp have shown that the enzyme complex can be arrested at different positions along the template strand during elongation, through the incorporation of chain-terminating nucleotides<sup>17</sup>. These complexes are heparin stable, thereby facilitating a ribonuclease footprinting approach that requires the preparation of arrested homogeneous enzyme complexes.

Chimeric RNA-DNA templates containing unique sites of incorporation for the chain-terminator 3'-dCTP were utilized as substrates for the BVDV polymerase (Fig. 1A). We tested the ability of BVDV RdRp to generate RNA/DNA hybrid products with chimeric templates R/D1 and R/D2 (Fig. 1B). We observed that the BVDV enzyme efficiently extends both templates to generate full-length products 36 nucleotides in length, as well as efficiently incorporates the CTP chain-terminator at position +26 or +29 for templates R/D1 or R/D2, respectively (Fig. 1B). The presence of homogenous products indicates that chain-termination is highly efficient.

**RNase H footprints of arrested polymerization complexes** – Throughout this study, we utilized a 5'-end labelled GG dinucleotide primer to monitor the formation of specific cuts generated after the addition of *E. coli* RNase H to arrested polymerization complexes. Given the low percentage of active BVDV enzyme complexes (Fig. 1B), the use of a labelled primer facilitates the analysis of only those complexes that are catalytically active. A schematic description detailing the components of the RNase H-based footprinting assay utilized is shown in Fig 2A. Essentially, the addition of *E. coli* RNase H to arrested polymerization complexes cleaves the RNA portion of the RNA-DNA hybrid product synthesized by the BVDV polymerase. With this approach, we compared the footprints generated when catalytically active enzyme complexes were arrested at either template position +26 (R/D1) or +29 (R/D2) (Fig. 2B). The resulting footprints show two specific cuts at positions +13 and +14 with both templates (Fig. 2B, right and left panels). The strong cut at position +13 corresponds to the template position 3 base pairs away from the RNA-DNA junction. The inability of *E.coli* RNase H to cleave up to the hybrid junction may result from steric effects or a loss of substrate specificity. We also observed the appearance of three additional cuts when the enzyme complex was arrested on template R/D2 as compared to R/D1 (Fig. 2B, right panel). This is consistent with the fact that the site of incorporation of 3'-dCTP is moved by 3 nucleotides, allowing the bases that are normally protected on the R/D1 template to become cleaved (Fig. 2B, right panel, lanes 2-4). Based on these results, we determined that the catalytically active enzyme complex sits on the template substrate with a protection of approximately 11 to 12 nucleotides in length, and that this protection moves

along the template according to the position where RNA synthesis is arrested (Fig. 2B and 2C).

The cleaved products appear to be RNase H-specific. The cuts increase with increasing amounts of *E.coli* RNase H, and are absent when RNase H is not added to the reaction (Fig. 2B, lane 1). The arrested enzyme complexes are also considerably stable. The fact that the site of protection is observed over the course of the reaction indicates that the interaction between the polymerase and the template substrate is stable. This protection is no longer visible when the complexes are heat inactivated at 95°C, prior to the addition of RNase H, as represented by a ladder of cleaved products (Fig. 2B, lane c). As well, the overall range of RNase H concentrations over which ‘single-hit’ conditions can be obtained was found to occur between 0.08 and 0.3 units (U) (Fig. 2B, lanes 2-4). Further increases in RNase H concentrations led to over-cleaved products (Fig. 2B, lanes 6-7). It is important to note that the amount of RNase H required for effective ‘single-hit’ conditions, such that less than 50% of the RNA is cut during the reaction, was optimized for each template utilized.

**Translocation of catalytically active enzyme complexes along the template strand** - We next modified our footprinting assay to include the use of short RNA-DNA-RNA chimeric templates for the following reasons: i) to arrest the BVDV enzyme complex on its natural RNA substrate; ii) to determine the minimum RNA template length required before the RNA-DNA junction to generate an RNase H-specific cut; iii) to change the site of incorporation of specific chain-terminators; and finally iv) to

confirm whether arrested enzyme complexes can move along the template strand (Fig. 3A).

The results of the footprinting analysis with chimeric templates R/D/R5-7 are consistent with the previous cleavage patterns obtained (Fig. 3B). With all templates, a strong cut was observed at position +13, located 4 base pairs away from the RNA-DNA junction (Fig. 3B, lane 3'-dCTP/+H). As noted previously, the RNase H enzyme induces cleavages not more than 3-5 nucleotides away from this junction, presumably because this positions its binding region on an RNA-RNA hybrid for which it exhibits significantly lower affinity. The RNA template length downstream of the RNA-DNA junction appears to have a direct effect on the number of cleaved products. The addition of RNase H to substrate R/D/R7, which contained the longest RNA region of 9 nucleotides when arrested with 3'-dATP, generated four specific cleavage products (Fig. 3B, right panel, lane 3'-dATP/+H). Increasing this length further did not generate a greater number of RNase H-specific cuts, as observed in the heat inactivation control (Fig. 3B, lane Heat/+H). Similarly, we were able to monitor enzyme translocation along the template strand. For instance, RNase H digestion of substrate R/D/R5 resulted in two cleavage products when the enzyme complex was arrested with 3'-dCTP, as opposed to three cleavage products when arrested one position further downstream with 3'-dATP (Fig. 3B, left panel). As in Fig.2, analysis of the RNase H digestion products suggests that the catalytically active enzyme complex generates a protection of approximately 11 to 12 nucleotides in length. Notably, the footprints generated with these substrates appear

to have a higher level of background cutting. This can be attributed to the presence of  $Mg^{2+}$  in the reaction.

## Discussion

Although considerable progress has been made in determining the structure of RdRps, little is known about specific interactions between the polymerase and its RNA template substrate after the initiation of RNA synthesis. Here we report the development of an RNase H-based footprinting technique that enables the study of the interaction between the BVDV polymerase and its nucleic acid substrate during elongation of RNA synthesis. An interpretation of our footprinting results is modeled in Figure 4. We designed our experiments to study footprints of arrested BVDV polymerization complexes. The results of our footprinting assay suggest that the catalytically active enzyme complex sits on the template substrate with a protection of approximately 11 to 12 nucleotides in length, and that this protection moves along the template strand according to the position where RNA synthesis is arrested. Studies on the *E.coli* RNase H enzyme have shown that 4 to 5 base pairs of the substrate are accommodated by the RNase H active center<sup>18</sup>. As such, we suggest that the active site of the BVDV RdRp contacts the newly synthesized RNA with approximately 6 to 7 base pairs. At this time, it is not known if the polymerase is completely stationary on the RNA template substrate, or if it can passively slide along the template strand. Sliding might allow bases that are normally protected to become susceptible to cleavage. Given these considerations, an exact length of protected bases would be difficult to state using this approach.



Nonetheless, it should be noted that our findings of a protection of 6 to 7 base pairs in length is in some agreement with molecular modeling studies on the HCV RdRp<sup>8; 9</sup>. In these studies, interactions of the HCV RdRp with a nucleic acid substrate, as inferred from the comparison with the crystal structure of HIV-1 RT in a ternary complex with DNA and incoming nucleotide, suggest that at least 5 nucleotides of the template region are in direct contact with the HCV polymerase<sup>9</sup>. Several other groups have analyzed RNA binding by RdRps during initiation of RNA synthesis<sup>21; 22; 23; 24; 25</sup>. For instance, Kim *et al.*<sup>22</sup> have determined that 7 nucleotides is the minimal size of RNA template required for stable binding of the HCV RdRp. Consistent with their findings are the results obtained in previous biochemical studies on the poliovirus 3D<sup>pol</sup><sup>23</sup>, the BVDV RdRp<sup>24</sup> and HCV polymerase<sup>21; 22; 25</sup>, all of which suggest that 6 to 8 nucleotides of the template RNA can interact with the RdRp to form a stable initiation complex. The RNase H-based footprinting assay described here, however, enables the study of catalytically active enzyme complexes after the initiation of RNA synthesis. The results of our study suggest that BVDV RdRp contacts the RNA template with approximately 6 to 7 base pairs during elongation. The priming strand beyond 6 to 7 base pairs is cleaved by *E. coli* RNase H. These findings further suggest that the primer and template maintain their duplex form and share the same exit. Based on this observation, we consider the possible positioning of the NS3 helicase upstream of the polymerase acting to unwind the double-stranded product as it exits the active site.

To date, this is the first footprinting of a viral RdRp enzyme complex on its RNA template substrate during elongation of RNA synthesis. An understanding of the nature of

the contacts made between the polymerase and its nucleic acid substrate during initiation or elongation of RNA synthesis may help determine the specific locations and functions of the accessory proteins within the RNA replication complex. The possibility that the RdRp-RNA interaction changes as the enzyme enters different stages of RNA synthesis cannot be excluded. Other polymerases, such as DNA-dependent RNA polymerases, are known to change their interactions with the template during different stages of transcription<sup>26; 27; 28</sup>. Several lines of evidence suggest that RdRps also adopt different conformations during different stages of RNA synthesis, or upon binding to different RNA templates<sup>14; 16; 29</sup>. It has been suggested that the thumb domain undergoes a conformational change involving the movement of the  $\beta$ -hairpin, to accommodate the growing double-stranded product during elongation<sup>16</sup>. The elucidation of two different crystal structures of the HCV RdRp from genotype 2a further demonstrates that the polymerase can exist in two different conformations; a “closed” conformation that is believed to be the active form of the enzyme, and an “open”, inactive form<sup>14</sup>. Finally, it has been demonstrated that the HCV polymerase alters its conformation to bind circular RNA, which then serve as templates for the initiation of RNA synthesis<sup>29</sup>.

Overall, the RNase H-based footprinting approach described in our study has provided novel insights into the binding properties of the BVDV polymerase during elongation. The development of this novel footprinting technique may be used in the future to facilitate the study of mechanisms involved in polymerase elongation and translocation. Ultimately, our data can aid in determining the effects of antiviral compounds on RdRp-RNA interactions. Information regarding this interaction would be

an obvious advantage when attempting to design specific inhibitors with improved antiviral efficacy.

# Figure 1

**A**

Template Name	Template Sequence
R/D1	5' CCT CTA TAC AGC TTC ATA CTT TCT AAu ucu cua uac 3'
	26
R/D2	5' CCT CTA TGC ACC TTC ATA CTT TCT AAu ucu cua uac 3'
	29

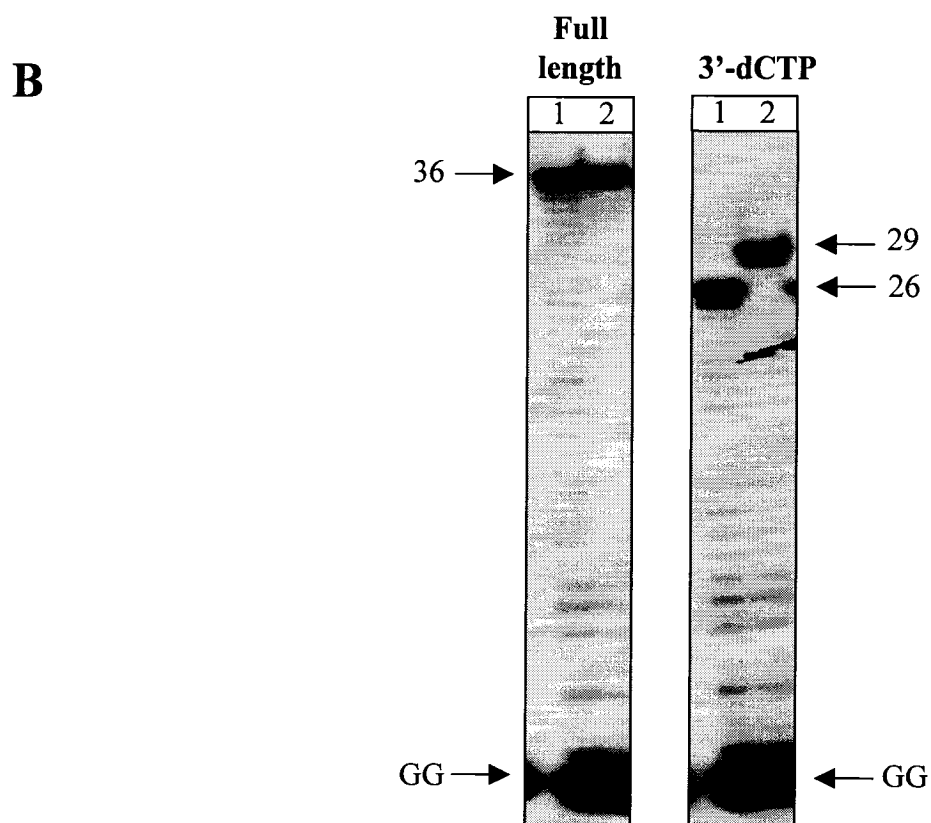
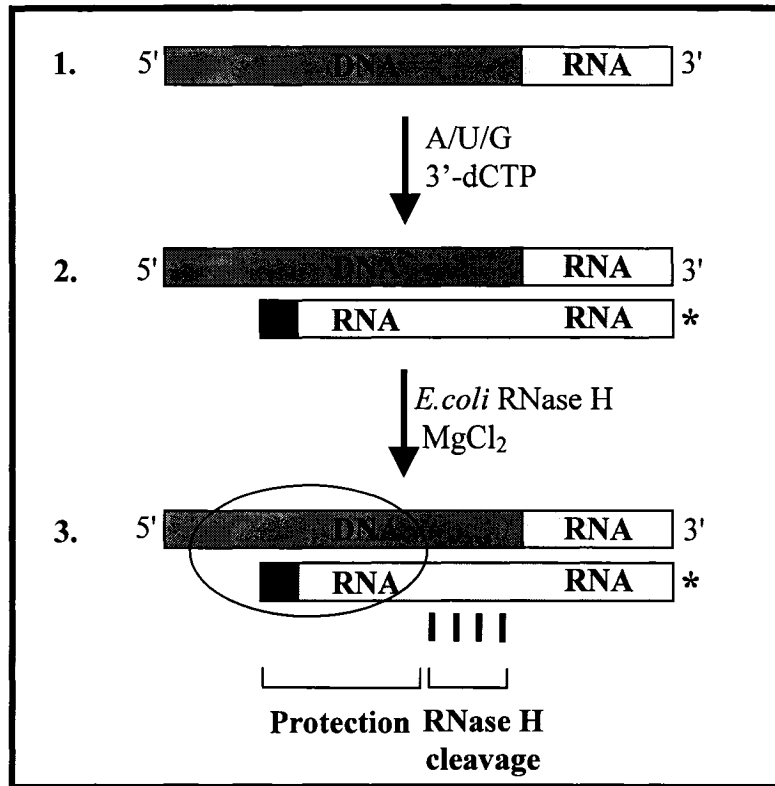


**Figure 1: Use of RNA-DNA chimeric templates as substrates for BVDV RdRp.**

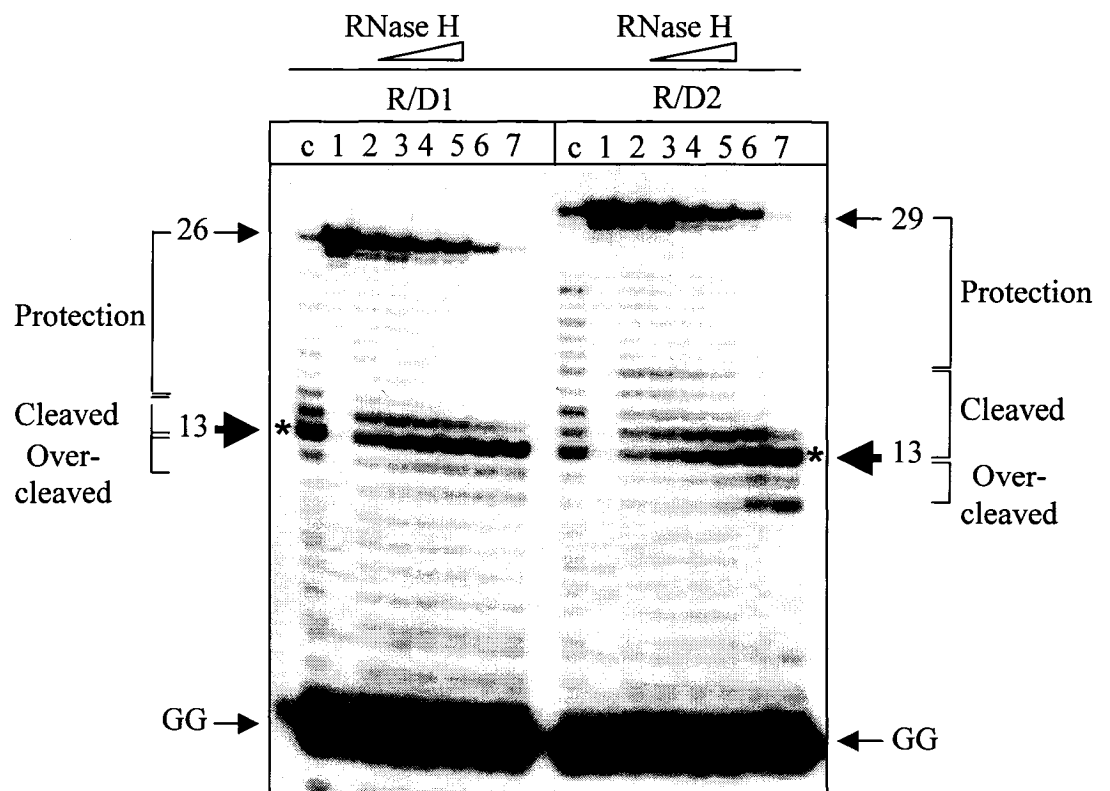
(A) Schematic representation of the chimeric RNA-DNA template systems, R/D1 and R/D2, utilized. The site of incorporation of 3'-dCTP is bolded. Note that the RNA portion of the template is represented by lower-case letters while the DNA portion is in upper-case letters. The template sequence that generates an RNA-DNA product is boxed in light grey. (B) Primer extension assay comparing full-length extension (left panel) and incorporation of 3'-dCTP (right panel) with templates R/D1 (lane 1) and R/D2 (lane 2). The site of incorporation for 3'-dCTP occurs at positions +26 (R/D1) or +29 (R/D2).

# Figure 2

**A**



**B**



C

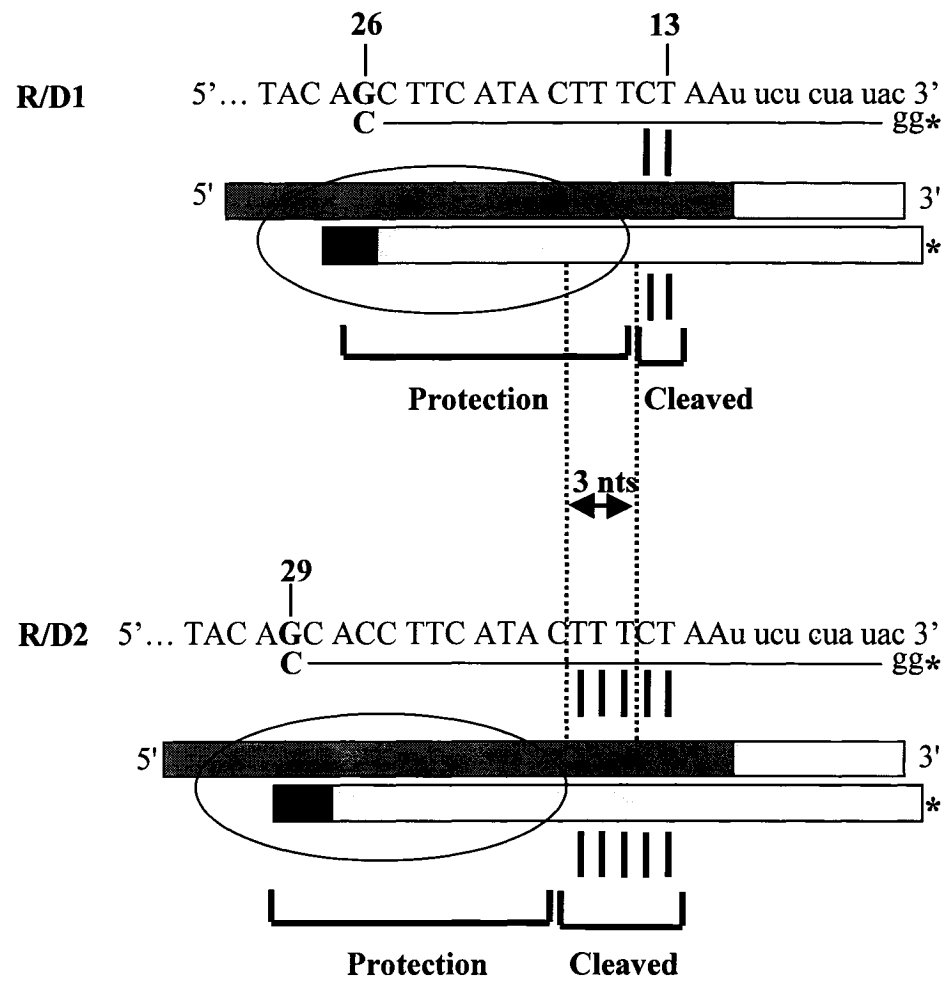


**Figure 2: Footprints of arrested polymerization complexes generate a protection of 11 to 12 nucleotides.** (A) Schematic description of the components involved in the RNase H-based footprinting assay. A series of RNA-DNA chimeric templates were utilized as substrates for BVDV RdRp (step 1). The RNA portion of the template is represented by the light grey box, while the DNA portion by the dark grey box. RNA synthesis is initiated through the extension of a 5'-end labeled dinucleotide primer (asterisk) bound to the 3'-end of the template and takes place until the incorporation of specific nucleoside analogues (black box), generating an RNA-DNA hybrid product (step 2). Addition of *E. coli* RNase H cleaves the RNA portion of the RNA-DNA hybrid that is not protected by the arrested polymerization complex, as visualized by a series of radiolabelled bands on denaturing polyacrylamide gels (step 3). (B) Comparison of the footprints generated by BVDV NS5B with chimeric templates R/D1 and R/D2. RNA synthesis proceeded until the incorporation of 3'-dCTP at position +26 (R/D 1, left panel) or +29 (R/D 2, right panel). Lane c shows a control reaction in which the arrested enzyme complex was heat inactivated at 95°C for 5 minutes, prior to the addition of 1.25U of *E. coli* RNase H. Lanes 1-7 show reactions in the presence of increasing concentrations of *E. coli* RNase H: 0U, 0.08U, 0.15U, 0.3U, 0.6U, 1.25U, and 2.5U. The asterisk represents a cut close to the RNA-DNA junction at template position +13. Note that the numbering refers to the length of the template. (C) Schematic description of the footprint pattern obtained in (A). The catalytically active enzyme complex (circle) sits on the template substrate with a protection of 11 to 12 nucleotides in length, and moves along the template according to the position where RNA synthesis is arrested.



# Figure 3

**A**

Template Name	Sequence	RNA portion
R/D/R5	5' cgu cua aac <u>ugc</u> cac a ACC CAC ACA CAC aca cac aac 3'    28 27	6 nts
R/D/R6	5' cgu cua aac <u>ugc</u> cac <u>ac</u> ACC CAC ACA CAC aca cac aac 3'    29 28	7nts
R/D/R7	5' cgu cua aac <u>ugc</u> cac <u>aac</u> ACC CAC ACA CAC aca cac aac 3'    30 29	8nts

**B**

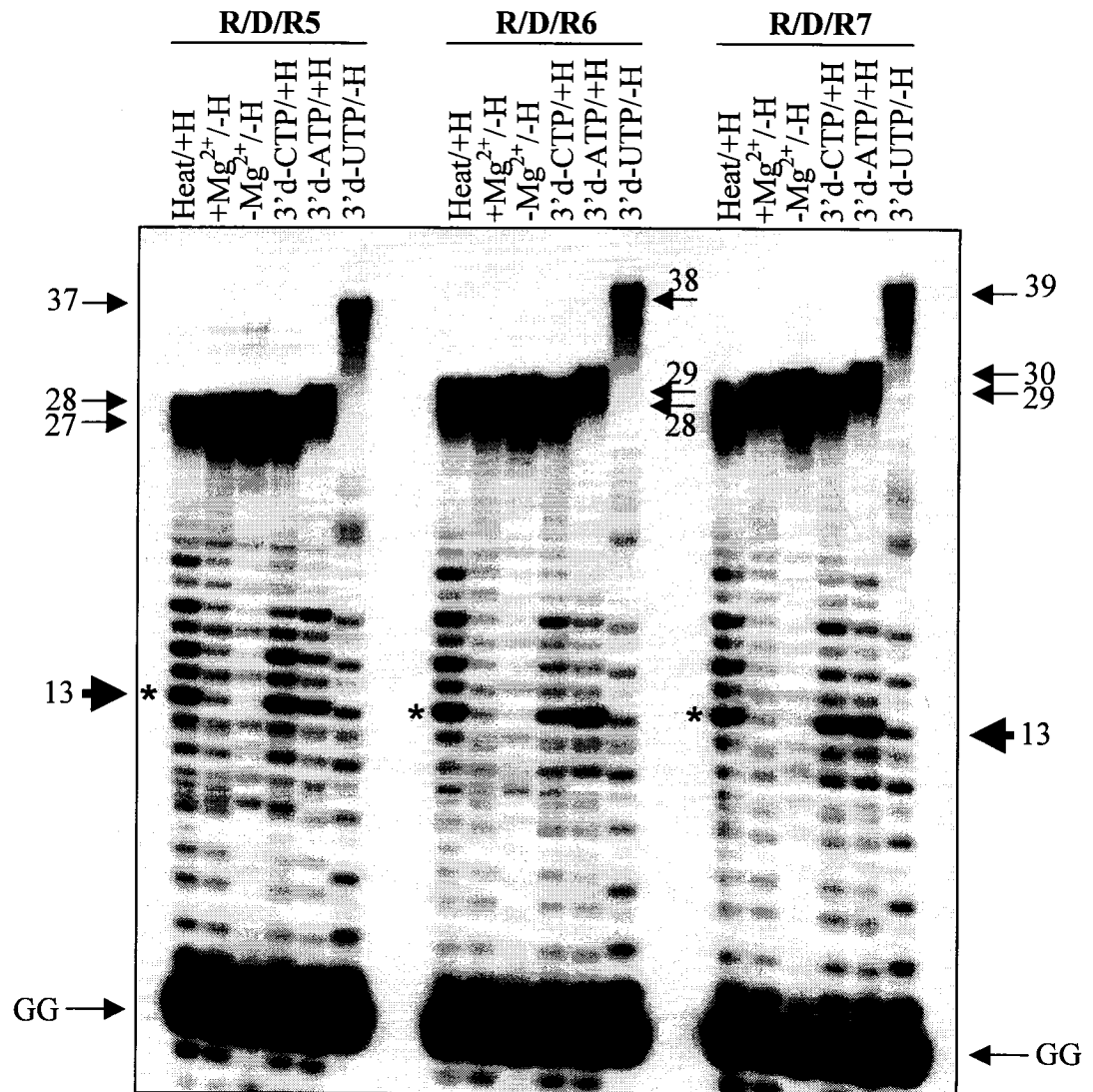


**Figure 3: Translocation of arrested enzyme complexes.** (A) Schematic representation depicting the modified chimeric RNA-DNA-RNA template systems (R/D/R 5-7) utilized in this experiment. Site of incorporation of chain-terminators, 3'-dCTP (bold) and 3'-dATP (shadowed), as well as the template length prior to the RNA-DNA junction (underlined) are highlighted. Note that the RNA portion of the template is represented by lower-case letters while the DNA portion in upper-case letters. (B) RNase H-based footprinting assay comparing the protection generated by arrested enzyme complexes on templates R/D/R5, R/D/R6 and R/D/R7. Incorporation of 3'-dUTP served as a control for the specific assignment of the positions of cleaved products obtained. The asterisk represents a cut close to the RNA-DNA junction at template position +13. Numbering refers to the length of the template.

**Figure 4**

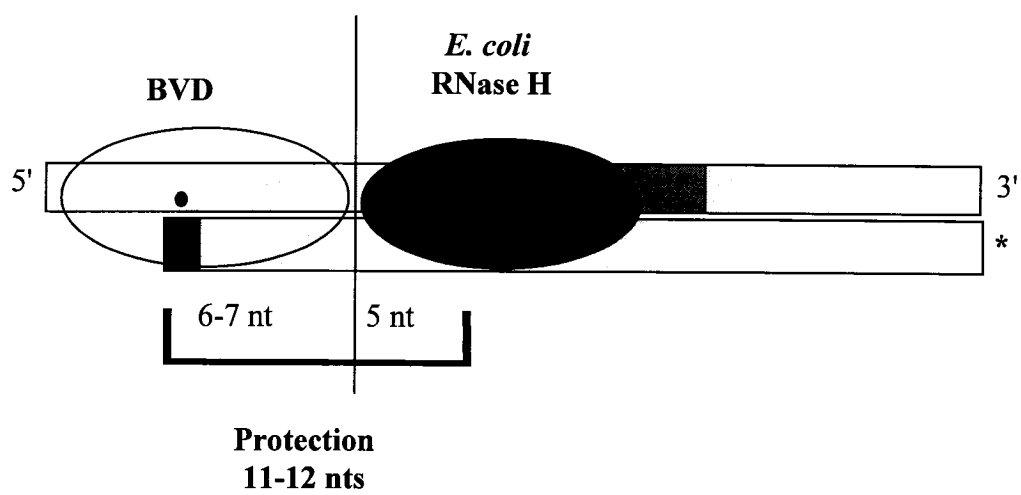


**Figure 4: Schematic model of the interaction between BVDV RdRp and its nucleic acid substrate during elongation.** Catalytically active enzyme complexes are arrested on RNA/DNA substrates (light grey /dark grey) through the incorporation of chain-terminating nucleotides (black square). An overall protection of 11-12 base pairs in length is generated, with the active site of the BVDV RdRp (clear circle) contacting the RNA template by 6 to 7 nucleotides, and the active site of *E. coli* RNase H (grey circle) accommodating 4 to 5 base pairs of the substrate.

## References:

1. Reed, K. E. & Rice, C. M. (2000). Overview of hepatitis C virus genome structure, polyprotein processing, and protein properties. *Curr Top Microbiol Immunol* **242**, 55-84.
2. Behrens, S. E., Tomei, L. & De Francesco, R. (1996). Identification and properties of the RNA-dependent RNA polymerase of hepatitis C virus. *Embo J* **15**, 12-22.
3. Ferrari, E., Wright-Minogue, J., Fang, J. W., Baroudy, B. M., Lau, J. Y. & Hong, Z. (1999). Characterization of soluble hepatitis C virus RNA-dependent RNA polymerase expressed in Escherichia coli. *J Virol* **73**, 1649-54.
4. Lohmann, V., Korner, F., Herian, U. & Bartenschlager, R. (1997). Biochemical properties of hepatitis C virus NS5B RNA-dependent RNA polymerase and identification of amino acid sequence motifs essential for enzymatic activity. *J Virol* **71**, 8416-28.
5. Yamashita, T., Kaneko, S., Shirota, Y., Qin, W., Nomura, T., Kobayashi, K. & Murakami, S. (1998). RNA-dependent RNA polymerase activity of the soluble recombinant hepatitis C virus NS5B protein truncated at the C-terminal region. *J Biol Chem* **273**, 15479-86.
6. Zhong, W., Gutshall, L. L. & Del Vecchio, A. M. (1998). Identification and characterization of an RNA-dependent RNA polymerase activity within the nonstructural protein 5B region of bovine viral diarrhea virus. *J Virol* **72**, 9365-9.
7. Ago, H., Adachi, T., Yoshida, A., Yamamoto, M., Habuka, N., Yatsunami, K. & Miyano, M. (1999). Crystal structure of the RNA-dependent RNA polymerase of hepatitis C virus. *Structure Fold Des* **7**, 1417-26.
8. Bressanelli, S., Tomei, L., Roussel, A., Incitti, I., Vitale, R. L., Mathieu, M., De Francesco, R. & Rey, F. A. (1999). Crystal structure of the RNA-dependent RNA polymerase of hepatitis C virus. *Proc Natl Acad Sci U S A* **96**, 13034-9.
9. Lesburg, C. A., Cable, M. B., Ferrari, E., Hong, Z., Mannarino, A. F. & Weber, P. C. (1999). Crystal structure of the RNA-dependent RNA polymerase from hepatitis C virus reveals a fully encircled active site. *Nat Struct Biol* **6**, 937-43.
10. Hansen, J. L., Long, A. M. & Schultz, S. C. (1997). Structure of the RNA-dependent RNA polymerase of poliovirus. *Structure* **5**, 1109-22.
11. Butcher, S. J., Grimes, J. M., Makeyev, E. V., Bamford, D. H. & Stuart, D. I. (2001). A mechanism for initiating RNA-dependent RNA polymerization. *Nature* **410**, 235-40.
12. Choi, K. H., Groarke, J. M., Young, D. C., Kuhn, R. J., Smith, J. L., Pevear, D. C. & Rossmann, M. G. (2004). The structure of the RNA-dependent RNA polymerase from bovine viral diarrhea virus establishes the role of GTP in de novo initiation. *Proc Natl Acad Sci U S A* **101**, 4425-30.
13. Sarafianos, S. G., Clark, A. D., Jr., Das, K., Tuske, S., Birktoft, J. J., Ilankumaran, P., Ramesha, A. R., Sayer, J. M., Jerina, D. M., Boyer, P. L., Hughes, S. H. & Arnold, E. (2002). Structures of HIV-1 reverse transcriptase with pre- and post-translocation AZTMP-terminated DNA. *Embo J* **21**, 6614-24.
14. Biswal, B. K., Cherney, M. M., Wang, M., Chan, L., Yannopoulos, C. G., Bilimoria, D., Nicolas, O., Bedard, J. & James, M. N. (2005). Crystal structures of

- the RNA-dependent RNA polymerase genotype 2a of hepatitis C virus reveal two conformations and suggest mechanisms of inhibition by non-nucleoside inhibitors. *J Biol Chem* **280**, 18202-10.
15. O'Farrell, D., Trowbridge, R., Rowlands, D. & Jager, J. (2003). Substrate complexes of hepatitis C virus RNA polymerase (HC-J4): structural evidence for nucleotide import and de-novo initiation. *J Mol Biol* **326**, 1025-35.
  16. Hong, Z., Cameron, C. E., Walker, M. P., Castro, C., Yao, N., Lau, J. Y. & Zhong, W. (2001). A novel mechanism to ensure terminal initiation by hepatitis C virus NS5B polymerase. *Virology* **285**, 6-11.
  17. D'Abramo, C. M., Cellai, L. & Gotte, M. (2004). Excision of incorporated nucleotide analogue chain-terminators can diminish their inhibitory effects on viral RNA-dependent RNA polymerases. *J Mol Biol* **337**, 1-14.
  18. Lima, W. F. & Crooke, S. T. (1997). Binding affinity and specificity of Escherichia coli RNase H1: impact on the kinetics of catalysis of antisense oligonucleotide-RNA hybrids. *Biochemistry* **36**, 390-8.
  19. Mendez, E., Ruggli, N., Collett, M. S. & Rice, C. M. (1998). Infectious bovine viral diarrhea virus (strain NADL) RNA from stable cDNA clones: a cellular insert determines NS3 production and viral cytopathogenicity. *J Virol* **72**, 4737-45.
  20. Huber, P. W. (1993). Chemical nucleases: their use in studying RNA structure and RNA-protein interactions. *Faseb J* **7**, 1367-75.
  21. Kao, C. C., Yang, X., Kline, A., Wang, Q. M., Barket, D. & Heinz, B. A. (2000). Template requirements for RNA synthesis by a recombinant hepatitis C virus RNA-dependent RNA polymerase. *J Virol* **74**, 11121-8.
  22. Kim, Y. C., Russell, W. K., Ranjith-Kumar, C. T., Thomson, M., Russell, D. H. & Kao, C. C. (2005). Functional analysis of RNA binding by the hepatitis C virus RNA-dependent RNA polymerase. *J Biol Chem* **280**, 38011-9.
  23. Beckman, M. T. & Kirkegaard, K. (1998). Site size of cooperative single-stranded RNA binding by poliovirus RNA-dependent RNA polymerase. *J Biol Chem* **273**, 6724-30.
  24. Kim, M. J., Zhong, W., Hong, Z. & Kao, C. C. (2000). Template nucleotide moieties required for de novo initiation of RNA synthesis by a recombinant viral RNA-dependent RNA polymerase. *J Virol* **74**, 10312-22.
  25. Zhong, W., Ferrari, E., Lesburg, C. A., Maag, D., Ghosh, S. K., Cameron, C. E., Lau, J. Y. & Hong, Z. (2000). Template/primer requirements and single nucleotide incorporation by hepatitis C virus nonstructural protein 5B polymerase. *J Virol* **74**, 9134-43.
  26. Tahirov, T. H., Temiakov, D., Anikin, M., Patlan, V., McAllister, W. T., Vassilyev, D. G. & Yokoyama, S. (2002). Structure of a T7 RNA polymerase elongation complex at 2.9 Å resolution. *Nature* **420**, 43-50.
  27. Ma, K., Temiakov, D., Jiang, M., Anikin, M. & McAllister, W. T. (2002). Major conformational changes occur during the transition from an initiation complex to an elongation complex by T7 RNA polymerase. *J Biol Chem* **277**, 43206-15.
  28. Cheetham, G. M. & Steitz, T. A. (2000). Insights into transcription: structure and function of single-subunit DNA-dependent RNA polymerases. *Curr Opin Struct Biol* **10**, 117-23.

29. Ranjith-Kumar, C. T. & Kao, C. C. (2006). Recombinant viral RdRps can initiate RNA synthesis from circular templates. *Rna* **12**, 303-12.

## **CHAPTER 5**

### **GENERAL DISCUSSION**



## **GENERAL DISCUSSION**

### **5.1 Initiation vs. Elongation**

The HCV replication complex is composed of several multi-domain enzymes that exhibit important activities such as unwinding, RNA synthesis, and protease activities. Elucidating the roles of the individual proteins will help advance both structural and functional studies on the replication complex as a whole. Currently, the structure and functions of many of the HCV non-structural proteins have been determined. While all proteins of the complex play an important role in replication, the RdRp is a key enzyme that is absolutely essential for the RNA replication process, and is often the target of antiviral drug development. To understand the polymerase, it is important to examine both the initiation and elongation stages of RNA synthesis. Despite the increasing number of studies on the characterization of RdRp activity and structure, the precise molecular mechanism of how HCV RNA synthesis is initiated, terminated, and regulated remains unclear. The fact that there are currently only poorly defined mechanisms of RNA synthesis impedes the precise evaluation of antiviral inhibitors that can specifically target the initiation and/or elongation stages of HCV replication. Evidently, precise knowledge of the different steps of RNA synthesis can serve as a molecular basis for the evaluation of antiviral compounds, as well as help determine the extent of discrimination of these inhibitors at the polymerase active site during initiation or elongation. A better understanding of the mechanism and regulation of HCV RNA replication is now possible with the use of replicons and the recent development of the JFH-1 model system, which ultimately permits the study of the entire HCV life cycle. At the time when I began my

PhD studies, these model systems were not available. Related viruses such as BVDV were used as surrogate model systems to study HCV replication. Despite the many similarities between both viruses in terms of their replication cycle and genetic organization, it is clear from the experiments described in this thesis that there are inherent differences in the activities of RdRp from HCV and BVDV, and that generally polymerases from the same viral families do not necessarily share a common, unifying mechanism of initiation of RNA synthesis.

The postulated HCV RNA replication process is a two-step mechanism. First, initiation of RNA synthesis begins at or near the 3' end of the positive strand RNA genome. Although still unclear, it is generally accepted that primer-independent (*de novo*) synthesis is the more biologically relevant mechanism of initiation for HCV and BVDV replication. *De novo* initiation consists of the addition of an NTP to the 3'-hydroxyl group of the first initiating nucleotide. During elongation, this nucleotidyl transfer reaction is repeated with subsequent NTPs to generate a complementary RNA product. In the past few years, *de novo* initiation of viral RNA synthesis has been the focus of many studies, which have provided most of what is known now about the specificity and requirements for initiating RNA synthesis *de novo*. For instance, the specificity of cytidylate as the preferred template initiation nucleotide has been identified<sup>195; 197; 199; 202</sup>, the involvement of the  $\beta$ -hairpin and the regulatory motif in the C-terminal tail of RdRp in this initiation process has been demonstrated<sup>191; 192; 194</sup>, and the requirements for high concentrations of the initiation nucleotide has been proven<sup>201; 202; 204; 205</sup>. However, the observation that both BVDV and HCV NS5B enzymes form

specific GTP binding sites<sup>182; 185</sup>, combined with the fact that GTP is the preferred NTPi *in vitro*, raised the possibility that the binding of GTP to the GTP-specific binding site might be an important step required during the initiation of RNA synthesis. In order to contribute to the characterization of the initiation step, we studied the functional role of this G-site during BVDV and HCV initiation. In the HCV enzyme, crystallographic data have pointed to the existence of a so-called “allosteric” or surface GTP binding site located behind the thumb domain, approximately 30Å away from the catalytic site<sup>182</sup>. In contrast, the structure of the BVDV polymerase bound to a GTP substrate revealed the existence of a G-site located in the vicinity of the active site of the BVDV enzyme, just upstream of the priming site (P-site) and nucleotide binding site (N-site)<sup>185</sup>. In Chapter 3, we showed that the binding of GTP to this G-site in the BVDV enzyme affects the precise positioning of the template during *de novo* synthesis, thereby stressing the functional importance of GTP binding to the G-site during initiation of RNA synthesis. Our data suggest that the bound GTP plays an important role in promoting *de novo* initiation by facilitating the alignment between the 3'terminus of the template and the priming nucleotide, and by preventing the template to overshoot and extend beyond the active site of the polymerase. Previous structural data on the BVDV polymerase has suggested that the 3'-hydroxyl group of the bound GTP may also help orient the 3'hydroxly group of NTPi to attack the first nucleotide substrate<sup>185</sup>. As such, we propose that the bound GTP plays a dual role during *de novo* initiation by orienting the priming nucleotide, and by controlling the positioning of the template. Such effects are not seen with the HCV enzyme, indicating that the requirement for high concentrations of GTP plays a different role in promoting efficient *de novo* synthesis. It is speculated that, in the

case of HCV NS5B, binding of GTP to the GTP binding site might trigger a conformational change in the enzyme. This change might involve movement of the  $\beta$ -hairpin away from the active site or allow for alternative interactions between the fingers and thumb domains which, in turn, may render efficient *de novo* initiation. Based on the results of Chapter 3, we also conclude that unlike the BVDV polymerase, the HCV enzyme does not contain a functionally equivalent GTP-specific binding site adjacent to the active site. This observation is in agreement with the HCV polymerase crystal structure which shows that this GTP position corresponds to a cavity filled with water molecules<sup>182</sup>, but differs from the structural model proposed by Ferron *et al.*<sup>249</sup>. In their model, a GTP molecule was docked in the HCV polymerase structure to determine whether a GTP pocket next to the active site can accommodate GTP in a similar manner as observed for BVDV RdRp. The model suggests that motif E, proposed to be part of the P-site, may also constitute a specific pocket to which the binding of a GTP molecule is needed to hold the initiation complex together. The role of this bound GTP comes into play once the first reaction of initiation occurs. Here the template enters the pocket and stacks against the guanine base of the motif E GTP. This stacking triggers a rearrangement of the guanine base pushing GTP toward the  $\beta$ -hairpin, which consequently induces a partial movement of the hairpin to accommodate the elongation of the growing RNA strand. This first rearrangement corresponds to previous kinetic data which shows that the N2 to N3 polymerization reaction is a rate-limiting step<sup>250</sup>. The authors also suggest that the reorganization of the thumb domain, through binding of a GTP molecule at the “allosteric” G-site located away from the active site, results in the complete opening of the  $\beta$ -hairpin, and allows the double-stranded RNA molecule to exit

the active site. Given that the corresponding  $\beta$ -thumb region in the BVDV RdRp shows higher conformational flexibility than that in HCV RdRp<sup>185</sup>, it is unlikely that GTP binding to the G-site in BVDV induces a similar conformational change. Additionally, the proposed role of GTP in HCV initiation is based on a structural model and not on experimental findings. The possibility that the role of GTP binding in the HCV NS5B enzyme may require different enzyme conformations with different catalytic properties remains to be established. Nonetheless, the structural model described above and the conclusions made in Chapter 3 highlight some of the significant differences in the role(s) of GTP during *de novo* initiation of RNA synthesis by both HCV and BVDV RdRps. Additional experiments exploring the role of GTP, especially in other experimental systems (i.e., subgenomic replicons, JFH-1 cell culture system, etc.) and with other related viruses will definitely provide a more accurate model of *de novo* synthesis, and aid in the characterization of the distinct steps involved in the initiation process. Precise knowledge of these steps is considerably important for the design of potent HCV inhibitors targeting the initiation of HCV RNA replication. This knowledge may also help in achieving optimal combinations of HCV polymerase inhibitors for effective therapeutic purposes. Given that initiation of RNA synthesis is likely the rate-limiting step in HCV replication, inhibitors targeting the initiation step might prove to be more potent than elongation inhibitors *in vivo*. For instance, it has been demonstrated that entecavir, a specific HBV initiation inhibitor, blocks viral genome replication with greater efficiency as compared to lamivudine (3TC), which inhibits the elongation step<sup>251</sup>.

Further investigation is also needed to confirm whether GTP is the preferred NTPi *in vivo*. In their study, Cai *et al.*<sup>252</sup> have found that the replication of both positive- and negative-strand RNAs of the subgenomic HCV replicon was selectively initiated with ATP rather than with GTP. The authors attributed this discrepancy due to differences in the sequence and/or structure of the HCV RdRp between different viral isolates. For this reason, it would be interesting to identify the specific amino acids and/or structures of the HCV polymerase that are involved in discriminating incoming NTPs for efficient initiation *in vivo*. Additional studies are required to determine whether the site of HCV replication or the nucleotide pools within the infected cell can affect the selection of nucleotides used. Alternatively, the environmental conditions within the infected cell, along with the presence of other viral and cellular proteins may also affect binding of GTP to the G-site in both HCV and BVDV RdRp. The possibility that occlusion of the active site by the C-terminal domain of the NS5B protein, which has been truncated in our studies, may effect template positioning and/or GTP binding during initiation cannot be excluded. Although it is certain that advances remain to be made, our model of *de novo* initiation reveals remarkable new facets into the role of GTP during *de novo* initiation of BVDV replication, and can be utilized to shed light on the similarities and differences between the initiation mechanisms among viral polymerases.

In line with the goal of examining the different stages involved in the viral replication process, we studied the interaction between the polymerase and its nucleic acid substrate during elongation of RNA synthesis. Although considerable progress has been made in determining the structure of viral RdRps, either alone or in the presence of

an incoming nucleotide<sup>179; 180; 181; 182</sup>, little data exists regarding how the enzyme interacts with its template after the initiation of RNA synthesis. The RNase H-based footprinting strategy devised in Chapter 4 has a generic application for the study of protein-nucleic acid complexes. Footprinting techniques serve as powerful tools that are often utilized for investigating the DNA or RNA binding sites of proteins, oligonucleotides, and small molecules. These methods provide rapid results pertaining to the sequence, location, size, and affinity of each site in a single molecule. We therefore designed our experiments to look at the footprinting pattern of arrested BVDV polymerization complexes. The combined results of our footprinting assay suggest that BVDV RdRp contacts the newly synthesized RNA with approximately 6 to 7 base pairs. At this time, it is not known if the polymerase is completely stationary on the RNA template substrate, or if it can passively slide along the template strand. Sliding might allow bases that are normally protected to become susceptible to cleavage. Given these considerations, an exact length of protected bases would be difficult to state using this approach. Nonetheless, it should be noted that our findings of a protection site of 6 to 7 base pairs in length is in some agreement with molecular modeling studies on the HCV RdRp<sup>181</sup>. To date, this is the first footprinting of a viral RdRp enzyme complex on its RNA template substrate during elongation. The development of this novel enzymatic footprinting technique may be used in the future to facilitate the study of mechanisms involved in polymerase elongation and translocation. As with HIV-1 RT, this technique can be expanded upon to study whether parameters such temperature, the nature of the nucleic acid substrate, the concentration of the next complementary nucleotide, or the mutational background of the enzyme can affect enzyme translocation. Our data can also aid in determining the effects of these

compounds on the RdRp-substrate interactions during inhibition of RNA synthesis. Additionally, the RNase H-based footprinting strategy can be used to characterize the binding properties of the polymerase with respect to other viral proteins within the replication complex. Based on our results, it is assumed that the NS3 helicase is positioned ahead of the polymerase to unwind the double-stranded product as it exits the active site. It would be interesting to confirm this observation and determine whether the presence of the NS3 helicase modifies the contact between the polymerase and its template substrate during polymerization.

A question that usually arises is whether the C-terminal domain of the NS5B protein should be included for enzymatic characterization studies. While it is true that the full-length protein is more native than its truncated version, the possibility that the presence of this hydrophobic anchor domain may cause aggregation or interfere with the stability of the remainder of the NS5B protein cannot be excluded. Given that the experiments presented in this thesis were conducted utilizing a C-terminal truncated form of the BVDV polymerase, it is important to explore whether the presence of this C-terminal domain plays a functional role during BVDV polymerization *in vivo*. The use of the full-length BVDV RdRp or the addition of crude extracts of virally-infected cells to the footprinting assay may help shed some light on this topic. The choice of probing nuclease also warrants discussion. While it is technically easier to utilize a nuclease that specifically degrades dsRNA molecules, *E. coli* RNase H was chosen for enzymatic probing to facilitate the analysis of only enzymatically active BVDV enzyme preparations, given that crystallographic data on *E. coli* RNase H is available<sup>253</sup>.



Overall, this classical footprinting approach has provided novel insights into the binding properties of the BVDV polymerase during elongation, and has initiated research into a relatively new field for viral RdRps. Eventually, this approach can be expanded upon to establish site-specific footprinting techniques that can be used to monitor the precise positioning of the protein on its nucleic acid substrate.

## **5.2 Future Therapeutic Implications**

The recurring theme throughout this thesis is to advance research with the ultimate goal of improving drug design for the development of effective polymerase inhibitors. As mentioned in Chapter 1, several anti-HCV nucleoside analogues have already yielded promising results in early clinical trials<sup>108</sup>. Most of our understanding of the mechanism of action of nucleoside analogues comes from studies performed on HIV-1-RT and its nucleoside inhibitors. Through these studies, it has been determined that there are two major biochemical mechanisms associated with resistance to this specific class of compounds, which include increased rates of phosphorolytic excision, or improved discrimination between the nucleoside analogue and its natural counterpart during incorporation<sup>254; 255</sup>. In Chapter 2, we addressed whether phosphorolytic excision is a possible mechanism that can also diminish the efficiency of nucleotide analogues directed against viral RdRps. We showed that the BVDV NS5B enzyme can excise incorporated obligate chain-terminators in PPi-dependent reactions and rescue RNA synthesis. Based on these results, we developed specific models to describe the events that take place directly at the active site of the BVDV polymerase during nucleotide

binding, chain-termination, phosphorolytic excision, and DEC formation. These models provide novel insights into the mechanism of translocation of viral RdRps, as well as describe how access to N- and P-sites is controlled by a translocational equilibrium that depends on multiple parameters. This precise positioning of the BVDV enzyme is a crucial parameter that can influence rates of excision of incorporated chain-terminators, and ultimately affect drug susceptibility. Studies with HIV-1 RT have shown that excision can only occur in a complex that contains the 3'end of the chain-terminated primer in the N-site (pre-translocation complex)<sup>256; 257</sup>. Upon binding of the next nucleotide, the polymerase translocates a single position further downstream, which brings the 3'end of the primer back to the P-site (post-translocation complex) and places the chain-terminator away from the active site, literally blocking excision. A similar scenario is described for the BVDV polymerase. We showed that the efficiency of excision and rescue of RNA synthesis critically depends on the concentration of PPi and NTPs. High NTP concentrations promote the formation of a DEC that diminishes excision, while high concentrations of PPi promote excision. Our laboratory further investigated whether obligate and non-obligate chain-terminators can also be excised by the HCV enzyme. It was determined that all inhibitors tested, including a broad panel of adenosine and cytidine analogues, as well as the clinically relevant non-obligate chain-terminator 2'-C-Me-CTP, are excised in the presence of physiological relevant concentrations of PPi. More importantly, it was determined that the efficiency of excision is largely influenced by the nature of the nucleobase, with pyrimidines being more efficiently excised than purines.

Taken together, the data obtained with both BVDV and HCV RdRps have important implications for future drug development. While metabolic activation of nucleoside analogue prodrugs, as well as the efficiency and accuracy of nucleotide incorporation are important factors that can influence susceptibility to this class of compounds *in vivo*, it cannot be excluded that phosphorolytic excision may also be relevant. As such, several approaches are needed to overcome the phosphorolytic removal of incorporated chain-terminators. These approaches, which are currently under investigation for HIV-1 RT, involve the identification of compounds that can trap the enzyme complex either pre- or post-translocation<sup>258</sup>. For instance, the development of small molecules that bind at or in close proximity to the N-site ultimately traps the complex post-translocation and blocks excision. In contrast, the development of small molecules that compete with the binding of PPi and/or PPi donor molecules traps the enzyme complex pre-translocation and diminishes excision by preventing the binding of PPi. Alternatively, our findings also warrant further investigation toward the development of novel purine analogues, given that they are less efficiently excised than pyrimidine analogues.

### 5.3 Final Conclusion

The research presented in this PhD thesis has answered several important basic questions regarding the different aspects of initiation and elongation of RNA synthesis of viruses belonging to the *Flaviviridae* family, in particular BVDV and HCV. Throughout this work, however, other questions have been raised, the answer to which will hopefully further our knowledge and understanding of the HCV replication process. This knowledge may potentially lead to the identification of novel targets, support the design of specific inhibitors that can block critical stages of the viral life cycle, and ultimately aid in the prevention of one of the most common causes of liver cirrhosis and HCC worldwide. It is my hope that the data presented in this thesis will provide the platform upon which further progress in the study of hepatitis C will proceed.

## CONTRIBUTION TO ORIGINAL KNOWLEDGE

The work presented below is a summary of the major findings contained in Chapters 2-4 of this thesis, which has been adapted from articles published or prepared for submission to refereed scientific journals. The focus of this thesis was to study the molecular mechanisms involved in initiation and elongation of viral RdRps.

**Chapter 2:** Prior to the initiation of projects detailed in this thesis, it has been determined that the NS5B protein of HCV and BVDV functions as an RNA-dependent RNA polymerase required for viral replication. Despite extensive biochemical and structural characterization of the polymerase, important and unresolved questions relating to the mechanisms of initiation and elongation of RNA synthesis remained. In this chapter, cell-free assays were established utilizing BVDV RdRp as a model system to study the fundamental aspects of the mechanisms of initiation and elongation of polymerases belonging to the *Flaviviridae* family. The first main objective was to assess the potential of chain-terminating nucleotides as antiviral agents. The major contribution of the work presented in Chapter 2 demonstrated for the first time that the incorporation of chain-terminating nucleotides by viral RdRps is not irreversible, and that the presence of PPi promotes the excision of the inhibitor and rescue of RNA synthesis. Given that phosphorolytic excision provides an important mechanism for HIV resistance, the results of Chapter 2 demonstrated that this PPi-dependent excision is also a possible mechanism that can diminish the efficiency of nucleotide analogues directed against viral RdRps.

**Chapter 3:** These chain-terminating nucleotides were utilized as tools to study the role of the GTP-specific binding site of BVDV NS5B during *de novo* initiation. Both HCV and BVDV NS5B have been co-crystallized with GTP<sup>182; 185</sup>. In the HCV enzyme, it has been demonstrated that GTP binds to the thumb domain at an allosteric GTP site that lies 30Å away from the polymerase active site. GTP binding to this site has been implicated in the regulation of the dynamic interactions between the fingers and thumb subdomains<sup>178; 182</sup>. In contrast, the G-site in BVDV NS5B is located ~ 4 to 6Å upstream of the polymerase active site<sup>185</sup>, thereby suggesting different yet important functions mediated by GTP binding during initiation of RNA synthesis. Strong biochemical evidence was presented in Chapter 3 to show that the G-specific binding site of BVDV NS5B controls the precise positioning of the template strand during *de novo* initiation. The other important results described in Chapter 3 showed that these effects were not observed with the HCV enzyme, indicating that the requirement for high concentrations of GTP plays a different role in promoting efficient *de novo* synthesis. As such, *de novo* initiation by BVDV and HCV RdRps is not based on a common, unifying mechanism.

**Chapter 4:** Although considerable progress has been made in defining the biochemical requirements during initiation and elongation, the detailed mechanism remains elusive. The RNA-RdRp interface has yet to be defined at different stages of RNA synthesis. In Chapter 4, a robust experimental system was established to study the protein-nucleic acid interactions at different stages during initiation and elongation. The results obtained provide the first footprints of elongation complexes of viral RdRps. Furthermore, the data suggest that this approach can be potentially used to study mechanisms involved in

polymerase elongation and translocation, as well as to study the effects of RNA, nucleotide, and/or inhibitor binding at different stages during initiation and elongation.

## References:

1. Choo, Q. L., Kuo, G., Weiner, A. J., Overby, L. R., Bradley, D. W. & Houghton, M. (1989). Isolation of a cDNA clone derived from a blood-borne non-A, non-B viral hepatitis genome. *Science* **244**, 359-62.
2. Kuo, G., Choo, Q. L., Alter, H. J., Gitnick, G. L., Redeker, A. G., Purcell, R. H., Miyamura, T., Dienstag, J. L., Alter, M. J., Stevens, C. E. & et al. (1989). An assay for circulating antibodies to a major etiologic virus of human non-A, non-B hepatitis. *Science* **244**, 362-4.
3. Bretner, M. (2005). Existing and future therapeutic options for hepatitis C virus infection. *Acta Biochim Pol* **52**, 57-70.
4. Shepard, C. W., Finelli, L. & Alter, M. J. (2005). Global epidemiology of hepatitis C virus infection. *Lancet Infect Dis* **5**, 558-67.
5. Hoofnagle, J. H. (2002). Course and outcome of hepatitis C. *Hepatology* **36**, S21-9.
6. Reddy, K. R., Wright, T. L., Pockros, P. J., Shiffman, M., Everson, G., Reindollar, R., Fried, M. W., Purdum, P. P., 3rd, Jensen, D., Smith, C., Lee, W. M., Boyer, T. D., Lin, A., Pedder, S. & DePamphilis, J. (2001). Efficacy and safety of pegylated (40-kd) interferon alpha-2a compared with interferon alpha-2a in noncirrhotic patients with chronic hepatitis C. *Hepatology* **33**, 433-8.
7. Glue, P., Rouzier-Panis, R., Raffanel, C., Sabo, R., Gupta, S. K., Salfi, M., Jacobs, S. & Clement, R. P. (2000). A dose-ranging study of pegylated interferon alfa-2b and ribavirin in chronic hepatitis C. The Hepatitis C Intervention Therapy Group. *Hepatology* **32**, 647-53.
8. Hadziyannis, S. J., Sette, H., Jr., Morgan, T. R., Balan, V., Diago, M., Marcellin, P., Ramadori, G., Bodenheimer, H., Jr., Bernstein, D., Rizzetto, M., Zeuzem, S., Pockros, P. J., Lin, A. & Ackrill, A. M. (2004). Peginterferon-alpha2a and ribavirin combination therapy in chronic hepatitis C: a randomized study of treatment duration and ribavirin dose. *Ann Intern Med* **140**, 346-55.
9. Fried, M. W., Shiffman, M. L., Reddy, K. R., Smith, C., Marinos, G., Goncales, F. L., Jr., Haussinger, D., Diago, M., Carosi, G., Dhumeaux, D., Craxi, A., Lin, A., Hoffman, J. & Yu, J. (2002). Peginterferon alfa-2a plus ribavirin for chronic hepatitis C virus infection. *N Engl J Med* **347**, 975-82.
10. Manns, M. P., McHutchison, J. G., Gordon, S. C., Rustgi, V. K., Shiffman, M., Reindollar, R., Goodman, Z. D., Koury, K., Ling, M. & Albrecht, J. K. (2001). Peginterferon alfa-2b plus ribavirin compared with interferon alfa-2b plus ribavirin for initial treatment of chronic hepatitis C: a randomised trial. *Lancet* **358**, 958-65.
11. Chambers, T. J., Hahn, C. S., Galler, R. & Rice, C. M. (1990). Flavivirus genome organization, expression, and replication. *Annu Rev Microbiol* **44**, 649-88.
12. Moradpour, D. & Blum, H. E. (2004). A primer on the molecular virology of hepatitis C. *Liver Int* **24**, 519-25.
13. Reed, K. E. & Rice, C. M. (2000). Overview of hepatitis C virus genome structure, polyprotein processing, and protein properties. *Curr Top Microbiol Immunol* **242**, 55-84.



14. Clarke, B. (1997). Molecular virology of hepatitis C virus. *J Gen Virol* **78** ( Pt **10**), 2397-410.
15. Branch, A. D., Stump, D. D., Gutierrez, J. A., Eng, F. & Walewski, J. L. (2005). The hepatitis C virus alternate reading frame (ARF) and its family of novel products: the alternate reading frame protein/F-protein, the double-frameshift protein, and others. *Semin Liver Dis* **25**, 105-17.
16. Walewski, J. L., Keller, T. R., Stump, D. D. & Branch, A. D. (2001). Evidence for a new hepatitis C virus antigen encoded in an overlapping reading frame. *Rna* **7**, 710-21.
17. Lo, S. Y., Selby, M., Tong, M. & Ou, J. H. (1994). Comparative studies of the core gene products of two different hepatitis C virus isolates: two alternative forms determined by a single amino acid substitution. *Virology* **199**, 124-31.
18. McLauchlan, J. (2000). Properties of the hepatitis C virus core protein: a structural protein that modulates cellular processes. *J Viral Hepat* **7**, 2-14.
19. Ray, R. B., Lagging, L. M., Meyer, K., Steele, R. & Ray, R. (1995). Transcriptional regulation of cellular and viral promoters by the hepatitis C virus core protein. *Virus Res* **37**, 209-20.
20. Ray, R. B. & Ray, R. (2001). Hepatitis C virus core protein: intriguing properties and functional relevance. *FEMS Microbiol Lett* **202**, 149-56.
21. Chou, A. H., Tsai, H. F., Wu, Y. Y., Hu, C. Y., Hwang, L. H., Hsu, P. I. & Hsu, P. N. (2005). Hepatitis C virus core protein modulates TRAIL-mediated apoptosis by enhancing Bid cleavage and activation of mitochondria apoptosis signaling pathway. *J Immunol* **174**, 2160-6.
22. Realdon, S., Gerotto, M., Dal Pero, F., Marin, O., Granato, A., Basso, G., Muraca, M. & Alberti, A. (2004). Proapoptotic effect of hepatitis C virus CORE protein in transiently transfected cells is enhanced by nuclear localization and is dependent on PKR activation. *J Hepatol* **40**, 77-85.
23. Jin, Y. H., Crispe, I. N. & Park, S. (2005). Expression of hepatitis C virus core protein in hepatocytes does not modulate proliferation or apoptosis of CD8<sup>+</sup> T cells. *Yonsei Med J* **46**, 827-34.
24. Yao, Z. Q., Eisen-Vandervelde, A., Waggoner, S. N., Cale, E. M. & Hahn, Y. S. (2004). Direct binding of hepatitis C virus core to gC1qR on CD4<sup>+</sup> and CD8<sup>+</sup> T cells leads to impaired activation of Lck and Akt. *J Virol* **78**, 6409-19.
25. Accapezzato, D., Francavilla, V., Rawson, P., Cerino, A., Cividini, A., Mondelli, M. U. & Barnaba, V. (2004). Subversion of effector CD8<sup>+</sup> T cell differentiation in acute hepatitis C virus infection: the role of the virus. *Eur J Immunol* **34**, 438-46.
26. Kittlesen, D. J., Chianese-Bullock, K. A., Yao, Z. Q., Braciale, T. J. & Hahn, Y. S. (2000). Interaction between complement receptor gC1qR and hepatitis C virus core protein inhibits T-lymphocyte proliferation. *J Clin Invest* **106**, 1239-49.
27. Grakoui, A., Wychowski, C., Lin, C., Feinstone, S. M. & Rice, C. M. (1993). Expression and identification of hepatitis C virus polyprotein cleavage products. *J Virol* **67**, 1385-95.
28. Cocquerel, L., Meunier, J. C., Op de Beeck, A., Bonte, D., Wychowski, C. & Dubuisson, J. (2001). Coexpression of hepatitis C virus envelope proteins E1 and

- E2 in cis improves the stability of membrane insertion of E2. *J Gen Virol* **82**, 1629-35.
29. Cocquerel, L., Meunier, J. C., Pillez, A., Wychowski, C. & Dubuisson, J. (1998). A retention signal necessary and sufficient for endoplasmic reticulum localization maps to the transmembrane domain of hepatitis C virus glycoprotein E2. *J Virol* **72**, 2183-91.
  30. Cocquerel, L., Duvet, S., Meunier, J. C., Pillez, A., Cacan, R., Wychowski, C. & Dubuisson, J. (1999). The transmembrane domain of hepatitis C virus glycoprotein E1 is a signal for static retention in the endoplasmic reticulum. *J Virol* **73**, 2641-9.
  31. Cocquerel, L., Wychowski, C., Minner, F., Penin, F. & Dubuisson, J. (2000). Charged residues in the transmembrane domains of hepatitis C virus glycoproteins play a major role in the processing, subcellular localization, and assembly of these envelope proteins. *J Virol* **74**, 3623-33.
  32. Flint, M., Thomas, J. M., Maidens, C. M., Shotton, C., Levy, S., Barclay, W. S. & McKeating, J. A. (1999). Functional analysis of cell surface-expressed hepatitis C virus E2 glycoprotein. *J Virol* **73**, 6782-90.
  33. Op De Beeck, A., Montserret, R., Duvet, S., Cocquerel, L., Cacan, R., Barberot, B., Le Maire, M., Penin, F. & Dubuisson, J. (2000). The transmembrane domains of hepatitis C virus envelope glycoproteins E1 and E2 play a major role in heterodimerization. *J Biol Chem* **275**, 31428-37.
  34. Patel, J., Patel, A. H. & McLauchlan, J. (2001). The transmembrane domain of the hepatitis C virus E2 glycoprotein is required for correct folding of the E1 glycoprotein and native complex formation. *Virology* **279**, 58-68.
  35. Ralston, R., Thudium, K., Berger, K., Kuo, C., Gervase, B., Hall, J., Selby, M., Kuo, G., Houghton, M. & Choo, Q. L. (1993). Characterization of hepatitis C virus envelope glycoprotein complexes expressed by recombinant vaccinia viruses. *J Virol* **67**, 6753-61.
  36. Deleersnyder, V., Pillez, A., Wychowski, C., Blight, K., Xu, J., Hahn, Y. S., Rice, C. M. & Dubuisson, J. (1997). Formation of native hepatitis C virus glycoprotein complexes. *J Virol* **71**, 697-704.
  37. Farci, P., Shimoda, A., Wong, D., Cabezon, T., De Gioannis, D., Strazzer, A., Shimizu, Y., Shapiro, M., Alter, H. J. & Purcell, R. H. (1996). Prevention of hepatitis C virus infection in chimpanzees by hyperimmune serum against the hypervariable region 1 of the envelope 2 protein. *Proc Natl Acad Sci U S A* **93**, 15394-9.
  38. Zibert, A., Schreier, E. & Roggendorf, M. (1995). Antibodies in human sera specific to hypervariable region 1 of hepatitis C virus can block viral attachment. *Virology* **208**, 653-61.
  39. Pileri, P., Uematsu, Y., Campagnoli, S., Galli, G., Falugi, F., Petracca, R., Weiner, A. J., Houghton, M., Rosa, D., Grandi, G. & Abrignani, S. (1998). Binding of hepatitis C virus to CD81. *Science* **282**, 938-41.
  40. Scarselli, E., Ansuini, H., Cerino, R., Roccasecca, R. M., Acali, S., Filocamo, G., Traboni, C., Nicosia, A., Cortese, R. & Vitelli, A. (2002). The human scavenger receptor class B type I is a novel candidate receptor for the hepatitis C virus. *Embo J* **21**, 5017-25.

41. Gardner, J. P., Durso, R. J., Arrigale, R. R., Donovan, G. P., Maddon, P. J., Dragic, T. & Olson, W. C. (2003). L-SIGN (CD 209L) is a liver-specific capture receptor for hepatitis C virus. *Proc Natl Acad Sci U S A* **100**, 4498-503.
42. Lozach, P. Y., Lortat-Jacob, H., de Lacroix de Lavalette, A., Staropoli, I., Foug, S., Amara, A., Houles, C., Fieschi, F., Schwartz, O., Virelizier, J. L., Arenzana-Seisdedos, F. & Altmeyer, R. (2003). DC-SIGN and L-SIGN are high affinity binding receptors for hepatitis C virus glycoprotein E2. *J Biol Chem* **278**, 20358-66.
43. Pohlmann, S., Zhang, J., Baribaud, F., Chen, Z., Leslie, G. J., Lin, G., Granelli-Piperno, A., Doms, R. W., Rice, C. M. & McKeating, J. A. (2003). Hepatitis C virus glycoproteins interact with DC-SIGN and DC-SIGNR. *J Virol* **77**, 4070-80.
44. Barth, H., Schafer, C., Adah, M. I., Zhang, F., Linhardt, R. J., Toyoda, H., Kinoshita-Toyoda, A., Toida, T., Van Kuppevelt, T. H., Depla, E., Von Weizsacker, F., Blum, H. E. & Baumert, T. F. (2003). Cellular binding of hepatitis C virus envelope glycoprotein E2 requires cell surface heparan sulfate. *J Biol Chem* **278**, 41003-12.
45. Saunier, B., Triyatni, M., Ulianich, L., Maruvada, P., Yen, P. & Kohn, L. D. (2003). Role of the asialoglycoprotein receptor in binding and entry of hepatitis C virus structural proteins in cultured human hepatocytes. *J Virol* **77**, 546-59.
46. Taylor, D. R., Shi, S. T., Romano, P. R., Barber, G. N. & Lai, M. M. (1999). Inhibition of the interferon-inducible protein kinase PKR by HCV E2 protein. *Science* **285**, 107-10.
47. Carrere-Kremer, S., Montpellier-Pala, C., Cocquerel, L., Wychowski, C., Penin, F. & Dubuisson, J. (2002). Subcellular localization and topology of the p7 polypeptide of hepatitis C virus. *J Virol* **76**, 3720-30.
48. Lohmann, V., Korner, F., Koch, J., Herian, U., Theilmann, L. & Bartenschlager, R. (1999). Replication of subgenomic hepatitis C virus RNAs in a hepatoma cell line. *Science* **285**, 110-3.
49. Sakai, A., Claire, M. S., Faulk, K., Govindarajan, S., Emerson, S. U., Purcell, R. H. & Bukh, J. (2003). The p7 polypeptide of hepatitis C virus is critical for infectivity and contains functionally important genotype-specific sequences. *Proc Natl Acad Sci U S A* **100**, 11646-51.
50. Harada, T., Tautz, N. & Thiel, H. J. (2000). E2-p7 region of the bovine viral diarrhea virus polyprotein: processing and functional studies. *J Virol* **74**, 9498-506.
51. Griffin, S. D., Beales, L. P., Clarke, D. S., Worsfold, O., Evans, S. D., Jaeger, J., Harris, M. P. & Rowlands, D. J. (2003). The p7 protein of hepatitis C virus forms an ion channel that is blocked by the antiviral drug, Amantadine. *FEBS Lett* **535**, 34-8.
52. Pavlovic, D., Neville, D. C., Argaud, O., Blumberg, B., Dwek, R. A., Fischer, W. B. & Zitzmann, N. (2003). The hepatitis C virus p7 protein forms an ion channel that is inhibited by long-alkyl-chain iminosugar derivatives. *Proc Natl Acad Sci U S A* **100**, 6104-8.
53. Premkumar, A., Wilson, L., Ewart, G. D. & Gage, P. W. (2004). Cation-selective ion channels formed by p7 of hepatitis C virus are blocked by hexamethylene amiloride. *FEBS Lett* **557**, 99-103.

54. Hijikata, M., Mizushima, H., Akagi, T., Mori, S., Kakiuchi, N., Kato, N., Tanaka, T., Kimura, K. & Shimotohno, K. (1993). Two distinct proteinase activities required for the processing of a putative nonstructural precursor protein of hepatitis C virus. *J Virol* **67**, 4665-75.
55. Pietschmann, T., Lohmann, V., Rutter, G., Kurpanek, K. & Bartenschlager, R. (2001). Characterization of cell lines carrying self-replicating hepatitis C virus RNAs. *J Virol* **75**, 1252-64.
56. Meyers, G. & Thiel, H. J. (1996). Molecular characterization of pestiviruses. *Adv Virus Res* **47**, 53-118.
57. Yamada, K., Mori, A., Seki, M., Kimura, J., Yuasa, S., Matsuura, Y. & Miyamura, T. (1998). Critical point mutations for hepatitis C virus NS3 proteinase. *Virology* **246**, 104-12.
58. Mori, A., Yuasa, S., Yamada, K., Nagami, Y. & Miyamura, T. (1997). The N-terminal region of NS3 serine proteinase of hepatitis C virus is important to maintain its enzymatic integrity. *Biochem Biophys Res Commun* **231**, 738-42.
59. Grakoui, A., McCourt, D. W., Wychowski, C., Feinstone, S. M. & Rice, C. M. (1993). Characterization of the hepatitis C virus-encoded serine proteinase: determination of proteinase-dependent polyprotein cleavage sites. *J Virol* **67**, 2832-43.
60. Love, R. A., Parge, H. E., Wickersham, J. A., Hostomsky, Z., Habuka, N., Moomaw, E. W., Adachi, T. & Hostomska, Z. (1996). The crystal structure of hepatitis C virus NS3 proteinase reveals a trypsin-like fold and a structural zinc binding site. *Cell* **87**, 331-42.
61. Yao, N., Reichert, P., Taremi, S. S., Prosise, W. W. & Weber, P. C. (1999). Molecular views of viral polyprotein processing revealed by the crystal structure of the hepatitis C virus bifunctional protease-helicase. *Structure* **7**, 1353-63.
62. Kim, J. L., Morgenstern, K. A., Lin, C., Fox, T., Dwyer, M. D., Landro, J. A., Chambers, S. P., Markland, W., Lepre, C. A., O'Malley, E. T., Harbeson, S. L., Rice, C. M., Murcko, M. A., Caron, P. R. & Thomson, J. A. (1996). Crystal structure of the hepatitis C virus NS3 protease domain complexed with a synthetic NS4A cofactor peptide. *Cell* **87**, 343-55.
63. McCoy, M. A., Senior, M. M., Gesell, J. J., Ramanathan, L. & Wyss, D. F. (2001). Solution structure and dynamics of the single-chain hepatitis C virus NS3 protease NS4A cofactor complex. *J Mol Biol* **305**, 1099-110.
64. Yan, Y., Li, Y., Munshi, S., Sardana, V., Cole, J. L., Sardana, M., Steinkuehler, C., Tomei, L., De Francesco, R., Kuo, L. C. & Chen, Z. (1998). Complex of NS3 protease and NS4A peptide of BK strain hepatitis C virus: a 2.2 Å resolution structure in a hexagonal crystal form. *Protein Sci* **7**, 837-47.
65. Di Marco, S., Rizzi, M., Volpari, C., Walsh, M. A., Narjes, F., Colarusso, S., De Francesco, R., Matassa, V. G. & Sollazzo, M. (2000). Inhibition of the hepatitis C virus NS3/4A protease. The crystal structures of two protease-inhibitor complexes. *J Biol Chem* **275**, 7152-7.
66. Arasappan, A., Njoroge, F. G., Chan, T. Y., Bennett, F., Bogen, S. L., Chen, K., Gu, H., Hong, L., Jao, E., Liu, Y. T., Lovey, R. G., Parekh, T., Pike, R. E., Pinto, P., Santhanam, B., Venkatraman, S., Vaccaro, H., Wang, H., Yang, X., Zhu, Z., McKittrick, B., Saksena, A. K., Girijavallabhan, V., Pichardo, J., Butkiewicz, N.,

- Ingram, R., Malcolm, B., Prongay, A., Yao, N., Marten, B., Madison, V., Kemp, S., Levy, O., Lim-Wilby, M., Tamura, S. & Ganguly, A. K. (2005). Hepatitis C virus NS3-4A serine protease inhibitors: SAR of P'2 moiety with improved potency. *Bioorg Med Chem Lett* **15**, 4180-4.
67. Arasappan, A., Njoroge, F. G., Parekh, T. N., Yang, X., Pichardo, J., Butkiewicz, N., Prongay, A., Yao, N. & Girijavallabhan, V. (2004). Novel 2-oxoimidazolidine-4-carboxylic acid derivatives as hepatitis C virus NS3-4A serine protease inhibitors: synthesis, activity, and X-ray crystal structure of an enzyme inhibitor complex. *Bioorg Med Chem Lett* **14**, 5751-5.
  68. Steinkuhler, C., Biasiol, G., Brunetti, M., Urbani, A., Koch, U., Cortese, R., Pessi, A. & De Francesco, R. (1998). Product inhibition of the hepatitis C virus NS3 protease. *Biochemistry* **37**, 8899-905.
  69. Ingallinella, P., Altamura, S., Bianchi, E., Taliani, M., Ingenito, R., Cortese, R., De Francesco, R., Steinkuhler, C. & Pessi, A. (1998). Potent peptide inhibitors of human hepatitis C virus NS3 protease are obtained by optimizing the cleavage products. *Biochemistry* **37**, 8906-14.
  70. Lamarre, D., Anderson, P. C., Bailey, M., Beaulieu, P., Bolger, G., Bonneau, P., Bos, M., Cameron, D. R., Cartier, M., Cordingley, M. G., Faucher, A. M., Goudreau, N., Kawai, S. H., Kukolj, G., Lagace, L., LaPlante, S. R., Narjes, H., Poupard, M. A., Rancourt, J., Sentjens, R. E., St George, R., Simoneau, B., Steinmann, G., Thibeault, D., Tsantrizos, Y. S., Weldon, S. M., Yong, C. L. & Llinas-Brunet, M. (2003). An NS3 protease inhibitor with antiviral effects in humans infected with hepatitis C virus. *Nature* **426**, 186-9.
  71. Perni, R. B., Almquist, S. J., Byrn, R. A., Chandorkar, G., Chaturvedi, P. R., Courtney, L. F., Decker, C. J., Dinehart, K., Gates, C. A., Harbeson, S. L., Heiser, A., Kalkeri, G., Kolaczowski, E., Lin, K., Luong, Y. P., Rao, B. G., Taylor, W. P., Thomson, J. A., Tung, R. D., Wei, Y., Kwong, A. D. & Lin, C. (2006). Preclinical profile of VX-950, a potent, selective, and orally bioavailable inhibitor of hepatitis C virus NS3-4A serine protease. *Antimicrob Agents Chemother* **50**, 899-909.
  72. Kwong, A. D., Kim, J. L. & Lin, C. (2000). Structure and function of hepatitis C virus NS3 helicase. *Curr Top Microbiol Immunol* **242**, 171-96.
  73. Lam, A. M. & Frick, D. N. (2006). Hepatitis C virus subgenomic replicon requires an active NS3 RNA helicase. *J Virol* **80**, 404-11.
  74. Borowski, P., Niebuhr, A., Schmitz, H., Hosmane, R. S., Bretner, M., Siwecka, M. A. & Kulikowski, T. (2002). NTPase/helicase of Flaviviridae: inhibitors and inhibition of the enzyme. *Acta Biochim Pol* **49**, 597-614.
  75. Borowski, P., Schalinski, S. & Schmitz, H. (2002). Nucleotide triphosphatase/helicase of hepatitis C virus as a target for antiviral therapy. *Antiviral Res* **55**, 397-412.
  76. Otsuka, M., Kato, N., Moriyama, M., Taniguchi, H., Wang, Y., Dharel, N., Kawabe, T. & Omata, M. (2005). Interaction between the HCV NS3 protein and the host TBK1 protein leads to inhibition of cellular antiviral responses. *Hepatology* **41**, 1004-12.
  77. Tellinghuisen, T. L. & Rice, C. M. (2002). Interaction between hepatitis C virus proteins and host cell factors. *Curr Opin Microbiol* **5**, 419-27.

78. Lin, C., Thomson, J. A. & Rice, C. M. (1995). A central region in the hepatitis C virus NS4A protein allows formation of an active NS3-NS4A serine proteinase complex in vivo and in vitro. *J Virol* **69**, 4373-80.
79. Lin, C., Wu, J. W., Hsiao, K. & Su, M. S. (1997). The hepatitis C virus NS4A protein: interactions with the NS4B and NS5A proteins. *J Virol* **71**, 6465-71.
80. Egger, D., Wolk, B., Gosert, R., Bianchi, L., Blum, H. E., Moradpour, D. & Bienz, K. (2002). Expression of hepatitis C virus proteins induces distinct membrane alterations including a candidate viral replication complex. *J Virol* **76**, 5974-84.
81. Dimitrova, M., Imbert, I., Kieny, M. P. & Schuster, C. (2003). Protein-protein interactions between hepatitis C virus nonstructural proteins. *J Virol* **77**, 5401-14.
82. Einav, S., Elazar, M., Danieli, T. & Glenn, J. S. (2004). A nucleotide binding motif in hepatitis C virus (HCV) NS4B mediates HCV RNA replication. *J Virol* **78**, 11288-95.
83. Asabe, S. I., Tanji, Y., Satoh, S., Kaneko, T., Kimura, K. & Shimotohno, K. (1997). The N-terminal region of hepatitis C virus-encoded NS5A is important for NS4A-dependent phosphorylation. *J Virol* **71**, 790-6.
84. Macdonald, A. & Harris, M. (2004). Hepatitis C virus NS5A: tales of a promiscuous protein. *J Gen Virol* **85**, 2485-502.
85. Evans, M. J., Rice, C. M. & Goff, S. P. (2004). Phosphorylation of hepatitis C virus nonstructural protein 5A modulates its protein interactions and viral RNA replication. *Proc Natl Acad Sci U S A* **101**, 13038-43.
86. Appel, N., Pietschmann, T. & Bartenschlager, R. (2005). Mutational analysis of hepatitis C virus nonstructural protein 5A: potential role of differential phosphorylation in RNA replication and identification of a genetically flexible domain. *J Virol* **79**, 3187-94.
87. Shirota, Y., Luo, H., Qin, W., Kaneko, S., Yamashita, T., Kobayashi, K. & Murakami, S. (2002). Hepatitis C virus (HCV) NS5A binds RNA-dependent RNA polymerase (RdRP) NS5B and modulates RNA-dependent RNA polymerase activity. *J Biol Chem* **277**, 11149-55.
88. Enomoto, N., Sakuma, I., Asahina, Y., Kurosaki, M., Murakami, T., Yamamoto, C., Ogura, Y., Izumi, N., Marumo, F. & Sato, C. (1996). Mutations in the nonstructural protein 5A gene and response to interferon in patients with chronic hepatitis C virus 1b infection. *N Engl J Med* **334**, 77-81.
89. Yi, M. & Lemon, S. M. (2004). Adaptive mutations producing efficient replication of genotype 1a hepatitis C virus RNA in normal Huh7 cells. *J Virol* **78**, 7904-15.
90. Lindenbach, B. D., Evans, M. J., Syder, A. J., Wolk, B., Tellinghuisen, T. L., Liu, C. C., Maruyama, T., Hynes, R. O., Burton, D. R., McKeating, J. A. & Rice, C. M. (2005). Complete replication of hepatitis C virus in cell culture. *Science* **309**, 623-6.
91. Wakita, T., Pietschmann, T., Kato, T., Date, T., Miyamoto, M., Zhao, Z., Murthy, K., Habermann, A., Krausslich, H. G., Mizokami, M., Bartenschlager, R. & Liang, T. J. (2005). Production of infectious hepatitis C virus in tissue culture from a cloned viral genome. *Nat Med* **11**, 791-6.

92. Zhong, J., Gastaminza, P., Cheng, G., Kapadia, S., Kato, T., Burton, D. R., Wieland, S. F., Uprichard, S. L., Wakita, T. & Chisari, F. V. (2005). Robust hepatitis C virus infection in vitro. *Proc Natl Acad Sci U S A* **102**, 9294-9.
93. Lanford, R. E., Bigger, C., Bassett, S. & Klimpel, G. (2001). The chimpanzee model of hepatitis C virus infections. *Hepatology* **42**, 117-26.
94. Mercer, D. F., Schiller, D. E., Elliott, J. F., Douglas, D. N., Hao, C., Rinfret, A., Addison, W. R., Fischer, K. P., Churchill, T. A., Lakey, J. R., Tyrrell, D. L. & Kneteman, N. M. (2001). Hepatitis C virus replication in mice with chimeric human livers. *Nat Med* **7**, 927-33.
95. Lindenbach, B. D. & Rice, C. M. (2005). Unravelling hepatitis C virus replication from genome to function. *Nature* **436**, 933-8.
96. Bartosch, B., Vitelli, A., Granier, C., Goujon, C., Dubuisson, J., Pascale, S., Scarselli, E., Cortese, R., Nicosia, A. & Cosset, F. L. (2003). Cell entry of hepatitis C virus requires a set of co-receptors that include the CD81 tetraspanin and the SR-B1 scavenger receptor. *J Biol Chem* **278**, 41624-30.
97. Cormier, E. G., Tsamis, F., Kajumo, F., Durso, R. J., Gardner, J. P. & Dragic, T. (2004). CD81 is an entry coreceptor for hepatitis C virus. *Proc Natl Acad Sci U S A* **101**, 7270-4.
98. Zhang, J., Randall, G., Higginbottom, A., Monk, P., Rice, C. M. & McKeating, J. A. (2004). CD81 is required for hepatitis C virus glycoprotein-mediated viral infection. *J Virol* **78**, 1448-55.
99. Flint, M., Maidens, C., Loomis-Price, L. D., Shotton, C., Dubuisson, J., Monk, P., Higginbottom, A., Levy, S. & McKeating, J. A. (1999). Characterization of hepatitis C virus E2 glycoprotein interaction with a putative cellular receptor, CD81. *J Virol* **73**, 6235-44.
100. Cocquerel, L., Voisset, C. & Dubuisson, J. (2006). Hepatitis C virus entry: potential receptors and their biological functions. *J Gen Virol* **87**, 1075-84.
101. Pestova, T. V., Shatsky, I. N., Fletcher, S. P., Jackson, R. J. & Hellen, C. U. (1998). A prokaryotic-like mode of cytoplasmic eukaryotic ribosome binding to the initiation codon during internal translation initiation of hepatitis C and classical swine fever virus RNAs. *Genes Dev* **12**, 67-83.
102. Spahn, C. M., Kieft, J. S., Grassucci, R. A., Penczek, P. A., Zhou, K., Doudna, J. A. & Frank, J. (2001). Hepatitis C virus IRES RNA-induced changes in the conformation of the 40s ribosomal subunit. *Science* **291**, 1959-62.
103. Grace, K., Gartland, M., Karayiannis, P., McGarvey, M. J. & Clarke, B. (1999). The 5' untranslated region of GB virus B shows functional similarity to the internal ribosome entry site of hepatitis C virus. *J Gen Virol* **80** ( Pt 9), 2337-41.
104. Poole, T. L., Wang, C., Popp, R. A., Potgieter, L. N., Siddiqui, A. & Collett, M. S. (1995). Pestivirus translation initiation occurs by internal ribosome entry. *Virology* **206**, 750-4.
105. Rijnbrand, R., van der Straaten, T., van Rijn, P. A., Spaan, W. J. & Bredenbeek, P. J. (1997). Internal entry of ribosomes is directed by the 5' noncoding region of classical swine fever virus and is dependent on the presence of an RNA pseudoknot upstream of the initiation codon. *J Virol* **71**, 451-7.
106. Hellen, C. U. & Sarnow, P. (2001). Internal ribosome entry sites in eukaryotic mRNA molecules. *Genes Dev* **15**, 1593-612.

107. Dasgupta, A., Das, S., Izumi, R., Venkatesan, A. & Barat, B. (2004). Targeting internal ribosome entry site (IRES)-mediated translation to block hepatitis C and other RNA viruses. *FEMS Microbiol Lett* **234**, 189-99.
108. De Francesco, R. & Migliaccio, G. (2005). Challenges and successes in developing new therapies for hepatitis C. *Nature* **436**, 953-60.
109. Gosert, R., Egger, D., Lohmann, V., Bartenschlager, R., Blum, H. E., Bienz, K. & Moradpour, D. (2003). Identification of the hepatitis C virus RNA replication complex in Huh-7 cells harboring subgenomic replicons. *J Virol* **77**, 5487-92.
110. Seeger, C. (2005). Salient molecular features of hepatitis C virus revealed. *Trends Microbiol* **13**, 528-34.
111. Smith, D. B. & Simmonds, P. (1997). Characteristics of nucleotide substitution in the hepatitis C virus genome: constraints on sequence change in coding regions at both ends of the genome. *J Mol Evol* **45**, 238-46.
112. Hofacker, I. L., Fekete, M., Flamm, C., Huynen, M. A., Rauscher, S., Stolorz, P. E. & Stadler, P. F. (1998). Automatic detection of conserved RNA structure elements in complete RNA virus genomes. *Nucleic Acids Res* **26**, 3825-36.
113. Tuplin, A., Wood, J., Evans, D. J., Patel, A. H. & Simmonds, P. (2002). Thermodynamic and phylogenetic prediction of RNA secondary structures in the coding region of hepatitis C virus. *Rna* **8**, 824-41.
114. You, S., Stump, D. D., Branch, A. D. & Rice, C. M. (2004). A cis-acting replication element in the sequence encoding the NS5B RNA-dependent RNA polymerase is required for hepatitis C virus RNA replication. *J Virol* **78**, 1352-66.
115. Friebe, P., Boudet, J., Simorre, J. P. & Bartenschlager, R. (2005). Kissing-loop interaction in the 3' end of the hepatitis C virus genome essential for RNA replication. *J Virol* **79**, 380-92.
116. Tsuchihara, K., Tanaka, T., Hijikata, M., Kuge, S., Toyoda, H., Nomoto, A., Yamamoto, N. & Shimotohno, K. (1997). Specific interaction of polypyrimidine tract-binding protein with the extreme 3'-terminal structure of the hepatitis C virus genome, the 3'X. *J Virol* **71**, 6720-6.
117. Chung, R. T. & Kaplan, L. M. (1999). Heterogeneous nuclear ribonucleoprotein I (hnRNP-I/PTB) selectively binds the conserved 3' terminus of hepatitis C viral RNA. *Biochem Biophys Res Commun* **254**, 351-62.
118. Gontarek, R. R., Gutshall, L. L., Herold, K. M., Tsai, J., Sathe, G. M., Mao, J., Prescott, C. & Del Vecchio, A. M. (1999). hnRNP C and polypyrimidine tract-binding protein specifically interact with the pyrimidine-rich region within the 3'NTR of the HCV RNA genome. *Nucleic Acids Res* **27**, 1457-63.
119. Spangberg, K., Wiklund, L. & Schwartz, S. (2001). Binding of the La autoantigen to the hepatitis C virus 3' untranslated region protects the RNA from rapid degradation in vitro. *J Gen Virol* **82**, 113-20.
120. Spangberg, K., Wiklund, L. & Schwartz, S. (2000). HuR, a protein implicated in oncogene and growth factor mRNA decay, binds to the 3' ends of hepatitis C virus RNA of both polarities. *Virology* **274**, 378-90.
121. Harris, D., Zhang, Z., Chaubey, B. & Pandey, V. N. (2006). Identification of cellular factors associated with the 3' nontranslated region of the hepatitis C virus genome. *Mol Cell Proteomics*.



122. Bartenschlager, R. & Lohmann, V. (2001). Novel cell culture systems for the hepatitis C virus. *Antiviral Res* **52**, 1-17.
123. Kato, N., Ikeda, M., Mizutani, T., Sugiyama, K., Noguchi, M., Hirohashi, S. & Shimotohno, K. (1996). Replication of hepatitis C virus in cultured non-neoplastic human hepatocytes. *Jpn J Cancer Res* **87**, 787-92.
124. Ito, T. & Lai, M. M. (1997). Determination of the secondary structure of and cellular protein binding to the 3'-untranslated region of the hepatitis C virus RNA genome. *J Virol* **71**, 8698-706.
125. Blight, K. J., Kolykhalov, A. A. & Rice, C. M. (2000). Efficient initiation of HCV RNA replication in cell culture. *Science* **290**, 1972-4.
126. Krieger, N., Lohmann, V. & Bartenschlager, R. (2001). Enhancement of hepatitis C virus RNA replication by cell culture-adaptive mutations. *J Virol* **75**, 4614-24.
127. Lohmann, V., Korner, F., Dobierzewska, A. & Bartenschlager, R. (2001). Mutations in hepatitis C virus RNAs conferring cell culture adaptation. *J Virol* **75**, 1437-49.
128. Lohmann, V., Hoffmann, S., Herian, U., Penin, F. & Bartenschlager, R. (2003). Viral and cellular determinants of hepatitis C virus RNA replication in cell culture. *J Virol* **77**, 3007-19.
129. Bukh, J., Pietschmann, T., Lohmann, V., Krieger, N., Faulk, K., Engle, R. E., Govindarajan, S., Shapiro, M., St Claire, M. & Bartenschlager, R. (2002). Mutations that permit efficient replication of hepatitis C virus RNA in Huh-7 cells prevent productive replication in chimpanzees. *Proc Natl Acad Sci U S A* **99**, 14416-21.
130. Bartenschlager, R., Kaul, A. & Sparacio, S. (2003). Replication of the hepatitis C virus in cell culture. *Antiviral Res* **60**, 91-102.
131. Blight, K. J., McKeating, J. A., Marcotrigiano, J. & Rice, C. M. (2003). Efficient replication of hepatitis C virus genotype 1a RNAs in cell culture. *J Virol* **77**, 3181-90.
132. Gu, B., Gates, A. T., Isken, O., Behrens, S. E. & Sarisky, R. T. (2003). Replication studies using genotype 1a subgenomic hepatitis C virus replicons. *J Virol* **77**, 5352-9.
133. Kato, T., Date, T., Miyamoto, M., Furusaka, A., Tokushige, K., Mizokami, M. & Wakita, T. (2003). Efficient replication of the genotype 2a hepatitis C virus subgenomic replicon. *Gastroenterology* **125**, 1808-17.
134. Pietschmann, T., Lohmann, V., Kaul, A., Krieger, N., Rinck, G., Rutter, G., Strand, D. & Bartenschlager, R. (2002). Persistent and transient replication of full-length hepatitis C virus genomes in cell culture. *J Virol* **76**, 4008-21.
135. Moradpour, D., Evans, M. J., Gosert, R., Yuan, Z., Blum, H. E., Goff, S. P., Lindenbach, B. D. & Rice, C. M. (2004). Insertion of green fluorescent protein into nonstructural protein 5A allows direct visualization of functional hepatitis C virus replication complexes. *J Virol* **78**, 7400-9.
136. Zhu, Q., Guo, J. T. & Seeger, C. (2003). Replication of hepatitis C virus subgenomes in nonhepatic epithelial and mouse hepatoma cells. *J Virol* **77**, 9204-10.
137. Lindenbach, B. D., Meuleman, P., Ploss, A., Vanwolleghem, T., Syder, A. J., McKeating, J. A., Lanford, R. E., Feinstone, S. M., Major, M. E., Leroux-Roels,

- G. & Rice, C. M. (2006). Cell culture-grown hepatitis C virus is infectious in vivo and can be recultured in vitro. *Proc Natl Acad Sci U S A* **103**, 3805-9.
138. Date, T., Kato, T., Miyamoto, M., Zhao, Z., Yasui, K., Mizokami, M. & Wakita, T. (2004). Genotype 2a hepatitis C virus subgenomic replicon can replicate in HepG2 and IMY-N9 cells. *J Biol Chem* **279**, 22371-6.
  139. Kato, T., Date, T., Miyamoto, M., Zhao, Z., Mizokami, M. & Wakita, T. (2005). Nonhepatic cell lines HeLa and 293 support efficient replication of the hepatitis C virus genotype 2a subgenomic replicon. *J Virol* **79**, 592-6.
  140. Miyamoto, M., Kato, T., Date, T., Mizokami, M. & Wakita, T. (2006). Comparison between subgenomic replicons of hepatitis C virus genotypes 2a (JFH-1) and 1b (Con1 NK5.1). *Intervirology* **49**, 37-43.
  141. Webster, G., Barnes, E., Brown, D. & Dusheiko, G. (2000). HCV genotypes--role in pathogenesis of disease and response to therapy. *Baillieres Best Pract Res Clin Gastroenterol* **14**, 229-40.
  142. Baginski, S. G., Pevear, D. C., Seipel, M., Sun, S. C., Benetatos, C. A., Chunduru, S. K., Rice, C. M. & Collett, M. S. (2000). Mechanism of action of a pestivirus antiviral compound. *Proc Natl Acad Sci U S A* **97**, 7981-6.
  143. Zitzmann, N., Mehta, A. S., Carrouee, S., Butters, T. D., Platt, F. M., McCauley, J., Blumberg, B. S., Dwek, R. A. & Block, T. M. (1999). Imino sugars inhibit the formation and secretion of bovine viral diarrhea virus, a pestivirus model of hepatitis C virus: implications for the development of broad spectrum anti-hepatitis virus agents. *Proc Natl Acad Sci U S A* **96**, 11878-82.
  144. Buckwold, V. E., Beer, B. E. & Donis, R. O. (2003). Bovine viral diarrhea virus as a surrogate model of hepatitis C virus for the evaluation of antiviral agents. *Antiviral Res* **60**, 1-15.
  145. Lindenbach, B. D. & Rice, C. M. (2003). Molecular biology of flaviviruses. *Adv Virus Res* **59**, 23-61.
  146. Mendez, E., Ruggli, N., Collett, M. S. & Rice, C. M. (1998). Infectious bovine viral diarrhea virus (strain NADL) RNA from stable cDNA clones: a cellular insert determines NS3 production and viral cytopathogenicity. *J Virol* **72**, 4737-45.
  147. Stuyver, L. J., Whitaker, T., McBrayer, T. R., Hernandez-Santiago, B. I., Lostia, S., Tharnish, P. M., Ramesh, M., Chu, C. K., Jordan, R., Shi, J., Rachakonda, S., Watanabe, K. A., Otto, M. J. & Schinazi, R. F. (2003). Ribonucleoside analogue that blocks replication of bovine viral diarrhea and hepatitis C viruses in culture. *Antimicrob Agents Chemother* **47**, 244-54.
  148. Sun, J. H., Lemm, J. A., O'Boyle, D. R., 2nd, Racela, J., Colonno, R. & Gao, M. (2003). Specific inhibition of bovine viral diarrhea virus replicase. *J Virol* **77**, 6753-60.
  149. Paeshuyse, J., Leyssen, P., Mabery, E., Boddeker, N., Vrancken, R., Froeyen, M., Ansari, I. H., Dutartre, H., Rozenski, J., Gil, L. H., Letellier, C., Lanford, R., Canard, B., Koenen, F., Kerkhofs, P., Donis, R. O., Herdewijn, P., Watson, J., De Clercq, E., Puerstinger, G. & Neyts, J. (2006). A novel, highly selective inhibitor of pestivirus replication that targets the viral RNA-dependent RNA polymerase. *J Virol* **80**, 149-60.

150. Behrens, S. E., Tomei, L. & De Francesco, R. (1996). Identification and properties of the RNA-dependent RNA polymerase of hepatitis C virus. *Embo J* **15**, 12-22.
151. Lohmann, V., Korner, F., Herian, U. & Bartenschlager, R. (1997). Biochemical properties of hepatitis C virus NS5B RNA-dependent RNA polymerase and identification of amino acid sequence motifs essential for enzymatic activity. *J Virol* **71**, 8416-28.
152. Yuan, Z. H., Kumar, U., Thomas, H. C., Wen, Y. M. & Monjardino, J. (1997). Expression, purification, and partial characterization of HCV RNA polymerase. *Biochem Biophys Res Commun* **232**, 231-5.
153. Yamashita, T., Kaneko, S., Shiota, Y., Qin, W., Nomura, T., Kobayashi, K. & Murakami, S. (1998). RNA-dependent RNA polymerase activity of the soluble recombinant hepatitis C virus NS5B protein truncated at the C-terminal region. *J Biol Chem* **273**, 15479-86.
154. Ferrari, E., Wright-Minogue, J., Fang, J. W., Baroudy, B. M., Lau, J. Y. & Hong, Z. (1999). Characterization of soluble hepatitis C virus RNA-dependent RNA polymerase expressed in *Escherichia coli*. *J Virol* **73**, 1649-54.
155. Al, R. H., Xie, Y., Wang, Y. & Hagedorn, C. H. (1998). Expression of recombinant hepatitis C virus non-structural protein 5B in *Escherichia coli*. *Virus Res* **53**, 141-9.
156. Johnson, R. B., Sun, X. L., Hockman, M. A., Villarreal, E. C., Wakulchik, M. & Wang, Q. M. (2000). Specificity and mechanism analysis of hepatitis C virus RNA-dependent RNA polymerase. *Arch Biochem Biophys* **377**, 129-34.
157. De Francesco, R., Behrens, S. E., Tomei, L., Altamura, S. & Jiricny, J. (1996). RNA-dependent RNA polymerase of hepatitis C virus. *Methods Enzymol* **275**, 58-67.
158. Schmidt-Mende, J., Bieck, E., Hugle, T., Penin, F., Rice, C. M., Blum, H. E. & Moradpour, D. (2001). Determinants for membrane association of the hepatitis C virus RNA-dependent RNA polymerase. *J Biol Chem* **276**, 44052-63.
159. Ivashkina, N., Wolk, B., Lohmann, V., Bartenschlager, R., Blum, H. E., Penin, F. & Moradpour, D. (2002). The hepatitis C virus RNA-dependent RNA polymerase membrane insertion sequence is a transmembrane segment. *J Virol* **76**, 13088-93.
160. Moradpour, D., Brass, V., Bieck, E., Friebe, P., Gosert, R., Blum, H. E., Bartenschlager, R., Penin, F. & Lohmann, V. (2004). Membrane association of the RNA-dependent RNA polymerase is essential for hepatitis C virus RNA replication. *J Virol* **78**, 13278-84.
161. Lee, K. J., Choi, J., Ou, J. H. & Lai, M. M. (2004). The C-terminal transmembrane domain of hepatitis C virus (HCV) RNA polymerase is essential for HCV replication in vivo. *J Virol* **78**, 3797-802.
162. Lohmann, V., Roos, A., Korner, F., Koch, J. O. & Bartenschlager, R. (1998). Biochemical and kinetic analyses of NS5B RNA-dependent RNA polymerase of the hepatitis C virus. *Virology* **249**, 108-18.
163. Carroll, S. S., Sardana, V., Yang, Z., Jacobs, A. R., Mizenko, C., Hall, D., Hill, L., Zugay-Murphy, J. & Kuo, L. C. (2000). Only a small fraction of purified hepatitis C RNA-dependent RNA polymerase is catalytically competent: implications for viral replication and in vitro assays. *Biochemistry* **39**, 8243-9.

164. Ishido, S., Fujita, T. & Hotta, H. (1998). Complex formation of NS5B with NS3 and NS4A proteins of hepatitis C virus. *Biochem Biophys Res Commun* **244**, 35-40.
165. Shimakami, T., Hijikata, M., Luo, H., Ma, Y. Y., Kaneko, S., Shimotohno, K. & Murakami, S. (2004). Effect of interaction between hepatitis C virus NS5A and NS5B on hepatitis C virus RNA replication with the hepatitis C virus replicon. *J Virol* **78**, 2738-48.
166. Piccininni, S., Varaklioti, A., Nardelli, M., Dave, B., Raney, K. D. & McCarthy, J. E. (2002). Modulation of the hepatitis C virus RNA-dependent RNA polymerase activity by the non-structural (NS) 3 helicase and the NS4B membrane protein. *J Biol Chem* **277**, 45670-9.
167. Wang, Q. M., Hockman, M. A., Staschke, K., Johnson, R. B., Case, K. A., Lu, J., Parsons, S., Zhang, F., Rathnachalam, R., Kirkegaard, K. & Colacino, J. M. (2002). Oligomerization and cooperative RNA synthesis activity of hepatitis C virus RNA-dependent RNA polymerase. *J Virol* **76**, 3865-72.
168. Qin, W., Luo, H., Nomura, T., Hayashi, N., Yamashita, T. & Murakami, S. (2002). Oligomeric interaction of hepatitis C virus NS5B is critical for catalytic activity of RNA-dependent RNA polymerase. *J Biol Chem* **277**, 2132-7.
169. Tu, H., Gao, L., Shi, S. T., Taylor, D. R., Yang, T., Mircheff, A. K., Wen, Y., Gorbalenya, A. E., Hwang, S. B. & Lai, M. M. (1999). Hepatitis C virus RNA polymerase and NS5A complex with a SNARE-like protein. *Virology* **263**, 30-41.
170. Watashi, K., Ishii, N., Hijikata, M., Inoue, D., Murata, T., Miyanari, Y. & Shimotohno, K. (2005). Cyclophilin B is a functional regulator of hepatitis C virus RNA polymerase. *Mol Cell* **19**, 111-22.
171. Kyono, K., Miyashiro, M. & Taguchi, I. (2002). Human eukaryotic initiation factor 4AII associates with hepatitis C virus NS5B protein in vitro. *Biochem Biophys Res Commun* **292**, 659-66.
172. Kim, S. J., Kim, J. H., Kim, Y. G., Lim, H. S. & Oh, J. W. (2004). Protein kinase C-related kinase 2 regulates hepatitis C virus RNA polymerase function by phosphorylation. *J Biol Chem* **279**, 50031-41.
173. Goh, P. Y., Tan, Y. J., Lim, S. P., Tan, Y. H., Lim, S. G., Fuller-Pace, F. & Hong, W. (2004). Cellular RNA helicase p68 relocalization and interaction with the hepatitis C virus (HCV) NS5B protein and the potential role of p68 in HCV RNA replication. *J Virol* **78**, 5288-98.
174. Hirano, M., Kaneko, S., Yamashita, T., Luo, H., Qin, W., Shiota, Y., Nomura, T., Kobayashi, K. & Murakami, S. (2003). Direct interaction between nucleolin and hepatitis C virus NS5B. *J Biol Chem* **278**, 5109-15.
175. Shimakami, T., Honda, M., Kusakawa, T., Murata, T., Shimotohno, K., Kaneko, S. & Murakami, S. (2006). Effect of hepatitis C virus (HCV) NS5B-nucleolin interaction on HCV replication with HCV subgenomic replicon. *J Virol* **80**, 3332-40.
176. Ranjith-Kumar, C. T., Gajewski, J., Gutshall, L., Maley, D., Sarisky, R. T. & Kao, C. C. (2001). Terminal nucleotidyl transferase activity of recombinant Flaviviridae RNA-dependent RNA polymerases: implication for viral RNA synthesis. *J Virol* **75**, 8615-23.

177. Oh, J. W., Ito, T. & Lai, M. M. (1999). A recombinant hepatitis C virus RNA-dependent RNA polymerase capable of copying the full-length viral RNA. *J Virol* **73**, 7694-702.
178. Cai, Z., Yi, M., Zhang, C. & Luo, G. (2005). Mutagenesis analysis of the rGTP-specific binding site of hepatitis C virus RNA-dependent RNA polymerase. *J Virol* **79**, 11607-17.
179. Ago, H., Adachi, T., Yoshida, A., Yamamoto, M., Habuka, N., Yatsunami, K. & Miyano, M. (1999). Crystal structure of the RNA-dependent RNA polymerase of hepatitis C virus. *Structure* **7**, 1417-26.
180. Lesburg, C. A., Cable, M. B., Ferrari, E., Hong, Z., Mannarino, A. F. & Weber, P. C. (1999). Crystal structure of the RNA-dependent RNA polymerase from hepatitis C virus reveals a fully encircled active site. *Nat Struct Biol* **6**, 937-43.
181. Bressanelli, S., Tomei, L., Roussel, A., Incitti, I., Vitale, R. L., Mathieu, M., De Francesco, R. & Rey, F. A. (1999). Crystal structure of the RNA-dependent RNA polymerase of hepatitis C virus. *Proc Natl Acad Sci U S A* **96**, 13034-9.
182. Bressanelli, S., Tomei, L., Rey, F. A. & De Francesco, R. (2002). Structural analysis of the hepatitis C virus RNA polymerase in complex with ribonucleotides. *J Virol* **76**, 3482-92.
183. O'Farrell, D., Trowbridge, R., Rowlands, D. & Jager, J. (2003). Substrate complexes of hepatitis C virus RNA polymerase (HC-J4): structural evidence for nucleotide import and de-novo initiation. *J Mol Biol* **326**, 1025-35.
184. Sarafianos, S. G., Clark, A. D., Jr., Das, K., Tuske, S., Birktoft, J. J., Ilankumaran, P., Ramesha, A. R., Sayer, J. M., Jerina, D. M., Boyer, P. L., Hughes, S. H. & Arnold, E. (2002). Structures of HIV-1 reverse transcriptase with pre- and post-translocation AZTMP-terminated DNA. *Embo J* **21**, 6614-24.
185. Choi, K. H., Groarke, J. M., Young, D. C., Kuhn, R. J., Smith, J. L., Pevear, D. C. & Rossmann, M. G. (2004). The structure of the RNA-dependent RNA polymerase from bovine viral diarrhea virus establishes the role of GTP in de novo initiation. *Proc Natl Acad Sci U S A* **101**, 4425-30.
186. Butcher, S. J., Grimes, J. M., Makeyev, E. V., Bamford, D. H. & Stuart, D. I. (2001). A mechanism for initiating RNA-dependent RNA polymerization. *Nature* **410**, 235-40.
187. Labonte, P., Axelrod, V., Agarwal, A., Aulabaugh, A., Amin, A. & Mak, P. (2002). Modulation of hepatitis C virus RNA-dependent RNA polymerase activity by structure-based site-directed mutagenesis. *J Biol Chem* **277**, 38838-46.
188. Biswal, B. K., Cherney, M. M., Wang, M., Chan, L., Yannopoulos, C. G., Bilimoria, D., Nicolas, O., Bedard, J. & James, M. N. (2005). Crystal structures of the RNA-dependent RNA polymerase genotype 2a of hepatitis C virus reveal two conformations and suggest mechanisms of inhibition by non-nucleoside inhibitors. *J Biol Chem* **280**, 18202-10.
189. O'Reilly, E. K. & Kao, C. C. (1998). Analysis of RNA-dependent RNA polymerase structure and function as guided by known polymerase structures and computer predictions of secondary structure. *Virology* **252**, 287-303.
190. Steitz, T. A. (1999). DNA polymerases: structural diversity and common mechanisms. *J Biol Chem* **274**, 17395-8.

191. Hong, Z., Cameron, C. E., Walker, M. P., Castro, C., Yao, N., Lau, J. Y. & Zhong, W. (2001). A novel mechanism to ensure terminal initiation by hepatitis C virus NS5B polymerase. *Virology* **285**, 6-11.
192. Cheney, I. W., Naim, S., Lai, V. C., Dempsey, S., Bellows, D., Walker, M. P., Shim, J. H., Horscroft, N., Hong, Z. & Zhong, W. (2002). Mutations in NS5B polymerase of hepatitis C virus: impacts on in vitro enzymatic activity and viral RNA replication in the subgenomic replicon cell culture. *Virology* **297**, 298-306.
193. Paul, A. V., van Boom, J. H., Filippov, D. & Wimmer, E. (1998). Protein-primed RNA synthesis by purified poliovirus RNA polymerase. *Nature* **393**, 280-4.
194. Leveque, V. J., Johnson, R. B., Parsons, S., Ren, J., Xie, C., Zhang, F. & Wang, Q. M. (2003). Identification of a C-terminal regulatory motif in hepatitis C virus RNA-dependent RNA polymerase: structural and biochemical analysis. *J Virol* **77**, 9020-8.
195. Luo, G., Hamatake, R. K., Mathis, D. M., Racela, J., Rigat, K. L., Lemm, J. & Colonno, R. J. (2000). De novo initiation of RNA synthesis by the RNA-dependent RNA polymerase (NS5B) of hepatitis C virus. *J Virol* **74**, 851-63.
196. Zhong, W., Uss, A. S., Ferrari, E., Lau, J. Y. & Hong, Z. (2000). De novo initiation of RNA synthesis by hepatitis C virus nonstructural protein 5B polymerase. *J Virol* **74**, 2017-22.
197. Kao, C. C., Yang, X., Kline, A., Wang, Q. M., Barket, D. & Heinz, B. A. (2000). Template requirements for RNA synthesis by a recombinant hepatitis C virus RNA-dependent RNA polymerase. *J Virol* **74**, 11121-8.
198. Sun, X. L., Johnson, R. B., Hockman, M. A. & Wang, Q. M. (2000). De novo RNA synthesis catalyzed by HCV RNA-dependent RNA polymerase. *Biochem Biophys Res Commun* **268**, 798-803.
199. Oh, J. W., Sheu, G. T. & Lai, M. M. (2000). Template requirement and initiation site selection by hepatitis C virus polymerase on a minimal viral RNA template. *J Biol Chem* **275**, 17710-7.
200. Zhong, W., Gutshall, L. L. & Del Vecchio, A. M. (1998). Identification and characterization of an RNA-dependent RNA polymerase activity within the nonstructural protein 5B region of bovine viral diarrhea virus. *J Virol* **72**, 9365-9.
201. Kao, C. C., Del Vecchio, A. M. & Zhong, W. (1999). De novo initiation of RNA synthesis by a recombinant flaviviridae RNA-dependent RNA polymerase. *Virology* **253**, 1-7.
202. Kim, M. J., Zhong, W., Hong, Z. & Kao, C. C. (2000). Template nucleotide moieties required for de novo initiation of RNA synthesis by a recombinant viral RNA-dependent RNA polymerase. *J Virol* **74**, 10312-22.
203. Shim, J. H., Larson, G., Wu, J. Z. & Hong, Z. (2002). Selection of 3'-template bases and initiating nucleotides by hepatitis C virus NS5B RNA-dependent RNA polymerase. *J Virol* **76**, 7030-9.
204. Lohmann, V., Overton, H. & Bartenschlager, R. (1999). Selective stimulation of hepatitis C virus and pestivirus NS5B RNA polymerase activity by GTP. *J Biol Chem* **274**, 10807-15.
205. Ranjith-Kumar, C. T., Gutshall, L., Kim, M. J., Sarisky, R. T. & Kao, C. C. (2002). Requirements for de novo initiation of RNA synthesis by recombinant flaviviral RNA-dependent RNA polymerases. *J Virol* **76**, 12526-36.

206. Zhong, W., Ferrari, E., Lesburg, C. A., Maag, D., Ghosh, S. K., Cameron, C. E., Lau, J. Y. & Hong, Z. (2000). Template/primer requirements and single nucleotide incorporation by hepatitis C virus nonstructural protein 5B polymerase. *J Virol* **74**, 9134-43.
207. Ranjith-Kumar, C. T., Kim, Y. C., Gutshall, L., Silverman, C., Khandekar, S., Sarisky, R. T. & Kao, C. C. (2002). Mechanism of de novo initiation by the hepatitis C virus RNA-dependent RNA polymerase: role of divalent metals. *J Virol* **76**, 12513-25.
208. Buck, K. W. (1996). Comparison of the replication of positive-stranded RNA viruses of plants and animals. *Adv Virus Res* **47**, 159-251.
209. Arnold, J. J., Ghosh, S. K. & Cameron, C. E. (1999). Poliovirus RNA-dependent RNA polymerase (3D(pol)). Divalent cation modulation of primer, template, and nucleotide selection. *J Biol Chem* **274**, 37060-9.
210. Arnold, J. J. & Cameron, C. E. (1999). Poliovirus RNA-dependent RNA polymerase (3Dpol) is sufficient for template switching in vitro. *J Biol Chem* **274**, 2706-16.
211. Neyts, J. (2006). Selective inhibitors of hepatitis C virus replication. *Antiviral Res.*
212. Crotty, S., Maag, D., Arnold, J. J., Zhong, W., Lau, J. Y., Hong, Z., Andino, R. & Cameron, C. E. (2000). The broad-spectrum antiviral ribonucleoside ribavirin is an RNA virus mutagen. *Nat Med* **6**, 1375-9.
213. Crotty, S., Cameron, C. E. & Andino, R. (2001). RNA virus error catastrophe: direct molecular test by using ribavirin. *Proc Natl Acad Sci U S A* **98**, 6895-900.
214. Contreras, A. M., Hiasa, Y., He, W., Terella, A., Schmidt, E. V. & Chung, R. T. (2002). Viral RNA mutations are region specific and increased by ribavirin in a full-length hepatitis C virus replication system. *J Virol* **76**, 8505-17.
215. Maag, D., Castro, C., Hong, Z. & Cameron, C. E. (2001). Hepatitis C virus RNA-dependent RNA polymerase (NS5B) as a mediator of the antiviral activity of ribavirin. *J Biol Chem* **276**, 46094-8.
216. Pfeiffer, J. K. & Kirkegaard, K. (2003). A single mutation in poliovirus RNA-dependent RNA polymerase confers resistance to mutagenic nucleotide analogs via increased fidelity. *Proc Natl Acad Sci U S A* **100**, 7289-94.
217. Stuyver, L. J., McBrayer, T. R., Whitaker, T., Tharnish, P. M., Ramesh, M., Lostia, S., Cartee, L., Shi, J., Hobbs, A., Schinazi, R. F., Watanabe, K. A. & Otto, M. J. (2004). Inhibition of the subgenomic hepatitis C virus replicon in huh-7 cells by 2'-deoxy-2'-fluorocytidine. *Antimicrob Agents Chemother* **48**, 651-4.
218. Shim, J., Larson, G., Lai, V., Naim, S. & Wu, J. Z. (2003). Canonical 3'-deoxyribonucleotides as a chain terminator for HCV NS5B RNA-dependent RNA polymerase. *Antiviral Res* **58**, 243-51.
219. Carroll, S. S., Tomassini, J. E., Bosserman, M., Getty, K., Stahlhut, M. W., Eldrup, A. B., Bhat, B., Hall, D., Simcoe, A. L., LaFemina, R., Rutkowski, C. A., Wolanski, B., Yang, Z., Migliaccio, G., De Francesco, R., Kuo, L. C., MacCoss, M. & Olsen, D. B. (2003). Inhibition of hepatitis C virus RNA replication by 2'-modified nucleoside analogs. *J Biol Chem* **278**, 11979-84.
220. Olsen, D. B., Eldrup, A. B., Bartholomew, L., Bhat, B., Bosserman, M. R., Ceccacci, A., Colwell, L. F., Fay, J. F., Flores, O. A., Getty, K. L., Grobler, J. A.,

- LaFemina, R. L., Markel, E. J., Migliaccio, G., Prhavc, M., Stahlhut, M. W., Tomassini, J. E., MacCoss, M., Hazuda, D. J. & Carroll, S. S. (2004). A 7-deaza-adenosine analog is a potent and selective inhibitor of hepatitis C virus replication with excellent pharmacokinetic properties. *Antimicrob Agents Chemother* **48**, 3944-53.
221. Eldrup, A. B., Prhavc, M., Brooks, J., Bhat, B., Prakash, T. P., Song, Q., Bera, S., Bhat, N., Dande, P., Cook, P. D., Bennett, C. F., Carroll, S. S., Ball, R. G., Bosserman, M., Burlein, C., Colwell, L. F., Fay, J. F., Flores, O. A., Getty, K., LaFemina, R. L., Leone, J., MacCoss, M., McMasters, D. R., Tomassini, J. E., Von Langen, D., Wolanski, B. & Olsen, D. B. (2004). Structure-activity relationship of heterobase-modified 2'-C-methyl ribonucleosides as inhibitors of hepatitis C virus RNA replication. *J Med Chem* **47**, 5284-97.
222. Tomassini, J. E., Getty, K., Stahlhut, M. W., Shim, S., Bhat, B., Eldrup, A. B., Prakash, T. P., Carroll, S. S., Flores, O., MacCoss, M., McMasters, D. R., Migliaccio, G. & Olsen, D. B. (2005). Inhibitory effect of 2'-substituted nucleosides on hepatitis C virus replication correlates with metabolic properties in replicon cells. *Antimicrob Agents Chemother* **49**, 2050-8.
223. Migliaccio, G., Tomassini, J. E., Carroll, S. S., Tomei, L., Altamura, S., Bhat, B., Bartholomew, L., Bosserman, M. R., Ceccacci, A., Colwell, L. F., Cortese, R., De Francesco, R., Eldrup, A. B., Getty, K. L., Hou, X. S., LaFemina, R. L., Ludmerer, S. W., MacCoss, M., McMasters, D. R., Stahlhut, M. W., Olsen, D. B., Hazuda, D. J. & Flores, O. A. (2003). Characterization of resistance to non-obligate chain-terminating ribonucleoside analogs that inhibit hepatitis C virus replication in vitro. *J Biol Chem* **278**, 49164-70.
224. Klumpp, K., Leveque, V., Le Pogam, S., Ma, H., Jiang, W. R., Kang, H., Granycome, C., Singer, M., Laxton, C., Hang, J. Q., Sarma, K., Smith, D. B., Heindl, D., Hobbs, C. J., Merrett, J. H., Symons, J., Cammack, N., Martin, J. A., Devos, R. & Najera, I. (2006). The novel nucleoside analog R1479 (4'-azidocytidine) is a potent inhibitor of NS5B-dependent RNA synthesis and hepatitis C virus replication in cell culture. *J Biol Chem* **281**, 3793-9.
225. Dhanak, D., Duffy, K. J., Johnston, V. K., Lin-Goerke, J., Darcy, M., Shaw, A. N., Gu, B., Silverman, C., Gates, A. T., Nonnemacher, M. R., Earnshaw, D. L., Casper, D. J., Kaura, A., Baker, A., Greenwood, C., Gutshall, L. L., Maley, D., DelVecchio, A., Macarron, R., Hofmann, G. A., Alnoah, Z., Cheng, H. Y., Chan, G., Khandekar, S., Keenan, R. M. & Sarisky, R. T. (2002). Identification and biological characterization of heterocyclic inhibitors of the hepatitis C virus RNA-dependent RNA polymerase. *J Biol Chem* **277**, 38322-7.
226. Love, R. A., Parge, H. E., Yu, X., Hickey, M. J., Diehl, W., Gao, J., Wriggers, H., Ekker, A., Wang, L., Thomson, J. A., Dragovich, P. S. & Fuhrman, S. A. (2003). Crystallographic identification of a noncompetitive inhibitor binding site on the hepatitis C virus NS5B RNA polymerase enzyme. *J Virol* **77**, 7575-81.
227. Chan, L., Reddy, T. J., Proulx, M., Das, S. K., Pereira, O., Wang, W., Siddiqui, A., Yannopoulos, C. G., Poisson, C., Turcotte, N., Drouin, A., Alaoui-Ismaili, M. H., Bethell, R., Hamel, M., L'Heureux, L., Bilimoria, D. & Nguyen-Ba, N. (2003). Identification of N,N-disubstituted phenylalanines as a novel class of inhibitors of hepatitis C NS5B polymerase. *J Med Chem* **46**, 1283-5.



228. Beaulieu, P. L., Bos, M., Bousquet, Y., DeRoy, P., Fazal, G., Gauthier, J., Gillard, J., Goulet, S., McKercher, G., Poupart, M. A., Valois, S. & Kukolj, G. (2004). Non-nucleoside inhibitors of the hepatitis C virus NS5B polymerase: discovery of benzimidazole 5-carboxylic amide derivatives with low-nanomolar potency. *Bioorg Med Chem Lett* **14**, 967-71.
229. Chan, L., Das, S. K., Reddy, T. J., Poisson, C., Proulx, M., Pereira, O., Courchesne, M., Roy, C., Wang, W., Siddiqui, A., Yannopoulos, C. G., Nguyen-Ba, N., Labrecque, D., Bethell, R., Hamel, M., Courtemanche-Asselin, P., L'Heureux, L., David, M., Nicolas, O., Brunette, S., Bilimoria, D. & Bedard, J. (2004). Discovery of thiophene-2-carboxylic acids as potent inhibitors of HCV NS5B polymerase and HCV subgenomic RNA replication. Part 1: Sulfonamides. *Bioorg Med Chem Lett* **14**, 793-6.
230. Chan, L., Pereira, O., Reddy, T. J., Das, S. K., Poisson, C., Courchesne, M., Proulx, M., Siddiqui, A., Yannopoulos, C. G., Nguyen-Ba, N., Roy, C., Nasturica, D., Moinet, C., Bethell, R., Hamel, M., L'Heureux, L., David, M., Nicolas, O., Courtemanche-Asselin, P., Brunette, S., Bilimoria, D. & Bedard, J. (2004). Discovery of thiophene-2-carboxylic acids as potent inhibitors of HCV NS5B polymerase and HCV subgenomic RNA replication. Part 2: tertiary amides. *Bioorg Med Chem Lett* **14**, 797-800.
231. Summa, V., Petrocchi, A., Matassa, V. G., Taliani, M., Laufer, R., De Francesco, R., Altamura, S. & Pace, P. (2004). HCV NS5b RNA-dependent RNA polymerase inhibitors: from alpha,gamma-diketoacids to 4,5-dihydroxypyrimidine- or 3-methyl-5-hydroxypyrimidinonecarboxylic acids. Design and synthesis. *J Med Chem* **47**, 5336-9.
232. Summa, V., Petrocchi, A., Pace, P., Matassa, V. G., De Francesco, R., Altamura, S., Tomei, L., Koch, U. & Neuner, P. (2004). Discovery of alpha,gamma-diketo acids as potent selective and reversible inhibitors of hepatitis C virus NS5b RNA-dependent RNA polymerase. *J Med Chem* **47**, 14-7.
233. Harper, S., Avolio, S., Pacini, B., Di Filippo, M., Altamura, S., Tomei, L., Paonessa, G., Di Marco, S., Carfi, A., Giuliano, C., Padron, J., Bonelli, F., Migliaccio, G., De Francesco, R., Laufer, R., Rowley, M. & Narjes, F. (2005). Potent inhibitors of subgenomic hepatitis C virus RNA replication through optimization of indole-N-acetamide allosteric inhibitors of the viral NS5B polymerase. *J Med Chem* **48**, 4547-57.
234. Beaulieu, P. L., Bousquet, Y., Gauthier, J., Gillard, J., Marquis, M., McKercher, G., Pellerin, C., Valois, S. & Kukolj, G. (2004). Non-nucleoside benzimidazole-based allosteric inhibitors of the hepatitis C virus NS5B polymerase: inhibition of subgenomic hepatitis C virus RNA replicons in Huh-7 cells. *J Med Chem* **47**, 6884-92.
235. Nguyen, T. T., Gates, A. T., Gutshall, L. L., Johnston, V. K., Gu, B., Duffy, K. J. & Sarisky, R. T. (2003). Resistance profile of a hepatitis C virus RNA-dependent RNA polymerase benzothiadiazine inhibitor. *Antimicrob Agents Chemother* **47**, 3525-30.
236. Tomei, L., Altamura, S., Bartholomew, L., Biroccio, A., Ceccacci, A., Pacini, L., Narjes, F., Gennari, N., Bisbocci, M., Incitti, I., Orsatti, L., Harper, S., Stansfield, I., Rowley, M., De Francesco, R. & Migliaccio, G. (2003). Mechanism of action

- and antiviral activity of benzimidazole-based allosteric inhibitors of the hepatitis C virus RNA-dependent RNA polymerase. *J Virol* **77**, 13225-31.
237. Tomei, L., Altamura, S., Bartholomew, L., Bisbocci, M., Bailey, C., Bosserman, M., Cellucci, A., Forte, E., Incitti, I., Orsatti, L., Koch, U., De Francesco, R., Olsen, D. B., Carroll, S. S. & Migliaccio, G. (2004). Characterization of the inhibition of hepatitis C virus RNA replication by nonnucleosides. *J Virol* **78**, 938-46.
  238. Wang, M., Ng, K. K., Cherney, M. M., Chan, L., Yannopoulos, C. G., Bedard, J., Morin, N., Nguyen-Ba, N., Alaoui-Ismaili, M. H., Bethell, R. C. & James, M. N. (2003). Non-nucleoside analogue inhibitors bind to an allosteric site on HCV NS5B polymerase. Crystal structures and mechanism of inhibition. *J Biol Chem* **278**, 9489-95.
  239. Di Marco, S., Volpari, C., Tomei, L., Altamura, S., Harper, S., Narjes, F., Koch, U., Rowley, M., De Francesco, R., Migliaccio, G. & Carfi, A. (2005). Interdomain communication in hepatitis C virus polymerase abolished by small molecule inhibitors bound to a novel allosteric site. *J Biol Chem* **280**, 29765-70.
  240. LaPlante, S. R., Jakalian, A., Aubry, N., Bousquet, Y., Ferland, J. M., Gillard, J., Lefebvre, S., Poirier, M., Tsantrizos, Y. S., Kukolj, G. & Beaulieu, P. L. (2004). Binding mode determination of benzimidazole inhibitors of the hepatitis C virus RNA polymerase by a structure and dynamics strategy. *Angew Chem Int Ed Engl* **43**, 4306-11.
  241. Ma, H., Leveque, V., De Witte, A., Li, W., Hendricks, T., Clausen, S. M., Cammack, N. & Klumpp, K. (2005). Inhibition of native hepatitis C virus replicase by nucleotide and non-nucleoside inhibitors. *Virology* **332**, 8-15.
  242. Biswal, B. K., Wang, M., Cherney, M. M., Chan, L., Yannopoulos, C. G., Bilimoria, D., Bedard, J. & James, M. N. (2006). Non-nucleoside Inhibitors Binding to Hepatitis C Virus NS5B Polymerase Reveal a Novel Mechanism of Inhibition. *J Mol Biol* **361**, 33-45.
  243. Powers, J. P., Piper, D. E., Li, Y., Mayorga, V., Anzola, J., Chen, J. M., Jaen, J. C., Lee, G., Liu, J., Peterson, M. G., Tonn, G. R., Ye, Q., Walker, N. P. & Wang, Z. (2006). SAR and mode of action of novel non-nucleoside inhibitors of hepatitis C NS5b RNA polymerase. *J Med Chem* **49**, 1034-46.
  244. Pfefferkorn, J. A., Greene, M. L., Nugent, R. A., Gross, R. J., Mitchell, M. A., Finzel, B. C., Harris, M. S., Wells, P. A., Shelly, J. A., Anstadt, R. A., Kilkuskie, R. E., Kopta, L. A. & Schwende, F. J. (2005). Inhibitors of HCV NS5B polymerase. Part 1: Evaluation of the southern region of (2Z)-2-(benzoylamino)-3-(5-phenyl-2-furyl)acrylic acid. *Bioorg Med Chem Lett* **15**, 2481-6.
  245. Pfefferkorn, J. A., Nugent, R., Gross, R. J., Greene, M., Mitchell, M. A., Reding, M. T., Funk, L. A., Anderson, R., Wells, P. A., Shelly, J. A., Anstadt, R., Finzel, B. C., Harris, M. S., Kilkuskie, R. E., Kopta, L. A. & Schwende, F. J. (2005). Inhibitors of HCV NS5B polymerase. Part 2: Evaluation of the northern region of (2Z)-2-benzoylamino-3-(4-phenoxy-phenyl)-acrylic acid. *Bioorg Med Chem Lett* **15**, 2812-8.
  246. Lai, V. C., Kao, C. C., Ferrari, E., Park, J., Uss, A. S., Wright-Minogue, J., Hong, Z. & Lau, J. Y. (1999). Mutational analysis of bovine viral diarrhea virus RNA-dependent RNA polymerase. *J Virol* **73**, 10129-36.

247. Arion, D., Kaushik, N., McCormick, S., Borkow, G. & Parniak, M. A. (1998). Phenotypic mechanism of HIV-1 resistance to 3'-azido-3'-deoxythymidine (AZT): increased polymerization processivity and enhanced sensitivity to pyrophosphate of the mutant viral reverse transcriptase. *Biochemistry* **37**, 15908-17.
248. Meyer, P. R., Matsuura, S. E., So, A. G. & Scott, W. A. (1998). Unblocking of chain-terminated primer by HIV-1 reverse transcriptase through a nucleotide-dependent mechanism. *Proc Natl Acad Sci U S A* **95**, 13471-6.
249. Ferron, F., Bussetta, C., Dutartre, H. & Canard, B. (2005). The modeled structure of the RNA dependent RNA polymerase of GBV-C virus suggests a role for motif E in Flaviviridae RNA polymerases. *BMC Bioinformatics* **6**, 255.
250. Dutartre, H., Boretto, J., Guillemot, J. C. & Canard, B. (2005). A relaxed discrimination of 2'-O-methyl-GTP relative to GTP between de novo and Elongative RNA synthesis by the hepatitis C RNA-dependent RNA polymerase NS5B. *J Biol Chem* **280**, 6359-68.
251. Levine, S., Hernandez, D., Yamanaka, G., Zhang, S., Rose, R., Weinheimer, S. & Colonno, R. J. (2002). Efficacies of entecavir against lamivudine-resistant hepatitis B virus replication and recombinant polymerases in vitro. *Antimicrob Agents Chemother* **46**, 2525-32.
252. Cai, Z., Liang, T. J. & Luo, G. (2004). Effects of mutations of the initiation nucleotides on hepatitis C virus RNA replication in the cell. *J Virol* **78**, 3633-43.
253. Lima, W. F. & Crooke, S. T. (1997). Binding affinity and specificity of Escherichia coli RNase H1: impact on the kinetics of catalysis of antisense oligonucleotide-RNA hybrids. *Biochemistry* **36**, 390-8.
254. Gotte, M. (2004). Inhibition of HIV-1 reverse transcription: basic principles of drug action and resistance. *Expert Rev Anti Infect Ther* **2**, 707-16.
255. Deval, J., Courcambeck, J., Selmi, B., Boretto, J. & Canard, B. (2004). Structural determinants and molecular mechanisms for the resistance of HIV-1 RT to nucleoside analogues. *Curr Drug Metab* **5**, 305-16.
256. Marchand, B. & Gotte, M. (2003). Site-specific footprinting reveals differences in the translocation status of HIV-1 reverse transcriptase. Implications for polymerase translocation and drug resistance. *J Biol Chem* **278**, 35362-72.
257. Sarafianos, S. G., Clark, A. D., Jr., Tuske, S., Squire, C. J., Das, K., Sheng, D., Ilankumaran, P., Ramesha, A. R., Kroth, H., Sayer, J. M., Jerina, D. M., Boyer, P. L., Hughes, S. H. & Arnold, E. (2003). Trapping HIV-1 reverse transcriptase before and after translocation on DNA. *J Biol Chem* **278**, 16280-8.
258. Gotte, M. (2006). Effects of Nucleotides and Nucleotide Analogue Inhibitors of HIV-1 Reverse Transcriptase in a Ratchet Model of Polymerase Translocation. *Curr Pharm Des* **12**, 1867-77.